

DEEPENING THE QUANTITATIVE UNDERSTANDING OF GROUNDWATER SYSTEMS IN DATA-SCARCE AREAS

Application in the Bandung Groundwater Basin, Indonesia



Steven Reinaldo Rusli

Propositions

- 1 | The primary consideration in undertaking water balance analysis is the rationale behind the selection of data sources.
(this thesis)
- 2 | Analysing groundwater storage has to consider the aquifer's stratification.
(this thesis)
- 3 | Developing methods to work in data-scarce areas inadvertently exacerbates the issue of data scarcity.
- 4 | Stereotyping represents an adequate statistical concept for understanding probability distributions.
- 5 | Promoting inclusivity leads to, paradoxically, non-inclusive environments.
- 6 | Working from home is as tragic as living in the office.

Propositions belonging to the thesis, entitled:

Deepening the quantitative understanding of groundwater systems in data-scarce areas: Application in the Bandung Groundwater Basin, Indonesia

Steven Reinaldo Rusli
Wageningen, 6 February 2024

Deepening the quantitative understanding of groundwater systems in data-scarce areas

Application in the Bandung Groundwater Basin, Indonesia

Steven Reinaldo Rusli

Thesis committee

Promotors

Prof. Dr A.H. Weerts

Special Professor, Hydrology Predictability

Wageningen University & Research

Dr V.F. Bense

Associate Professor, Hydrology and Environmental Hydraulics

Wageningen University & Research

Other members

Prof. Dr C. Kroeze, Wageningen University & Research

Prof. Dr M. Bierkens, Utrecht University, The Netherlands

Prof. Dr M. Huysmans, Vrije Universiteit Brussel, Belgium

Prof. Dr N. van de Giesen, Delft University of Technology, The Netherlands

This research was conducted under the auspices of the Graduate School for Socio-Economic and Natural Sciences of the Environment (SENSE)

Deepening the quantitative understanding of groundwater systems in data-scarce areas

Application in the Bandung Groundwater Basin, Indonesia

Steven Reinaldo Rusli

Thesis

submitted in fulfillment of the requirements for the degree of doctor
at Wageningen University

by the authority of the Rector Magnificus,

Prof. Dr A.P.J. Mol,

in the presence of the

Thesis Committee appointed by the Academic Board

to be defended in public

on Tuesday, 6 February 2024

at 1.30 p.m. in the Omnia Auditorium.

Steven Reinaldo Rusli

Deepening the quantitative understanding of groundwater systems in data-scarce areas
Application in the Bandung Groundwater Basin, Indonesia

214 pages.

PhD thesis, Wageningen University, Wageningen, The Netherlands (2024)

With references, with summary in English and Dutch

ISBN 978-94-6447-956-0

DOI <https://doi.org/10.18174/640983>

With love, to my wife, Marlitha Egi
With faith, in my son, Gavriel Brandon Rusli
With hope, for my future child(ren)

With respect, to my fathers, Eric and Hagi
With honor, to my mothers, Lily and Enie
With strength, for my sisters, Stella, Marcella, and Marien

With compassion, to my grandparents
and with goodwill, to the extended family and relatives

This book is dedicated to you all

Contents

	Page
Contents	vii
Summary	ix
Samenvatting	xiii
Chapter 1 Introduction	1
Chapter 2 The Bandung Groundwater Basin	17
Chapter 3 Water balance components and their uncertainty bounds	27
Chapter 4 Hydrological and groundwater flow model one-way coupling	49
Chapter 5 Aquifer interaction induced by multi-layer abstraction	73
Chapter 6 Future groundwater availability projection	105
Chapter 7 Synthesis	131
References	145
Statement of authorship contribution	177
Acknowledgements	179
About the author	181

Summary

Groundwater serves 95% of the total non-frozen freshwater in, on, and above the earth. With the increasing water demand due to population growth, abstracting groundwater is an unavoidable need for society. Understanding the groundwater system's response in flow, head, table, and storage to anthropogenic activities is, therefore, crucial for developing sustainable groundwater management, policies, and strategies.

In recent decades, groundwater flow modeling has been a major contributor to advancing the understanding of groundwater resources. However, many obstacles persist in developing and implementing groundwater flow modeling; data scarcity being one among many. Due to this issue, maximizing the groundwater flow model's capability to unravel subsurface processes and mechanisms in data-scarce areas remains challenging to this day.

The situation is also particularly applicable to the Bandung groundwater basin, Indonesia. Only a few groundwater-related research were conducted in the area. Several factors, primarily data availability, have hindered further progress in understanding the groundwater system. As a result, the quantification of groundwater-related variables in this area lacks the depth found in data-sufficient areas. For that reason, the main aim of this study is to deepen the quantitative understanding of the groundwater system in the Bandung groundwater basin, Indonesia. In achieving the primary goal, four topics are covered: (1) estimating water balance components, (2) developing a one-way coupled hydrological and groundwater flow model, (3) model evaluation using (ancillary) environmental water tracers data, and (4) projecting future groundwater availability.

This thesis begins with an introduction in Chapter 1, briefly describing groundwater in general, and laying out the basic idea and principles of groundwater flow modeling. It is also complemented by other fundamental materials, such as aquifers, groundwater abstraction, and the link between hydrological and groundwater flow simulation. All the academic journal articles resulting from this thesis share a common study area of the Bandung groundwater basin. Thus, most of the essential details of the study area are elaborated in Chapter 2. These include location overview, hydrological and hydrogeological settings, anthropogenic footprint, and data availability, including those collected during the field campaign conducted in 2020.

Chapter 3 explores the estimation of the Bandung groundwater basin's water balance and investigates the associated uncertainty bounds. Using a series of estimates for each water balance component, it is aimed that the definitive conclusion on the basin's current water storage change status could be derived. Multiple water balance components' estimates are collated from ground measurements, interpolated gauge-based datasets, and remote-sensing products, to hydrological model-based estimates. Further, their uncertainties are quantified by applying the Extended Triple Collocation technique. The analysis leads to the conclusion that the integration of a dedicated groundwater flow model is imperative for mitigating the uncertainty surrounding the estimates of water balance components, particularly when conducting assessments of basin water storage changes.

In Chapter 4, a one-way coupled hydrological and groundwater flow model is constructed and calibrated. The hydrological model is based on the Wflow_sbm model, following up the model-based estimates discussed in Chapter 3. In the model setup, we incorporate one additional parameter, *MaxLeakage*, to estimate groundwater recharge. Using information obtained from field campaigns and collaborations with several government and private sectors, a parsimonious groundwater flow model is developed using the MODFLOW model. The simulation output is evaluated by comparing a number of variables: (1) the river discharge simulated by the hydrological model with discharge observation data, (2) the groundwater head simulated by the groundwater flow model with observed groundwater head, and (3) the basin's water storage changes simulated by the one-way coupled model with gravimetric satellite estimates of GRACE. All designated evaluations produce satisfactory metrics: KGE (Kling-Gupta Efficiency) of 0.46, r^2 (coefficient of determination) of 0.895, and cross-correlation coefficient of 0.502, to name a few. It is concluded in this chapter that gravimetric satellite data of GRACE could be used as a supplementary model evaluation tool, even in basin-scale models. Having said that, the local features of the basin and the GRACE's footprint due to the potential spatial coverage differences are of substantial importance to be considered.

Chapter 5 further explores the details of the one-way coupled model simulation results. To increase confidence in the model results, the model is evaluated, qualitatively, by comparing the pattern produced by the one-way coupled model with the ones derived from environmental water tracer data analysis. The collated environmental water tracer data include major ion elements, groundwater age estimates, and stable isotope data. Agreement was met between the two approaches from the perspective of groundwater recharge spatial distribution, regional groundwater flow direction, groundwater age estimates, and aquifer interaction identification. The previously hypothesized aquifer interaction induced by multi-layer groundwater abstraction then becomes quantifiable using the model simulation output. Within this chapter, the understanding of the groundwater system is further deepened: the parsimonious groundwater flow model is able to simulate the groundwater flow processes from the unconfined aquifer and mountainous area which compensates for the volume of groundwater abstracted from the confined aquifer.

In Chapter 6, the now-established one-way coupled model is used to project future groundwater availability. The projected climate forcings are taken from the Coupled Model Intercomparison Project Phase 6 (CMIP6), under two greenhouse gas concentration trajectory scenarios: RCP (Representative Concentration Pathway) 4.5 and 8.5. Before being forced into the Wflow_sbm model to obtain the projected groundwater recharge, the climate forcing projections are first bias-corrected using the method tailored to the Inter-Sectoral Impact Model Intercomparison Project phase 3b (ISIMIP3b). Further, the computed groundwater recharge drives the groundwater flow simulation, set up under multiple groundwater abstraction scenarios. The scenarios are developed across a range, including scenarios of increasing and decreasing groundwater abstraction. It considers a wide range of potential future possibilities, including the very tangible capital city relocation plan of Indonesia. This implementation reveals that anthropogenic activities exert dominant control over regulating the groundwater regime in the study area, even when compared with the influence of climatic factors.

Chapter 7 provides a comprehensive synthesis of the findings from the four fundamental chapters in this thesis. First, it highlights the importance of a devoted groundwater flow model to narrow the uncertainty associated with water balance components' estimation, especially in evaluating a basin's water storage changes. Second, incorporating multiple sources of data provides significant support in evaluating hydrological and groundwater flow models. This is shown by the assimilation of GRACE and environmental water tracer data, which helps in understanding the groundwater flow system in the study area. Third, the study reveals that the management of groundwater abstraction is of paramount importance for ensuring future groundwater availability in the Bandung groundwater basin. Additionally, Chapter 7 addresses each research question arising from the specific objectives and offers a comprehensive discussion of lessons learned, including the study's limitations, uncertainties, challenges, and potential future opportunities.

Samenvatting

Grondwater is goed voor 95% van de totale niet-bevroren zoetwatervoorraad onder, op en boven het aardoppervlak. Door de toenemende vraag naar water als gevolg van de bevolkingsgroei is het onttrekken van grondwater een onvermijdelijke maatschappelijke behoefte. Inzicht in de impact van menselijke activiteiten op het grondwatersysteem in stroming, stijghoogte, grondwaterstand, en opslag is daarom cruciaal voor de ontwikkeling van beleid en strategieën voor een duurzaam grondwaterbeheer.

In de afgelopen decennia heeft het modelleren van grondwaterstromingen veel bijgedragen aan een beter begrip van grondwatervoorraden. Er bestaan echter veel obstakels bij het ontwikkelen en implementeren van grondwaterstromingsmodellering; gegevensschaarste is er daar één van. Vanwege dit probleem blijft het maximaliseren van het vermogen van het grondwaterstromingsmodel om ondergrondse processen en mechanismen in gebieden met weinig gegevens te ontrafelen tot op de dag van vandaag een uitdaging.

De situatie is ook in het bijzonder van toepassing op het grondwaterbekken van Bandung, Indonesië. Er is slechts weinig grondwatergerelateerd onderzoek uitgevoerd in het gebied. Verschillende factoren, voornamelijk de beschikbaarheid van gegevens, hebben verdere vooruitgang in het begrijpen van het grondwatersysteem belemmerd. Het gevolg is dat de kwantificering van grondwatergerelateerde variabelen in dit gebied niet de diepgang heeft die wel beschikbaar is in gebieden met voldoende gegevens. Daarom is het hoofddoel van deze studie het verdiepen van het kwantitatieve begrip van het grondwatersysteem in het Bandung grondwaterbekken, Indonesië. Om dit doel te bereiken, worden vier onderwerpen behandeld: (1) het schatten van waterbalanscomponenten, (2) het ontwikkelen van een eenzijdig gekoppeld hydrologisch en grondwaterstromingsmodel, (3) modevaluatie met behulp van (aanvullende) gegevens van omgevingswatertracers, en (4) het voorspellen van de toekomstige beschikbaarheid van grondwater.

Dit proefschrift begint met een inleiding in hoofdstuk 1, waarin grondwater in het algemeen wordt beschreven en het basisidee en de principes van grondwaterstromingsmodellering worden uiteengezet. Hoofdstuk 1 wordt aangevuld met ander fundamenteel materiaal, zoals watervoerende lagen, grondwateronttrekking en het verband tussen hydrologische simulatie en simulatie van grondwaterstromen. Alle in academische tijdschriften gepubliceerde artikelen die uit dit proefschrift voortkomen, hebben als gemeenschappelijk studiegebied

het Bandung grondwaterbekken. Daarom worden de meeste essentiële details van het studiegebied in hoofdstuk 2 uitgewerkt. Deze omvatten een overzicht van de locatie, hydrologische en hydrogeologische settings, de antropogene voetafdruk en de beschikbaarheid van gegevens, inclusief de gegevens die zijn verzameld tijdens de veldcampagne die in 2020 is uitgevoerd.

Hoofdstuk 3 behandelt de schatting van de waterbalans van het Bandung grondwaterbekken en de bijbehorende onzekerheidsgrenzen. Met behulp van een reeks schattingen voor elke waterbalanscomponent wordt geprobeerd om een definitieve conclusie te trekken over de huidige mate van verandering in de watervoorraad van het stroomgebied. De schattingen van meerdere waterbalanscomponenten worden samengevoegd, van grondmetingen, geïnterpoleerde meetgegevens en teledetectieproducten tot schattingen op basis van hydrologische modellen. Verder worden de onzekerheden gekwantificeerd door de Extended Triple Collocation techniek toe te passen. De analyse leidt tot de conclusie dat de integratie van een specifiek grondwaterstromingsmodel noodzakelijk is om de onzekerheid rond de schattingen van waterbalanscomponenten te verminderen, met name bij het uitvoeren van beoordelingen van veranderingen in de wateropslag in het stroomgebied.

In hoofdstuk 4 wordt een eenzijdig gekoppeld hydrologisch en grondwaterstromingsmodel geconstrueerd en gekalibreerd. Het hydrologische model is gebaseerd op het Wflow_sbm model, voortbouwend op de modelgebaseerde schattingen die in hoofdstuk 3 zijn besproken. In de modelopzet nemen we een extra parameter op, *MaxLeakage*, om de grondwateraanvulling te schatten. Met behulp van informatie verkregen uit veldcampagnes en samenwerkingsverbanden met verschillende overheids- en particuliere sectoren wordt een eenvoudig grondwaterstromingsmodel ontwikkeld met behulp van het MODFLOW model. De simulatieresultaten worden geëvalueerd door een aantal variabelen te vergelijken: (1) De door het hydrologische model gesimuleerde rivierafvoer met waargenomen afvoerdata, (2) de door het grondwaterstromingsmodel gesimuleerde grondwaterstand met de waargenomen grondwaterstand, en (3) de door het eenzijdig gekoppelde model gesimuleerde veranderingen in de wateropslag in het stroomgebied met gravimetrische satelliet-schattingen van GRACE. Alle toegewezen evaluaties leveren bevredigende metriecken op: Een KGE (Kling-Gupta Efficiëntie) van 0,46, r^2 (determinatiecoëfficiënt) van 0,895 en kruisrelatiecoëfficiënt van 0,502, om er een paar te noemen. In dit hoofdstuk wordt geconcludeerd dat gravimetrische satellietgegevens van GRACE kunnen worden gebruikt als een aanvullend instrument voor modevaluatie, zelfs in modellen op schaal van het rivierbekkenniveau. Dit gezegd hebbende, is het van groot belang om rekening te houden met de lokale kenmerken van het rivier bekken en de voetafdruk van GRACE vanwege de mogelijke ruimtelijke dekkingsverschillen.

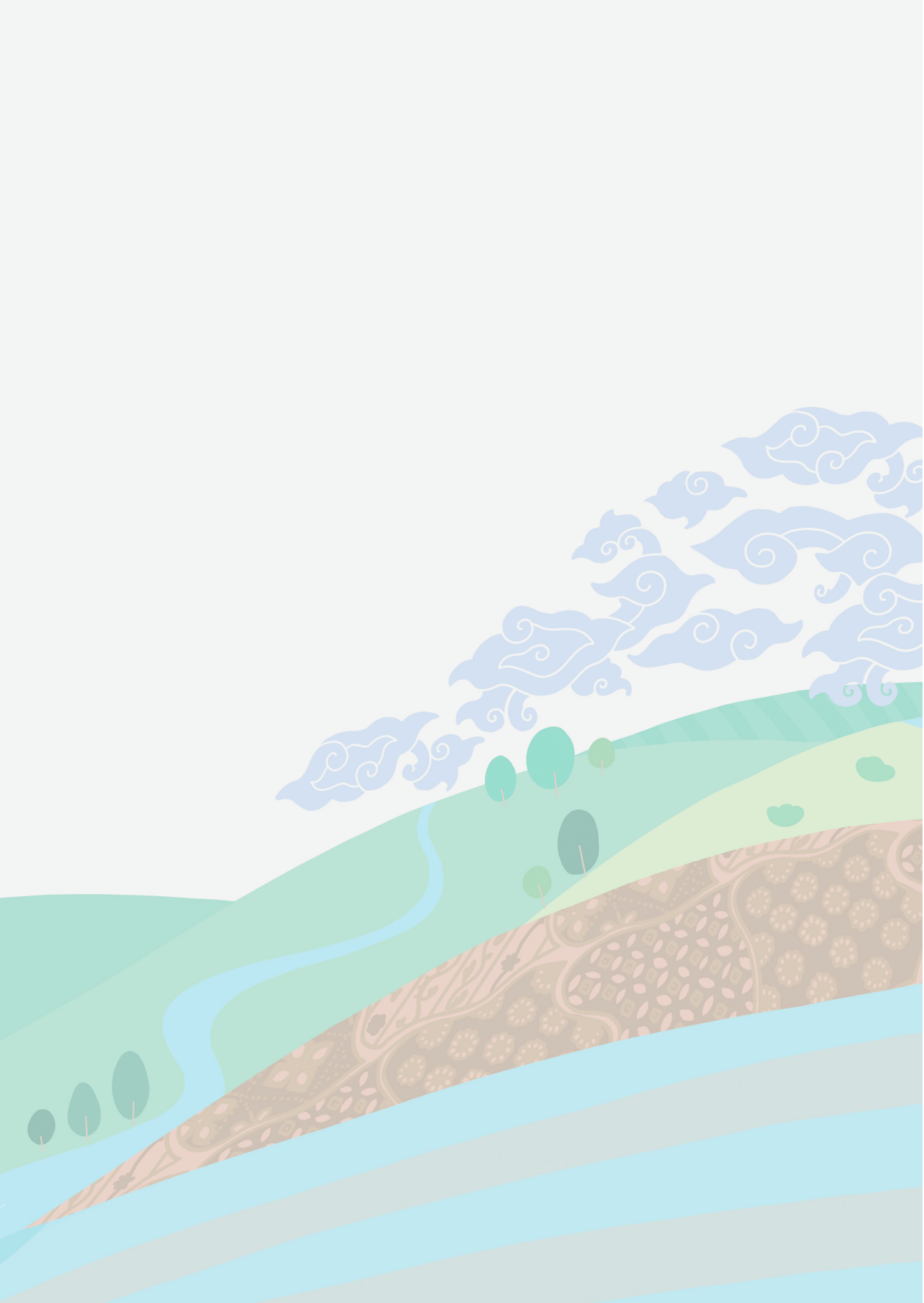
Hoofdstuk 5 gaat verder in op de simulatieresultaten van het eenzijdig gekoppelde model. Om de betrouwbaarheid van de modelresultaten te vergroten, wordt het model kwalitatief geëvalueerd door het patroon dat door het eenzijdig gekoppelde model wordt geproduceerd

te vergelijken met de patronen die zijn afgeleid uit de analyse van omgevingswatertracerdata. Dit zijn onder meer elementen van belangrijke ionen, grondwater-leeftijdsisotopen en stabiele isotopengegevens. Er was overeenstemming tussen de twee benaderingen wat betreft de ruimtelijke verdeling van de grondwateraanvulling, de richting van de regionale grondwaterstroming, de schatting van de grondwaterleeftijd en de identificatie van de interactie tussen watervoerende pakketten. De eerder genoemde aquiferinteractie veroorzaakt door meerlagige grondwateronttrekking wordt vervolgens kwantificeerbaar met behulp van de modelsimulatie-uitvoer. In dit hoofdstuk wordt het begrip van het grondwatersysteem verder verdiept: het grondwaterstromingsmodel is in staat om de grondwaterstromingsprocessen uit de niet-gesloten watervoerende laag en het bergachtige gebied te simuleren, waardoor het volume grondwater dat wordt onttrokken uit de ingesloten watervoerende laag wordt gecompenseerd.

In hoofdstuk 6 wordt het nu ontwikkelde eenzijdig gekoppelde model gebruikt om de toekomstige beschikbaarheid van grondwater te simuleren. De voorspelde klimaatscenario's zijn afkomstig van het Coupled Model Intercomparison Project Phase 6 (CMIP6), onder twee scenario's voor broeikasgasconcentraties: RCP (Representative Concentration Pathway) 4.5 en 8.5. Voordat het hydrologische Wflow_sbm model hiermee geforceerd wordt om de geprojecteerde grondwateraanvulling te krijgen, worden de klimaatprojecties eerst gecorrigeerd met behulp van de methode die ook gebruikt is in het Inter-Sectoral Impact Model Intercomparison Project fase 3b (ISIMIP3b). Verder stuurt de berekende grondwateraanvulling de simulatie van de grondwaterstroming aan, welke zijn opgezet onder meerdere grondwateronttrekkingsscenario's. Verschillende scenario's zijn ontwikkeld, inclusief scenario's van toenemende en afnemende grondwateronttrekking. Er wordt rekening gehouden met een breed scala aan toekomstige mogelijkheden, waaronder het zeer concrete plan voor de verplaatsing van de hoofdstad van Indonesië. De simulaties laten zien dat antropogene activiteiten een dominante invloed hebben op de regulering van het grondwaterregime in het studiegebied, zelfs in vergelijking met de invloed van veranderde klimatologisch factoren.

Hoofdstuk 7 geeft een synthese van de bevindingen uit de vier fundamentele hoofdstukken in dit proefschrift. Ten eerste benadrukt het het belang van een toegewijd grondwaterstromingsmodel om de onzekerheid in verband met de schatting van waterbalanscomponenten te beperken, vooral bij de evaluatie van de veranderingen in de wateropslag in een rivierbekken. Ten tweede biedt de integratie van meerdere gegevensbronnen een belangrijke ondersteuning bij de evaluatie van hydrologische en grondwaterstromingsmodellen. Dit getoond door het gebruik van GRACE en watertracerdata, wat helpt bij het begrijpen van het grondwaterstromingssysteem in het studiegebied. Ten derde toont het onderzoek aan dat het beheer van grondwateronttrekking van het grootste belang is om de toekomstige beschikbaarheid van grondwater in het Bandung grondwaterbekken te garanderen. Hoofdstuk 7 gaat in op elke onderzoeksvraag die voortvloeit uit de specifieke doelstellin-

gen en biedt een uitgebreide bespreking van de geleerde lessen, inclusief de beperkingen, onzekerheden, uitdagingen en mogelijke toekomstige kansen van het onderzoek.



Chapter 1

Introduction



1.1 Groundwater in essence

The water cycle concept is often used to introduce hydrology-related science. While enveloping many processes from atmospheric, hydrologic, to geologic layer, one supplementary information that would benefit from its frequent sharing is the proportion of water volume involved within each process. From the book *Water in Crisis: A Guide to the World's Fresh Water Resources* (Thomas, 1994) (see Figure 1.1), it is known that only 2.5% of the total water volume on, in, and above the planet Earth is non-saline water. Without taking into account the frozen glaciers and ice caps, there is less than 40% of the already small proportion of non-saline water available in a liquid state. Within such a tiny fraction remains the 11.1 million km³ of freshwater that humans strive to manage.

It is a lot of water. In fact, it is so much water, that if the freshwater is spread all over the Earth's land surface area, the whole planet would be inundated by more than 21 meters of water columns. Unfortunately, not all of the freshwater on the planet Earth is easily accessible. Over 10.5 million km³, equivalent to roughly 95%, of the available non-frozen freshwater is accumulated under the surface, between the tiny open spaces between rock and sand, soil, and gravel, known as the **groundwater** (Schneider et al., 2011).

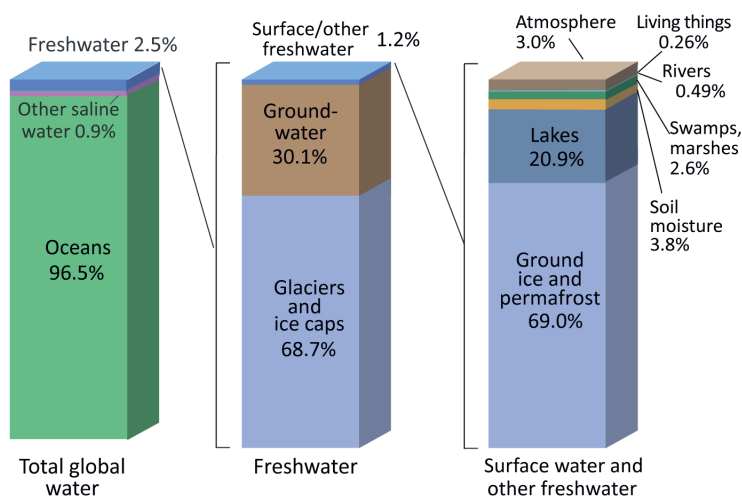
1.1.1 Innate natural attributes of groundwater system

In many ways, groundwater and surface water share many fundamentally common features. Physically, both groundwater and surface water travel from locations with higher energy to those with lower energy. When they are still, they are both storable, although each storage of groundwater and surface water has its own inflow and outflow budget within the water cycle conceptual framework. On the other hand, they also have key differences within their flow and storage systems, regulated by different mechanisms and processes.

Analogous to reservoirs and/or water bodies for surface water, groundwater is deposited in **aquifers**. It is defined as subsurface geological formations with the capability of storing and transmitting groundwater. Each aquifer has its own properties, such as porosity, permeability, storage capacity, thickness, soil stratigraphy, etc. These properties are molded and shaped by unique (hydro)geological processes: weathering, erosion, deposition, compaction, burial, and so forth. Often, aquifer properties are found to be heterogeneous (varying among locations) and anisotropic (varying among directions).

When groundwater flows, many physical attributes are involved in driving such a motion, contributed dominantly by aquifer properties: available pore spaces among soil particles, rock size distribution, retention capacity, and so on. Another key component, that is often disregarded, is the properties of the flowing fluid: density, viscosity, etc. Encompassing all controlling factors of groundwater flow, **hydraulic conductivity** represents the easiness of certain fluid, in most cases the groundwater, to flow through porous media.

Where is Earth's Water?



Credit: U.S. Geological Survey, Water Science School. <https://www.usgs.gov/special-topic/water-science-school>
 Data source: Igor Shiklomanov's chapter "World fresh water resources" in Peter H. Gleick (editor), 1993, *Water in Crisis: A Guide to the World's Fresh Water Resources*. (Numbers are rounded).

Figure 1.1: Water distribution across the globe, taken from the United States Geological Survey (USGS).

In addition to aquifer/soil control, groundwater movement is also regulated, naturally, by **surface water**. Water bodies such as rivers, lakes, and/or even oceans frequently act as boundary conditions for the water exchange between groundwater and surface water, displayed in Figure 1.2. These interactions also propagate from higher to lower energy. Therefore, in an area where the groundwater level is higher compared to the surface water elevation, groundwater seeps as river baseflow (Figure 1.2 [top]). Otherwise, the water bodies are losing water (Figure 1.2 [bottom]) by infiltrating into the soil and filling the groundwater storage.

1.1.2 Society's role on groundwater

As the largest freshwater storage on earth, groundwater has never been and could not be detached from society. In many ways, the regime of groundwater is partly regulated by **anthropogenic activities**, besides its natural control described in the section above. For that reason, the correlation between societal roles and groundwater management is an interesting and important topic in itself (Scholz et al., 2000; Mitchell et al., 2012). Changes in land use and land cover, for example, alter the amount and pattern of groundwater

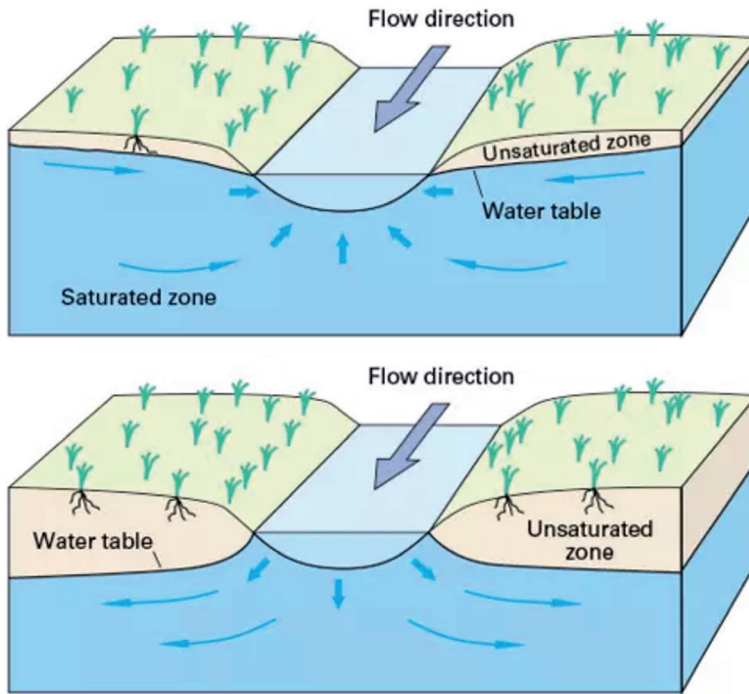


Figure 1.2: Schematics of groundwater and surface water interaction where the river gains water [top figure] and loses water [bottom figure], taken from Alley et al. (1999).

recharge, which is the main inflow into a groundwater system. Anthropogenic influence on surface water also indirectly affects groundwater, as surface water control on groundwater is briefly mentioned above. However, among many human interventions, one activity with the most direct impact is **groundwater abstraction**, carried out by physically pumping groundwater out from an aquifer.

Human civilization has been abstracting groundwater to meet its water demand since the prehistorical age (Angelakis et al., 2016; Voudouris et al., 2018). Water requirements for irrigation, domestic uses, and industrial needs are some examples of pivotal usage of groundwater. Globally, the spatial distribution of groundwater abstraction is highly non-uniform. Despite global average annual groundwater abstraction estimates (de Graaf et al., 2014) being lower than global average annual groundwater recharge estimates (de Graaf et al., 2016), many places on regional and catchment scales have been experiencing the opposite. When inflow to a system (in this case, groundwater recharge) is lower than outflow from the system (in this case, groundwater abstraction), considering also the net flow of other budgets (for example, river baseflow, head boundary conditions, etc), **groundwater storage depletes**.

Such a situation can be found all across the world, starting from Asia in northern India (Chatterjee et al., 2018), Bangladesh (Shahid et al., 2015), northwest China (Hu et al., 2019; Lili et al., 2020), Jordan (Al-Zyoud et al., 2015), Europe in Spain (Closas et al., 2017) and its archipelago (Custodio et al., 2016), Denmark (Henriksen et al., 2008), Africa in Algeria (Khezzani and Bouchemal, 2018), Ghana (Yidana et al., 2019), South Africa (Sorensen et al., 2021), to the American continent in northeast Brazil (Luna et al., 2017), Mexico (Ochoa-González et al., 2018), and California, United States of America (Holland et al., 2022). Many issues arise as consequences of groundwater storage depletion: land subsidence (Shen and Xu, 2011; Figueroa-Miranda et al., 2018), saltwater intrusion (Kim and Yang, 2018; Mabrouk et al., 2018), surface water level decrease (Lin et al., 2018; Wu et al., 2018), etc. Therefore, the aftermath of groundwater abstraction and its impact on groundwater table and storage is important to be understood and quantified as inputs and benchmarks for groundwater management, policies, and strategies.

1.1.3 Multi-layer groundwater abstraction

As the subsurface is shaped by varying geological processes, often there are, vertically, multiple layers of aquifers with distinct characteristics. For example, some aquifers could hold and/or release more groundwater, some are more permeable, some are thicker in depth, and so forth. Based on their confining condition, there are two categorizations of aquifers: (1) **unconfined aquifer**, and (2) **confined aquifer**, which deliver different responses to groundwater abstraction. The (simplified) physical differences between the two types of aquifers are visually shown in Figure 1.3.

An unconfined aquifer has a **free water table** on its upper facet to regulate its change in energy. The free water table is defined as the dividing line between vadose zones (unsaturated soil moisture) and fully saturated soil. It is usually found near surface elevation and sometimes has direct proximity to surface water. Treating an unconfined aquifer as a hydrological bucket, its typical water budget is classified as inflow (recharge, surface water - groundwater interaction), outflow (groundwater abstraction from shallow wells, baseflow contribution), and storage change (fluctuating groundwater table).

When groundwater is pumped out from an unconfined aquifer, the groundwater level in the abstraction well dwindles as a result of water leaving the pores and spaces between the soil. Depending on the soil/aquifer properties, groundwater around a point of abstraction will eventually flow into the abstraction well. This occurs as the hydraulic head in the abstraction well, represented by the groundwater table, is lower than its surroundings. Flowing at relatively low velocities, the groundwater table profile around an abstraction well is generally manifested in curvy instead of straight lines. The area where the groundwater table profile is impacted by groundwater abstraction is known as the cone of depression. In short, an unconfined aquifer response to groundwater abstraction is reflected entirely through groundwater table decrease.

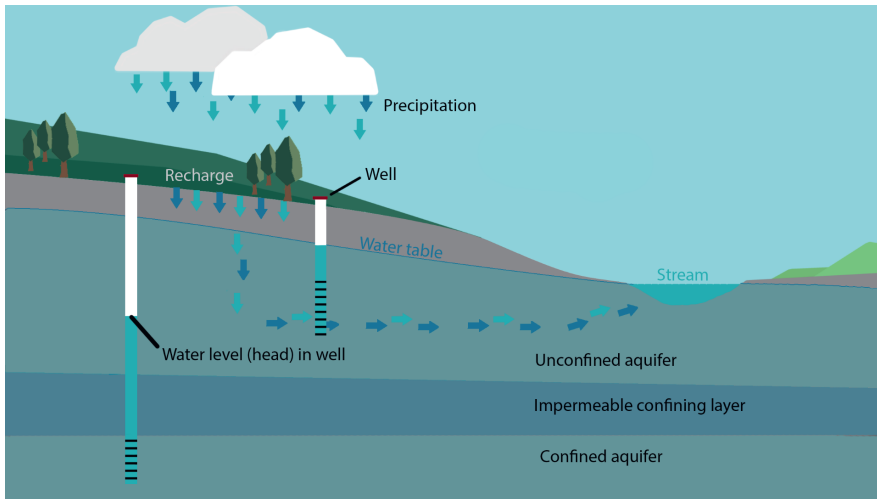


Figure 1.3: Confining conditions of unconfined and confined aquifers, taken from Land (2020).

On the other hand, a confined aquifer is bounded by a relatively impermeable layer on its upper facet, causing the layer to be practically **under pressure**. Because of the pressurized system, often the water level in a well penetrating into such an aquifer rises above the top of the confined layer. Additionally, due to the less permeable layer on its top, a confined aquifer rarely has direct contact with groundwater recharge, thus making it more difficult to replenish. It is generally not in touch with surface water, too, as a confined aquifer is mostly found at a relatively deeper depth than an unconfined aquifer.

When groundwater is pumped out from a confined aquifer, pores and spaces between soil are depressurized instead of drained, as the ecosystem within the layer being abstracted is fully saturated. Decreasing water pressure provides less support to the overbearing geological formation above, paving the way for the overlaying geological formation to potentially compact and subside. Generally, a confined aquifer's response to groundwater abstraction is observable through a change in the hydraulic head (piezometric head) at a much widespread distance from the abstraction well.

Under an equilibrium state, the groundwater table of an unconfined aquifer and the piezometric head of a confined aquifer in the same location, but at different depths, are expected to be in balance. However, changes in groundwater's hydraulic head are unavoidable when groundwater abstraction is in place. With discrepancies in responses to groundwater abstraction, hydraulic heads' changes in unconfined and confined aquifers also often diverge. Further, this stimulates groundwater flow among the vertical layers of aquifers. Extensively discussed in previous studies (Russo and Lall, 2017; Wang et al., 2019), the so-called **aquifer interaction** is also explored later in this study.

1.2 Quantification of groundwater flow

To understand and analyze the groundwater system, such as flow rate, groundwater head, and storage changes, along with other parameters and variables, it becomes more and more popular to develop and implement **groundwater modeling** through a numerical approach. One of the reasons for its growing recognition and demand is the reliability of numerical groundwater model simulation results to be translated into management practices (Singh, 2014; Yeh, 2015). Therefore, this section is dedicated to discussing the current status of groundwater modeling; its relationship with hydrological modeling, typical conceptual framework, data requirement, assessed output, and involved uncertainties.

1.2.1 Role of hydrological simulation: groundwater recharge estimates

Groundwater flow is primarily driven by **groundwater recharge**. However, groundwater recharge is not available as observation data in most cases. Instead, it is often estimated by hydrological modeling (Armanuos et al., 2016; Melati et al., 2019; Nolte et al., 2021). Therefore, simulating groundwater flow, more often than not, is closely linked with hydrological modeling, which also serves a considerable part of this thesis.

In **hydrological modeling**, often the conventional 'hydrological buckets' concept constitutes the water cycle (Staudinger et al., 2021; Turek et al., 2022). Within a particular catchment area as the simulated domain over a certain period, and considering the law of mass conservation, precipitation (P) typically serves as the main input, evapotranspiration (ET) and volumetric river discharge (Q) as the output, and change of volumes in water bodies, soil moisture, and subsurface bucket as the storage changes (ΔS) of a hydrological system. The classic and simple correlation among the inflow, outflow, and storage changes is expressed in Equation 1.1. Typically, to evaluate and validate the quality and accuracy of a hydrological simulation, each of the elements in Equation 1.1, ideally, is either determined by or compared with observation data and/or estimates.

$$I = O + \Delta S \iff P = ET + Q + \Delta S \quad (1.1)$$

The precipitation component in hydrological modeling, in a majority of instances, is a 'known variable', despite its inherited uncertainties (Bárdossy et al., 2022). In recent decades, multiple approaches have been developed in observing/estimating precipitation: rain gauges, remote-sensing, numerical modeling, re-analysis products, etc (Tapiador et al., 2012; Sun et al., 2018). Each method offers unique advantages (and drawbacks) in spatial and temporal coverage, spatial and temporal resolution, involved bias and uncertainties, and so on. As the input variable into a hydrological simulation, and considering the multiple options for precipitation estimates, the center of precipitation-related matter in hydrological modeling generally focuses on the selection and/or blending method of the available products (Mazzoleni et al., 2019; Yin et al., 2021; Hafizi and Sorman, 2022).

From the output side of hydrological modeling, at the moment, the most common variable used as the benchmark of simulation reliability is river discharge (Jian et al., 2017; Pandi et al., 2021; Westerberg et al., 2022). Similar to precipitation, there are also multiple methods to estimating river discharge: field measurements, and even reanalysis (Alfieri et al., 2020; Harrigan et al., 2020) as well as remote sensing-based approach (Bjerklie et al., 2005; Li et al., 2018). Inevitably, there are also uncertainties within each method. Generally, hydrological modeling of river discharge is compared with river discharge observation/estimates for model calibration, validation, and/or evaluation.

Besides its primary input and output comparison, a hydrological simulation could also be evaluated by assessing its 'inner process' component (Bouaziz et al., 2021). It is, admittedly, not a common procedure. For example, comparing simulated groundwater recharge with groundwater recharge field measurement involves large uncertainties as the latter is difficult to conduct. It is also controlled by many spatially non-uniform variables in different layers: rainfall, land cover and land use, topography, soil type, and more. However, in a data-scarce area, assessing hydrological simulation components using variables other than rainfall or river discharge, to complement model validation, should be considered in the effort to increase confidence in the modeling's dependability.

As an inner process component in a hydrological simulation, groundwater recharge plays a very crucial role in groundwater flow modeling (Sanford, 2002). Analogous to hydrological simulation, groundwater recharge serves the same purpose as precipitation: the main inflow to the simulated system. Therefore, establishing a hydrological simulation to produce **reliable estimates of groundwater recharge** is the first step toward a reliable groundwater model.

1.2.2 Groundwater flow modeling framework

In addition to reliable groundwater recharge estimates, other essential prerequisites for a robust numerical groundwater flow model are the model construction and parameterization. A groundwater flow model is always unique from one to another; each system is governed by distinct hydro(geo)logical boundaries. Within its development, a numerical groundwater flow model is an evolution from a **conceptual groundwater flow model**. Typically, it involves an interpretation of the actual physical configuration of the target system; the aquifer geometry, hydrodynamic and hydrogeologic properties, and water exchange fluxes (Izady et al., 2014). A reliable conceptual model is important to be well-established before, subsequently, a numerical groundwater flow is constructed based upon it.

In **constructing and parameterizing** a numerical groundwater flow model, a modeler translates the variables of the settled conceptualization into numerical values and expressions (Mary P. Anderson and Hunt, 2015). For example, an abstraction well is conceptually represented as the removal of a certain volume of groundwater (sink). Numerically, it is translated to values of a specified rate, applied at a specified time, to a specified location

and depth. Another example is groundwater recharge, which is conceptually represented as an addition of water (source). Numerically, groundwater recharge is also manifested in a specified rate, applied at a specified time, to a specified location and depth. Similar 'numerical translations' are applied for other head boundary conditions (surface water level, subsurface head control, etc) and flow boundary conditions (losing river, water transfer, etc). Besides the 'fluxes', the 'pools' of groundwater flow are also required to be parameterized (Mary P. Anderson and Hunt, 2015). Certain parameters are ingrained in each of the physical 'pool' representations, referred to as soil/aquifer properties in the previous section. A cell of soil/aquifer, for example, has its own value for storage coefficient, hydraulic conductivity, anisotropy, etc, that regulates the flow of groundwater into and out from the cell itself.

A groundwater flow model simulation is capable of producing several types of output; groundwater table, groundwater storage, water budgets, intercell flow, groundwater and surface water interaction, and more. The selected variables to be assessed depend on the aim and the focus of the modeling practice itself; whether it is to understand subsurface processes, to estimate changes in groundwater table and groundwater storage, to assist in deriving groundwater policies and management strategies, or other goals. Similar to a hydrological model, a good groundwater flow model needs to be calibrated. Analogous to river discharge variables in hydrological modeling, groundwater head (groundwater table for unconfined aquifer and piezometric head for confined aquifer) is typically used as the benchmark for groundwater flow model evaluation, quantified by the agreement between simulation results and observations.

1.2.3 Data acquisition strategy

From the description of a typical groundwater flow model framework, it is shown that a numerical groundwater flow model requires a lot of data input, starting from soil stratigraphy, soil/aquifer properties, and boundary conditions' parameterization, to groundwater head observation data. The first three types of data mentioned are useful for conceptualizing the actual groundwater flow system, constructing the groundwater flow model structure, and quantifying model parameters. The latter-mentioned groundwater head observation data, meanwhile, is key to ensuring an adequate confidence level in using the groundwater flow model simulation results. Considering their all-encompassing function and role within the groundwater flow modeling framework, both **data quantity and data quality** hold a crucially important role in producing a sound numerical groundwater flow model.

There are a number of approaches to collecting data for groundwater flow model parameterization. For soil/aquifer properties, a regional geological map commonly is the very first step of information available to a modeler. For a smaller/local spatial scale, field tests could be performed to gather auxiliary data and/or to validate larger-scale information. Series of laboratory tests are often also feasible for small-scale explorations.

Soil investigation reports are traditionally dependable and resourceful in understanding geological formations in the vertical direction, too. Accumulation of numerous reports, distributed spatially within a domain, could provide valuable insight into soil/aquifer's spatial variability. Through these data sources, however, it is not unusual to find discrepancies among datasets. After all, each type of information has different measurement methods, spatial scales, spatial coverages, and data time frames. Therefore, to reduce the width of uncertainties, known as the uncertainty bounds, it is important to take into account **multiple data sources** in parameterizing a numerical groundwater flow model.

Improving groundwater model quality is intrinsically intertwined with better groundwater observation data quality (Rajabi et al., 2018; Condon et al., 2021). In selecting observation wells' data, it is important to consider numerous aspects, such as the wells' location and network design, the available metadata, etc. Well-designed observation wells network could minimize uncertainty and exploration cost and was extensively discussed in previous studies (Pesti et al., 1994; Chen et al., 2003). Similar to the discussed topic of the hydrological model evaluation, in **data-scarce areas** where groundwater calibration data are limited, additional methods in the effort to evaluate a groundwater flow model and to increase confidence in the model's dependability are necessary.

1.2.4 Limitation and uncertainties

Akin to every other environmental science and modeling subject, the effort to understand and imitate real-world processes under numerical environments is **confined by many factors**: finite knowledge, sparse and/or scarce field measurements, inadequate data availability, insufficient computational power, and imminent uncertainties. Real-world systems are so complicated that it is impossible to capture the entire sub-processes in detail. Even if it was possible, accurate and precise estimates of the variables in focus would not be available, both in quantity and quality. Systematic bias and error are ingrained in many measurement techniques, too. Uncertainties also come from multiple stages in a modeling study: measured parameters and forcings, model structure, and calibration data. Therefore, within this study, in order to produce dependable model results, the inherently prevailing uncertainties and the strategies to respond to and minimize their influence in arriving at conclusions and suggestions are addressed in every chapter.

One notable source of uncertainty comes from the innate nature of the involved properties' **spatial and temporal variability and coverage**. On this subject, each variable/property embodies its own details. Take, for example, groundwater table observation data as an illustration. Two nearby observation wells might record two different point-data values. This could occur due to, for instance, variation in topography within the very spatial grid that covers both observation wells, hence two different observed groundwater tables. Two different observations could also happen between two instances that measured groundwater tables before and after a rainfall event that is covered within a single

timestep. On the other hand, a numerical groundwater flow model simulation represents a grid-averaged value at an aggregated time. In such a scenario, it is entirely possible to have multiple (and different) values which all are correct, but do represent separate circumstances. The inconsistency, for such an instance, is materialized due to the uncertainty of model structure; which in this case is the model's spatial and temporal resolution. In larger-scale simulation, it is sometimes not feasible to inspect such a case-by-case event, as it could also happen to all other variables: soil/aquifer properties, surface water parameters, groundwater recharge estimates, and many more. Therefore, **data pre-processing** and screening play an important role in reducing misinterpretation and uncertainties.

Encountering a situation where typical data availability is **scarce and/or sparse** is also widely plausible. Fortunately, there are plenty of remote-sensing products that could be used as a source of estimates, especially those of surface water cycle components. Secondary data from literature reviews, investigation reports, and collaboration with government agencies are also very useful in collating valuable information. Considering the broad scope of the current science, insights from inter- and multi-disciplinary data might reveal unexpected yet beneficial perspectives. Especially in data-scarce areas, it is recommended to consider multiple sources of information and associated data in constructing and evaluating a numerical groundwater flow model.

1.3 Research framework

In previous sections, the general concept of groundwater flow controlling factors and the effort to quantify its system through groundwater modeling have been described. The distinctive nature of groundwater flow in different areas, with unique properties and boundary conditions, has also been explored, together with the extended risks of groundwater abstraction from multiple depths of aquifers. In addition to that, challenges that might arise due to data scarcity-related issues are briefly mentioned. Therefore, this section attempts to put together and implement the knowledge, as well as to formulate the objective and research questions of this study under a systematic thought process for a specific study area.

1.3.1 Objectives and research questions

The primary goal of this thesis, as suggested by the book title, is to deepen, in detail, the **quantitative understanding** of a **groundwater system** in data-scarce areas. The study focuses on the Bandung groundwater basin in Indonesia. In achieving the primary objective, four specific objectives are defined, accompanied by research questions that form the structure of this thesis, described below. The overall structure of the study is visually represented in Figure 1.4.

Estimating water balance components and their uncertainty bounds. Within this objective, the status of water storage change within the Bandung groundwater basin is determined. Each component of the water cycle is quantified, taking into account the uncertainty bounds attached to each estimate. Further, the assessment of the water storage status is calculated using the simple Equation 1.1. To fulfill the first research objective, several research questions arise as follows:

- To what extent do different datasets and products differ in estimating water balance components in the Bandung groundwater basin?
- How well does a hydrological simulation using the Wflow_sbm model perform in comparison with other estimation methods?
- Considering the uncertainty bounds in each of the surface water balance components, to what extent the definitive basin water storage change status can be determined?

Constructing a one-way coupled hydrological and groundwater flow model. In this objective, the previously established Wflow_sbm hydrological model and a MODFLOW groundwater flow model are one-way coupled. Using the data collated from field measurements, government agencies' collaboration, and literature reviews, a parsimonious groundwater flow model is constructed. Given the limited availability of hydraulic head calibration data, the model evaluation is complemented with the utilization of open-source gravimetric satellite data of GRACE. This approach takes into consideration spatial scaling and resolution differences. The research questions that emerge in the attempt to accomplish the second research objective are as follows:

- How can the recharge estimates from the Wflow_sbm hydrological model be incorporated into groundwater flow simulation?
- To what extent can a parsimonious, yet reliable, groundwater flow model in the study area be constructed, considering the limited hydrogeological data availability?
- What factors need to be considered in utilizing and, more importantly, contextualizing open-source remote-sensing-based global estimates of terrestrial water storage change (GRACE) in basin-scale model evaluation?

Quantifying aquifer interaction induced by multi-layer groundwater abstraction. Following the established one-way coupled model, the impact of multi-layer groundwater abstraction on internal groundwater flow among aquifers, termed 'aquifer interaction', is delved deeper. A number of environmental water tracers (EWT) data that were previously measured are utilized to investigate the groundwater flow patterns within and among the subsurface layers. The assimilated EWT data include major ion elements, groundwater age estimates, and stable isotopes. The research questions developed within the process of answering this particular specific objective are as follows:

- To what extent can the result of a parsimonious groundwater flow model, built on limited hydrogeological data availability, be explored?

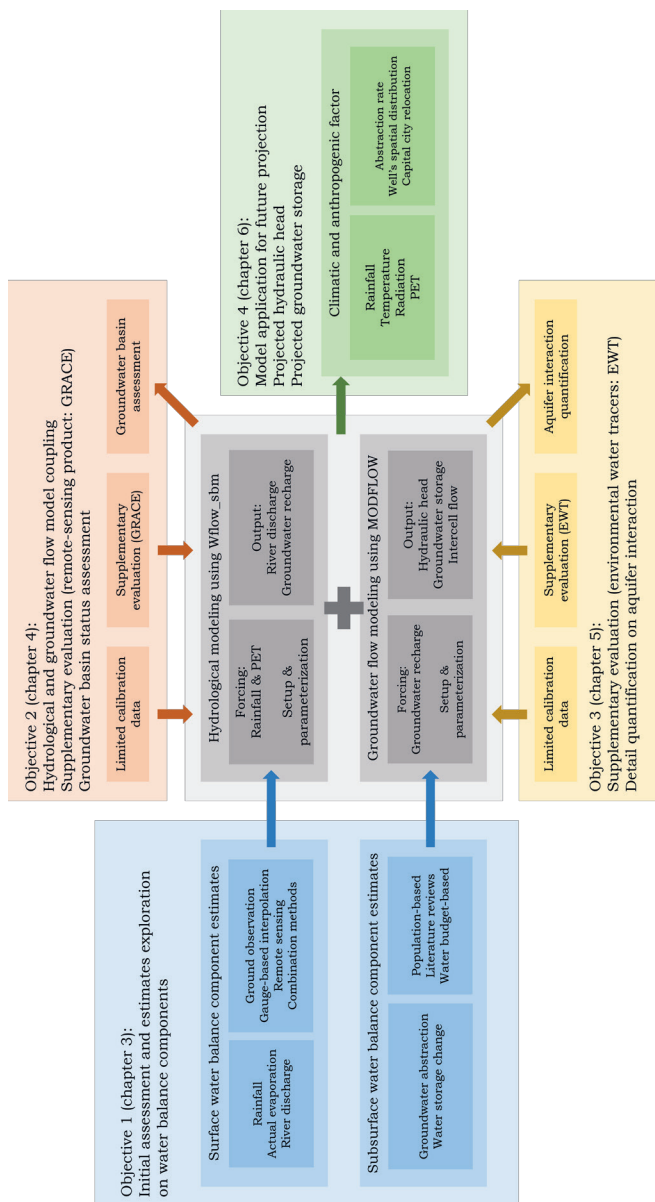


Figure 1.4: Research structure in this thesis. Each colored box represents one milestone of a research objective and/or working stage.

- To what extent can EWT data analysis be incorporated in evaluating a groundwater flow model?
- What is the impact of simultaneously abstracting groundwater from multiple depths and aquifers on groundwater head, storage, and aquifers' internal processes?

Projecting future groundwater status. With increasing confidence in the one-way coupled model's reliability through multiple model evaluation, the model is used to project future groundwater availability under multiple climatic and anthropogenic scenarios. The climatic factors are explored through changes in rainfall and potential evapotranspiration. Meanwhile, the anthropogenic factors are developed through changes in groundwater abstraction rate and spatial distribution. For the fourth specific objective, the emerged research questions are as follows:

- How do the projected changes in climate variables in the Bandung groundwater basin influence groundwater recharge?
- What are the possibilities of groundwater abstraction changes in the Bandung groundwater basin, considering the capital city relocation plan of Indonesia?
- To what extent do the changes in climatic forcing and anthropogenic activities, both each and combined, influence the future groundwater availability in the study area?

1.3.2 Thesis outline

In the current section of the Introduction, general information about groundwater, basic principles of groundwater flow modeling, and its typical challenges are laid out. It is supplemented by rudimentary materials related to aquifer properties, groundwater flow driving factors, groundwater abstraction, and hydrological simulation role as well as data collection strategy in constructing a groundwater flow model. The research's overall and specific objectives are also displayed in Figure 1.4, along with the flow of the research framework, written from chapter to chapter.

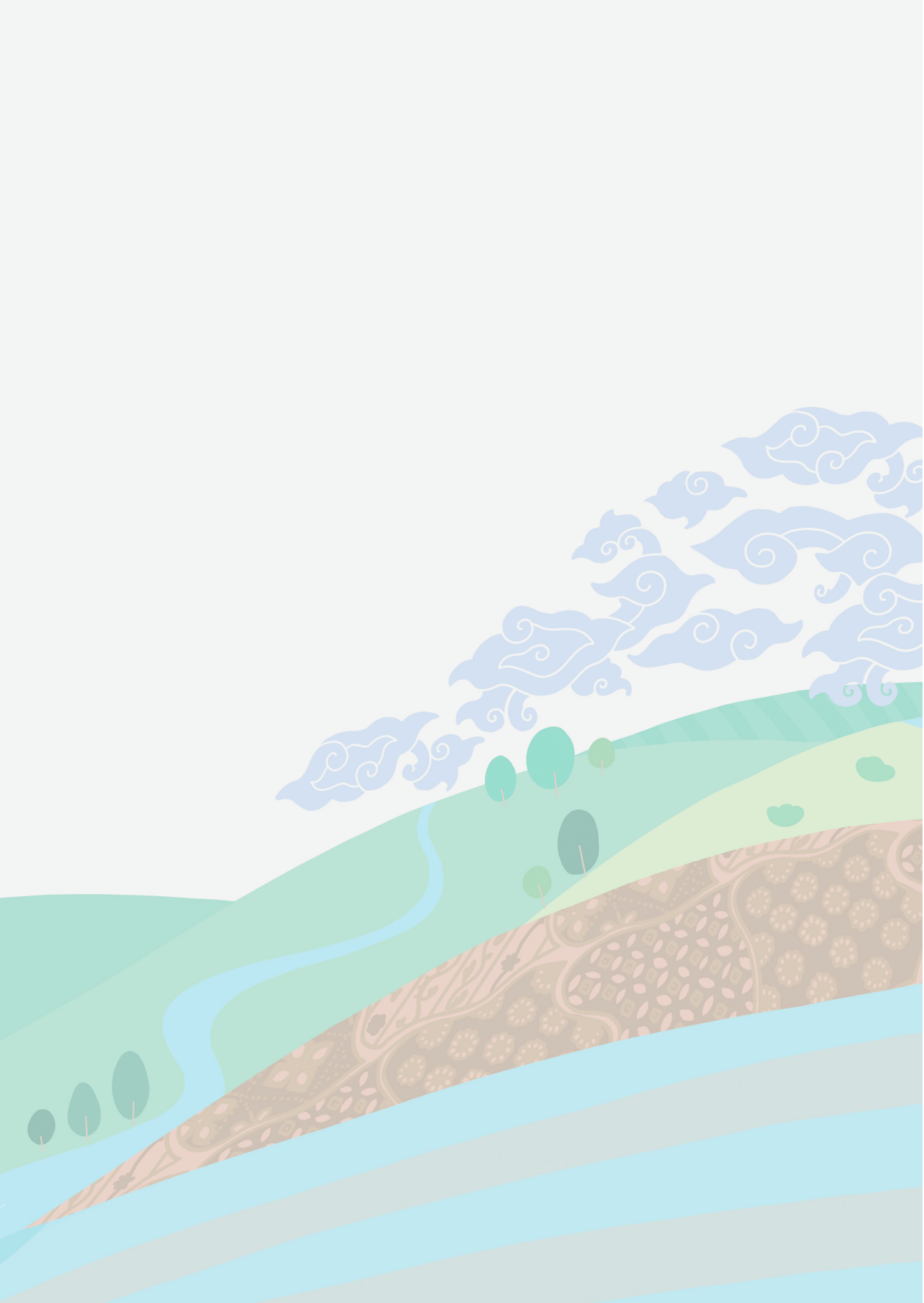
For all the academic journal articles resulting from this thesis, there is one common study area, which could be referred to either as the Upper Citarum River basin or the Bandung groundwater basin. To avoid repetitive information on the basic features of the study area, Chapter 2 elaborates on most of the essential details of the Bandung groundwater basin, such as location overview, hydrological and hydrogeological settings, anthropogenic footprint, and data availability as well as field campaign conducted in 2020.

In Chapter 3, a quantitative review of the water balance in the study area is presented. It is accomplished by collating multiple water balance components' estimates and their uncertainty bounds. Ground-based measurements, interpolated gauge-based datasets, remote-sensing products, and hydrological model-based estimates are all considered. The water storage change status is also determined considering the wide range of available estimates, therefore achieving the first specific objective.

A one-way coupled hydrological and groundwater flow model is constructed, evaluated, and established in the following two subsequent chapters, while also answering the second and third specific objectives. Groundwater flow model evaluation using limited calibration data is accompanied by the model assessment on groundwater storage changes using GRACE data in Chapter 4. Chapter 5 provides a qualitative perspective on groundwater flow model evaluation using environmental tracer data analysis, while also quantifying aquifer interaction induced by multi-layer groundwater abstraction.

In Chapter 6, the fourth specific objective is accomplished by using the established one-way coupled model to project future groundwater availability. It is initiated by hydrological simulation under projected climatic forcings that result in projected groundwater recharge. Further, the projected groundwater recharge drives the groundwater flow simulation, which is set up under multiple and diverging abstraction scenarios, resulting in projected hydraulic head and groundwater storage.

Last but not least, the synthesis of the research is presented in Chapter 7. The final chapter also addresses the primary objective of the research as well as discusses the limitations, uncertainties, challenges, and future opportunities.



Chapter 2

The Bandung Groundwater Basin



This chapter introduces the area to which all the studies within this thesis are applied. Having said that, there are two non-identical names used to refer to the site: the Upper Citarum River Basin (UCRB) and the Bandung groundwater basin (BGB). Pragmatically, they cover very comparable, although not equal, areas of interest. However, they are conceptually defined by two distinct parameters. The UCRB is delineated on the basis of the surface topography, while the BGB is of the subsurface lithology. In this chapter, the study area features and characteristics, from its natural attributes of climatic, hydrological, and hydrogeological setting, to its anthropogenic influence of groundwater abstraction, as well as our fieldwork campaign, are thoroughly described.

2.1 Physical characteristics

The study area is located in the West Java Province, Indonesia. Estimated from the Multi-Error-Removed-Improved-Terrain Digital Elevation Model (MERIT-DEM) (Yamazaki et al., 2017), the UCRB, whose boundaries are portrayed by the red dashed lines in Figure 2.1, covers an area of 1,823 km². Geographically, it is located between 6°43'S 107°22'E and 7°15'S 107°57'E, with its outlet at 6°56'S 107°30'E. Administratively, it covers two cities, Bandung and Cimahi, and three other smaller regencies of Bandung, West Bandung, and Sumedang. According to the West Java Central Bureau of Statistics, the UCRB was populated by no less than 9.6 million people in 2017. Situated in varying elevated terrains, the UCRB is surrounded by mountainous areas around its periphery with the highest elevation of 2,586 m above sea level (ASL). Its outlet elevation is at 640 m ASL. Figure 2.1 also shows the topographical distribution of the UCRB, with a vast and relatively flat landscape distributed primarily in the middle part of the basin, where urban and industrial areas have mostly developed.

While the UCRB is the domain of analysis in Chapter 3, the rest of the analysis from Chapter 4 to Chapter 6 focuses on the BGB area (see Figure 2.1). BGB's boundary is delineated on the basis of subsurface lithology, and legally regulated under the Indonesian law of the Office of Mineral and Energy Resources Ministerial Regulation number 2, 2017 (Indonesia, 2017). According to the information mentioned in the regulation, it is determined by considering the hydrogeological, geological, and groundwater hydraulics properties data. As we cannot find any access to the cited data, we refine the border of the regulated basin delineation by evaluating its consonance with the surface topography profile from MERIT-DEM data (Yamazaki et al., 2017). Figure 2.1 portrays the final domain of our study. Although separated from the surface catchment boundary, BGB's coverage area of 1,700 km² is relatively similar to that of the UCRB. The most visible difference between the UCRB and the BGB, conceivably, is the northern part of the area. In that area, lies a geological fault named Lembang, known as "Sesar Lembang" in the Indonesian language. The Lembang Fault acts as a barrier for the groundwater flow from the northern more elevated area of the UCRB to the areas covered by BGB (Delinom,

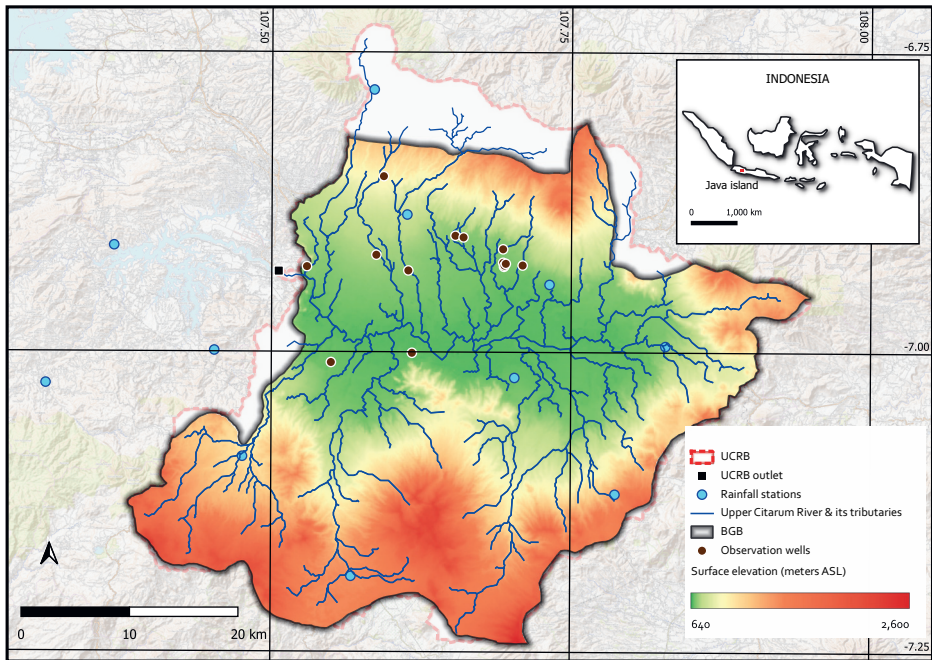


Figure 2.1: Overview of the Bandung Groundwater Basin (BGB). The upper right locator map shows the location of the study area relative to Indonesia. The main panel shows the geographical location, river system, and topographical distribution of the BGB based on the Multi-Error-Removed-Improved-Terrain Digital Elevation Model (Yamazaki et al., 2017). The Upper Citarum River Basin (UCRB) delineation is shown by the dashed red line in the background. Important data points of rainfall stations and observation wells are also pointed.

2009), physically separating the UCRB and BGB boundaries, and therefore represented as the Neumann no-flow boundary condition in the numerical model of this thesis. Other slight differences in the UCRB and the BGB spatial coverages occur due to the slope variability between the surface elevation and the subsurface geological layer.

2.2 Hydrological situation

There are eleven rainfall stations spatially distributed within and around the UCRB (blue circles in Figure 2.1). Based on these rainfall stations' data between 2005 and 2015, provided by the Indonesian National Meteorology, Climatology, and Geophysical Agency (BMKG), the Thiessen polygon-interpolated average annual rainfall in the UCRB is 1,971 mm. These measurements, however, involve huge uncertainties and errors as there exist notable periods when potentially missing data were not properly gauged. There is also relatively significant spatial variability of rainfall measured by these rainfall stations.

The potential of incorporating rainfall estimates from remote sensing and/or reanalysis products in UCRB is comprehensively discussed in Chapter 3. The rainfall seasonal pattern is divided into dry and rainy seasons, occurring annually from April to September and October to March, respectively. As the UCRB is located in a tropical region, rainfall is dominantly the only source of precipitation throughout the year.

The UCRB is the upstream part of a bigger watershed system, the Citarum River basin, whose main river flows to the Java Sea. Three cascading dams are constructed along the main river: Saguling, Cirata, and Jatiluhur dams. Saguling reservoir, the most upstream among the three, is located just downstream of the Nanjung discharge measurement station. Pinpointed as the UCRB outlet in Figure 2.1, Nanjung station monitors the river discharge flowing through the Upper Citarum River. The streamflow data are made available by the Indonesia Research Center for Water Resources (PUSAIR). Between 2005 and 2018, the minimum and maximum recorded daily discharge in Nanjung station were 4.08 m³/s and 469.29 m³/s respectively, with an average of 73.86 m³/s. Peak flows are frequently found, with events of daily discharge surpassing 450 m³/s (approximately the 95th percentile) occurring 6 times during the mentioned period.

The climate in the UCRB is a tropical monsoon climate, with relatively constant temperatures. According to the BMKG climatology data between 2005 and 2014, the mean annual temperature in the URCB is measured at 23.4°C, with a very narrow range of average monthly temperatures between 22.5°C and 24.8°C. The temperature is even more varied spatially than temporally, with an average of 15.3°C around the mountainous area. Similar to other typical tropical climate regions, the UCRB has high potential evapotranspiration, estimated at 1,560 mm annually (Siswanto and Francés, 2019).

2.3 Hydrogeological setting

The hydrogeological data of the BGB is available through previous studies (Hutasoit, 2009; Taufiq et al., 2017), especially one from Rahiem (2020). The latter collated field data from 189 geological boreholes, although they are non-uniformly distributed across the BGB. The data are, to a large extent, concentrated only at the flat and lower elevated terrain towards the UCRB outlet. Figure 2.2 shows the location of the boreholes that are located within the BGB boundaries. Despite more than half of the data being incomplete and some are even located outside the BGB domain, the project provides substantially useful insights into the BGB's lithological and geological profile.

Further, Figure 2.3 shows the graphical representation of the hydrogeological setting in the BGB's north-south cross-section, adapted from Hutasoit (2009) and Rusli et al. (2021). The subsurface is comprised of a three-layer geological structure: a thick sandy, breccia, and tuff-mixed aquifer, interspersed with layers of clayey aquitard, sitting on a volcanic rock basement formation. The primary aquifer's lithological structure, the Cibereum

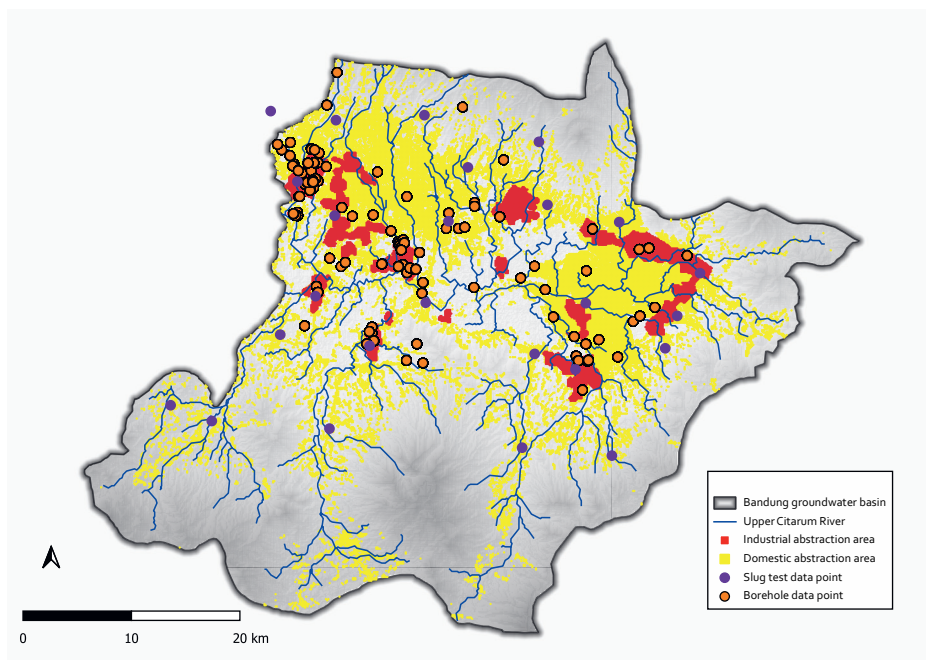


Figure 2.2: Map view for borehole and slug test data point, as well as the estimates of domestic and industrial groundwater abstraction area. The borehole data is collated from Rahiem (2020), the slug test data from our field campaign, and the groundwater abstraction area is described in Section 2.4.

formation, is formed by partially consolidated volcanic deposits from the late Pleistocene – Holocene age (Hutasoit, 2009). In many locations, it is interspersed by layers of clay from the Kosambi formation, which is dominated by the lake deposits of consolidated clay from the Holocene age. These interspersions separate the aquifer into two layers: the shallow unconfined upper aquifer and the deep confined lower aquifer. The Cikapundung formation, with a high degree of compacted volcanic deposits, forms the basement of the basin below the lower aquifer of the Cibereum formation. On average, the thickness of the upper aquifer and the scattered interspersing aquitard layers are 75 meters and 30 meters, respectively. The rock basement elevation is assumed constant at the elevation of 300 meters above sea level, according to the lowest borehole point data.

This is, naturally, a simplification of the actual more complex hydrogeological setting. However, we believe that our approach to interpreting the available groundwater basin’s actual geophysical condition into a simplified aquifer system diagram is the appropriate strategy considering the (lack of) data availability. Further complexification would be an effort that cannot be justified by data or observations, as the lithological data in the mountainous and highly elevated areas are plainly not available.

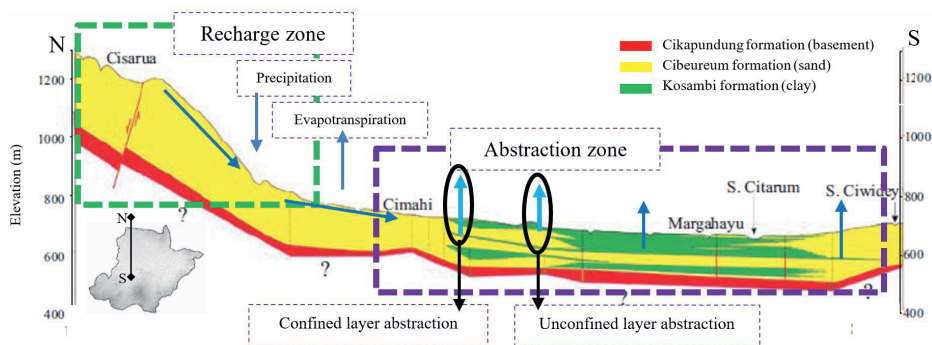


Figure 2.3: Graphical interpretation of the BGB hydrogeological setting through the north-south cross-section, modified from Hutasoit (2009). The north part (left in the picture) of the basin acts, presumably, as recharge zones (green box), while groundwater is mainly abstracted in the middle part of the basin (purple box) from both unconfined aquifers by the domestic sector and confined aquifers by the industrial sector (annotated by blue arrows). The red, yellow, and green layers represent a layer-cake type of rock formation in the UCRB/BGB.

2.4 Anthropogenic footprint

With the rising pressure of the expanding population, groundwater resources in the BGB have been necessarily abstracted to fulfill the increasing water demands. As the most upstream part of the Citarum watershed system, the groundwater resources' demand for irrigation in the UCRB is, fortunately, negligible. Still, groundwater over-exploitation has been long known as a threatening problem in the BGB (Gumilar et al., 2015; Tirtomihardjo, 2016), with the domestic sector pumping from shallow aquifers and the industrial sector from deep aquifers. Previous studies have quantified the consequences of the current groundwater abstraction rate, for example, land subsidence rate between 8 cm/year (Abidin et al., 2012) and 18.7 cm/year (Ryagus et al., 2023) on average, and even up to 2 meters in several industrial zones (Gumilar et al., 2015).

There is no monitoring initiative, unfortunately, for the domestic groundwater abstraction in the BGB. According to the local regulations, it is entirely legal to pump shallow groundwater for household needs. In this study, the domestic groundwater abstraction volume is therefore estimated from the population number (data from the West Java Central Bureau of Statistics), the population growth estimate (Tarigan et al., 2016), the average daily water consumption per person, and the water supply coverage from Municipal Drinking Water Company (PDAM) (Moersidik et al., 2015) (see Table 2.1). Under such circumstances, between 2005 and 2018, the average domestic groundwater abstraction volume is calculated at 122 million m^3 per year, equivalent to 0.18 mm/day.

Table 2.1: Estimated domestic-only groundwater abstraction volume in the UCRB

Year	Basin population	Average water consumption	Total domestic water demand	Government water supply	Domestic groundwater abstraction
	people	liter/person/day	Mm ³ /year	Mm ³ /year	Mm ³ /year
2005	6,269,003		274.58	178.48	96.10
2006	6,496,376		284.54	184.95	99.59
2007	6,731,996		294.86	191.66	103.20
2008	6,976,162		305.56	198.61	106.94
2009	7,229,183		316.64	205.81	110.82
2010	7,491,382		328.12	213.28	114.84
2011	7,763,090		340.02	221.02	119.01
2012	8,044,653	120	352.36	229.03	123.32
2013	8,336,428		365.14	237.34	127.80
2014	8,638,785		378.38	245.95	132.43
2015	8,952,109		392.10	254.87	137.24
2016	9,276,797		406.32	264.11	142.21
2017	9,613,261		421.06	273.69	147.37
2018	9,949,726		435.80	283.27	152.53
Average volumes of the annual domestic groundwater abstraction					122.39

Regarding the industrial sector groundwater abstraction, the existing regulation theoretically imposes strict rules on deep aquifer groundwater abstraction. Unfortunately, there has been a lack of focus on enforcing water-related regulations in Indonesia (Braadbaart and Braadbaart, 1997; Listiyani and Said, 2018). Regarding groundwater institutional management, the Office of Mineral and Energy Resources (ESDM) of the West Java Province is the responsible organization for deriving, implementing, and evaluating groundwater abstraction-related policies. Currently, the groundwater abstraction volumes from the industrial sector's registered deep wells have been known to be partly monitored by ESDM since 2017.

In 2017, there were 377 deep wells operated by the industries, with a total annual groundwater abstraction volume of 6.8 million m³ reported to ESDM within the BGB. However, such numbers are believed to be significantly higher in reality. In his study, Tirtomihardjo (2016) reported the annual industrial sector's groundwater abstraction estimate of 47.6 million m³ in 2008. Further, Taufiq et al. (2017) estimated the actual industries' groundwater abstraction between 2010 and 2015 to be 14 times higher than the reported volumes (see Figure 2.4 [bottom]). Having said that, Figure 2.4 [bottom] shows a positive trend of industrial groundwater abstraction decrease since 2005. The trend is agreed by gravimetric satellite data of GRACE in the study area (Figure 2.4 [top]); a remote-sensing-based product estimating the terrestrial water storage change (TWSC). The indicated trend of positive water storage changes is a logical agreement when compared with the decreasing industrial groundwater abstraction rate. Yet, it is in contrast with the result of some studies (Gumilar et al., 2015; Tirtomihardjo, 2016) that presented dwindling groundwater tables. At length, from field observation to direct interviews with site officers, the average annual industry-driven groundwater pumping values in this study are estimated at 255 million m³, equivalent to 0.38 mm/day.

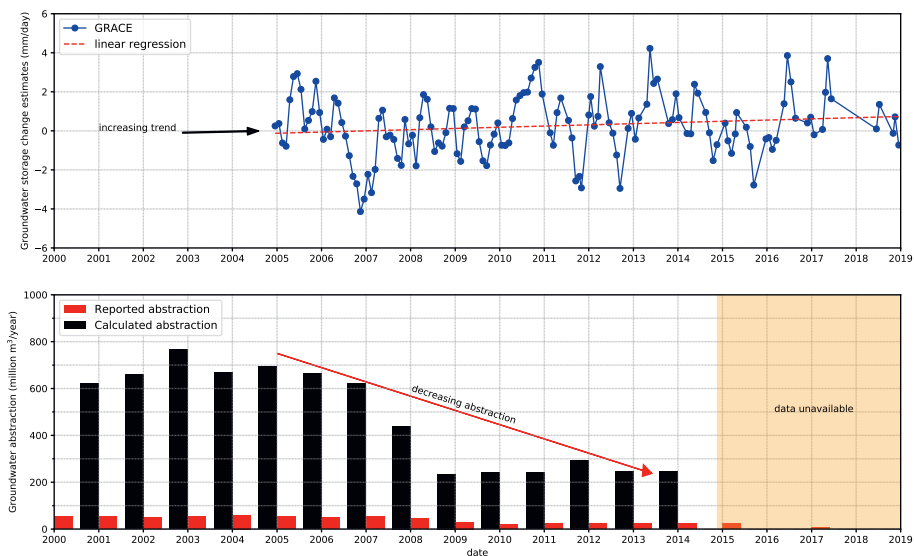


Figure 2.4: Correlation between GRACE estimates on the terrestrial water storage change (top) and annual reported and estimated actual groundwater pumping volumes by the industrial sector in the BGB (adapted from Taufiq et al., 2017) (bottom). GRACE estimates show an increasing trend of terrestrial storage change, agreed by a decreasing trend of groundwater abstraction during the same period. There was an organizational management shuffle of groundwater monitoring policies in the UCRB after 2015 and data were missing for some years. The data were made available again in 2017, only to show significantly further drops in the reported - not the actual - groundwater abstraction volumes.

Besides the estimation of the groundwater abstraction volume, its spatial distribution is also important to be approximated. The Indonesia geospatial database is utilized to determine the location of the domestic groundwater abstraction. Parts of the BGB with land use of residential, building, and high-rise buildings are merged into the domestic abstraction area (see Figure 2.2). For the industrial abstraction, available location information from previous research that focused on the industrial activities in the UCRB is used (Ginkel, 2016), validated by the data from the groundwater abstraction report from the industries to ESDM in 2017 (again, see Figure 2.2).

In summary, the UCRB/BGB is a highly groundwater-dependent region as the majority of its water demand is fulfilled by abstracting water from the sub-surface. From the above description of domestic and industrial demand, approximately 370 million m³ of groundwater, equivalent to 0.57 mm/day, is believed to be abstracted annually. With such a massive abstraction volume, it is hypothesized that groundwater abstraction has a significant influence on other components of the basin water cycle and possibly impacts its total water storage negatively.

2.5 Groundwater-related data availability

2.5.1 Field campaign and laboratory measurement

To discern the soil properties in the study area, twenty-five locations within and around the BGB domain were selected for in-situ measurements during a field campaign in 2020 (Figure 2.2). Horizontal hydraulic conductivities from the shallow soil layers between 5 and 10 meters below the ground surface were measured using slug test. At each testing point, soil samples were taken for laboratory measurements of vertical hydraulic conductivities (flow-through test and grain-size analysis). The spatial distribution of the field campaign data points is designed to be more outspread compared to other data to get a better sense of the soil spatial variability.

The in-situ measurements (slug test) result in varying horizontal hydraulic conductivity values (K_h), ranging between 0.15 and 0.35 m/day depending on the location. Meanwhile, the laboratory measurements (flow-through test) appraise the vertical hydraulic conductivity values (K_v) between 3×10^{-4} and 6×10^{-4} m/day. These numbers indicate moderate to low heterogeneity of the upper soil of the BGB, shown by the lowest and the highest K_h and K_v values, which are measured at the same degree of magnitude. In general, the northeast area of the BGB is observed to be the less permeable area, while slightly more porous soil is found more frequently in the southwest part of the study area.

2.5.2 Observation wells data

There are only twenty-six observation wells being consistently monitored within the BGB domain, although not regularly enough (low-frequency monitoring). Most of these observation wells suffer from several issues: short data periods, observation frequency, and/or data reliability. Twelve observation wells are situated very close to surrounding abstraction wells. This causes the observed groundwater level to be largely influenced by local drawdowns, especially those measuring the piezometric head from the deep aquifers considering the higher industrial abstraction intensity compared to the domestic ones. Most of the observation wells' locations are also concentrated in the lower elevated part of the BGB. Despite these concerns, the observation wells data are used to assess the groundwater flow model simulation results considering the lack of options.

Figure 2.1 shows the location of the observation wells in which data were used. Primarily, we use the measurement data in 2004 from the observation wells with depths of less than the interpolated upper aquifer thickness. The groundwater table depth data from these observation wells ranged between 8 and 25 meters from the surface. We also use the data of the observation wells that measure the piezometric head of the deep aquifers, whose values are, generally, lower than the phreatic groundwater level. Hypothetically, this is caused by more spatially intense and higher volumes of groundwater abstraction from the confined aquifer.

2.5.3 Environmental water tracers data

With limited groundwater table data for model calibration, auxiliary groundwater-related documentation is highly welcomed. In this study, once-at-a-time (OAT) measurement of environmental water tracers (EWT) data in the BGB is available. They were collected in more than 20 different projects pre-2008, before being collated into one integrated open-source groundwater database, funded by the Directorate General of Higher Education and Ministry of Research of Indonesia in 2016. The data include major ion elements (Na^+/K^+ , Ca^{2+} , Mg^{2+} , Cl^- , HCO_3^- , and SO_4^{2-}), groundwater age estimates derived from radiocarbon (^{14}C) content, and stable isotopes of deuterium ($\delta^2\text{H}$ or δD) and oxygen-18 ($\delta^{18}\text{O}$). All the EWT data analyzed in this study are freely available and developed in an open repository QGIS-cloud platform (Irawan et al., 2016). These datasets, unfortunately, are not measured continuously, thus time-series analysis is not feasible. Having said that, in this study, they are all combined with the additional EWT data that was later measured for prior studies (Taufiq et al., 2017) to assist in making qualitative interpretations and evaluating the numerical model simulation.

The samples for OAT major ion elements measurement are spread in 65 locations; 30 points for the deep aquifer, 19 for the shallow aquifer, 3 for water springs, and 13 for the surface water (river). There are also 72 points of OAT stable isotope measurements of deuterium ($\delta^2\text{H}$ or δD) and oxygen-18 ($\delta^{18}\text{O}$); 36 samples are from the deep aquifer, 19 from the shallow aquifer, 14 from the river water, and 3 from the rainfall. Most of these points are located near the major ion elements measurement location. The radiocarbon (^{14}C) contents were also OAT measured in 22 locations to estimate the groundwater age, including their uncertainties, all from the deep aquifer. The handling, usage, and contribution of these EWT data to our study are fully described in Chapter 5.

2.5.4 Secondary data from ESDM

Data availability of this study is also supported by the Office of Mineral and Energy Resources (ESDM) of West Java Province. They provide secondary data, where field measurements and reports were conducted previously. Twenty-three pumping test reports are made available to us. Later in this study, these data are used to estimate the specific storage parameter and the hydraulic conductivity of the deep aquifer.



Chapter 3

Water balance components and their uncertainty bounds



This chapter is mostly based on and adapted from:

S. Rusli, A. Weerts, A. Taufiq, and V. Bense (2021). “Estimating water balance components and their uncertainty bounds in highly groundwater-dependent and data-scarce area: An example for the Upper Citarum basin”.

Journal of Hydrology: Regional Studies 37, 100911.
doi: <https://doi.org/10.1016/j.ejrh.2021.100911>

Abstract

Study Region: Upper region of the Citarum basin in Indonesia.

Study focus: Assessing water balance components in data-scarce regions using different approaches could result in different outcomes. In the upper reaches of the Citarum River in West Java, Indonesia, for example, many previous studies found the groundwater storage to be depleting, while GRACE identifies a contrasting trend of increasing terrestrial water storage change (TWSC). Therefore, in this study, we aim to improve the accuracy of water balance component estimates in the Upper Citarum River Basin (UCRB). Firstly, we estimate groundwater abstraction volumes based on population size and a review of literature. Estimates of the other water balance components, namely the rainfall, actual evaporation, discharge, and groundwater storage change are derived from various global datasets and available measurements. We also use a distributed hydrological model, Wflow_sbm, to yield additional estimates of discharge and actual evaporation. We compare each basin water balance estimate and quantify the uncertainty of some components using the Extended Triple Collocation (ETC) method.

New hydrological insights for the region: ETC application on four different rainfall estimates suggests a preference of using CHIRPS product in the study area as it delivers r^2 of 0.56 and RMSE of 6.52 mm/day, compared to estimates from rainfall station ($r^2 = 0.39$, RMSE = 8.57 mm/day), SACA&D ($r^2 = 0.29$, RMSE = 10.46 mm/day), and TRMM ($r^2 = 0.56$, RMSE = 8.61 mm/day). With CHIRPS rainfall forcing, Wflow_sbm model estimates of average daily actual evaporation and discharge are obtained. The results for actual evaporation (2.67 mm/day) are plausible with a narrow difference of less than 0.50 mm/day among other estimates. The simulated discharge results in a daily average of 5.38 mm/day, estimated between observation data (3.65 mm/day) and GloFAS-ERA5 product (6.12 mm/day). Combining precipitation, actual evaporation, and discharge with a groundwater abstraction estimate of 0.57 mm/day, the Wflow_sbm-based groundwater storage change is estimated at a daily storage depletion of 0.82 mm/day. Using GLEAM actual evaporation estimates (3.13 mm/day) and observed daily discharge, on the other hand, results in surplus water of 0.45 mm/day for groundwater storage change. These results demonstrate the high uncertainty in capturing subsurface hydrological processes, although the groundwater storage change estimates are found close to the TWSC estimates based upon GRACE gravimetric satellite data of 0.25 mm/day, with a variance of 1.57 mm/day. To aid in estimating current and future basin-scale groundwater level changes to support operational water management and policy in the Citarum basin, considering the massive groundwater abstraction, a focus on subsurface hydrological components quantification is of great importance for future research.

3.1 Introduction

Groundwater has been used for water supply purposes since prehistorical ages (Angelakis et al., 2016; Voudouris et al., 2018). Since then, its exertion has developed from fulfilling life's basic needs to meeting various demands from domestic, industrial, and agricultural sectors. However, groundwater resources are increasingly over-exploited globally (de Graaf et al., 2016) from Central Asia (Chatterjee et al., 2018; Hu et al., 2019), the Middle East (Al-Zyoud et al., 2015), South Europe (Closas et al., 2017), Africa (Khezzani and Bouchemal, 2018; Mokadem et al., 2018), to Central America (Ochoa-González et al., 2018). Groundwater over-abstraction leads to dwindling groundwater tables and often to deteriorating water quality. In many ways, it also poses threats to the security of water resources on a scale of the water cycle as a whole when the regulatory role of groundwater flow to other hydrological fluxes is considered (Chambel, 2015).

Groundwater table fluctuation generally influences other water balance internal processes. For example, changes in groundwater recharge-discharge pattern affect surface water system (Earman and Dettinger, 2011), groundwater flow pattern (Pétre et al., 2019a), runoff generation process (Abe et al., 2020), and rate of evapotranspiration (Lurtz et al., 2020). More consequences unavoidably occur once more factors are involved, such as groundwater quality, anthropogenic influence (Zhu et al., 2019a; Lin et al., 2020), climate change (Zhu et al., 2020b), and land cover and land use (LULC) development (Lamichhane and Shakya, 2019; Shawul et al., 2019).

Additionally, interactions among hydrological cycle, groundwater resources, and human interference are also mutually influential as changes in water balance internal processes have a chain-reaction effect in increasing groundwater abstraction from both unconfined and confined aquifers (Ali et al., 2012). Change in precipitation pattern has been found to have a strong relationship with groundwater abstraction volume, too (Asoka et al., 2017). It is clearly shown that groundwater is very closely connected with basin water cycle processes, although it flows on a spatially and temporally different scale.

Unfortunately, in determining water balance components with good accuracy, the required hydrological and hydrogeological information is often unavailable, particularly in developing countries. The usage of global open-source datasets, as well as remote sensing techniques (Rodell et al., 2009; Vorobevskii et al., 2020), provides the opportunity to cope with the challenge of data scarcity. However, water balance estimates determined using freely available, often open-source, tools should be accompanied by the awareness of each method's uncertainties, assumptions, and embedded errors.

The Upper Citarum River Basin (UCRB), located in West Java, Indonesia is an example of a region that is data-scarce as well as highly groundwater dependent. At least 50 million cubic meters of groundwater was estimated to be abstracted in 1990, and it grows to 300 million cubic meters in 2006 (Tirtomihardjo, 2016). Added to this fact, other studies also

indicate groundwater storage depletion in the basin (Gumilar et al., 2015). Such a massive volume and impact of groundwater abstraction, unfortunately, is not well-managed and monitored. Groundwater abstraction data are hardly available, accessible, and reliable for public information.

Based on the rainfall stations' measurement, the average daily rainfall in the UCRB between 2005 and 2015 is of 5.40 mm/day (1971.77 mm/year), with a variance of 7.03 mm/day (617.91 mm/year). Meanwhile, according to ERA5 reanalysis products (Hersbach et al., 2020), the average daily actual evaporation is estimated at 2.82 mm/day (1028.88 mm/year) with a variance of 0.55 mm/day (36.03 mm/year). The remaining water from the precipitation and the actual evaporation estimates suggests a lower average potential daily inflow of 2.58 mm/day compared to the observed average daily outflow of 3.65 mm/day, barring more water is still lost due to groundwater abstraction. However, this seems to be in contrast with the Gravity Recovery and Climatic Experiment (GRACE) estimate that shows increasing terrestrial water storage change (TWSC) in the last 15 years. The absence of reliable hydrology and hydrogeology data makes it difficult to accurately capture the hydrological behavior of the UCRB and verify the true status of the groundwater storage change. It further stipulates the importance of more comprehensive and accurate estimates of the water balance components in the UCRB.

Therefore, the primary focus of this research is to provide improved estimates of the water balance components in a groundwater-dependent and data-scarce region of the UCRB, in particular the rainfall, actual evaporation, discharge, groundwater abstraction, and groundwater storage change. Each component is estimated based not only on ground measurement but also on various approaches and sources: open-source global datasets, remote-sensing-based estimates, and hydrological simulation using Wflow_sbm model (Schellekens et al., 2020). Uncertainty bounds of each water balance component are also quantified, more importantly, to appraise the accuracy of each estimate using the Extended Triple Collocation (ETC) method (McColl et al., 2014).

3.2 Methods

3.2.1 Data sources and availability

The UCRB is a data-scarce region with limited information and access to local observations and measurements. Therefore, we explore various sources of literature, site survey, and global datasets. A major portion of secondary data is provided by government organizations previously mentioned: ESDM, BMKG, and PUSAIR. Several numbers of available global datasets are taken into account to provide additional information on unmeasured water budget variables and to validate the uncertainty of each estimate. In summary, Table 3.1 lists the major data sources used in this study.

Table 3.1: Major data sources list

Data	Source
Precipitation	BMKG rainfall station (2000 - 2015)
	Interpolated gauge-based SACA&D (1981 - 2018)
	Satellite products of CHIRPS (1981 - 2018)
Potential evapotranspiration	Tropical Rainfall Measuring Mission (TRMM) (1998 - 2018)
Actual evaporation	ECMWF Re-Analysis product of ERA5
	Global Land Evaporation Amsterdam Model (GLEAM)
	ECMWF Re-Analysis product of ERA5
Discharge	Hydrological model-based estimate (Wflow_sbm)
	Automatic Water Level Recorder measurement by PUSAIR
	Hydrological model-based estimate (Wflow_sbm)
Groundwater abstraction	Global Flood Awareness System (GloFAS)-ERA5
	Official reports and previous research results
Groundwater storage estimate	Population data-based estimate
Topography data	Gravity Recovery and Climate Experiment (GRACE)
	MERIT-DEM

There are four sources of rainfall estimates considered in this study. The first two rainfall datasets, BMKG and SACA&D, are sourced and derived from rainfall-station-based measurements. BMKG rainfall station data are available from eleven stations shown in Figure 2.1. SACA&D (Besselaar et al., 2017) are interpolated gauge-based precipitation products applied in the South East Asia region by using an optimum interpolation method (Hofstra et al., 2008) implemented in European Climate Assessment and Dataset (ECA&D) project (Haylock et al., 2008). The other two data sources are satellite-based data, TRMM3B43 (further referred to as 'TRMM') and CHIRPS (Funk et al., 2015); both are gauge-based corrected estimates. TRMM products have been widely used in Indonesia (Prasetia et al., 2012; As-syakur et al., 2013) as well as CHIRPS (Setiawan et al., 2017; Narulita and Ningrum, 2018). Additionally, both datasets were also found superior to drive the hydrological model of SWAT to produce satisfying simulation results even when compared with rain gauge data (Luo et al., 2019).

There are three sources of daily actual evaporation estimates: GLEAMv3.3a (further referred to as 'GLEAM') (Miralles et al., 2011; Martens et al., 2017), ERA5 (Hersbach et al., 2020), and Wflow_sbm model simulation results. Particularly for Indonesia, GLEAM estimates have been tested and deliver good performance in the western part of Java Island (Wati et al., 2018), with a spatial resolution of $0.25^0 \times 0.25^0$. ERA5 data, meanwhile, is available in a finer spatial resolution of $0.1^0 \times 0.1^0$. Wflow_sbm model calculates daily actual evaporation using the potential evaporation estimated based on downscaled ERA5 temperature and global radiation, a method suggested by Bruin et al., 2016.

Observed daily discharge data are provided by PUSAIR. Additionally, two more discharge estimates from Wflow_sbm model simulation and the Global Flood Awareness System (GloFAS)-ERA5 are used. Wflow_sbm model and its parameterization are based upon the method of (pedo)transfer function (Imhoff et al., 2020) described in Section 3.2.3. GloFAS-ERA5 is a global river discharge reanalysis product, whose accuracy, unfortunately,

decreases as the catchment size becomes smaller (Harrigan et al., 2020), to the accuracy of average KGE of 0.21 for catchment size between 500 and 2,500 km², a range suitable to the UCRB. Therefore, GloFAS-ERA5 estimates are used more as a comparison tool rather than an applicable estimate in this study.

Groundwater abstraction is estimated from the population data (Table 2.1) and literature reviews of industrial pumping. Further, the discrepancy between the basin inflow (precipitation) and outflow (evaporation, river discharge, and groundwater abstraction) determines groundwater storage change. As an additional benchmark, the terrestrial water storage change (TWSC) is also estimated from the GRACE dataset of gridded monthly global water storage (NASA/JPL, 2019). Since GRACE is measured in $1^0 \times 1^0$ resolution, it is necessary to reconcile the spatial resolution difference between GRACE and catchment size (Landerer and Swenson, 2012). In fact, the GRACE estimates have been used mostly in large basins, and their application on local-scale groundwater basins has been limited due to their inherent uncertainties (Sun, 2013). However, considering the uniformly distributed hydrological characteristics of rainfall patterns, population density, and urban development in the area surrounding the UCRB, we currently assume that the footprint of these remainder areas captured by GRACE is a good representation of the study area itself. The detail of such scaling uncertainties is discussed in Chapter 4. Moreover, using GRACE data as a verification tool still has its merit as Humphrey et al. (2016) demonstrated GRACE meaningful hydrological signal in high frequency (monthly) temporal variability, which is what we use in this study. GRACE has also been used as a terrestrial water storage reference in Indonesia (Han et al., 2017).

3.2.2 Extended Triple Collocation (ETC method)

Uncertainty of each water balance component estimate is quantified using the extended triple collocation (ETC) technique (McColl et al., 2014), the improved uncertainty estimation method from the standard triple collocation (TC) (Stoffelen, 1998). Practically, both TC and ETC methods have been applied to many geophysical parameters, such as soil moisture data (Gruber et al., 2016; Chen et al., 2018a), sea surface temperature data (Saha et al., 2020), and ice concentration data (Scott, 2020). It is important to realize that ETC does not reduce uncertainty. Instead, it quantifies uncertainties to assist in selecting the least uncertain product among the numbers of estimates.

In principle, the ETC method evaluates uncertainty by deriving the correlation coefficient of each measurement system with respect to an unknown target variable (McColl et al., 2014) and is expressed through RMSE and r^2 parameter (Wu et al., 2019). It assumes the existence of a linear relationship between independent dataset X_i and hypothetical ‘true value’ T , with Equation 3.1:

$$X_i = \alpha_i + \beta_i T + \epsilon_i \quad (3.1)$$

where α_i and β_i are calibration parameters and ϵ_i is the corresponding random error. Further, covariances between different measurements, used to directly determine the designated objective function of RMSE and r^2 , are calculated using Equation 3.2:

$$Q_{i,j} = cov(X_i, X_j) = E(X_i X_j) - E(X_i)E(X_j) \quad (3.2)$$

where $Q_{i,j}$ represents covariance between two datasets, X_i and X_j . As the ETC method requires three unique datasets for each analysis ($i, j = 1, 2, 3$), there are six different covariance values based on three dataset permutations (Q_{11} , Q_{12} , Q_{13} , Q_{22} , Q_{23} , and Q_{33}). These covariances are used to calculate two objective functions:

$$RMSE^2 = \begin{bmatrix} Q_{11} - \frac{Q_{12}Q_{13}}{Q_{23}} \\ Q_{22} - \frac{Q_{12}Q_{23}}{Q_{13}} \\ Q_{33} - \frac{Q_{13}Q_{23}}{Q_{12}} \end{bmatrix} \quad (3.3)$$

$$r^2 = \begin{bmatrix} \frac{Q_{12}Q_{13}}{Q_{11}Q_{23}} \\ \frac{Q_{12}Q_{23}}{Q_{22}Q_{13}} \\ \frac{Q_{13}Q_{23}}{Q_{33}Q_{12}} \end{bmatrix} \quad (3.4)$$

where each element in each matrix represents the subsequent objective function value of each dataset. It is widely known that the closer RMSE and r^2 values to 0 and 1, respectively, the better the simulation performs.

3.2.3 Wflow_sbm model and its parameterization

Wflow_sbm model (Schellekens et al., 2020), modification of the previous topog_sbm model (Vertessy and Elsenbeer, 1999), is used to simulate the hydrological cycle in the UCRB. It is built on PCRaster (Karszenberg et al., 2010) and Python language. Figure 3.1 displays an overview of the simulated processes and fluxes within the model framework. One of the Wflow_sbm primary strengths is the model parameters that mostly represent physical characteristics, making it easier to interpret and correlate their values with physical catchment properties (Vertessy and Elsenbeer, 1999). It has been used in broad applications on hydrological modeling, delivering good performance, too (López et al., 2016; Hassaballah et al., 2017; Gebremicael et al., 2019; Wannasin et al., 2021b).

We use a similar setup as Imhoff et al. (2020) for model parameterization. The high-resolution model is parameterized based on point-scale (pedo)transfer functions (PTFs), followed by scaling to model resolution. This method has been applied to other tropical catchments with good results (Wannasin et al., 2021a). Soil-related parameters are estimated based on soil types from the SoilGrids database (Hengl et al., 2017). Monthly

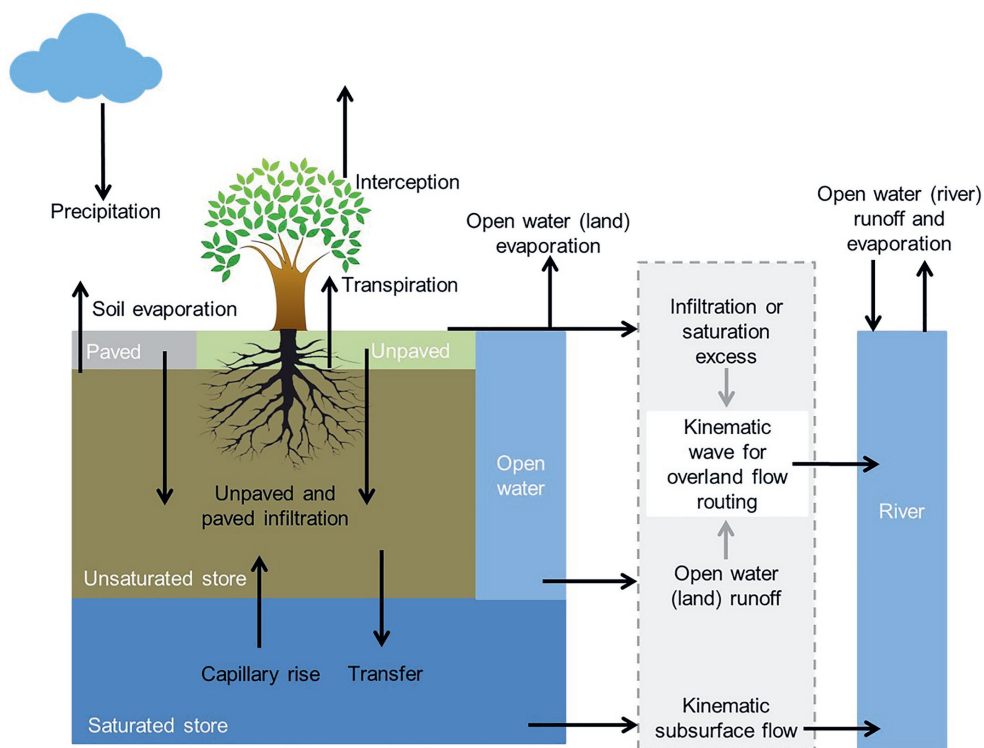


Figure 3.1: Overview of processes and fluxes in Wflow_sbm model framework (Schellekens et al., 2020)

Leaf Area Index (LAI) climatology is used for calculating daily interception using the model of Gash (1979) and derived from MODIS. For river network, slope, and river slope, we use Eilander et al. (2020) method based on MERIT-DEM dataset (Yamazaki et al., 2017). For deriving parameter values coupled to land use, we use the vito land use map (Buchhorn et al., 2020). The parameter controlling recharge to deep groundwater (*MaxLeakage*) is set to zero. To limit computing time, we use one day timestamp with fixed sub-timesteps for kinematic wave iterations; 900 seconds for river cells and 3,600 seconds for land cells.

The model is forced with CHIRPS rainfall data (spatial resolution of $0.1^\circ \times 0.1^\circ$) and PET derived from ERA5 reanalysis (Bruin et al., 2016). For spatial downscaling of ERA5 2m temperature to the model grid, we use a fixed lapse rate of $0.65^\circ/100\text{m}$. For the period of simulation, we simulate the hydrological cycle between 2005 and 2018 where all the hydrological components data are available or have been created.

3.2.4 Groundwater storage change estimate

As there is no snow-formed precipitation and notable reservoir/lake/water bodies within the basin spatial domain, the UCRB storage involves only subsurface storage, both in soil moisture storage (vadose zones) and/or groundwater storage (saturated zones), referred to as 'groundwater storage' in this chapter. Change in the groundwater storage (ΔS) is therefore determined by all the abovementioned water balance components of precipitation (P) as the inflow, and actual evaporation (AE), river discharge (Q_r), and groundwater abstraction (Q_a) as the outflow, calculated using Equation 3.5.

$$\Delta S = I - O = P - (AE + Q_r + Q_a) \quad (3.5)$$

On the other hand, recharge is a very important flux to consider in groundwater storage change assessment. However, from a whole catchment perspective, recharge is an internal process within the water cycle, not a water balance component that flows into (like precipitation) or out from (like actual evaporation, river discharge, and groundwater abstraction) a catchment directly itself and therefore not included in Equation 3.5. In this study, we report the average daily recharge estimates based on the Wflow_sbm model simulation. It is important to note that these estimates vary in space and time.

3.2.5 Uncertainty bounds experimental setup

Using two rainfall-station-based and two satellite-based measurements, the uncertainty of each rainfall dataset is evaluated based on each value and measurement technique. The spatial resolution of the rainfall data is selected on the same resolution of $0.25^0 \times 0.25^0$. As the four rainfall data sources have different temporal coverages (see Table 3.1), the overlapping data availability period between 2000 and 2015 is selected. The calculated objective functions, RMSE and r^2 , are averaged within grids bounding the UCRB.

ETC method requires data grouping of three different datasets to be evaluated, while there are four different rainfall data sources listed in Table 3.1. Therefore, four ETC dataset groups are constructed to utilize all available data, while at the same time conforming to ETC input requirements, named ETC_1, ETC_2, ETC_3, and ETC_4. ETC_1 consists of rainfall station data, SACA&D, and CHIRPS. ETC_2 consists of rainfall station data, SACA&D, and TRMM. ETC_3 consists of rainfall station data, CHIRPS, and TRMM. Lastly, ETC_4 consists of SACA&D, CHIRPS, and TRMM. The rainfall estimate with the highest r^2 and the lowest RMSE is used to drive the Wflow_sbm model.

Furthermore, with various estimates obtained from numerous approaches, we derive uncertainty bounds of each water balance component by calculating some statistical distribution of the inter-annual estimates during the simulated period between 2005 and 2018, namely the mean, 1st, and 3rd quartile. For rainfall estimates, we put our main focus on the best estimates according to the ETC application following the rainfall data

screening. For actual evaporation and river discharge estimates, we define two sets of estimates: ETC-based and Wflow_sbm-based estimates. ETC-based estimates consist of the rainfall, actual evaporation, and discharge estimates with the highest r^2 and the lowest RMSE based on ETC application on each component, added with the estimated groundwater abstraction, which leads to the groundwater storage change estimate. The Wflow_sbm-based estimates, on the other hand, consist of an identical set of estimates, except the actual evaporation and discharge estimates are obtained from the Wflow_sbm hydrological model simulation.

3.3 Results

3.3.1 Data quality screening

Two observed data that are mainly checked and screened prior to further estimates are the observed rainfall and discharge. We examine the number of non-rainy days in all rainfall estimates to inspect their reliability regarding potentially missing measurements. For discharge data, we compare the rising and falling pattern of daily discharge observation with CHIRPS rainfall and qualitatively derive judgment based on their agreement.

Between 2005 and 2015 when all rainfall station data are available, each rainfall station has on average 233 non-rainy days each year. The station with the most non-zero data available, Cisondari rainfall station, has on average 208 non-rainy days annually, while other stations have 257 non-rainy days at most. This number does not correspond well with rainfall characteristics in a tropical region (in this instance the UCRB) where there are only two seasons during a year, rainy and dry, with roughly similar temporal lengths. In contrast, SACA&D, CHIRPS, and TRMM rainfall estimates, respectively, have significantly fewer non-rainy days of only 161, 133, and 170. This fact shows the unreliability of the rainfall station data, specifically in the UCRB, as these non-rainy days might not actually have happened. Instead, there were rainfall occurrences unrecorded during actual precipitation. Moreover, the amount of non-rainy days is not related to missing data in certain prolonged periods as well, since the longest consecutive non-rainy day in the Cisondari rainfall station is found at 22 days, reflecting the absence of a dry season. With such ambiguous observation, considering and further utilizing other rainfall estimates is unavoidable, hence the application of the ETC technique to the rainfall estimates becomes even more important.

In response to the dubious rainfall data quality, the discharge data screening is performed by comparing the observed discharge, not to the observed rainfall but to CHIRPS rainfall estimates. Figure 3.2 shows the rising and falling pattern of the observed discharge due to the stimuli of CHIRPS rainfall estimates from 2005 to 2015. We can see the seasonal pattern from both data: a trend of higher rainfall and discharge that starts during September/October and ends during June/July. The rainfall plot presents little variance

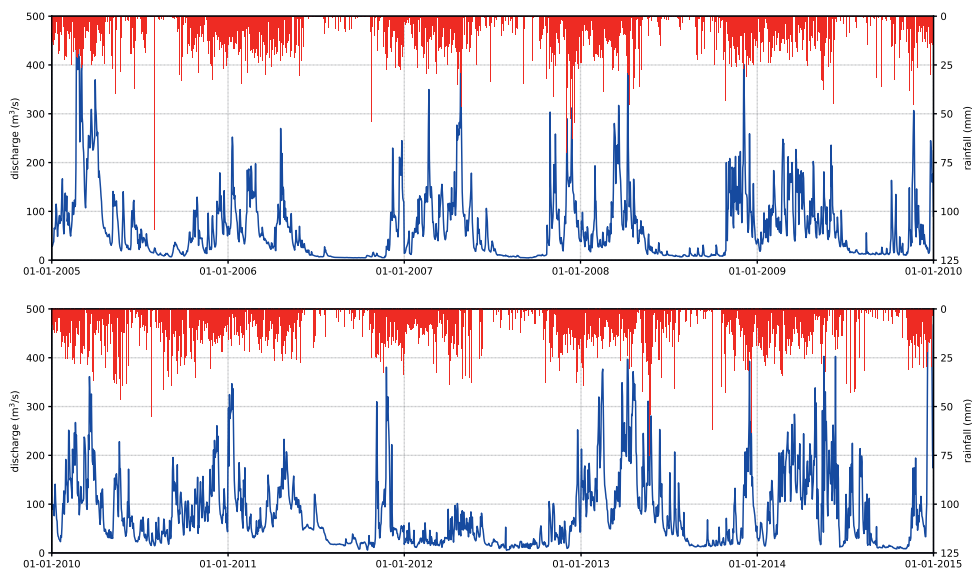


Figure 3.2: Plot between CHIRPS rainfall estimate (red bar - right axis) and observed discharge (blue line - left axis). The disagreement of the rising and falling pattern between the two fluxes is shown in several periods and taken into account in the succeeding analysis.

between wet and dry years, although it is still visible. For example, 2011 was a relatively dry year with less rainfall than the average, while 2013 was much wetter. The pattern is, however, dissimilar to the observed discharge. The basin response is sometimes inconsistent with the rainfall pattern. In 2012, for instance, the continuous rainfall early during the year was not followed by a rising discharge, instead, it shows a series of consistent low flows. Thus, in subsequent analysis, the calculation of average discharge does not consider data from 2012.

3.3.2 Rainfall estimates

Figure 3.3a shows a comparison between various estimates of annual rainfall in the UCRB. It suggests that satellite-based measurements of CHIRPS and TRMM result in an estimate of precipitation that is higher (2,872 mm/year and 2,863 mm/year respectively) than that of station-based measurements (1,972 mm/year for rainfall station and 2,426 mm/year for SACA&D). This is agreed by the data screening which shows numerous potentially missing data in the rainfall station record. Secondly, Figure 3.3b reports the result of ETC application to the daily rainfall estimates. The left- and right-side y-axis show the r^2 and RMSE values, respectively.

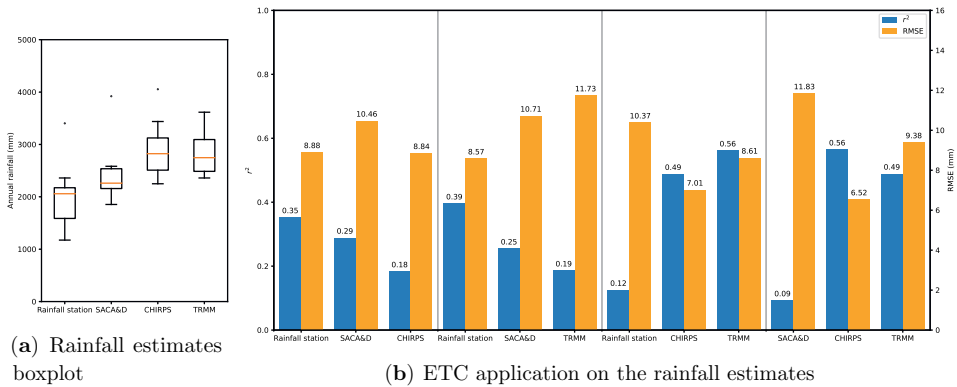


Figure 3.3: The rainfall estimates analysis. Figure (a) shows the statistical distribution of each annual rainfall estimate. Figure (b) shows the results of the ETC application on the rainfall forcing data. Two results on the left part show the combination of two rainfall station data with one satellite-based measurement (ETC.1 and ETC.2), while the other two results on the right part show the combination of one rainfall station data with two satellite-based measurements (ETC.3 and ETC.4) (Section 3.2.5).

Figure 3.3a in combination with r^2 metric in Figure 3.3b show that rainfall estimates sourced from more similar measurement techniques tend to be in a better agreement compared to estimates from different approaches. r^2 of both rainfall station and SACA&D data are higher than the satellite-based measurements in ETC.1 and ETC.2, while similar patterns are found in r^2 of CHIRPS and TRMM in ETC.3 and ETC.4. Furthermore, while the satellite estimates have low r^2 in ETC.1 and ETC.2 (0.18 for each estimate), their values in ETC.3 and ETC.4 improve to 0.52. Similar improvements are also found for the rainfall-station-based measurement, but they occur at a much lower rate. The r^2 of rainfall station and SACA&D data in ETC.3 and ETC.4 of 0.12 and 0.09, respectively, have improved only to 0.37 and 0.27 on average. Based on the evaluation of r^2 and rainfall data screening in Section 3.3.1, the satellite-based rainfall estimates are preferable to be used than the rainfall-station-based estimates.

To select the satellite data with the least uncertainty, the calculated RMSEs are considered. ETC application shows distinct and obvious results in this regard. Comparing the two satellite-based rainfall measurements, all ETC datasets agree that CHIRPS estimates have less uncertainties compared to TRMM. From ETC.1 and ETC.2, the RMSE of CHIRPS (8.84 mm/day) is lower than those of TRMM (11.73 mm/day), which is in agreement with ETC.3 and ETC.4 results.

In conclusion, according to the ETC application to the four rainfall estimates using the r^2 , similar measurement techniques produce estimates that are in better agreement with those estimated using different measurement techniques. Furthermore, based on the evaluation of

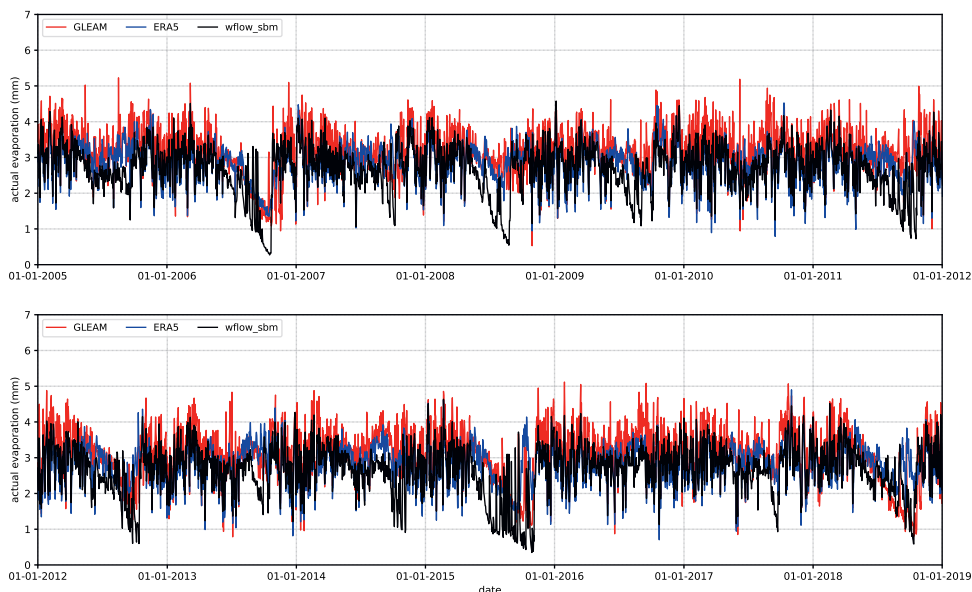


Figure 3.4: Comparison of actual evaporation values from three estimates: GLEAM (red line), ERA5 (blue line), and Wflow_sbm model (black line). The simulation period is between 2005 - 2018.

RMSE, CHIRPS rainfall estimates have the lowest RMSE among the considered estimates. Therefore, the rainfall input for the Wflow_sbm model simulation in this study is based on CHIRPS forcing.

3.3.3 Actual evaporation estimates

Based upon the Wflow_sbm simulation that uses CHIRPS rainfall estimates as the model input, the Wflow_sbm-based actual evaporation estimates are shown in Figure 3.4, compared with GLEAM and ERA5 estimates. We can see notable periods when the Wflow_sbm model produces lower estimates than the other two actual evaporation products, mostly during dry season periods in the latter part of each year. The water-height-equivalents of average daily actual evaporation, however, are not largely diverse as GLEAM, ERA5, and Wflow_sbm estimates are 3.13, 2.82, and 2.67 mm/day respectively. The contrast in the temporal fluctuation of these estimates is quantified by the variance, with the highest variability shown by GLEAM and Wflow_sbm simulation, estimated at approximately 0.73 mm/day. However, the Wflow_sbm simulation has lower estimates ranging between 0.11 and 4.54 mm/day, while GLEAM has the same variables on higher notes between 0.53 and 5.23 mm/day. The ERA5 actual evaporation estimates stand in between, ranging from 0.70 to 4.90 mm/day.

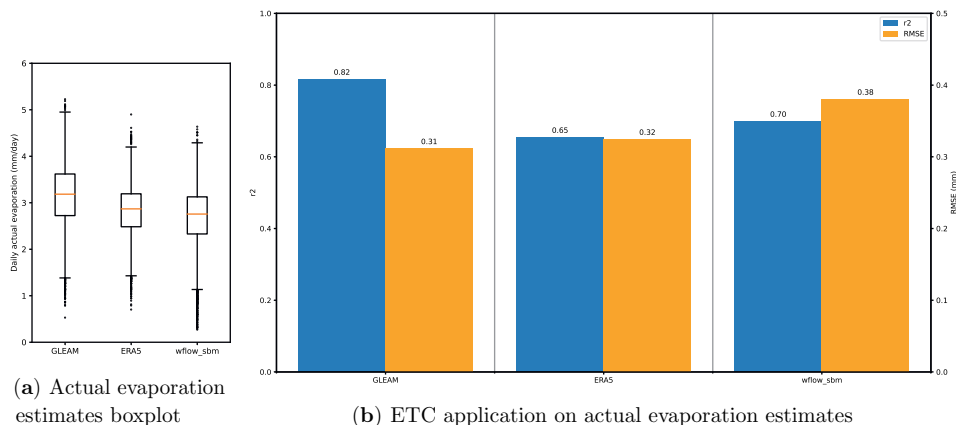


Figure 3.5: Actual evaporation estimates analysis. Figure (a) shows the statistical distribution of each estimate. Figure (b) shows the results of extended triple collocation application on actual evaporation estimates.

Furthermore, Figure 3.5a shows a boxplot comparison of daily actual evaporation estimates. It supports the Figure 3.4 interpretation of actual evaporation estimate distribution that shows higher values of GLEAM, and lower values of Wflow_sbm simulation, with ERA5 values placed in between. The results of ETC application on actual evaporation estimates are shown in Figure 3.5b, indicating GLEAM estimates to have the highest r^2 of 0.82 and the lowest RMSE of 0.31 mm/day. ERA5 and Wflow_sbm estimates have comparable results, with r^2 values of 0.65 and 0.70, and RMSE of 0.32 and 0.38 mm/day, respectively. Uncertainty quantification suggests a justifiable approximation of actual evaporation, ranging between 2.67 and 3.13 mm/day.

3.3.4 River discharge estimates

Three river discharge estimates of observed data, Wflow_sbm simulation, and GloFAS-ERA5, are plotted in Figure 3.6. GloFAS-ERA5 and observation data are directly available, while Wflow_sbm-based estimates are simulated through the setup described in Section 3.2.3. Visually, the oscillation pattern of discharge in the UCRB is quite distinct in Figure 3.6. From all discharge estimates, dry periods are found in the latter part of each year after June, while wet periods start around late October until early May. Additionally, there is no significant time lag noticed among the estimates. However, peak extreme values are not in agreement, for example during early and late 2016. Low flows during dry periods, on the other hand, are mostly in agreement among estimates.

Figure 3.6 also shows that GloFAS-ERA5 has the highest discharge estimate, followed by Wflow_sbm simulation and observation data. The water-height-equivalent average discharge of GloFAS-ERA5 estimates is 6.12 mm/day, while Wflow_sbm and observation estimates

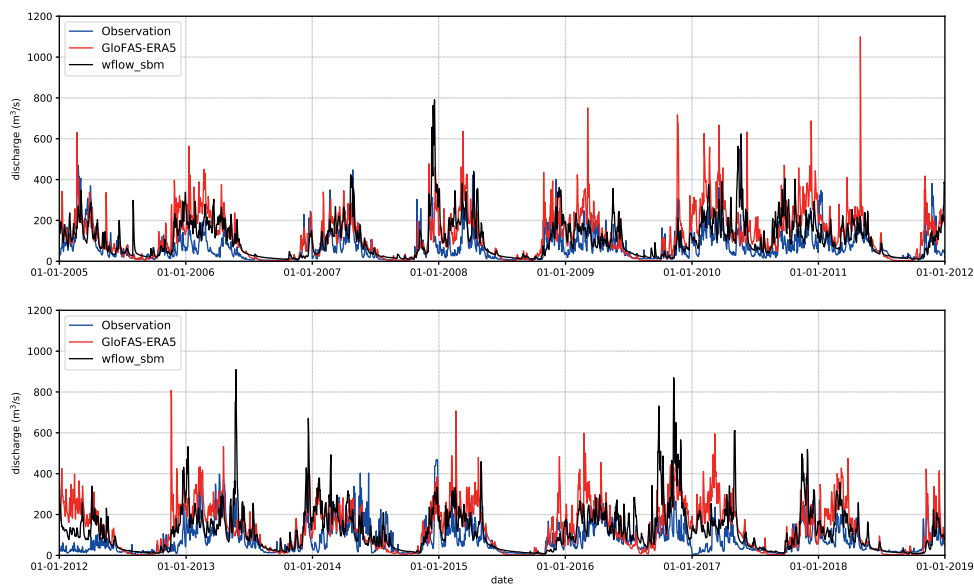


Figure 3.6: Three different river discharge estimates in the UCRB. The blue line represents observed river discharge data, the red lines GloFAS-ERA5 river discharge estimates, and the black lines Wflow_sbm model simulation results. The simulation period is between 2005 - 2018.

are 5.38 and 3.65 mm/day respectively. Although the rising and falling discharge pattern is mostly in agreement, there are periods where certain estimate delivers significantly higher values than others. Specifically, GloFAS-ERA5 and Wflow_sbm over-reactions to precipitation are quantitatively shown by high statistical variances of 5.38 and 4.82 mm/day respectively, while the same metric on discharge observation is calculated at only 3.36 mm/day.

GloFAS-ERA5 overestimation on discharge observation compared to Wflow_sbm simulation is also agreed by three objective functions of Kling-Gupta Efficiency (KGE) (Gupta et al., 2009), Nash-Sutcliffe (NSE) (Nash and Sutcliffe, 1970), and Root Mean Square Error (RMSE), calculated using *hydroeval* Python package (Hallouin, 2019). It is important to consider that these metrics are calculated accordingly to the observed discharge, in which the accountability and accuracy have been discussed in Section 3.3.1. Instead of entirely relying on the numbers, qualitative interpretations of discharge estimates are no less important than the KGEs, NSEs, and RMSEs. Nevertheless, results show that the objective functions of GloFAS-ERA5 estimates are worse than the ones of the Wflow_sbm simulation. While the KGE for Wflow_sbm simulation to river discharge observation is calculated at 0.18, the one for GloFAS-ERA5 is -0.03. The same goes with NSE, as one from Wflow_sbm (-0.76) is higher than one from GloFAS-ERA5 (-1.17). Last but not least,

Table 3.2: Average daily water balance components estimates in the UCRB (mm/day)

	Data	Average	Variance
Precipitation	Rainfall station	5.40	7.03
	SACA&D	6.47	12.25
	TRMM	7.50	11.73
	CHIRPS	7.80	9.33
	GLEAM	3.13	0.73
Actual evaporation	ERA5	2.82	0.55
	Wflow_sbm model-based estimate	2.67	0.73
Discharge	Observation	3.65	3.36
	GloFAS-ERA5	6.12	5.38
	Wflow_sbm model-based estimate	5.38	4.82
Groundwater abstraction	Domestic estimate	0.18	0.03
	Industrial estimate	0.38	0.06
Change in groundwater storage	ETC-based estimate	+0.45	8.64
	Wflow_sbm-based estimate	-0.82	7.31
	GRACE	0.25	1.57

Table 3.3: The UCRB water balance estimate summary (mm/day)

Flux	Source	Estimate range
Inflow	Precipitation	7.80
Outflow	Actual evaporation	2.67 - 3.13
	Discharge	3.65 - 5.38
	Groundwater abstraction	0.57
Groundwater storage change	ETC- and Wflow_sbm-based estimate	-0.82 - +0.45

the RMSE of Wflow_sbm and GloFAS-ERA5 are calculated at 94.15 and 104.53 m³/s, respectively. Considering the values from three discharge estimates, the calculated metrics, and GloFAS-ERA5's tendency to decrease in accuracy in smaller catchments (Harrigan et al., 2020), the water-height-equivalent average daily discharge component is estimated between 3.65 and 5.38 mm/day.

3.3.5 Groundwater storage change estimates

As discussed in Section 3.2.4, the 'groundwater storage' change estimates are calculated based on the discrepancy between the basin inflow (precipitation) and outflow (actual evaporation, river discharge, and groundwater abstraction). Each water balance component, however, has multiple estimates that vary in magnitude. Therefore, we categorize two groups of estimates: 'ETC-based' and 'Wflow_sbm-based' estimates (Section 3.2.5). In order to assist the calculation, Table 3.2 elaborates the statistical distribution of all mentioned water balance components estimates and Table 3.3 additionally synthesizes them to total inflow and outflow, along with groundwater storage change estimate in the UCRB. The average daily recharge calculated by the Wflow_sbm model, meanwhile, results in an estimate of 2.63 mm/day. It is important to take into account that great parts of the recharge flow horizontally in the soil moisture layer and subsequently become a part of river discharge as baseflow, and only the rest of it permeates vertically into the saturated zones and fills the groundwater storage.

Based on the ETC-based estimates, there is an indication of a positive recharging trend to the UCRB groundwater storage of 0.45 mm/day, despite the state of massive groundwater abstraction. On the other hand, the Wflow_sbm-based estimates result in an opposite groundwater storage change status of negative 0.82 mm/day, indicating water deficits in the groundwater storage are further aggravated by groundwater abstraction. Although the estimates range is in agreement with GRACE measures of, on average, 0.25 mm/day with a variance of 1.57 mm/day, the contrast between the two estimates demonstrates notable uncertainty in groundwater storage change estimate despite considering numerous approaches from measurements to modeling techniques on the water balance components.

3.3.6 The uncertainty bounds of the UCRB water balance estimate

To summarize all the above estimates, we plot the inter-annual time-series of average daily estimates of rainfall, actual evaporation, discharge, and groundwater storage change in Figure 3.7 for the Wflow_sbm-based and in Figure 3.8 for the ETC-based estimate. We also plot the first and third quartiles of the inter-annual estimates to show the width of the inter-annual variance of each estimate. Additionally, we plot the average monthly values for each component to show the consistency between daily and monthly estimates.

From Figure 3.7 and Figure 3.8, we can see a narrow variance in evaporation and discharge estimates. More importantly, there are good correlations among these estimates, with a correlation value of 0.76 between the Wflow_sbm simulation and GLEAM estimates of actual evaporation, and 0.56 between the discharge observed and simulated by the Wflow_sbm model. Consistent patterns between daily and monthly averages are also visible in these two components from both estimates. The Wflow_sbm-based discharge shows a little disruption during September as there are some years when rainy seasons started earlier compared to the average, resulting in an inter-annual outlier of discharge whose values skew the average.

In contrast, the groundwater storage change estimates show different features. A broad range of estimates from -0.82 mm/day to +0.45 mm/day can be interpreted either way as long-term recharging or discharging process from or to the groundwater storage. Although such estimates are found in the range that is in agreement with GRACE measures, the uncertainty bounds are too wide to enable us to derive a strong conclusion on the groundwater storage status in the UCRB. The relatively higher variances of the groundwater storage change estimates compared to the other water balance components shown in Table 3.2 further support our interpretation. Moreover, the pattern of the inter-annual average monthly estimates of GRACE is relatively dissimilar with both the ETC-based and Wflow_sbm-based estimates and dominantly found in different sides of positive and negative values. All these facts underpin the absence of accurate estimates of groundwater storage change despite the ability to accurately estimate the other water balance components of rainfall, actual evaporation, and river discharge.

3.4 Discussion

3.4.1 Alternative of forcing estimates and data sources

In this study, the results of ETC application to four rainfall estimates favor the use of satellite-based forcing data compared to rainfall-station-based data. This is further supported by the concerning rainfall station data quality where suspiciously numerous missing data exist due to an under-expected number of annual non-rainy days. It is also noted from the ETC application on rainfall estimates, supporting previous studies by Boluwade (2020), that similar measurement techniques have higher agreements between their products in comparison to data measured by different methods.

The considered rainfall data in this study are sourced only from rainfall-station-based and satellite-based measurements. Therefore, it is possible for future research to also observe the accuracy of other measurement techniques, for example, radar (Sauvageot, 1994), crowd-sourcing personal weather stations (Vos et al., 2017), or commercial microwave link networks (Overeem et al., 2011). Similar opportunities apply to other water balance components' estimates.

3.4.2 Results interpretation to the field situation

The results summarized in Table 3.2 show notable discrepancies among the estimated water balance components. It is important to consider, nevertheless, that the UCRB is a data-scarce area, from both aspects of quantity and quality. Although the ETC technique is applied to quantify the estimates' uncertainty, the true values of the hydrological forcing remain unknown. In this case, ETC applications do not reduce the uncertainty of the estimates. Instead, it quantifies the confidence level of each estimate, supporting the decision-making in selecting the best estimate for each water balance component.

In comparison to previous studies in the Citarum basin, our estimates of each water balance component are reliably verified. The average daily rainfall estimates between 5.40 and 7.80 mm/day in the UCRB is in agreement with the previous approximation by Jaya et al. (2020) with 6.30 mm/day and Salim et al. (2019) with a range between 5.38 and 7.12 mm/day. In the same study, Salim et al. (2019) estimated an average discharge equivalent to 4.49 mm/day, which is well within the estimated range of this study between 3.65 and 5.38 mm/day. Average discharge during dry and wet periods simulated by Julian et al. (2019) at 3.40 mm/day is also closely approximated within our uncertainty bounds.

However, earlier studies did not consider potential changes in groundwater storage. In this study, the groundwater storage change is estimated using three approaches - ETC-based estimate, Wflow_sbm-based estimate, and remote sensing-based gravimetric satellite estimates of GRACE - dependent on the water balance components estimates of rainfall, actual evaporation, discharge, and groundwater abstraction. These estimates result in

diverging trends from -0.82 to $+0.45$ mm/day, suggesting a high variance and uncertainties in the estimates of the water balance components, which eventually lead to a pending groundwater storage change status.

Considering the positive ETC-based estimate of groundwater storage change, increases in such components would coincide with rising groundwater tables, which unfortunately are not reinforced by the results of previous studies as they showed dwindling groundwater tables (Gumilar et al., 2015; Tirtomihardjo, 2016). Gumilar et al. (2015) found trends of groundwater table decline in eleven wells within the BGB. However, those wells are located in industrial zones and are used to abstract the groundwater. Thus, the observed groundwater tables in those wells would certainly involve biases in their measurements. The same findings by Tirtomihardjo (2016) also contain similar issues as the direct quotes from the study were 'groundwater levels in industrial areas are on the decline'. To capture the overview of the groundwater table fluctuation, groundwater table data with less bias regarding groundwater abstraction need to be collected and analyzed.

While groundwater table data are point-based and often involve biases, groundwater storage change estimate is an integrated metric of a whole basin. Comparing the results from previous studies of dwindling groundwater tables that are in conflict with two of our estimates, ETC-based and GRACE, points to a possibility of spatially varying states of groundwater storage change. There could be zones with dwindling groundwater tables, while the basin's overall groundwater storage is indeed increasing, and vice versa. A more comprehensive study on the UCRB subsurface processes could unravel the spatial distribution of groundwater storage changes and map as well as separate recharging and discharging area of groundwater storage.

Furthermore, by comparing the decreasing groundwater abstraction rate (Figure 2.4) with the uncertain groundwater storage change estimates, changing trends in the groundwater storage status could be plausible. Therefore, temporally fluctuating trends of groundwater storage state are necessary to be further explored. Time-series simulations of subsurface internal processes need to be performed in the future, taking into account groundwater flow and groundwater-related data reliability as the gap of knowledge in the UCRB.

3.4.3 The opportunities for future research

Despite involving some errors and uncertainties, surface water balance components in the UCRB (rainfall and discharge) are in principle directly observable. In contrast, groundwater abstraction, instead of being directly measured, is roughly estimated using population data and modeling results from other research. The credibility of the available industrial groundwater abstraction report is also questionable since the reported values are significantly lower than previous estimates (Taufiq et al., 2017). Hence, the groundwater storage change estimate as a result of all other estimates is highly uncertain.

Moreover, there are still issues to consider such as water balance spatial distribution, temporal variance, and groundwater flow system. To improve the accuracy and narrow the range of subsurface water balance estimates, the internal subsurface hydrological processes involving hydrogeological characteristics, soil parameters, etc, should be explored, simulated, and validated. Currently, the continuation of this study is being conducted by collating groundwater-related data from the UCRB.

3.5 Conclusions

In this paper, we improve the accuracy of the water balance components' estimates and their uncertainty bounds in a highly groundwater-dependent and data-scarce region of the UCRB between 2005 and 2018. The analysis starts from hydrological data collection to hydrological simulation using the Wflow_sbm model, which allows uncertainty quantification of water balance components as estimated from these data.

The rainfall data are sourced from rainfall-station-based (rainfall station and SACA&D) and satellite-based (TRMM and CHIRPS) measurements. The uncertainty analysis using the ETC method indicates a preference towards satellite data, which is supported by initial rainfall data screening that shows many potentially missing data recorded by the rainfall stations. In subsequent analysis, CHIRPS rainfall data, with an average daily rainfall estimate of 7.80 mm/day, are used to drive the Wflow_sbm model.

Hydrological simulation using the Wflow_sbm model results in two water balance components' estimates: actual evaporation and discharge. The actual evaporation is compared to the other two remote sensing estimates: GLEAM and ERA5. All the estimates result in very similar values, with ETC application on actual evaporation in favor of GLEAM. The simulated discharge of 5.38 mm/day is compared to both observation data and the GloFAS-ERA5 estimate, with observed data of 3.65 mm/day endorsed by the ETC.

We developed two scenarios in estimating groundwater storage change: ETC-based and Wflow_sbm model-based estimate. Both scenarios involve CHIRPS rainfall estimates and groundwater abstraction estimates based on population data and industrial abstraction literature. The ETC-based estimates consist of GLEAM actual evaporation and observed discharge, resulting in an average daily groundwater storage change of +0.45 mm/day. The Wflow_sbm model-based estimates, on the other hand, consist of evaporation and discharge estimates produced by Wflow_sbm simulation, delivering a result of -0.82 mm/day. Additionally, GRACE satellite observation estimates a similar metric of +0.25 mm/day, with a variance of 1.57 mm/day. Such a wide range of groundwater storage change estimates reflects substantial uncertainties and knowledge gaps on subsurface hydrological behavior in the UCRB. Further, it leads to a need for the next research step to simulate subsurface hydrological processes and to validate that with the available groundwater head measurements, which are currently being developed.

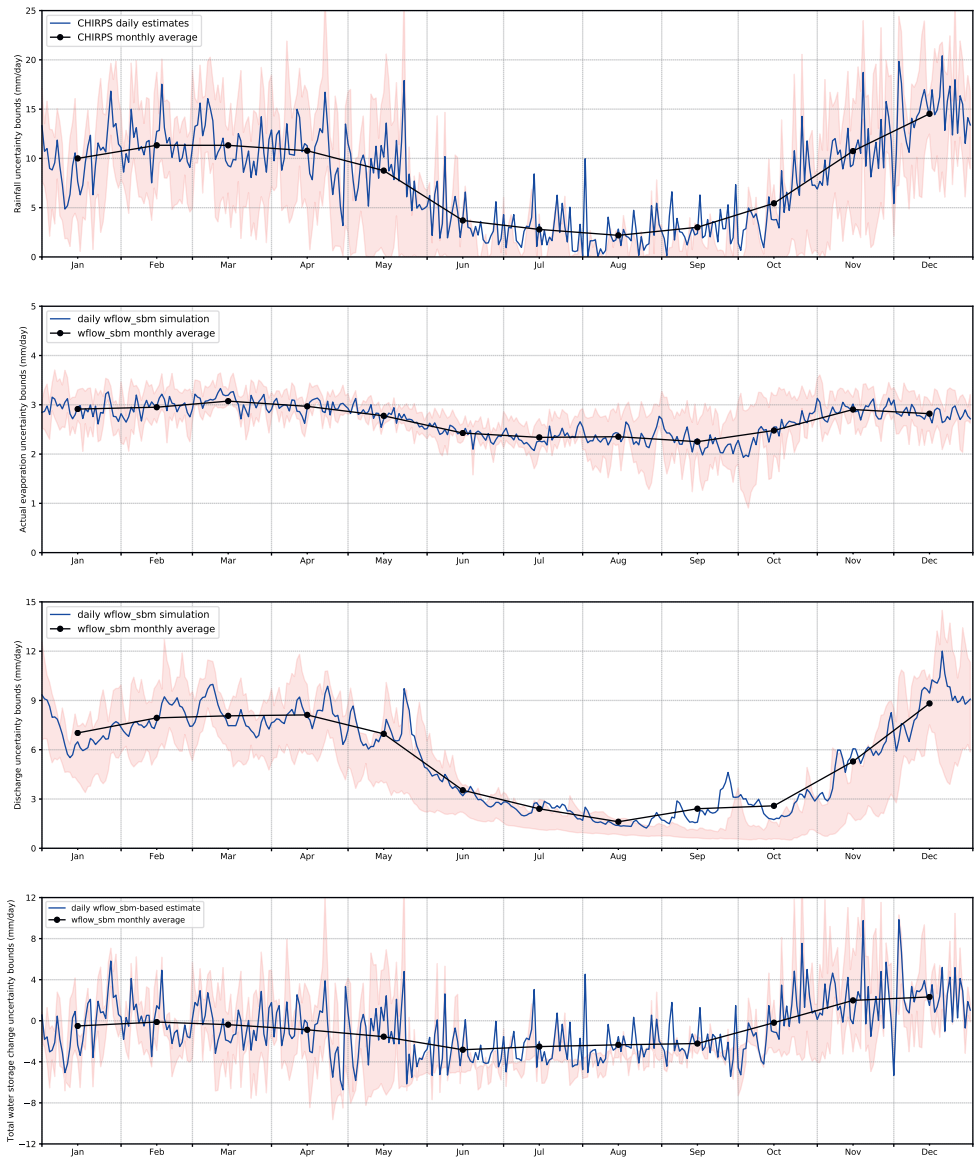


Figure 3.7: Plot of inter-annual average daily estimates of [from top to bottom] rainfall, actual evaporation, discharge, and groundwater storage change based on the Wflow_sbm simulation. The light red areas represent the width between the first and third quartiles of each component estimate.

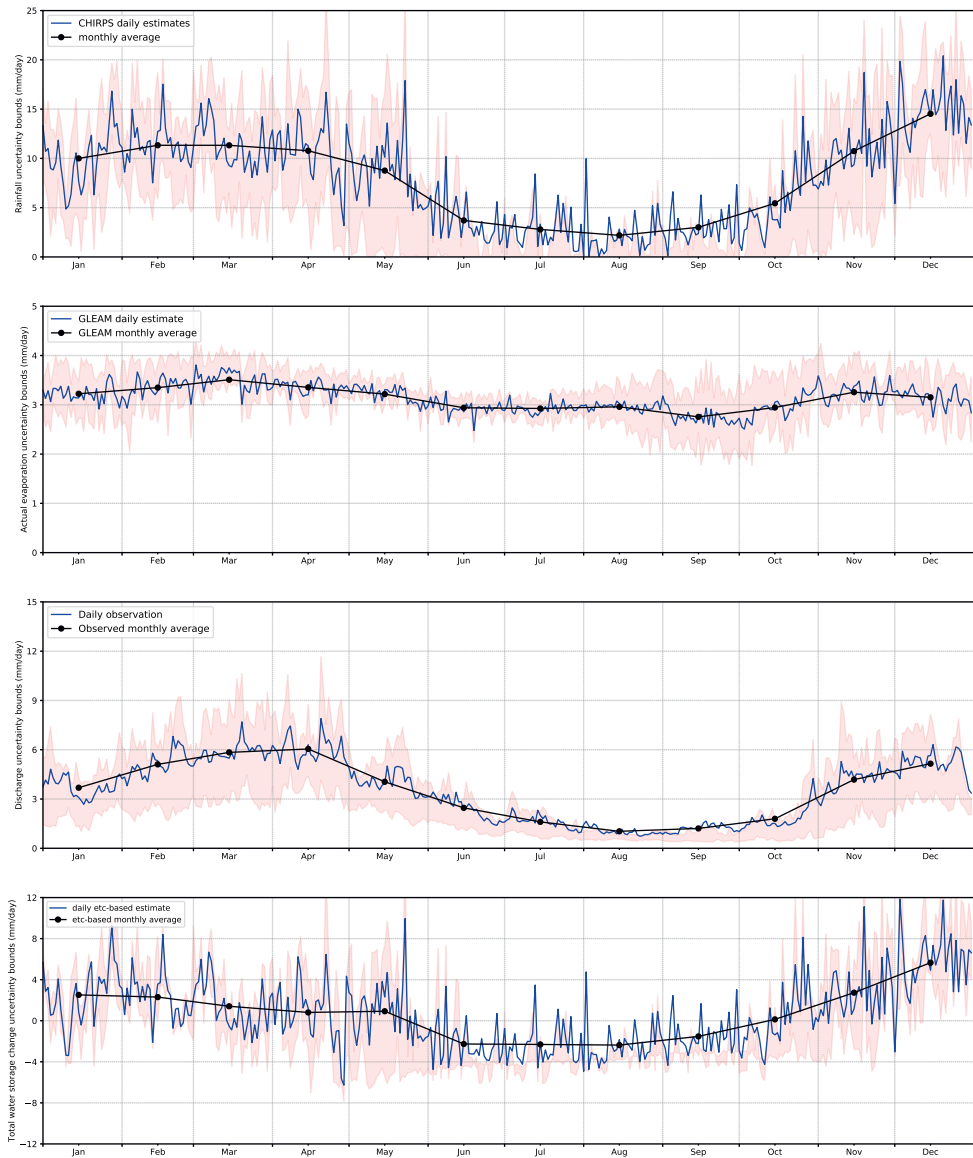
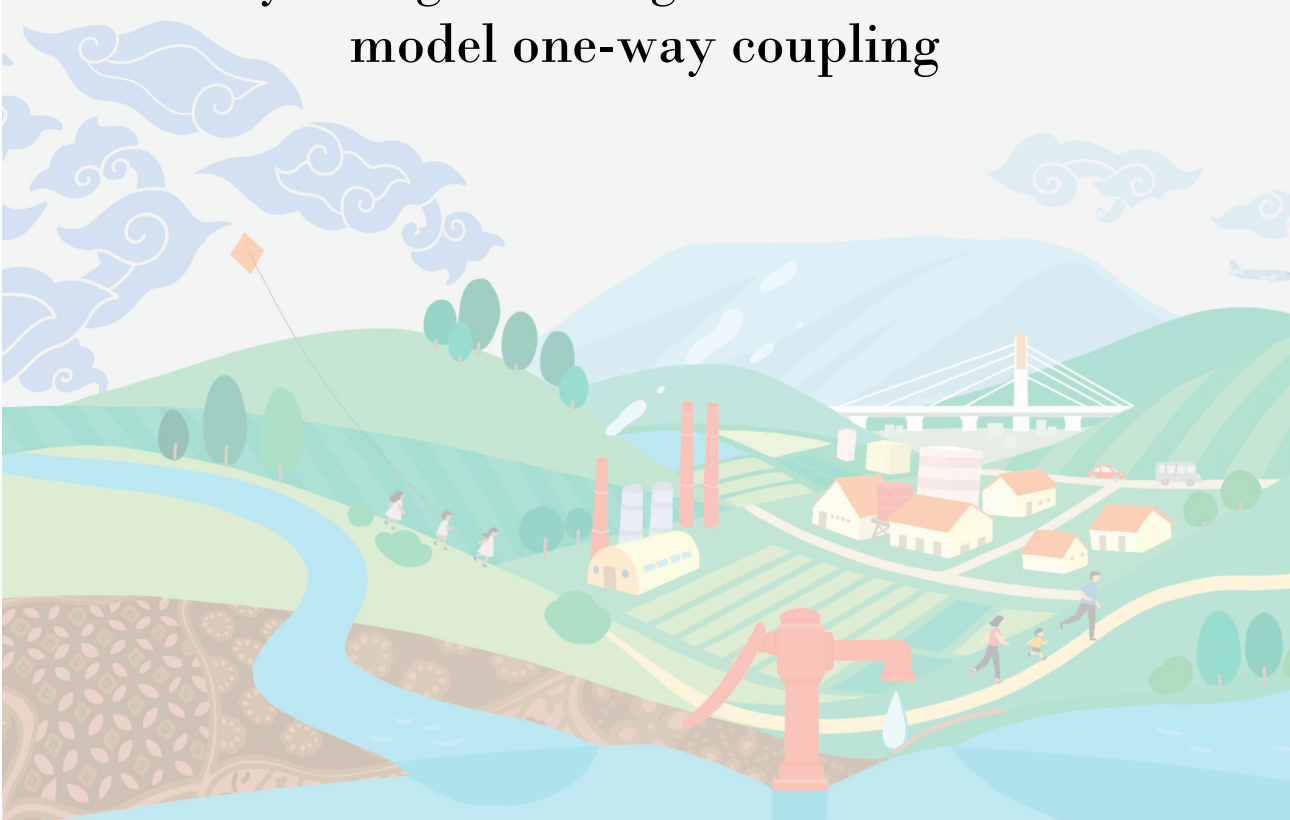


Figure 3.8: Plot of inter-annual average daily estimates of [from top to bottom] rainfall, actual evaporation, discharge, and groundwater storage change based on the ETC application. The light red areas represent the width between the first and third quartiles of each component estimate.



Chapter 4

Hydrological and groundwater flow model one-way coupling



This chapter is mostly based on and adapted from:

S. Rusli, V. Bense, A. Taufiq, and A. Weerts (2023a). “Quantifying basin-scale changes in groundwater storage using GRACE and one-way coupled hydrological and groundwater flow model in the data-scarce Bandung groundwater Basin, Indonesia”.

Groundwater for Sustainable Development 22, 100953.

doi: <https://doi.org/10.1016/j.gsd.2023.100953>

Abstract

Assessing basin-scale groundwater storage changes is often difficult when groundwater table data are scarce. In this study, we quantify the groundwater storage changes by using the Wflow_sbm hydrological model coupled with the MODFLOW groundwater model in the data-scarce area of the Bandung Groundwater Basin (BGB), Indonesia. The soil moisture storage change calculated by Wflow_sbm plus the groundwater storage change calculated by MODFLOW is compared to the water storage change estimated by the GRACE satellite between 2005 and 2015. The calculated cross-correlation coefficient is 0.502, and 62.1% of the simulated water storage change falls within GRACE's estimated uncertainty bounds. The important context in the water storage comparison are GRACE temporally local time-lags, data gaps in GRACE datasets, and differences in model seasonal performance and analyzed domain characteristics. The two latter factors highlight the importance of considering local groundwater-related information over large-scale global datasets in basin-scale groundwater storage change assessment. Based on the groundwater flow model, the current predicament of groundwater abstraction in the Bandung groundwater basin is highly unsustainable for future groundwater uses. On average, the groundwater storage in the study area is dwindling at the rate of 87 million m³/year between 2005 and 2018, dominantly a consequence of groundwater abstraction, whose effect is rippled to further impact the whole groundwater flow regime. Agreed by the situation shown by the limited data, the simulated groundwater table drawdown, spatially, is found to be locally and non-uniformly distributed. The capability of a one-way coupled hydrological and groundwater model to investigate basin-scale groundwater storage change, with comparable estimates to the GRACE dataset, unravel the opportunity of using such methods to estimate the behavior of future groundwater storage dynamics under the changing anthropogenic and climatic factors in catchment-scale studies.

4.1 Introduction

Groundwater is the world's most abundant freshwater resource, on which nearly half of the total world's population depends as the source for drinking water supply and industrial uses (Oki and Kanae, 2006). However, human dependencies on groundwater have vastly impacted the subsurface water tables and aquifer storage. Between 1960 and 2010, for example, global groundwater depletion is estimated at no less than 7 trillion m³ due to various factors (de Graaf et al., 2016). Among those are anthropogenic activities, which frequently act as the primary cause of storage depletion (Döll et al., 2012; Huo et al., 2016). In many places, practices of unsustainable groundwater use, where groundwater abstraction exceeds its sustainable yield, are constantly happening and difficult to control (Chinnasamy and Agoramoorthy, 2015; Wang et al., 2019; Dangar et al., 2021).

While the influence of anthropogenic factors on groundwater is strong, the natural hydrological cycle also holds a key role in regulating aquifer status. Even without abstraction, groundwater storage anomalies would still naturally occur due to the changing precipitation and soil moisture (Asoka and Mishra, 2020). The impact of climate change on the alteration of groundwater recharge has also been shown (Meixner et al., 2016; Tillman et al., 2016; Smerdon, 2017). Currently, although precipitation intensity is generally increasing (Trenberth, 2011; Li et al., 2019), the recharge to the groundwater is often found at a decreasing rate (Serrat-Capdevila et al., 2007; Holman et al., 2009; Dams et al., 2012), with numerous factors involved in the process.

The impact of both anthropogenic and climatic factors on groundwater storage is commonly monitored via groundwater table measurements. In recent times, gravimetric satellite data from the Gravity Recovery and Climate Experiment (GRACE) mission are often used to observe the terrestrial water storage change. Its derived groundwater storage proportion is then commonly validated by available in-situ measurements (Shen et al., 2015; Chen et al., 2016; Du et al., 2018). GRACE data, however, are measured on a spatial resolution of a few hundred kilometers (Frappart and Ramillien, 2018) (specifically at 1°×1°), although resampled data are available on a higher resolution of 0.5°×0.5°. To investigate groundwater storage change in basins whose total area is significantly smaller than those of GRACE spatial resolution (a grid size of 1°×1° is equivalent to approximately 12,000 km² along the equator), another method is needed.

In the Bandung groundwater basin (BGB), Indonesia, whose total area of 1,699 km² is a lot smaller than one GRACE grid, estimating the water storage change through various modeling approaches results in uncertain outcomes (Rusli et al., 2021). Although GRACE estimates are found in agreement with the values determined from several methods, the status of the BGB storage change and its subsurface hydrological components remains unknown (Rusli et al., 2021). In addition, using time-series groundwater level observation data to understand the trend, dynamics, and magnitude of groundwater storage change

is hardly possible as the observation wells are neither designed spatially as part of a network, nor they are temporally monitored frequently and regularly enough. The spatial distribution of the data is not uniform across the basin; most of the boreholes and measured groundwater table data are concentrated in the lower elevated area and hardly available in the mountainous area. Besides, most of the data also have either incomplete information (for example the lack of well construction details) or missing periods of observation. Therefore, to assess the groundwater storage status in the BGB, a solution is required to tackle the data scarcity and spatial coverage challenges.

One approach is to use numerical modeling. A groundwater model is capable of simulating groundwater storage dynamics, with groundwater recharge as the surface boundary condition provided by hydrological modeling. Therefore, in this study, our objective is to simulate the water storage change in the data-scarce area of the BGB by applying a one-way model coupling between Wflow_sbm hydrological model (Schellekens et al., 2020) and MODFLOW groundwater model. We validate our one-way coupled model by comparing its output in terms of water storage change to GRACE estimates. Additionally, we also investigate the current state of groundwater storage in the study area considering the changing climatic and anthropogenic situation.

4.2 Methods

4.2.1 GRACE estimates: products and application

The GRACE mission is a remote-sensing satellite-based mission that estimates the terrestrial water storage change (TWSC) dynamic based on the measurements of gravity anomalies (Frappart and Ramillien, 2018). Practically, TWSC is a quantity of vertical water mass changes, consisting of snow, surface water, soil moisture, and groundwater storage in a unit of GRACE measurement grid of $1^\circ \times 1^\circ$. Due to its large measurement grid area, GRACE-related applied studies have been mostly conducted in large basins with reliable data, such as the Amazon (Pokhrel et al., 2013), the Colorado (Rahaman et al., 2019), the Upper Nile (Shamsudduha et al., 2017), and the Heihe basins (Cao et al., 2012). In these studies, GRACE-derived groundwater storage changes are compared to in-situ water table measurements with a relatively similar spatial scale.

In small basin applications, the GRACE estimates' spatial scaling uncertainty inflates a concern. To tackle the issue, there have been numerous efforts to downscale GRACE products to basin-scale estimates (Miro and Famiglietti, 2018; Yin et al., 2018; Chen et al., 2019; Verma and Katpatal, 2020). GRACE dataset statistical downscaling (Yin et al., 2018) was applied in areas where the relationship between GRACE-derived groundwater storage and evapotranspiration is strong. In a highly groundwater-dependent area like the BGB, the groundwater storage change is influenced not only by evapotranspiration but also mostly by groundwater abstraction. Another method (Miro and Famiglietti,

2018) downscales GRACE to the resolution of $0.25^\circ \times 0.25^\circ$, however, it requires a lot of machine learning processing of numerous hydrological variables, whose data are not available in the study area. In this study, we incorporate GRACE estimate' uncertainty bounds (NASA/JPL, 2019) as one approach to tackle the spatial scale uncertainty and validate our model simulation results.

With various GRACE products available, the used version in this study is the JPL GRACE and GRACE-FO Mascon Ocean, Ice, and Hydrology Equivalent Water Height Coastal Resolution Improvement (CRI) filtered release 06 version 02 (NASA/JPL, 2019). It is selected as it, importantly, incorporates the CRI algorithm. The GRACE grid that covers the study area has a long coastal line of the Indian Ocean along its southern border, making the CRI algorithm application relevant. With the absence of snow and negligible surface water components in the study area, the GRACE estimates of water storage change in the BGB should consist only of soil moisture and groundwater storage components (Equation 4.1). The groundwater storage component consists of the specific yield (S_y) and specific storage (S_s) components from the unconfined and confined aquifers, respectively. Therefore, in this study, the GRACE TWSC estimates are comparable with the sum of soil moisture change, determined by the hydrological model of `Wflow_sbm`, and groundwater storage change, simulated using the groundwater model of MODFLOW.

$$\Delta_{water} = \Delta_{surfacewater} (\approx 0) + \Delta_{soilmoisture} + \Delta_{groundwater} (= \Delta_{S_s} + \Delta_{S_y}) \quad (4.1)$$

A change in basin water storage results from the discrepancy between inflow and outflow. In the BGB, the only water inflow comes from rainfall and consequent groundwater recharge. Therefore, we expect a strong consistency and correlation between the rainfall and the water storage change estimated in the study area. In this study, we use the CHIRPS dataset (Funk et al., 2015) for our rainfall estimate, and GRACE along with the one-way coupled model simulation result, later on, as the estimate for water storage change.

By comparison with the GRACE dataset, the CHIRPS dataset is available in a much higher spatial resolution of $0.05^\circ \times 0.05^\circ$. Hence, it offers a more detailed representation of rainfall across the study area. As the GRACE water storage change estimates cover a larger spatial domain, its values are less sensitive to changes over smaller sub-areas. Comparing both spatial coverages, the Upper Citarum River Basin (UCRB)/BGB, as the most upstream part of a larger watershed system, has steeper slopes and higher elevation. Meanwhile, the larger spatial domain covered by the GRACE grid partly also covers the lower elevated and more flat area downstream of the basin. This results in discrepancies in the hydrological response to rainfall. For example, the smaller and steeper area of the UCRB requires a shorter time to generate surface runoff compared to ones of the GRACE grid spatial domain. The same things apply in the required time to adjust the BGB's water storage. For that reason, occasional lags in the timing of the GRACE water storage change signal compared to the timing of the CHIRPS rainfall estimates are expected.

Besides the expected difference in detecting changes using the two datasets, we note some missing values in the GRACE dataset. In the earlier period of our simulation between 2005 and 2015, as low as 9.8% of the data is missing. The unavailable values, fortunately, do not appear in a prolonged continuous period. However, between 2016 and 2018, it increases to 52.8%, which we judge as too poor of temporal coverage to be used as the benchmark for our simulation. To tackle this issue, we do not take into account the latter periods of the GRACE dataset when assessing the quality of our simulation.

4.2.2 Hydrological Wflow_sbm model setup and recharge estimates

Both river discharge and groundwater recharge are outputs of the hydrological model Wflow_sbm (Schellekens et al., 2020) that is set up and described in Chapter 3. A high-resolution model is first parameterized based upon point-scale (pedo)transfer functions (Imhoff et al., 2020) before being scaled to the designated model resolution. The model assigned elevation is derived from the MERIT-DEM dataset (Yamazaki et al., 2017). The soil-related parameters, daily interception calculation, river network delineation, and land use-related parameters are set in a similar fashion to the previous studies (Rusli et al., 2021). The same goes for model timestamps and kinematic wave iterations' sub-timesteps. The model is forced with CHIRPS rainfall (Funk et al., 2015) and ERA5-derived potential evapotranspiration (Bruin et al., 2016). The simulation period is set from 2005 to 2018, with the actual simulation period being extended to one year before the designated period in order to diminish the effect of the initial condition uncertainty, commonly known as the 'model warm-up' period (Yu et al., 2019).

The Wflow_sbm parameter that is directly related to the amount of water recharging the upper aquifer in the MODFLOW model is *MaxLeakage*. Numerically, it acts as the maximum threshold of water leaving the subsurface's unsaturated to the saturated zones. A higher *MaxLeakage* parameter increases the recharge and decreases the surface water discharge. By applying the *MaxLeakage* parameter to our previously built model (Rusli et al., 2021), we simultaneously are able to compare two variables. First, the calculated discharge with the observation data. Secondly, the simulated groundwater table from the groundwater model, forced with the calculated recharge, with the observed groundwater table. According to previous studies focussing on the groundwater recharge quantification in the study area, the annual recharge in the Bandung groundwater basin is estimated between 300 and 450 mm (Hutasoit, 2009; Tirtomihardjo, 2016).

4.2.3 Groundwater model setup

We use the MODFLOW python package developed by Bakker et al. (2016) to build our groundwater model. MODFLOW is an open-source groundwater flow model distributed by the U.S. Geological Survey (USGS) and written using a modular object-oriented design (Hughes et al., 2017). These modular objects are packages assignable to the main model

and simulations, with applications that are independently unique from one case to another. In this study, we use MODFLOW6, which solves the Darcy three-dimensional groundwater flow equation (Equation 4.2) using the control-volume finite-difference (CVFD) method (Langevin et al., 2017).

$$\frac{\partial}{\partial x} \left(K_{xx} \frac{\partial h}{\partial x} \right) + \frac{\partial}{\partial y} \left(K_{yy} \frac{\partial h}{\partial y} \right) + \frac{\partial}{\partial z} \left(K_{zz} \frac{\partial h}{\partial z} \right) + Q_s = S_S \frac{\partial h}{\partial t} \quad (4.2)$$

where K is the hydraulic conductivity in corresponding directions, Q_s is the volumetric flux per unit volume representing sources and sinks, and S_S represents the storage parameters of the porous material.

We discretize the study domain of the BGB, vertically, into a 3-layer model, with each layer representing the upper aquifer, the aquitard layer, and the bottom aquifer that lies on the bedrock basement. The horizontal grid size is set to 100m \times 100m, generating 481 rows and 646 columns within the model domain. The assigned surface elevation is derived from the MERIT-DEM dataset (Yamazaki et al., 2017), identical to the Wflow_sbm model. The initial K_h for the upper aquifer are spatially interpolated from slug test data, ranging between 0.15 and 0.35 m/day depending on the location. The K_v are interpolated from the lab tests where soil samples were taken during the slug tests, varying between 3×10^{-4} and 6×10^{-4} m/day. For the aquitard layer, we assign a multiplication factor of 0.1 to both the K_h and K_v of the first layer. For the bottom aquifer, the K_h and K_v are interpolated from 23 pumping test reports, ranging between 0.18 and 0.58 m/day. As both the first and third model layer are actually formed by the same geological formation, the similarities between the initial K_h are, in fact, encouraging.

The groundwater recharge is calculated from the Wflow_sbm simulation at a daily time step and then forced to the groundwater flow model. The controls on the uptake and release from the elastic and water table storage, the specific yield (S_y) and the specific storage (S_s) respectively, are only applied during the transient simulation. In Equation 4.2, the S_y takes over the S_s when the calculated groundwater table is lower than the cell top elevation. While the sieve analysis indicates very sandy soil and a low S_y of 0.05, we initiate the S_y at 0.2 to ease the model convergence. The S_s values are averaged from the pumping test reports documented by ESDM, resulting in a value of $8.7 \times 10^{-3} \text{ m}^{-1}$. The river paths are delineated using the ArcGIS hydrology toolset and parameterized using groundwater level observations data along the river. The river depth is derived from the difference between the surface water level and the groundwater level observations. We do not directly input the actual river depth as the grid size of 100m \times 100m is generally wider than the river itself. The riverbed hydraulic conductance is determined via model calibration. The groundwater abstraction is set according to estimates from our previous study (Rusli et al., 2021), increasing annually. The spatial distribution of the abstraction wells, as mentioned previously, is assigned based on the land-use map of the study area.

We use the groundwater flow simulation setup whose steps have been proven successful in a previous study (Karimi et al., 2019). First, steady-state simulation is performed to obtain the initial condition for the period as early as 1990. Second, we used transient model spin-up until 2004 to achieve dynamic steady-state conditions. The dynamic steady-state condition is achieved when the groundwater state is relatively stable. The model is simultaneously calibrated by comparing the simulated groundwater table elevation with the observation data. We finally run the final simulation between 2005 and 2018 using the calculated head in 2004 as the initial condition using the calibrated parameters. The model parameterization during the final simulation is set constant throughout the model run, as adjusting model parameters in a shorter period to improve model output does not imply more reliable simulations (Rusli et al., 2015).

We believe that our approach to translating the interpretation of the groundwater basin's actual geophysical condition into the numerical groundwater flow model is the best strategy considering the (lack of) data availability. Further model complexification would be an effort that cannot be justified by data or observations. This parsimonious modeling philosophy has been applied in other studies (Voss and Soliman, 2013; Kumar et al., 2019; Liu and Rahman, 2022), where all implementations have been conducted under data scarcity conditions, similar to the situation in our study area. A previous study has also proved that the GRACE dataset is better compared to the 'simple' aquifer system (Katpatal et al., 2018), which is represented by our approach.

4.2.4 Coupling of Wflow_sbm and MODFLOW model

One-way coupling between a hydrological and a groundwater flow model has been applied in many studies (Yuanyuan et al., 2013; Jing et al., 2018; Elliott et al., 2022). In such a scheme, two different simulations are run in separate software packages instead of being integrated into one fully coupled simulation (Haque et al., 2021). In this study, while the two models are coupled via the recharge variable, the Wflow_sbm model is simulated in a separate environment from the MODFLOW model. Each model is independently calibrated and validated. The discharge simulated by the Wflow_sbm model is compared with the observed discharge, while the groundwater model is calibrated using the groundwater level observation data in 2004 using dynamic steady-state simulation. The transient simulation of groundwater flow is calibrated by comparing the total water storage change, which includes the groundwater storage change component, with the GRACE estimates.

In calculating the total water storage change based on the one-way coupled model simulation, we sum the soil moisture change calculated from the hydrological simulation and the groundwater storage change calculated from the groundwater flow simulation. The soil moisture calculation in the Wflow_sbm model involves two main partitions: the unsaturated and the saturated stores of the shallow soil. The unsaturated store includes the soil layer close to the root zone, while the saturated store is the fluctuating shallow or

perched groundwater table (the S_y part of the groundwater flow model). Both of the results are also temporally resampled from daily to monthly. The groundwater storage change of the MODFLOW simulation is on monthly timesteps, although calculated in half-daily sub-timesteps. The phreatic water table storage from the MODFLOW simulation is still considered, as the saturated zones in the Wflow_sbm model only involve the first 2 meters of depth of soil. Figure 4.1 summarizes the full methodologies used in this study.

4.2.5 Model calibration

Following up the Wflow_sbm model setup, we calibrate the *MaxLeakage* parameter by optimizing the KGE metric (Kling et al., 2012), calculated based upon the simulated discharge compared to the discharge observation data. Additionally, we also evaluate the quality of our simulation under the current setup to our previous results (Rusli et al., 2021), by looking at the improvement of three metrics, the Kling-Gupta efficiency (KGE) (Gupta et al., 2009; Kling et al., 2012), the Nash-Sutcliffe efficiency (NSE) (Nash and Sutcliffe, 1970), and the Root Mean Square Error (RMSE), as well as the average discharge value between the observation and the simulation.

For the MODFLOW model calibration, we manually adjust the spatially varying hydraulic conductivity parameter, which we evaluate using the determination coefficient (r^2) calculated based upon the simulated water table elevation under the dynamic steady-state condition and the observed groundwater table data. We also assess the transient simulation, by taking into account the simulated groundwater storage change in the total water storage change estimates and comparing it to the GRACE estimates.

Pearson correlation coefficient is used to evaluate our one-way coupled model simulation results, by comparing the simulated water storage change estimates with the GRACE estimates. Spatial assessment metrics are not preferred as the spatial resolution of the two compared samples are hardly similar; there are 163,337 grid cells in our one-way coupled model, while there are only 4 GRACE grids covering the same domain. To tackle the Pearson correlation coefficient's high sensitivity to outliers, we also assess both estimates visually to avoid such issues. In addition to that, to take into account the GRACE measurement uncertainties, we also quantify the percentage of feasible simulated water storage change estimates. In this study, the feasible simulated water storage change estimates are defined as the simulated water storage change results that fall within the range of GRACE uncertainty bounds, provided alongside the GRACE water storage change estimates data (NASA/JPL, 2019). The percentage is calculated by fractionating the number of feasible simulated water storage change estimates with the total number of available estimates during the simulation period.

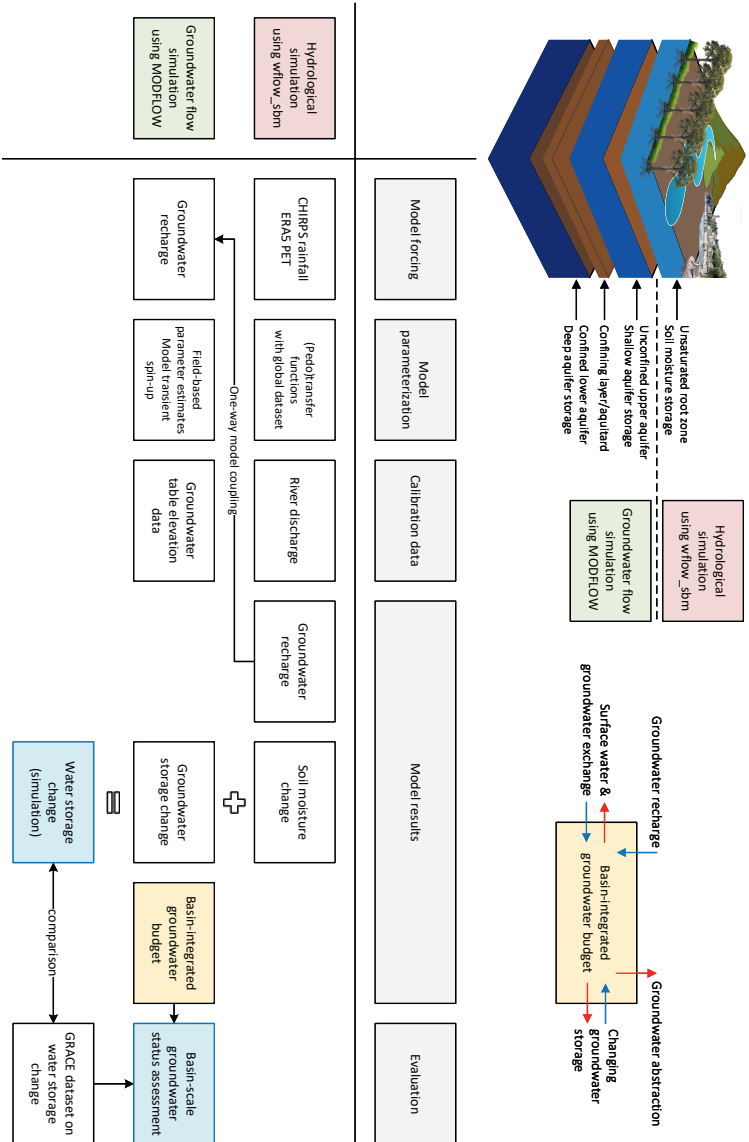


Figure 4.1: Flowchart of the research methods and workflow. The upper left figure portrays the vertical partition of different water storage in the model simulation. The upper right figure simplifies the basin-integrated groundwater budget components. The simulation flow diagram is shown in the bottom figure.

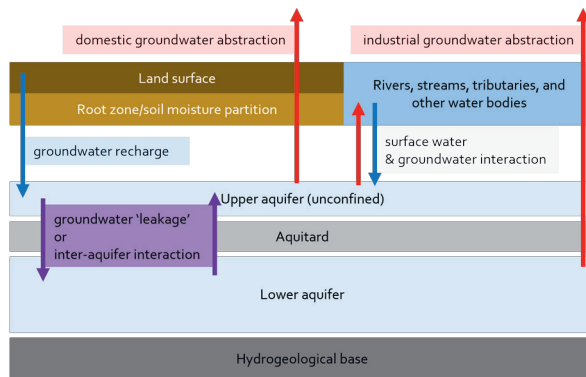


Figure 4.2: Simplified conceptualization of groundwater fluxes within the groundwater model.

4.2.6 GRACE dataset screening

Regarding GRACE applicability to be used as the point of reference to our one-way coupled model simulation, we first evaluate the correlation between the CHIRPS rainfall and the GRACE TWSC estimates. The evaluation is done by calculating the Pearson correlation coefficient between the two variables. To take into account the limitations and uncertainties of GRACE estimates described in Section 4.2.1, we apply two independent adjustments. On the subject of the expected lags of the GRACE signals' timing, we use the cross-correlation coefficient as the evaluation metric. Previous hydrological studies have attested to the use of such metric as it considers the time lag of the interaction among hydrological variables (Seo et al., 2019; Wang et al., 2021b). Regarding the occasionally missing GRACE dataset, we calculate both the r and cross-correlation coefficient during only the period where the data are mostly complete, e.g. between 2005 and 2015. In this way, we ensure that we put sufficient consideration to the context of spatial resolution, scaling, and data quality and availability in comparing our water storage change simulation results to the GRACE estimates.

4.2.7 Groundwater storage change assessment

Using the calibrated MODFLOW model, we assess the groundwater storage change in the BGB. Three fluxes influence the groundwater storage 'bucket' in the study area: groundwater recharge, groundwater abstraction, and the interaction between surface water and groundwater (Figure 4.2). The latter water flux is strongly controlled by the two former most important budgets: the groundwater recharge as the inflow and the groundwater abstraction as the outflow. The trends of these two key components, together with the groundwater storage, are analyzed and quantified.

We also assess the groundwater storage change by plotting the groundwater table and the piezometric head fluctuation for the upper and the bottom aquifer respectively. As the changes for both variables are spatially distributed, we assess two values - the average and the largest changes - for each layer of the aquifers. By analyzing the spatial distribution of the changes, we can determine the impact of groundwater abstraction on the groundwater table profile, and identify the occurrence of local drawdown.

4.3 Results

4.3.1 Hydrology model Wflow_sbm calibration and output

In calibrating the Wflow_sbm model, the KGE values vary between 0.35 and 0.48 when the *MaxLeakage* parameter is set between 0.0 and 1.5 mm/day. There is, however, less than a 1% difference between the lowest and the highest KGE under the *MaxLeakage* range of 0.9 and 2.0 mm/day. As all the calculated KGE satisfy the suggested minimum value of -0.41 (Knoben et al., 2019), we set the *MaxLeakage* parameter at 0.9 mm/day, taking into consideration the results of recharge estimates from previous studies (Hutasoit, 2009; Tirtomihardjo, 2016), resulting in an average annual recharge of 317 mm.

Figure 4.3 plots the simulated discharge and the observation data. Compared to our previous study, incorporating the *MaxLeakage* parameter in the Wflow_sbm model visually improves its performance. It is quantitatively confirmed by the improved KGE, NSE, and RMSE metrics, calculated using the *hydroeval* package (Hallouin, 2019). The KGE increases from previously 0.35 to currently 0.46, the NSE improves from -0.76 to -0.58, and the RMSE decreases from 94.15 m³/s to 90.78 m³/s. The average observed discharge of 83.16 m³/s that was previously simulated at 113.57 m³/s, now is more accurately simulated at 96.48 m³/s. We further use the calculated recharge under these current sets of parameters as the driving force to the groundwater model simulation.

Besides the groundwater recharge, another result from the Wflow_sbm model is the soil moisture. It is calculated in a daily time step and aggregated to a monthly time step before the changes are calculated. The calculated daily soil moisture is shown in Figure 4.4, with the dynamic that is in agreement with the rainfall input.

4.3.2 Groundwater model calibration

Figure 4.5a shows the comparison between the observed and the simulated groundwater table elevation based on the calibrated groundwater model, with an r^2 of 0.895. The calibrated K_h in the upper and bottom aquifers are within a range between 0.15 and 0.35 m/day, and between 0.14 and 0.46 m/day, respectively. These values are very similar to the values measured from the fieldwork. The optimum K_h for the aquitard layer is between 0.017 and 0.039 m/day. For the vertical properties, the optimum K_v in the upper

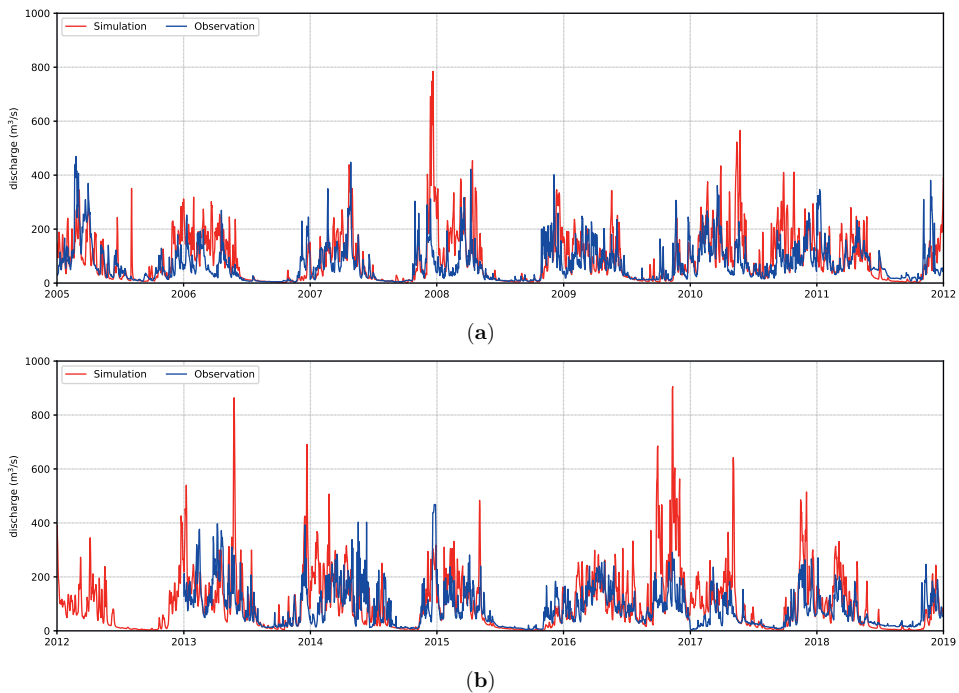


Figure 4.3: The comparison between the observed and the simulated discharge during (a) the first half (2005 to 2011) and (b) the second half (2012 to 2018) of the simulation period.

aquifer is between 3×10^{-3} and 6×10^{-3} m/day, which is one degree of magnitude higher than the values of the soil samples' K_v measured in the laboratory. The anisotropy factor of 0.1 and 1.0, respectively, are the most optimum for the aquitard and bottom aquifer. The riverbed hydraulic conductance is at its optimum at $75 \text{ m}^2/\text{day}$. The river base elevation is also calibrated and normalized to its respective grids. The calibrated river base elevation parameter of 23.5 meters below the surface is validated by groundwater level elevations located near river streams. Through the calibration phase, the model led to groundwater level distribution shown in Figure 4.5b. It clearly reflects the influence of surface topography on the basin's groundwater flow direction. The high groundwater table is higher along the basin's outside perimeter, which is the location of mountainous areas on the surface, and drops off towards the vast flat terrain in the center of the basin.

4.3.3 Screening result of the GRACE data

Figure 4.6 presents the time-series plot between CHIRPS monthly rainfall estimates and two water storage change estimates. The latter is represented by two independent products: (1) the one-way coupled model-based water storage change simulated in the spatial domain

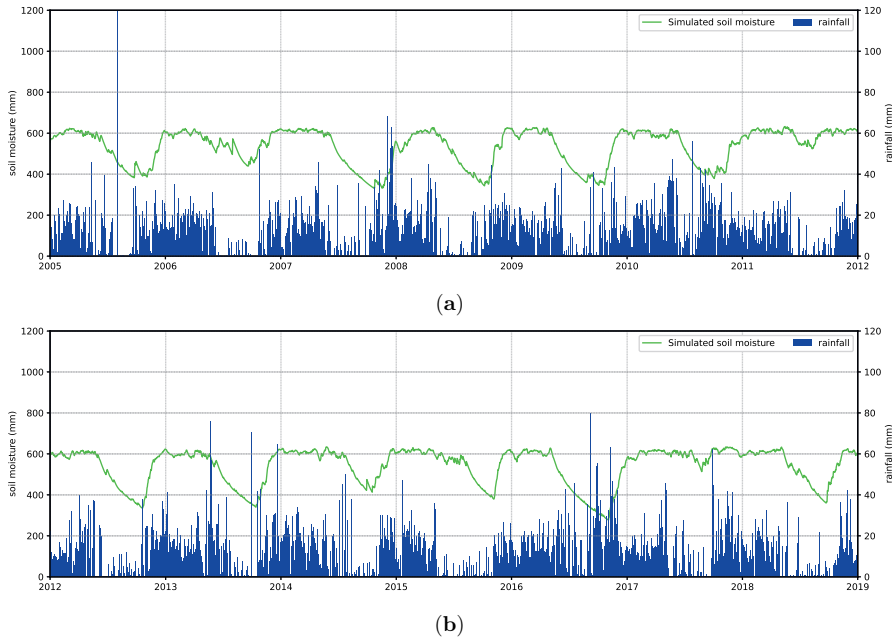


Figure 4.4: The simulated soil moisture under the Wflow_sbm model setup, plotted side by side with the CHIRPS rainfall data, during (a) the first half (2005 to 2011) and (b) the second half (2012 to 2018) of the simulation period. The model response based on the seasonal change is clearly indicated by the increasing soil moisture during the rainy season and the decreasing soil moisture during the dry season.

of the BGB, and (2) the GRACE water storage change estimated for the spatial domain of the GRACE grid surrounding (and including) the study area, plus its uncertainty bounds. As CHIRPS rainfall estimates are available in a higher resolution than GRACE, the rainfall estimates cover the same domain as the model-based estimates; and a smaller domain than the GRACE-based estimates at the same time.

Visually, the fluctuations of the rainfall estimates are predominantly in agreement with both water storage change estimates' dynamics, although several discrepancies remain. The seasonal patterns are well-captured. During the dry season between April and September, the values of both rainfall quantity and water storage changes generally fall. In contrast, during the rainy season between October and March, all of the variables' values appear to rise, although the two water storage estimates often increase to different extents. The discrepancies between the variables' dynamics become more apparent after 2015. During this period, as mentioned in Section 4.2.1, the GRACE dataset contains several missing values. With more detailed observation, we can also see the expected small time-lags of GRACE signal to the rainfall input compared to the simulated water storage change.

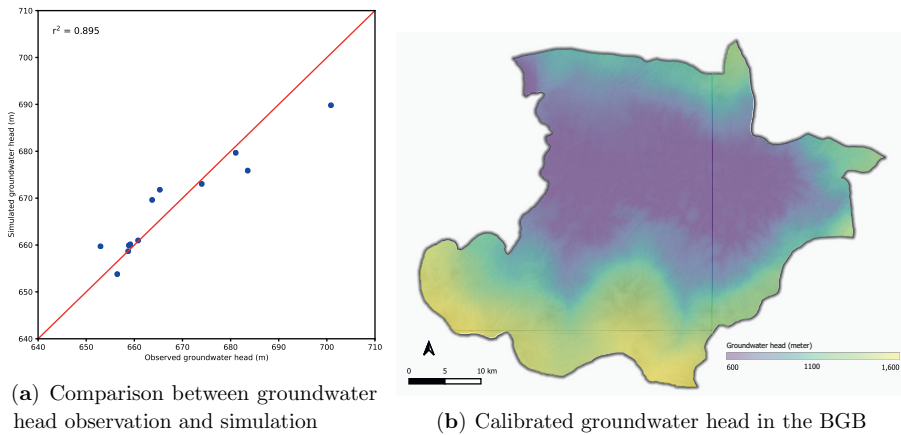


Figure 4.5: The groundwater model calibration results. Figure (a) shows the plot comparing the observed and simulated groundwater head in wells located in the flat terrain of the Bandung groundwater basin, with r^2 value of 0.895. Figure (b) shows the distribution and contour of the calculated groundwater head based on the calibrated parameters, indicating the influence of the surface topography on the groundwater table elevation.

The Pearson correlation coefficient between the input rainfall and GRACE estimates is calculated at 0.537. Meanwhile, the cross-correlation coefficient is calculated at 0.601, with an optimum temporal shift of one time-step. This means that on average, the GRACE-based water storage change estimates are lagging by a month compared to the rainfall. The Pearson correlation coefficient between the rainfall data and the simulated total water storage change, on the other hand, is higher compared to those with GRACE estimates, calculated at 0.706.

4.3.4 Water storage change estimates

The GRACE TWSC estimates including its uncertainty bounds and the one-way coupled model-based simulated water storage change are also shown in Figure 4.6. The simulated water storage change is equal to the sum of the soil moisture storage changes calculated by the Wflow_sbm and the groundwater storage changes calculated by the MODFLOW. Parallel to the rainfall visual assessment, the two water storage change estimates show similar dynamics, especially during the earlier period of the simulation between 2005 and 2015. Likewise, the timing between the two signals also seems to differ. The GRACE estimates tend to rise or fall one month behind the simulation. This is agreed by the previous cross-correlation analysis between the rainfall and the GRACE estimates. The peak magnitude, on the other hand, is arguably less consistent. During some peak water storage changes, the one-way coupled model simulation generates higher values compared to the GRACE estimates. A more comprehensive discussion on the matter is presented in

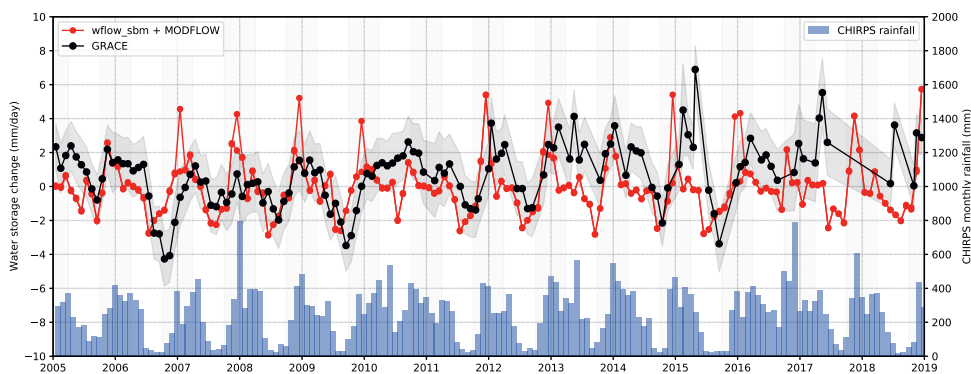


Figure 4.6: Time-series comparison between two water storage change estimates and the monthly CHIRPS rainfall data in the BGB. The two water storage change estimates are the model-based water storage change simulated under the spatial domain of specifically the BGB (red lines), and the GRACE-based water storage change estimated under the spatial domain of the GRACE grid surrounding (and including) the study area (black lines), plus its uncertainty bounds (grey-hatched area).

Section 4.4.2. On the whole, focusing on the period between 2005 and 2015 and considering the uncertainty bounds due to different spatial scales of the analyzed/measured domain, 62.1% of the simulated water storage change is calculated within GRACE estimates uncertainty bounds, with the Pearson correlation coefficient of 0.502.

4.3.5 Groundwater storage change simulation

Focusing on the governing budgets over the groundwater flow regime, as mentioned in Section 4.2.7, Figure 4.7 shows the simulated dynamic budgets of the groundwater recharge, groundwater abstraction, and groundwater storage changes in the BGB. Using the calculated values, we are able to determine the overall status of certain groundwater budget trends during the simulation period. The groundwater storage change is calculated at -0.14 mm/day on average, and its long-term trend clearly indicates a sustained decline. Our results also suggest that the groundwater storage of the BGB is depleting at an average rate of 87 million m^3/year .

Groundwater storage depletion is reflected through dwindling groundwater tables. Figure 4.8 shows the time series of the average and largest groundwater head changes in both the unconfined and confined aquifers. In the unconfined aquifer, the water table elevation along the smaller upstreams locally rises as much as 5 cm/year on average, seemingly by gaining water from the river baseflow (orange line). In other locations, especially the flat terrain area of the basin, the water table elevation is slowly and steadily falling (yellow line). The maximum water table drawdown (pink line) is found near the center of the

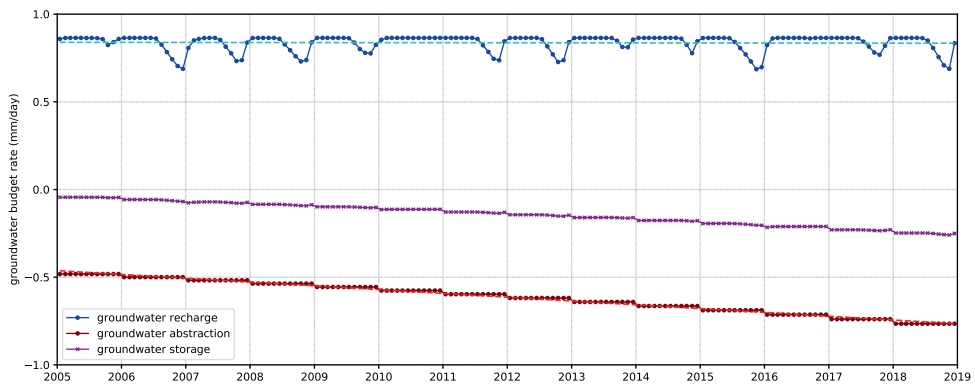


Figure 4.7: The time-series plot of the groundwater storage change simulation result, including its governing budgets of groundwater recharge and groundwater abstraction. The trend lines show that despite a relatively constant recharge average, groundwater storage in the BGB is depleting at an even faster rate than the groundwater abstraction increase, indicating the domino effect of groundwater abstraction on the dwindling groundwater table.

basin, in the intersection between the domestic and industrial abstraction areas. Although a total water table decrease of 2.7 meters does not seem significant, it represents the whole grid size of 100 m x 100 m. The local drawdown around the associated abstraction well is theoretically much higher than the grid-representative groundwater head decrease. On the other hand, in the confined aquifer where there is more concentrated and intense groundwater abstraction, the groundwater head drawdown is found more profound than those in the unconfined layer. There is a stark difference between the average and the maximum groundwater head drawdown in the unconfined aquifer (purple line). The fact that the maximum groundwater head drawdown is located under the industrial abstraction area indicates the severe effect of local drawdown in the confined aquifer. However, the average groundwater head changes of the confined aquifer are relatively similar to those of the unconfined aquifer, discussed in Section 4.4.4.

4.4 Discussion

4.4.1 Assumptions and limitations of the simulations

Uncertainties and limitations are always present in hydrological research, albeit from the quality of the input data, measurements and calibration variables, model structure and parameterization, etc (Liu and Gupta, 2007; Ahmadi and Nasseri, 2020; Moges et al., 2021). The fact that the BGB is a data-scarce area and several assumptions have to be made throughout the research propagates the uncertainties to the research outcome.

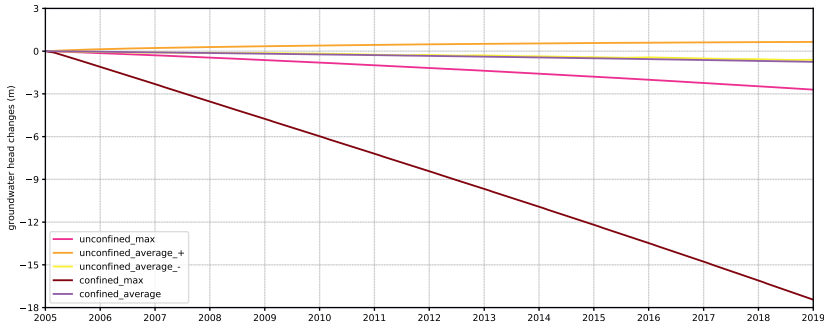


Figure 4.8: The time-series simulation of the average and maximum groundwater head changes in both the unconfined and confined aquifers. The ‘_average’ variables are taken from the spatial mean values, while the ‘_max’ values are found at the center of the basin under the intersection between the domestic and industrial abstraction area for the unconfined layer, and the north-west periphery section for the confined layer.

In this study, groundwater recharge is a very important variable as it couples the `Wflow_sbm` to the MODFLOW model. Under a more ideal situation, the `Wflow_sbm` model could be better calibrated by comparing the simulation results with direct recharge measurement. Previous studies have shown the benefit of using such an approach (Misstear et al., 2009; Dong et al., 2021). However, since recharge measurement data are not available, we instead calibrate the hydrological model on the basis of river discharge comparison. In addition to that, for a catchment with relatively high annual rainfall like the BGB, the uncertainties of the estimated recharge in terms of spread are found to be wider compared to ones with lower rainfall (Zhu et al., 2020a). This is, however, unavoidable considering the data availability.

There are also several assumptions made for the groundwater flow model parameterization. The soil data, including the hydraulic conductivities, storage parameters, and lithology profiles, are mostly concentrated in a few locations, while these properties in the more elevated areas are largely unknown. For the global groundwater flow modeling, this might not be an issue with the availability of global gridded hydrogeological datasets, such as GLHYMPS (Gleeson et al., 2014) and its updated version of GLHYMPS2.0 (Huscroft et al., 2018). For regional groundwater flow models, however, using these data is not scale-wise fitting. Additional future field campaigns and in-situ measurements could increase the dependability of the groundwater model parameterization. The groundwater flow model is also calibrated in a steady-state simulation, as time series of groundwater level measurements are not available. Should the groundwater monitoring management has improved, calibrating the groundwater flow model on transient simulation would strengthen the level of confidence and reliability of the simulation.

The assumption of negligible surface water storage components from the GRACE estimates could also be criticized (see Equation 4.1). Within the GRACE grid covering the BGB, there are three concentrated surface water reservoirs. This could influence the GRACE estimation of the TWSC, especially considering the nature of the non-uniform spatially distributed surface water that plays an important role in GRACE accuracy over the TWSC estimates (Longuevergne et al., 2013). In this study, the surface water component is assumed negligible as they are located outside of the BGB (despite still falling within the GRACE measurement grid). Their total surface area of less than 200 km² is also assumed relatively insignificant compared to the GRACE grid size of approximately 12,000 km² along the equator. In future studies, nonetheless, there is an opportunity to incorporate their effects into the GRACE water storage estimates analysis.

4.4.2 Model simulation and GRACE comparison in estimating TWSC

The hydrological simulation using `Wflow_sbm` improves the results from previous study (Rusli et al., 2021), shown by the closer estimates of average simulated discharge to the observation and the improved KGE (Kling et al., 2012), NSE (Nash and Sutcliffe, 1970), and RMSE. The groundwater flow simulation has an r^2 of 0.895 between the simulated and observed water table elevation during model calibration. The combination of two well-grounded simulations increases the confidence in water storage change estimates calculated by the one-way coupled models.

The visible time lags between the GRACE and model-simulated water storage change estimates, where GRACE estimates are mostly found to lag, are not spotted for the first time. This trend is also noticed in previous research (Zhong et al., 2019; Neves et al., 2020; Salam et al., 2020). Some research found that the lag-time ranges between two and four months (Hachborn et al., 2017; Rahimzadegan and Entezari, 2019; Fatolazadeh and Goïta, 2021), and was spatially variable. Considering the seasonal pattern in the BGB, the water storage change simulation tends to overestimate GRACE only during the wet seasons (grey light-hatched zones, Figure 4.6), and gives better results in dry seasons. While its performance to detect seasonal trends has been evaluated in a number of studies (Getirana et al., 2020; Tangdamrongsub and Šprlák, 2021), research focusing on GRACE accuracy varying between different seasons is very limited. Additionally, in this study, the simulated water storage change is estimated in a basin where the slope is steeper and the elevation is higher compared to the larger area measured by GRACE. The behavior of different responses in the water storage change during the wet seasons does make sense considering the respective associated basin characteristics. With all the above-mentioned contexts involved, the r between the simulation and GRACE estimates of 0.502 is considered acceptable, as it is comparable with other basin-scale research on the same topic (Yirdaw and Snelgrove, 2011; Tang et al., 2017; Zhong et al., 2018; Liu et al., 2020; Jyolsna et al., 2021).

4.4.3 GRACE aptness to assess basin-scale groundwater storage change

The spatial scale difference between the GRACE measurements and the basin size, as well as the local hydrological and hydrogeological properties, is one of the key reasons behind the discrepancies between TWSCs in Figure 4.6. Although both lines represent the estimated water storage change, they are measured/simulated under different (albeit overlaying) domains. The results in this paper are fully agreed with previous studies which show that despite having good agreement on water storage change estimates on a regional scale, related local data/measurements are found to have higher variance in their values compared to GRACE dataset whose estimates are based on larger spatial domain (Zhang et al., 2019; Rzepecka and Birylo, 2020; Li et al., 2021). This highlights the importance of considering the spatial scale and local/regional features when applying GRACE to assess basin-scale groundwater storage changes.

In addition, it is also important to recognize the dominant water storage component. In the BGB, the status of the soil moisture and the groundwater storage change, according to the one-way coupled model simulation, are occasionally found in reverse; the soil moisture storage often decreases at the same time the groundwater storage increases. This trend is also supported in other research (Pokhrel et al., 2013). During periods when they are identified under the same state, the water storage change is dominated by the change of the soil moisture component, contributing up to 74.8% of the total water storage change. Therefore, the signals captured by GRACE are contributed mostly by the water storage change in the shallow soil layer instead of the deeper saturated zones. While both soil moisture and groundwater storage are considered the subsurface component of the water storage, the term 'subsurface' includes numerous spatial coverages from the root zones, shallow vadose zones, to the elastic and storage partitions of the groundwater system.

Nevertheless, in many basin-scale data-scarce areas where groundwater storage assessment is limited by the availability of direct observation data, GRACE estimates are undeniably valuable (Rodell et al., 2007). However, although it could be utilized as an alternative tool to observe the groundwater storage general trend, even on a basin-scale domain (Skaskevych et al., 2020), its spatial footprint should always be taken into account. It covers the local contexts, for example, related to the existence of lakes, reservoirs, and coastal lines, as well as the incorporated spatial characteristics variability (slope, elevation, land use, land cover, etc) within the measurement domain. Indeed, general conclusions are derivable from GRACE estimates in regional-scale basins (Abou Zaki et al., 2019), however, the importance of local data, when available, should always be prioritized. The hydrological attributes of the basin surrounding the measurement area could also impact the quality of GRACE estimation. In this study, for example, the local impact of groundwater abstraction has to be detected from groundwater table measurements in observation wells near the abstraction wells. GRACE estimates, in comparison, measure the storage changes on a much larger scale and are relatively insensitive to local groundwater table changes.

In fact, it has been shown in previous studies that GRACE groundwater storage depletion often underestimates global hydrologic model output in heavily exploited aquifers (Rateb et al., 2020). While both GRACE and modeling methods could be well-quantified, putting context and critical thinking in interpreting each estimate is indispensable.

4.4.4 Present status of the BGB groundwater storage

The result of groundwater storage simulation (Figure 4.7), indicates unsustainable groundwater management, involving many aspects from groundwater recharge to groundwater abstraction. Surprisingly, the groundwater recharge's trend is shown not to be falling, which is in contrast to some of the previous research results of decreasing groundwater recharge under changing climates (Serrat-Capdevila et al., 2007; Holman et al., 2009; Dams et al., 2012). However, despite the positive gradient of the recharge regression line, it is visually apparent that the recharge generally gets lower towards the end of the simulation period. The fact that 2010 was a significantly wet year with a high number of rainy days induces the recharge to be constantly high throughout the year. By removing the extreme wet year of 2010, the trend of the recharge would reverse to a declining direction. On the other hand, the increasing groundwater abstraction is clearly indicated by the red bottom lines. It constantly increases during the simulation period, starting from an average equivalent of 0.48 mm/day in 2005 to 0.76 mm/day in 2018. In practice, groundwater abstraction has been expanding not only in its volume but also in its flow rate and its spatial distribution. In summary, the combination of the changing groundwater recharge and groundwater abstraction drives groundwater storage depletion. Although several methods in separating climatic and anthropogenic factors to the groundwater storage changes have been developed (Wang et al., 2019; Zhong et al., 2019; Su et al., 2022), our assessment clearly indicates the dominance of the human factor in the current groundwater storage depletion. Given the water demand situation in the study area, such groundwater exploitation might be unavoidable. However, active actions are still necessary to be taken in response to the currently depleting groundwater storage.

Focusing on groundwater abstraction, it is important to recognize the potential effect of multi-layer pumping. Not only do they dwindle groundwater table but also, to certain extents, influence regional groundwater flow regime (Wang et al., 2019). Directly, spatially concentrated abstractions create local cones of depression (Sun et al., 2011). Indirectly, groundwater abstraction from deeper aquifers impacts the groundwater table in shallow aquifers, as decreasing groundwater head in lower aquifers means increasing head gradient between aquifers (Zimmermann et al., 2017). In the BGB, specifically, the interaction between the shallow and the deep aquifer through vertical flow leakage was identified. Previous results on high dichlorodifluoromethane (CFC-12) tracing reveal young groundwater from samples taken in the upper layer of the deeper aquifers (Taufiq et al., 2017). In our study, such leakage is hypothesized through groundwater head changes of the confined aquifer under the industrial abstraction area (Figure 4.8). Despite having spatially more

concentrated and higher volumes of groundwater abstractions, the average groundwater head decrease in the confined layer is relatively similar to one in the unconfined layer, seemingly due to the potential leakage from the upper to the lower aquifer. The dwindling groundwater tables from the upper aquifers also impact the flow characteristics exchanged between the groundwater and surface waters, especially along rivers. The different gradient of groundwater storage depletion compared to the gradient of increasing groundwater abstraction (Figure 4.7) indicates that the groundwater storage change processes cannot be explained solely by the dynamics of groundwater abstraction, as they involve numerous feedback among variables associated in subsurface flows. This hypothesis is further tested and analyzed in Chapter 5.

Alarming, based on the groundwater storage budget shown in Figure 4.7, the withering groundwater storage rate is calculated at approximately 87 million m³/year. The long-term average groundwater storage change in the BGB has been negative since the beginning of the simulation. The fact that the groundwater storage depletion rate is simulated in a comparable degree to both the groundwater abstraction increasing rate and the recharge decreasing rate combined signals a warning. The combination of multiple groundwater table drawdowns, as a consequence of human exploitation of groundwater, has causal sequences on the groundwater flow regime in a bigger picture when it impacts the flow between the groundwater, the river baseflow, and the constant head boundaries. Under the currently increasing groundwater abstraction, the negative trend of groundwater storage changes points out the unsustainable groundwater management policy in the BGB.

4.5 Conclusions

In this study, our objective is to quantify the basin-scale water storage change in the BGB. We achieve this by one-way coupling of the hydrological model Wflow_sbm to the groundwater model MODFLOW, where groundwater recharge generated by the Wflow_sbm model simulation is used to drive the groundwater flow model. The simulation result is compared to GRACE estimates, including its uncertainty bounds, with the simulation period between 2005 and 2015.

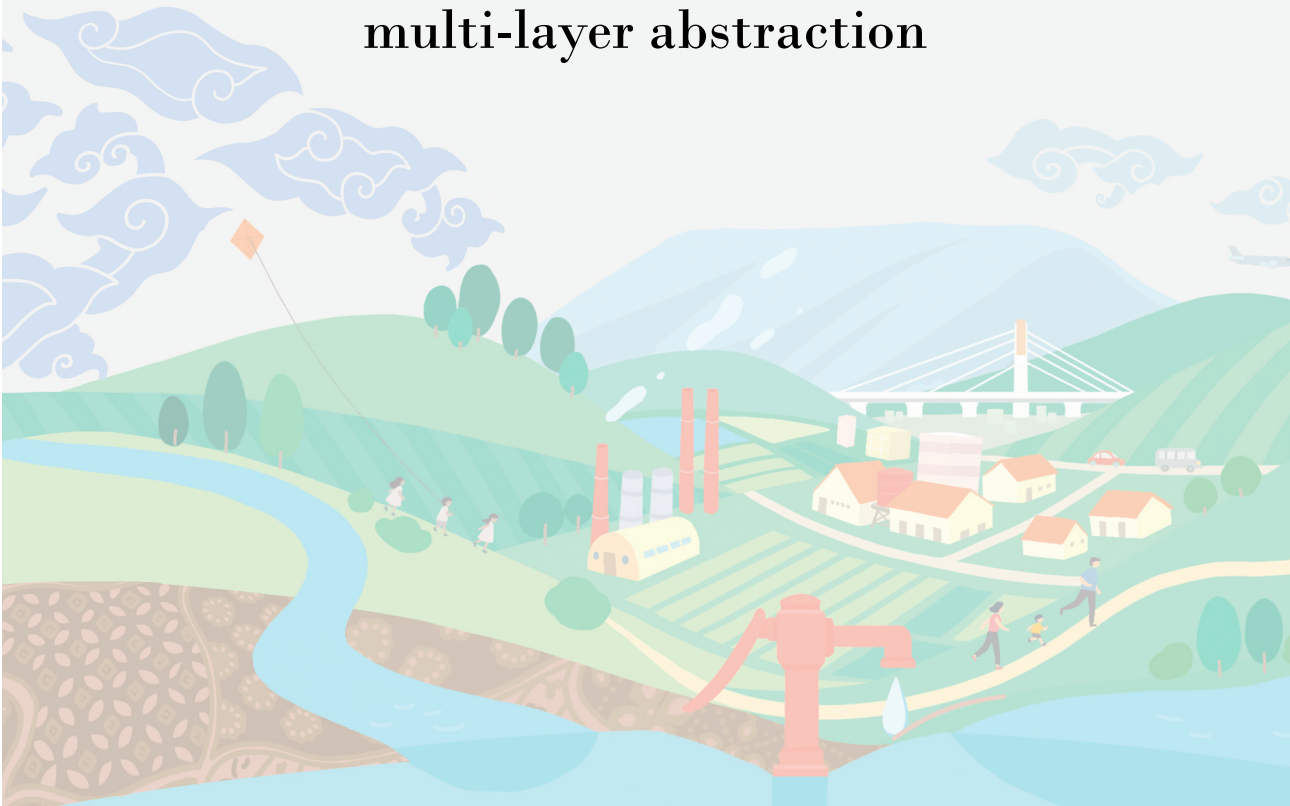
The Wflow_sbm model is forced with CHIRPS rainfall data and ERA5-derived potential evapotranspiration. The groundwater flow model is parameterized using fieldwork-based data. We simulate the groundwater flow under changing recharge (monthly) and abstraction (annually) to assess the dynamics of the groundwater storage change. To ensure consistency between the GRACE estimates and the rainfall data, we filter out the periods after 2015 where several GRACE estimates are missing. We also implement a cross-correlation function in addition to the Pearson correlation coefficient to take into account the expected signal time lag that occurred due to the spatial scale differences between the GRACE measurement and the one-way coupled model domain. This led to a cross-correlation coefficient of 0.601.

The combination of soil moisture storage change from Wflow_sbm and groundwater storage change from MODFLOW is compared with the GRACE water storage change estimates. Visual comparison suggests good agreement between the two estimates with a cross-correlation coefficient of 0.502, and 62.1% of the simulated water storage change falls within the GRACE estimates uncertainty bounds. Based on the groundwater flow model simulations, the BGB storage is currently depleting at a rate of approximately 87 million m³/year. Our model simulations expose the unsustainability of the current groundwater management. Further research on aquifers' response to groundwater abstraction, both locally and regionally, and from both of the layers (upper and lower aquifers), could be paramount in deriving suitable future groundwater management policy in the BGB and other similar basins in data-scarce areas.



Chapter 5

Aquifer interaction induced by multi-layer abstraction



This chapter is mostly based on and adapted from:

S. Rusli, A. Weerts, S. Mustafa, D. Irawan, A. Taufiq, and V. Bense (2023b).
“Quantifying aquifer interaction using numerical groundwater flow model
evaluated by environmental water tracer data: Application to the data-scarce
area of Bandung groundwater basin, West Java, Indonesia”.

Journal of Hydrology: Regional Studies 50, 101585.
doi: <https://doi.org/10.1016/j.ejrh.2023.101585>

Abstract

Study Region: Bandung Groundwater Basin (BGB), Indonesia.

Study focus: Groundwater abstraction of various magnitudes, pumped out from numerous depths in a multitude of layers of aquifers, stimulates different changes in hydraulic head distribution, including ones under vertical cross-sections. This generates groundwater flow in the vertical direction, where groundwater flows within its storage from the shallow to the underlying confined aquifers. In the BGB, previous studies have identified such processes, but quantitative evaluations have never been conducted, with data scarcity mainly standing as one of the major challenges. In this study, we utilize the collated (1) environmental water tracer data, including major ion elements (Na^+/K^+ , Ca^{2+} , Mg^{2+} , Cl^- , SO_4^{2-} , HCO_3^-), stable isotope data (^2H and $\delta^{18}\text{O}$), and groundwater age determination (^{14}C), in conjunction with (2) groundwater flow modeling to quantify the aquifer interaction, driven mainly by the multi-layer groundwater abstraction in the BGB, and demonstrate their correspondence. In addition, we also use the model to quantify the impact of multi-layer groundwater abstraction on the spatial distribution of the groundwater level changes.

New hydrological insights for the region: In response to the limited calibration data availability, we expand the typical model calibration that makes use of the groundwater level observations, with in-situ measurement and a novel qualitative approach using the collated environmental water tracers (EWT) data for the model evaluation. The analysis in the study area using EWT data and quantitative methods of numerical groundwater flow modeling is found to collaborate with each other. Both methods show agreement in their assessment of (1) the groundwater recharge spatial distribution, (2) the regional groundwater flow direction, (3) the groundwater age estimates, and (4) the identification of aquifer interaction. On average, the downwelling to the deeper aquifer is quantified at 0.110 m/year, which stands out as a significant component compared to other groundwater fluxes in the system. We also determine the unconfined aquifer storage volume decrease, calculated from the change in the groundwater table, resulting in an average declining rate of 51 Mm^3/year . This number shows that the upper aquifer storage is dwindling at a rate disproportionate to its groundwater abstraction, hugely influenced by losses to the deeper aquifer. The outflow to the deeper aquifer contributes to 60.3% of the total groundwater storage lost, despite representing only 32.3% of the total groundwater abstraction. This study shows the possibility of quantification of aquifer interaction and groundwater level change dynamics driven by multi-layer groundwater abstraction in a multi-layer hydrogeological setting, even in a data-scarce environment. Applying such methods can assist in deriving basin-scale groundwater policies and management strategies under the changing anthropogenic and climatic factors, thereby ensuring sustainable groundwater management.

5.1 Introduction

The impact of anthropogenic factors on water storage depletion, especially through groundwater abstraction, has been detected from catchment to global scales. In the Heihe River basin, China, the human-induced footprint is quantified to cause a net negative to the terrestrial water storage (TWS) change derived from the gravimetric satellite data of Gravity Recovery and Climate Experiment (GRACE), despite the positive climate-driven TWS anomalies simulated by land surface models of Global Land Data Assimilation System (GLDAS) (Zhong et al., 2019). In the transboundary Aral Sea basin of the Eurasian region, up to 75.24% of the basin TWS change is influenced by human activities (Yang et al., 2021). In a global-scale analysis, the anthropogenic factor has been identified as exerting dominant control over the continuous decline of TWS in major river basins between 2002 and 2010 (Felfelani et al., 2017). These depleting groundwater storages encompass changes on multiple hydrogeological partitions, including processes in both shallow unconfined aquifers and deep confined aquifers (McNamara et al., 2011). As groundwater abstraction is the direct factor in contact with these subsurface stratifications, the ability to quantify its impact on the changes in groundwater storage and its flow regime is highly important.

In areas whose hydrogeological profile consists of vertically diverse lithologies, groundwater abstraction affects not only the groundwater storage dynamics but also the overall groundwater system, both directly and indirectly (Wang et al., 2019). Directly, groundwater abstraction depletes groundwater storage and dwindles the groundwater table or the piezometric head of the respective aquifers it extracts from. Indirectly, the steeper groundwater head gradient between overlying aquifers, resulting from groundwater abstraction across multiple aquifer layers, stimulates inter-aquifer groundwater movement from upper to lower aquifers (Russo and Lall, 2017). This flow is referred to as aquifer interaction. As a result, the deep aquifers' storage eventually gains water while the shallow aquifers' storage, in contrast, loses water, without influencing the groundwater storage change as a whole. The cumulative impact of the internal water movement leads to potentially severe groundwater-related problems that could not be understated. In Beijing, China, land subsidence is analyzed to be influenced by not only the groundwater abstraction but also the subsurface hydrogeological layer structure (Li et al., 2017), which, as described above, is the primary factor driving the aquifer interaction. In the Western part of the United States, the confined groundwater storage loss due to aquifer compaction driven by groundwater abstraction has caused soil stability perturbation that poses significant damages to infrastructure (Smith and Majumdar, 2020). Therefore, in-depth storage partition-based analysis with an emphasis on aquifer interaction, complementing the integrated groundwater storage change analysis, is crucially relevant to support the development of sustainable groundwater management practices.

To investigate subsurface water movement and groundwater flow, transport, and dynamics, analysis using environmental water tracers' (EWT) properties have been widely applied (Turnadge and Smerdon, 2014; Chambers et al., 2019; Kurukulasuriya et al., 2022). EWT has also been used to gain a conceptual understanding of a hydrogeological system behavior (Cowie et al., 2014; Doveri and Mussi, 2014). However, it is often necessary to incorporate other perspectives to enhance groundwater system assessment, as the EWT method possesses numerous limitations from uncertainties (Larocque et al., 2009), measurement bias (McCallum et al., 2014), to cost, time, and expertise (Kurukulasuriya et al., 2022), and more importantly, it does not always come up with quantitative values in its output. In data-scarce areas, additionally, EWT measurement data often suffer from low quality, including incomplete variables, lack of metadata, basic descriptions, and inconsistent measurements. In these types of data-restricted areas, unfortunately, other hydrogeological data such as lithological profiles and groundwater table measurements are usually also in short supply. Such a case appears in the data-scarce area of Bandung Groundwater Basin (BGB), Indonesia. The situation of limited groundwater-related data availability in the study area has been previously reported (Rusli et al., 2021; Rusli et al., 2023a). Regarding aquifer interaction, a prior study in the BGB identified vertical groundwater leakage from the shallow to the deep aquifer through high dichlorodifluoromethane (CFC-12) tracing that reveals young groundwater in the upper layer of the deeper aquifers (Taufiq et al., 2017). Such a proposition, however, is based on only a one-time sampling and measurement, and was only qualitatively interpreted, but not quantitatively constrained.

Sustainable groundwater management and policy planning require accurate spatiotemporal groundwater flow quantification, including ones among and within the aquifers. While some EWT data are available in the BGB, it is challenging to translate the EWT-based hypothesis to a tangible groundwater management policy without detailed quantification of the internal fluxes among the aquifers. Although it is possible to take a quantitative approach by constructing a site-specific numerical groundwater flow model, such an approach has not been extensively explored. Primarily, this occurs due to the limited availability of groundwater table data that are typically used as groundwater flow model calibration data. Granted such data are available, however, their spatial and temporal distribution and density could be deemed insufficient, leaving a gap within the groundwater flow model evaluation. In this context, the integration of these two approaches could emerge as the optimal alternative in regions with limited data availability. This concept of combining EWT data and hydrological models has been demonstrated to offer valuable insights in data-scarce environments. Therefore, in this study, we propose a framework to utilize EWT data in conjunction with a numerical groundwater flow model to quantify the aquifer interaction driven by multi-layer groundwater abstraction in the BGB. Using our framework, we intend to in concert assess both the EWT measurements and the numerical groundwater flow model. We compare and demonstrate their compatibility to reinforce each method's output. The EWT data-driven qualitative analysis is used

to conceptually evaluate the numerical groundwater flow model simulation. Meanwhile, the numerical model fills the quantitative and spatial information gap resulting from the limited availability of EWT data. Using the groundwater flow model, we are also able to quantify the impact of the aquifer interaction, driven by the multi-layer groundwater abstraction, on the basin groundwater level changes. We expect that the outcome of this research will greatly assist in deriving future groundwater regulation and management in the BGB.

5.2 Material and methods

5.2.1 Environmental water tracers data

All the EWT data analyzed in this study are freely accessible and hosted on an open repository QGIS-cloud platform (Irawan et al., 2016). They were collected in more than 20 different projects conducted between 2007 and 2009. Subsequently, these datasets were collated into one integrated open-source groundwater database, funded by the Directorate General of Higher Education and the Ministry of Research of Indonesia in 2016. It's worth noting that these datasets were not collected continuously, thus time-series analysis is hardly feasible. Nevertheless, for the purposes of this study, they have been combined with additional EWT data collected in 2015 (Taufiq et al., 2017). This combined dataset aids in qualitative interpretations and in evaluating the numerical model simulations.

There are a total of 65 sampling locations for major ion element measurements, distributed as follows: 30 points for the deep aquifer, 19 for the shallow aquifer, 3 for water springs, and 13 for surface water (river). The measured chemical components include the cations of Na^+/K^+ , Ca^{2+} , and Mg^{2+} , and the anions of Cl^- , HCO_3^- , and SO_4^{2-} . The data are, unfortunately, spatially clustered dominantly in the northern part of the flat terrain of the basin for the deep groundwater samples and the western part for the shallow groundwater samples. There are also 72 points of stable isotope measurements of deuterium ($\delta^2\text{H}$ or δD) and oxygen-18 ($\delta^{18}\text{O}$). These measurements are distributed as follows: 36 samples from the deep aquifer, 19 from the shallow aquifer, 14 from river water, and 3 from rainfall. Most of these sampling points are located in proximity to the major ion element measurement locations. The radiocarbon (^{14}C) content was measured in 22 locations to estimate groundwater age, along with their associated uncertainties. These measurements were exclusively conducted in the deep aquifer. The locations and measurement data for all these samples are depicted in Figure 5.1.

The groundwater flow model parameterization involves fieldwork and data collection in the study area in 2020. These efforts produce estimates of the upper aquifer's hydraulic conductivities. Specifically, we conducted slug tests at 25 spatially distributed locations to measure the horizontal hydraulic conductivities of the soil. Additionally, soil samples were taken from these locations for grain size analysis, and flow-through tests in the laboratory

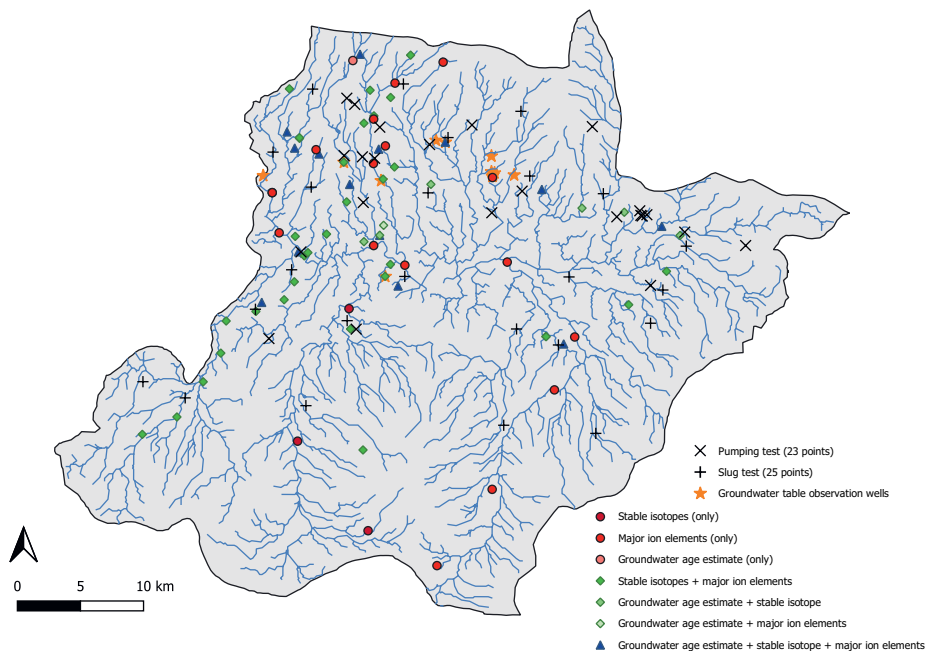


Figure 5.1: Groundwater data location in the BGB. These data encompass stable isotopes, major ion elements, and groundwater age estimates. Different types of measurements at each location are indicated by distinct symbols: red circles for locations with only one type of measurement available, green diamonds for locations with two types of measurements, and blue triangles for locations with all three types of measurements. This spatial representation helps visualize the distribution and coverage of groundwater data across the basin.

were conducted to measure vertical hydraulic conductivity. We gathered 23 validated pumping test reports, conducted in 2019, to estimate the specific storage parameter and the hydraulic conductivity of the deep aquifer. All of the data of the groundwater flow model were also used in our previous studies (Rusli et al., 2023a), and their locations are also shown in Figure 5.1. Given the limitations in terms of data depth and quantity, we recalibrated the model parameters during the model spin-up phase. This recalibration involved comparing the model's groundwater head simulation results with observation data. However, it's important to mention that only a limited number of groundwater observation wells are consistently monitored within the basin. We have addressed the parameter calibration and data limitation comprehensively in our previous study (Rusli et al., 2023a). To enhance the model prediction's reliability, additional model evaluation is necessary due to the differing purpose of the current study. Therefore, we assessed the model's simulation capability by utilizing the available EWT data.

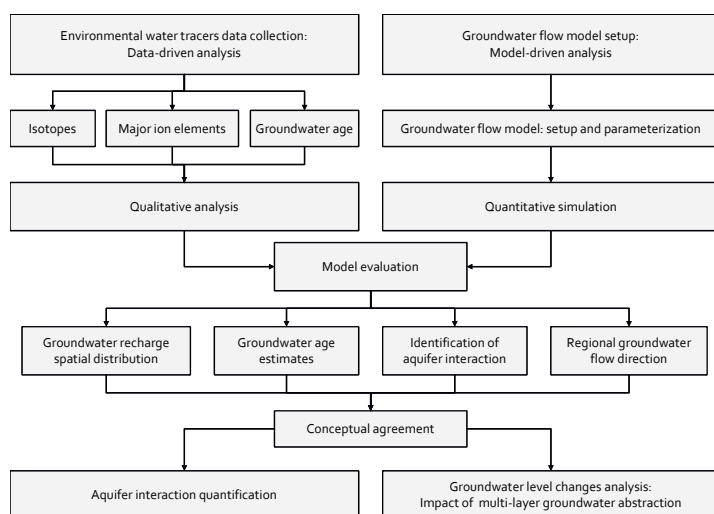


Figure 5.2: The detailed flowchart of the research methodologies. The analysis is divided into two main parts: the data-driven analysis based on hydrogeochemistry data on the left and the model-driven analysis based on the groundwater flow model simulation on the right. After the model evaluation, the assessment focuses on the quantification of inter-aquifer interaction and its impact on groundwater level changes.

5.2.2 Experimental design

The research framework involves two initially independent processes: (1) a qualitative data-driven analysis using the collated EWT data and (2) a quantitative model-driven approach using the numerical groundwater flow model. Once each part has been established, they are mutually assessed and evaluated in terms of the groundwater recharge spatial distribution, regional groundwater flow direction, groundwater age estimates, and the identification of aquifer interactions. Following this assessment, the numerical groundwater flow model is employed for further analysis of the BGB. This analysis focuses on aquifer interaction and changes in the groundwater table over the simulation period. The overall research framework is depicted in Figure 5.2.

5.2.3 Environmental water tracer data analysis

In deriving the qualitative data-driven analysis, we focus on three different EWT data: (1) the major ion elements data, (2) the groundwater age data, and (3) the stable isotope data. Our analysis revolves around their spatial patterns, including their distribution across the basin, variations in their values across different locations, and their potential relationships with other pertinent information such as land use and land cover data or groundwater abstraction zones. In some instances, we employ spatial interpolation techniques to assess how these values are distributed in and around unmeasured locations.

We assess the major ion element data by plotting the measured values in Stiff diagrams (Stiff, 1951), categorizing the data according to the samples' sources (rainfall, river, shallow, and deep groundwater). The stiff diagram describes the chemical state of the water samples by assembling the cations on the left side of the box, with sodium-potassium (Na^+/K^+) at the top, calcium (Ca^{2+}) at the middle and magnesium (Mg^{2+}) at the bottom and the anions on the right side (chlorine/ Cl^- at the top, sulfate/ SO_4^{2-} in the middle, and bicarbonate/ HCO_3^- at the bottom). We visualize the spatial distribution of the major ion element data by overlaying the Stiff diagrams on the BGB map. We also combine our analysis with information that we have from other studies on major ion elements (Taufiq et al., 2017), which include an additional 40 samples from shallow groundwater and 65 samples from deep groundwater.

The groundwater age estimates are calculated based on the radiocarbon (^{14}C) content of 22 samples collected from confined aquifers with a screen depth of more than 100 meters. We overlay this data with the BGB map and deep groundwater abstraction zones to explore potential correlations between these variables. Due to the limited data points, we spatially interpolate the point-based groundwater age estimates to rasterized area estimates based on the inverse distance weighting (IDW) interpolation. Having said that, it's crucial to interpret these groundwater age profiles cautiously, as they are spatially poorly distributed. Additionally, field conditions often hold more complexities and processes due to spatial heterogeneities and transient effects (Post et al., 2013).

The stable isotope data are sourced from four water sample categories: rainfall, surface water (river), shallow groundwater, and deep groundwater. Similar to the previous two EWT data, we overlay the stable isotope data on the BGB map, categorized by the samples' sources, this time according to the $\delta^{18}\text{O}$ value. We also plot the correlation between the $\delta^2\text{H}$ and $\delta^{18}\text{O}$ and compare the calculated local meteoric water line (LMWL) with the global meteoric water line (GMWL) to assess the processes of the water cycle, starting from the precipitation as the input source (Wang et al., 2018; Chen et al., 2021). To investigate the subsurface water processes and the pattern of how the stable isotope composition alters over depth, we plot the correlation between the $\delta^{18}\text{O}$ of the groundwater sample and the depth at which the samples were taken from.

5.2.4 Groundwater flow model setup

The groundwater flow model setup in this study is the continuation of our previous version (Rusli et al., 2023a), built using the MODFLOW python package flopy (Bakker et al., 2016). MODFLOW is an open-source, spatially distributed, groundwater flow model developed by the U.S. Geological Survey (USGS), written using a modular object-oriented design (Hughes et al., 2017). These modular objects are expressed as packages in MODFLOW and are assignable to the main model and simulations. Physically, these objects distinctly represent, for example, rivers, abstraction wells, etc. Such a concept creates unique applications

of the packages from one case to another, as any available modules can be attached or detached from the model structure. In this study, we use the latest MODFLOW version 6 (MODFLOW6), which solves the three-dimensional groundwater flow equation described by Darcy's law (Equation 5.1) using control-volume finite-difference (CVFD) method (Langevin et al., 2017).

$$\frac{\partial}{\partial x} \left(K_{xx} \frac{\partial h}{\partial x} \right) + \frac{\partial}{\partial y} \left(K_{yy} \frac{\partial h}{\partial y} \right) + \frac{\partial}{\partial z} \left(K_{zz} \frac{\partial h}{\partial z} \right) + Q_s = S_S \frac{\partial h}{\partial t} \quad (5.1)$$

where K is the hydraulic conductivity in corresponding directions, Q_s is the volumetric flux per unit volume representing sources and sinks, and S_S represents the specific storage component of the porous material.

In accordance with the simplified interpretation of the BGB's hydrogeological setting (Figure 2.3), the numerical groundwater flow model is spatially discretized into a vertically 3-layer model, with a horizontal grid size of 100m \times 100m. The surface elevation is determined based on MERIT-DEM data (Yamazaki et al., 2017). The thickness of each layer is interpolated based on the available borehole data (Rahiem, 2020). The hydraulic and aquifer properties, including the horizontal (K_h) and vertical (K_v) hydraulic conductivities of each layer and the storage parameters of both specific yield (S_y) and the specific storage (S_s), are taken from fieldwork data and official reports to the government described in Chapter 2. The simulation is forced with the groundwater recharge calculated by the previously established hydrological model `wflow_sbm` (Rusli et al., 2023a), during the period between 2005 and 2018. River boundaries are delineated using the hydrology toolbox in ArcGIS. The MODFLOW well package is configured to simulate groundwater abstraction from areas estimated based on land use data. Wells are assigned to each grid cell that intersects with building-related land use from the national land use database. Within this set of wells, domestic groundwater abstraction is applied to the upper aquifer (unconfined) layer, with the abstraction rates' distribution derived from the total estimated groundwater withdrawal presented in Table 5.1 and the number of intersected cells. For the confined layer, wells are assigned to each grid that intersects with the industrial area and applied to the lower aquifer (confined) layer. The abstraction volume is implemented transiently with an annual increase to account for changing abstraction rates over time, estimated in our previous study (Rusli et al., 2021). A no-flow boundary is set up along the basin's perimeter, given its location in the uppermost part of the watershed system. The higher elevated area in the northern part of the basin does not serve as a flow boundary due to the presence of a geological fault named the Lembang fault, which separates the groundwater flow system. A constant head boundary is applied at the downstream part of the basin, following the water table in the downstream reservoir. Table 5.1 below lists all the groundwater flow model parameters and setup used in this study. Further, Figure 5.3 shows the north-south and the west-east cross-section of the numerical groundwater flow model. The red, blue, and green bars, respectively, scattered in the model cross-section,

Table 5.1: Groundwater flow model parameter

Parameters and/or forcing data		Values (in range, optimized, and vary spatially/temporally)
Grid size	horizontal direction	100m × 100m
	vertical direction	3-layers, varying elevation
Initial condition (head) ¹	layer 1	627.5m to 1608.0m
	layer 2	565.9 m to 1206.1m
	layer 3	504.2m to 1344.2m
Groundwater recharge	calculated via wflow_sbm	317 mm/year (on average)
Hydraulic conductivities ²	horizontal - upper aquifer (K_{h_1})	0.15 to 0.35 m/day
	vertical - upper aquifer (K_{v_1})	3×10^{-3} to 6×10^{-3} m/day
	horizontal - aquitard (K_{h_2})	0.0165 to 0.0385 m/day
	vertical - aquitard (K_{v_2})	3.3×10^{-4} to 6.6×10^{-4} m/day
	horizontal - lower aquifer (K_{h_3})	0.144 to 0.464 m/day
Storage parameters	vertical - lower aquifer (K_{v_3})	3×10^{-3} to 6×10^{-3} m/day
	specific yield (S_y)	0.2
River parameters	specific storage (S_s)	8.7×10^{-3} /m
	average river conductance	75 m ² /day
Groundwater abstraction ²	average river depth	2 meters
	domestic abstraction	96.1 to 152.5 Mm ³ /year
	industrial abstraction	202.9 to 322 Mm ³ /year

¹ Calculated based upon dynamic steady-state model spinup² Optimized under steady-state simulation, interpolated spatially using Rbf (radial basis function) method³ Increase in annual timestep

represent the groundwater abstraction, river, and no flow boundary conditions assigned to the respective cells. The dark grey area at the left, right, and bottom part of the cross-section represents the inactive cells with no flow boundary condition.

The groundwater flow simulation setup follows a proven procedure (Karimi et al., 2019), involving a steady-state run, a transient model spin-up, and the final transient simulation. The steady-state run is used to obtain the initial condition for the model spin-up, which is further used to achieve the dynamic steady-state condition of the groundwater system. We compare the dynamic steady-state groundwater level in 2004 with the observed data, which have resulted in an r^2 of 0.895 in our previous study (Rusli et al., 2023a). The final transient simulation between 2005 and 2018 uses the simulated groundwater level under the dynamic steady-state condition as the initial condition. The final transient simulation is run under a monthly timesteps setup with quarter-daily sub-timesteps.

We have also developed an additional steady-state simulation that excludes the abstraction boundaries. This scenario serves the specific purpose of conducting particle tracking analysis using MODPATH (Pollock, 2016). MODPATH is a post-processing program designed to work in conjunction with MODFLOW. It complements the groundwater age analysis by allowing us to track the movement of particles in the groundwater system. By assigning particles in the cell where the groundwater samples were taken for the ¹⁴C content measurement, MODPATH is capable of conducting time-series backward particle-tracking analysis. The results of this particle tracking analysis yield travel time estimates, which are comparable to groundwater age estimates. This additional analysis helps us gain insights into the movement and residence times of groundwater in the study area.

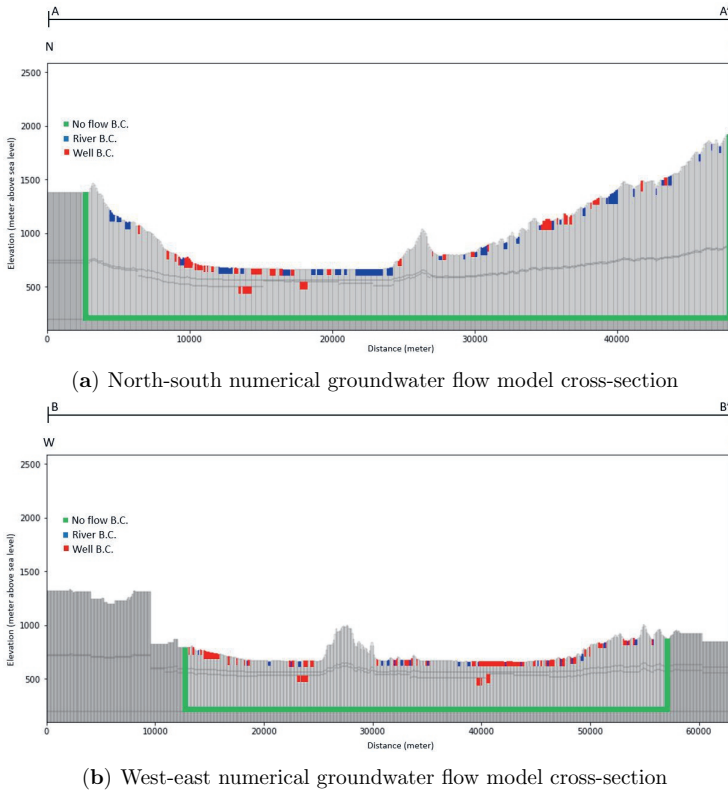


Figure 5.3: The cross-section of the numerical groundwater flow model of the BGB in north-south and west-east directions. The red, blue, and green bars, respectively, scattered in the model cross-section, represent the groundwater abstraction, river, and no flow boundary conditions assigned to the respective cells. The dark grey area at the left, right, and bottom part of the cross-section represents the inactive cells with no flow boundary condition.

5.2.5 Model evaluation

Considering the limited number of calibration data in the BGB, supplementary model evaluation is necessary. GRACE-based additional evaluation on terrestrial water storage change estimates has been described in our previous study (Rusli et al., 2023a). In this study, we further evaluate the model performance by comparing the EWT data-driven interpretations with the model-driven outcomes. The particular model evaluation process serves as a crucial step to validate to an even greater extent the groundwater flow model’s performance and, more importantly, its ability to capture the behavior of the real-world groundwater processes in the BGB. It ensures that the model not only reproduces groundwater levels and storage but also represents the broader behavior of the groundwater system in response to various factors. The evaluation involves several points

of view; (1) the groundwater recharge distribution, (2) the regional groundwater flow direction, (3) groundwater age estimates, and (4) the identification of aquifer interaction, as shown in Figure 5.2.

Following the one-way coupled model evaluation, we use the simulation results not only to quantify the aquifer interaction but also to assess the groundwater level changes. In quantifying the internal groundwater vertical movement, we put the intercell flow simulation results together with the groundwater storage analysis of the groundwater flow model itself. The aquifer interaction, while being an important part of the groundwater storage, is not actually portrayed in such a value coherently as the 'groundwater storage change' is an aggregation of the processes that occurred in each layer of the upper, the lower aquifer, and the aquitard. The direct implication of the groundwater level changes, which is straightforwardly connected with the upper aquifer storage, has precisely a similar attribute. While it is inherently attached to the groundwater storage, it does represent just a partition and not the whole solitary hydrological compartment. Therefore, we also analyze the groundwater level change; its magnitude, its spatial distribution pattern, and its correlation with the groundwater abstraction zones.

5.3 Results

5.3.1 Major ion elements data analysis

Figure 5.4 displays the Stiff diagram overlaid on the BGB map, depicting the spatial distribution of the water samples. Specifically, Figure 5.4a represents samples from water springs and rivers, Figure 5.4b illustrates the shallow groundwater samples, and Figure 5.4c showcases the deep groundwater samples. To avoid repetition in each plot, we've standardized the north direction to point upwards in all figures.

The dominance of HCO_3^- anion elements in the springs and river water of the BGB suggests the influence of volcanic rocks in the upper layer of the geological formation within the study area (Meybeck, 2003). While major ion composition in water is also affected by climatic, proximity to the ocean, and human factors, the major ion elements measured in Figure 5.4a are primarily located in river upstream areas where non-lithologic factors have minimal impact. However, a noticeable variation is evident in the center of the basin, where one Stiff diagram exhibits a sudden increase in sodium concentration. This variation corresponds to samples collected in the textile industrial area where groundwater is abstracted from the deeper aquifer. Previous studies have confirmed that textile wastewater can introduce bleaching agents, including sodium silicate (Wang et al., 2011; Rashidi et al., 2021). Additionally, a relatively higher sodium concentration near the basin outlet and along the main river, though lower compared to the industrial area, indicates a distributed source of wastewater and underscores the potential for the river's self-restoration capacity.

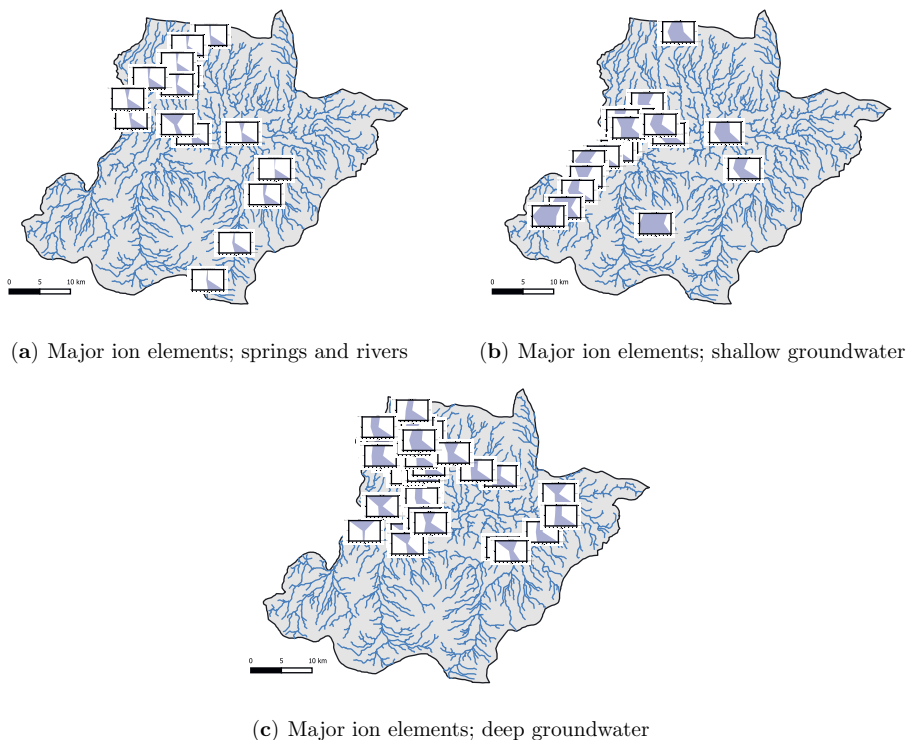


Figure 5.4: The spatial distribution of Stiff diagrams plotted from water samples measured from (a) surface water, (b) shallow groundwater, and (c) deep groundwater. From the bottom left corner, in a clockwise direction, the Stiff diagrams represent the Mg^{2+} , Ca^{2+} , Na^+/K^+ , Cl^- , SO_4^{2-} , and HCO_3^- .

The analysis of shallow groundwater samples reveals changing trends in major ion elements, characterized by higher concentrations of Na^+/K^+ , Ca^{2+} , Mg^{2+} , and Cl^- compared to the water from springs and rivers. When combined with data presented in Taufiq et al. (2017), the increased sodium concentration highlights the impact of industrial wastewater, particularly from areas located upstream in the basin, on the shallow groundwater. Additionally, the dominance and uniform spatial distribution of Ca^{2+} in the cation elements suggest that shallow groundwater is recharged uniformly throughout the basin, despite variations in topographical distribution. Previous studies have identified CaHCO_3 as the common major ion properties in groundwater recharge (Li et al., 2008; Mora et al., 2017). Meanwhile, the increase in Cl^- concentration is likely influenced lithologically and may be attributed to sedimentary rock resulting from the lake deposits in the upper layer of the flat terrain in the basin.

Deep groundwater samples exhibit interestingly distinct features. While samples from the northern part of the basin still show a dominance of CaHCO_3 type water, this dominance is not as pronounced as in the shallow groundwater samples. Furthermore, samples from locations near the basin outlet and the upstream industrial area indicate sudden decreases in Ca^{2+} and, in most cases, higher sodium concentrations compared to the shallow groundwater samples. These abrupt reductions in Ca^{2+} levels suggest cation exchange processes that can be interpreted in various ways. In a previous study, Eeman et al. (2017) proposed that the horizontal component of water flow has minimal impact on chemical composition changes in the vertical direction due to cation exchange. Therefore, we can infer that the cation exchange process, reflected by the decrease in Ca^{2+} concentration, is the result of vertical groundwater flow, or in other words, aquifer interaction.

5.3.2 Groundwater age data analysis

The plot in Figure 5.5 displays the groundwater age data points, their spatial interpolation, and the estimated industrial area where deep groundwater abstraction takes place. Generally, the groundwater age profile around the basin's periphery, especially in the higher elevation areas to the east, exhibits younger ages and gradually matures as it approaches the basin outlet. This pattern aligns with the topographical profile of the surface and suggests the propagation of confined groundwater flow from the mountainous region to the lower plains, as groundwater age has previously been employed to determine regional groundwater flow direction (Tanachaichoksirikun and Seeboonruang, 2020).

However, deep groundwater abstraction in the BGB has introduced some local interference. In the abstraction area toward the eastern part of the basin, for example, where samples are collected from four locations, the ages of two middle samples indicate younger groundwater age compared to the other two flanking them. This phenomenon can theoretically occur only if those two middle samples are, in fact, groundwater leaking from the shallow aquifer, which is expected to have a younger age. It also suggests the presence of vertical cross-formational groundwater flow, influencing groundwater age mass dispersion alongside horizontal advection along aquifers (Bethke and Johnson, 2002).

Another noteworthy observation is that only four data points have groundwater age estimates exceeding 10,000 years. Using MODPATHV7.2, we later compare the younger groundwater age estimates (with age estimates of less than 10,000 years) derived from ^{14}C content with the travel times obtained from backward particle tracking analysis.

5.3.3 Stable isotopes data analysis

The locations of the stable isotope samples are visualized in Figure 5.6a. Each data point represents a geographical location and the $\delta^{18}\text{O}$ value of the water sample, indicated by the size of the data points. The $\delta^{18}\text{O}$ values range between -10.5‰ (smallest circle) and -2.5‰ (largest circle). Additionally, Figure 5.6b showcases the correlation between $\delta^2\text{H}$

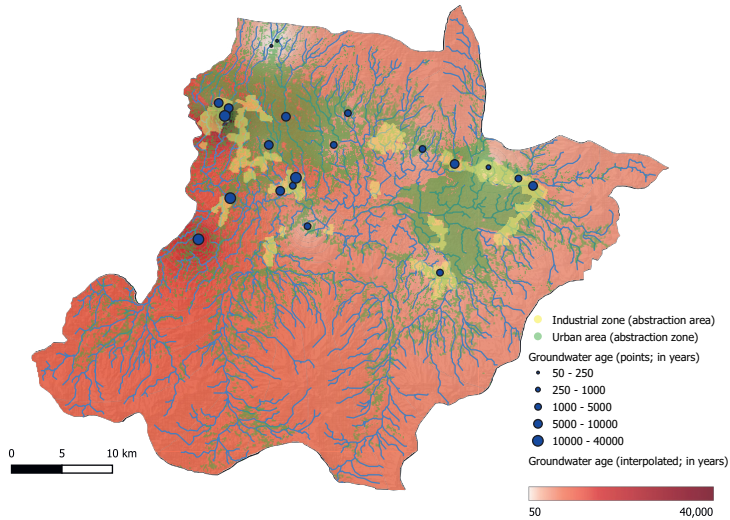


Figure 5.5: Groundwater age estimates (blue points) in confined aquifers from the BGB. These estimates are overlaid with the industrial area marked in yellow. Additionally, the map displays the interpolation of groundwater age estimates using the Inverse Distance Weighting (IDW) method, represented by the red areas. While the overall pattern of groundwater age distribution appears relatively consistent, some localized anomalies are evident, particularly in close proximity to the industrial zones where groundwater is abstracted from the deep aquifer.

and $\delta^{18}\text{O}$ values of the samples, categorized by the water samples' sources. Furthermore, Figure 5.6c and Figure 5.6d illustrate the relationship between the measured $\delta^{18}\text{O}$ and $\delta^2\text{H}$ values of the samples and the depth at which these samples were obtained.

There are only three locations inside the BGB domain where rainfall samples are taken for stable isotope measurements shown in Figure 5.6a. To increase the sample size, we use four additional points outside the basin boundary to calculate the local meteoric water line (LMWL) equation: $\delta^2\text{H} = 7.76 \delta^{18}\text{O} + 12.67$. The LMWL gradient of 7.76 is very close to one of the global meteoric water line (GMWL) of 8, indicating the approaching equilibrium processes of the local precipitation in the BGB, behaving similarly to the average global spatial relationship between $\delta^2\text{H}$ and $\delta^{18}\text{O}$ in precipitation (Putman et al., 2019). However, the intercept value of 12.67 in the LMWL equation, in contrast to the GMWL's intercept value of 10.00, raises the possibility of rainfall evaporation. This could be attributed to the tropical climate in the basin. It's important to note that this interpretation is based on a limited dataset of less than 10 non-time series measurements. Therefore, it comes with a significant degree of uncertainty and should be utilized in conjunction with other investigative methods to obtain the most accurate understanding of the system (Kendall and McDonnell, 1998; Coplen et al., 2000).

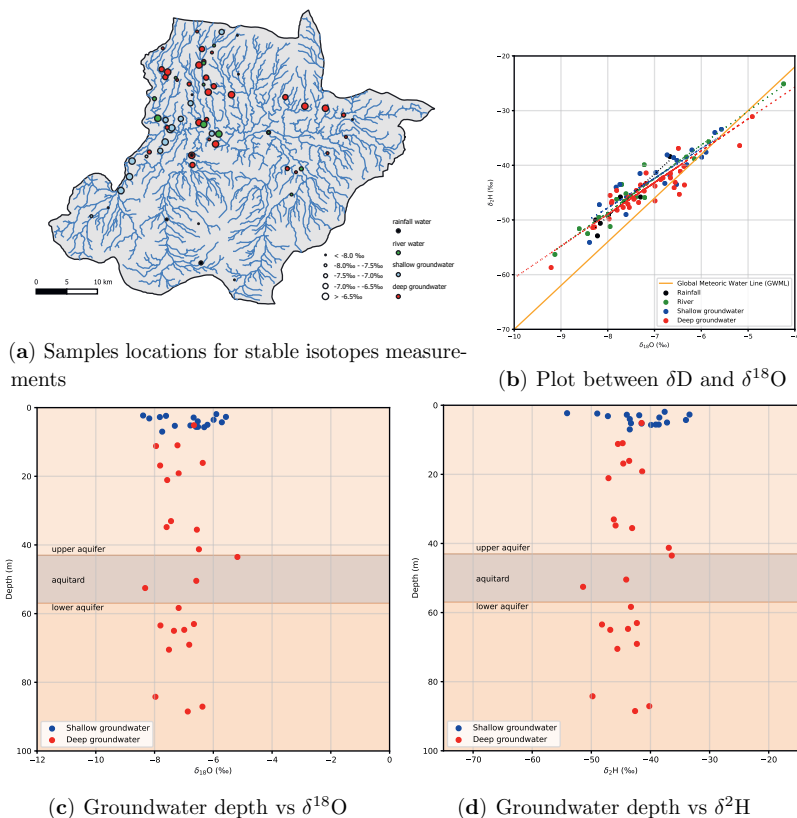


Figure 5.6: The stable isotope measurements data, covering (a) the spatial distribution of the measurements, (b) the local meteoric water line (LMWL), (c) the $\delta^{18}O$ -depth profile, and (d) the δ^2H -depth profile. Figures (c) and (d) are overlaid with the average thickness of each layer derived from the borehole data.

The meteoric water lines' gradient, divided according to the samples' sources, could also provide insights into the local hydrological process. In the case of the rainfall, river, shallow, and deep groundwater stable isotopes, the gradient values are 7.76, 6.17, 5.44, and 5.81, respectively. The notably distinct gradient between rainfall and river water samples suggests that dominant evaporation processes are occurring in the BGB, corroborating our previous study (Rusli et al., 2021). On the other hand, the small differences in the gradient values among the river and groundwater samples indicate water recycling, especially between the shallow and deep groundwater. The effect of local groundwater head drawdown due to deep groundwater abstraction can also be observed from the d-excess values. In the BGB, the deep groundwater's d-excess values average around 12.98‰, with a relatively low variability compared to values from other studies (Sreedevi et al.,

2021; Al-Gburi et al., 2022). This suggests that the recharge water in the basin primarily originates from specific sources, likely dominated by rainfall, with a minimal contribution from streams and water bodies. To some extent, this may also reflect the low spatial variability or heterogeneity of soil properties, which aligns with fieldwork measurements and findings.

Figure 5.6a shows the $\delta^{18}\text{O}$ of samples collected in close proximity. Many data points tend to cluster within groups marked by similarly-sized circles. This clustering strengthens the hypothesis of aquifer interaction, indicated by the consistent $\delta^{18}\text{O}$ compositions in neighboring samples, even though they are collected from various depths. Additionally, there is a trend of lighter water compositions upstream transitioning to heavier compositions downstream, which aligns with the regional groundwater flow direction estimated from interpolated groundwater age data. This method of inferring flow direction based on $\delta^{18}\text{O}$ values has also been corroborated in another study (Zhu et al., 2019b).

Figure 5.6b displays the correlation between stable isotopes $\delta^2\text{H}$ and $\delta^{18}\text{O}$, with nearly every point situated above the Global Meteoric Water Line (GMWL). The Local Meteoric Water Lines (LMWLs) of the river, shallow groundwater, and deep groundwater indicate a significant similarity in stable isotope compositions among these water samples. The gradients of these water lines suggest the order of flow, starting from rainfall (water line gradient of 7.76), progressing to river water (6.17), and eventually reaching the groundwater (5.44 for shallow groundwater and 5.81 for deep groundwater).

Figure 5.6c illustrates the correlation between the depth of groundwater samples and their $\delta^{18}\text{O}$ values, overlaid with an approximation of the average depths of the upper aquifer, aquitard, and lower aquifer based on lithological profile data from the relatively flat part of the basin. Since the borehole locations differ from the water samples and the two fieldwork activities were conducted at separate times, this approximation helps provide context. The $\delta^{18}\text{O}$ values, ranging between -6% and -8% , are relatively wide for stable isotope measurements, particularly for samples collected from deep groundwater. The broadest range is observed at depths between 40 and 60 meters below the surface elevation, which coincides with the aquitard's boundary that typically separates the upper and lower aquifers. This finding further supports the aquifer interaction hypothesis, as it indicates the likelihood of mixing processes due to vertical groundwater flow conveyance. The elevated stable isotope values at around 40 meters depth suggest that groundwater is temporarily impeded and mixed vertically by the aquitard. After breaching the aquitard layer, stable isotope profiles in the lower aquifer closely resemble those in the upper aquifer, which aligns with the similarity in geological formation and soil properties in both aquifers. A comparable analysis can be made from Figure 5.6d.

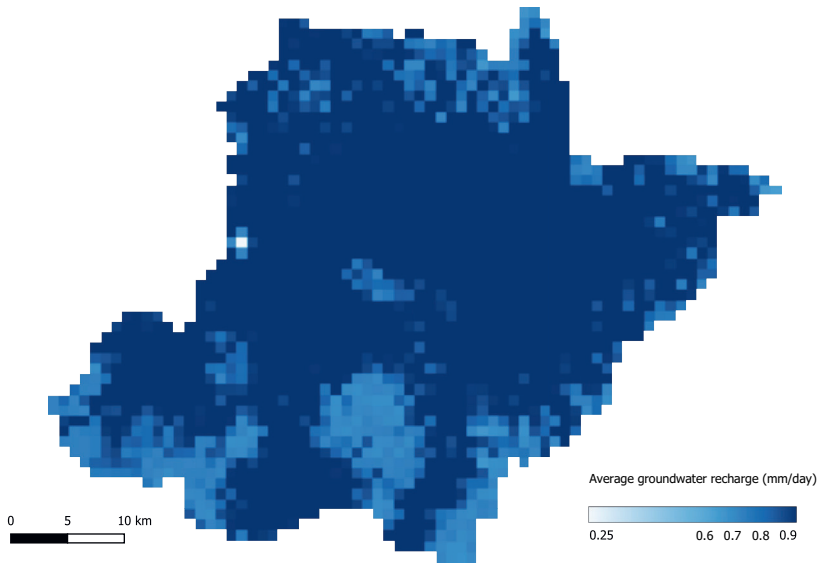


Figure 5.7: The spatial distribution of the simulated groundwater recharge in the BGB, averaged between 2005 and 2018.

5.3.4 Model simulation: Groundwater recharge spatial distribution

The groundwater recharge, utilized as input for the groundwater flow model, is computed through hydrological simulations conducted using the Wflow_sbm model, as detailed in (Rusli et al., 2023a). Originally, these simulations are carried out on a daily basis and are subsequently aggregated into monthly time steps to align with the temporal resolution of the groundwater flow model. Given the region's wet and humid climate, the variation in groundwater recharge between the rainy and dry seasons is relatively limited. Figure 5.7 illustrates the spatial distribution of the average groundwater recharge within the BGB between 2005 and 2018.

The calculated values primarily fall within the range of 0.6 to 0.9 mm/day and exhibit spatial variability in response to the terrain's slope. In areas with steep slopes, surface water tends to run off more readily due to gravitational forces, making vertical infiltration through the soil less common. Consequently, the groundwater recharge in mountainous regions is relatively lower, typically around 0.6 to 0.7 mm/day. In areas with gentler slopes, groundwater recharge rates increase to approximately 0.8 and 0.9 mm/day.

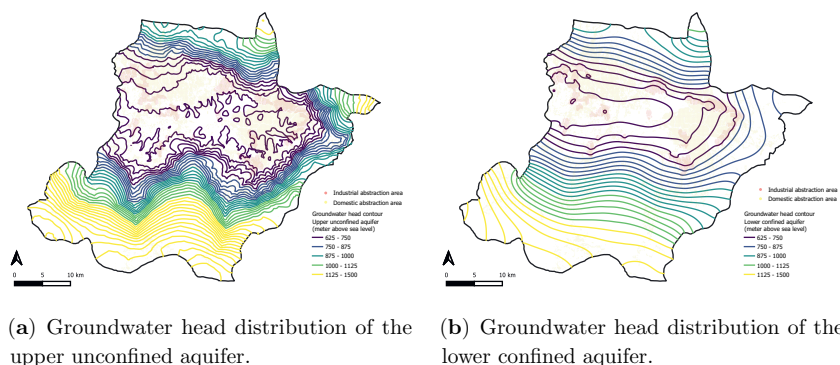


Figure 5.8: The spatial distribution of the simulated groundwater head contour in the (a) upper unconfined layer and (b) lower confined layer. Both figures are in agreement with the topographical profile of the basin surface, although the profile of the groundwater head in the unconfined aquifer is more responsive compared to the ones from the confined aquifer.

5.3.5 Model simulation: Regional groundwater flow direction

The determination of the regional groundwater flow direction is facilitated through contour plots representing the distribution of groundwater heads. In line with the principles of groundwater flow, where water naturally moves from areas of higher hydraulic heads to those with lower heads, a flow direction is symbolized by perpendicular lines between the head contour lines. This relationship is based on the assumption of horizontally isotropic conditions, which is a fundamental premise of the groundwater flow model. Figures 5.8a and 5.8b illustrate the simulated distribution of groundwater levels within the upper (unconfined) and lower (confined) aquifers, respectively, as simulated by our groundwater flow model at the end of the simulation time (2018).

In general, these contours align with the topographical profile of the basin, where groundwater primarily flows from the periphery of the basin towards its central region, characterized by lower elevations and milder surface slopes. However, there are noteworthy differences between the upper and lower aquifers. The groundwater head contours in the upper aquifer exhibit more variability and steeper gradients due to the larger area of groundwater abstraction and the influence of groundwater recharge.

The impact of groundwater abstraction on the groundwater heads is partially visible in Figure 5.8a, depicted by the local closed contour lines near the eastern part of the groundwater abstraction areas. Given that the values of the local groundwater drawdown are generally lower than the contour interval of 25 meters, it may not be readily discernible in the figure. To provide a more detailed representation of groundwater table drawdown, Section 5.3.8 provides the result of the simulated groundwater table drawdown presented not in contour form but as a raster-based display.

On the other hand, the impact of groundwater recharge on groundwater storage is apparent in the differences in groundwater head values: the groundwater head in the upper aquifer reaches heights of up to 1500 meters above sea level (ASL), while in the lower aquifer, it only extends to around 1300 meters ASL. On the other hand, the lower values of the groundwater head in both aquifers are relatively consistent, typically ranging between 625 and 675 meters ASL.

5.3.6 Model simulation: Groundwater age estimates

The groundwater age estimates are approximated with two methods in this study: radiocarbon (^{14}C) content measurements and the MODPATH backward particle tracking analysis. Considering most of the groundwater age estimates are younger than 10,000 years, Figure 5.9 shows the comparison between both approximations within the dominant range. The uncertainty bounds in each axis are illustrated by the error bars. The uncertainties of the measurement-based estimates come from the multiple samples taken for multiple measurements in one point location. The ones of simulated-based estimates come from the temporal precision of the MODPATH simulation. Initially, the simulation is set up with groundwater abstraction as a constant boundary condition, following the current model setup. The result of this initial run is shown in Figure 5.9a. The Pearson coefficient correlation between the two estimates, however, is as low as 0.05, as we see the dots are widely spread across the graph. This occurs due to the model setup, as there was supposedly no groundwater abstraction in the far past. Removing such a boundary condition from the simulation improves the Pearson coefficient correlation between the two age estimates to 0.77. Visually, the improvement is also shown in Figure 5.9b.

5.3.7 Model simulation: Identification of aquifer interaction

The presence of aquifer interaction in the numerical groundwater flow model is inferred through the analysis of intercell flow. To begin with, the groundwater budget is divided into distinct vertical layers, and the fluxes between cells within each layer are then collectively assessed. It's worth noting that intercell flow differs from the specific discharge in the vertical direction (q_z), as reported by MODFLOW output. q_z takes into account various flow boundaries within the cells or layers, including contributions from sources such as rivers, wells, recharge, etc., and cumulatively represents the net change in flow over time. In contrast, intercell flows exclusively quantify the rate at which groundwater moves from one cell to an adjacent cell in a specific direction. This flow occurs as a consequence of differences in pressure between the two neighboring cells.

Figures 5.10a and 5.10b illustrate the spatial distribution of vertical intercell flow, specifically from the upper aquifer to the lower aquifer. The patterns observed in both figures exhibit a certain symmetry, highlighting the equilibrium of groundwater movement between the aquifers. In the upper aquifer, there are areas around the midstream of the river where

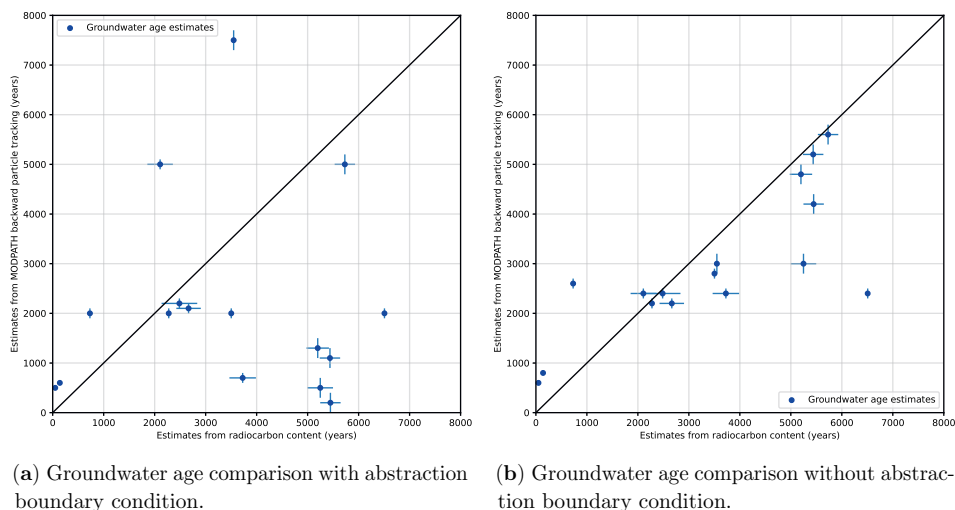


Figure 5.9: The comparison between groundwater age estimates from water samples measured radiocarbon content (x-axis) and from MODPATH backward particle tracking analysis (y-axis). Figure (a) shows the result when the model is simulated with groundwater abstraction, while Figure (b) is without groundwater abstraction. The error bars indicate the uncertainty of the groundwater age estimates, sourced from multiple measured samples for the x-axis and temporal precision of the MODPATH simulation for the y-axis.

upward fluxes (indicated by positive values) are noticeable. In these regions, groundwater from the lower aquifer, characterized by undisturbed confined groundwater pressure, moves upwards into the upper aquifer. This movement occurs because the unconfined groundwater table in the upper aquifer has been diminished due to shallow groundwater abstraction. The average upward flux is estimated at 0.47 mm/day, which is equivalent to 90.10 million cubic meters per year (Mm^3/year). In contrast, the majority of areas, particularly beneath the zones of deep groundwater abstraction, experience a general downward movement of groundwater. The substantial and concentrated industrial abstraction from the deep groundwater significantly reduces confined groundwater pressure, increases the hydraulic gradient between the aquifers, and forces groundwater from the upper aquifer to move downward. On average, the downward flux is calculated at 0.68 mm/day, equivalent to 289.30 Mm^3/year . This value increases to -1.08 mm/day, equivalent to 31.36 Mm^3/year , under the estimated industrial areas. It's important to note that the relationship between the flux rates and volumes is non-linear due to variations in the sizes of the areas involved. When aggregated across the entire groundwater basin, the aquifer interaction is quantified at an average rate of 0.30 mm/day, which amounts to a substantial 187.70 Mm^3/year of groundwater movement within the groundwater storage between the aquifers.

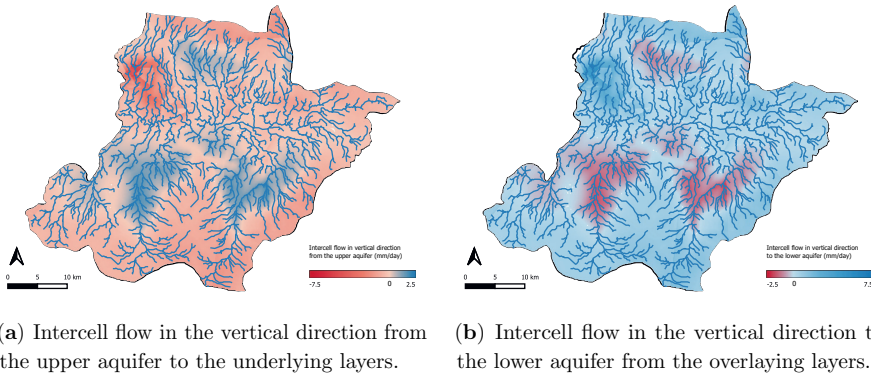
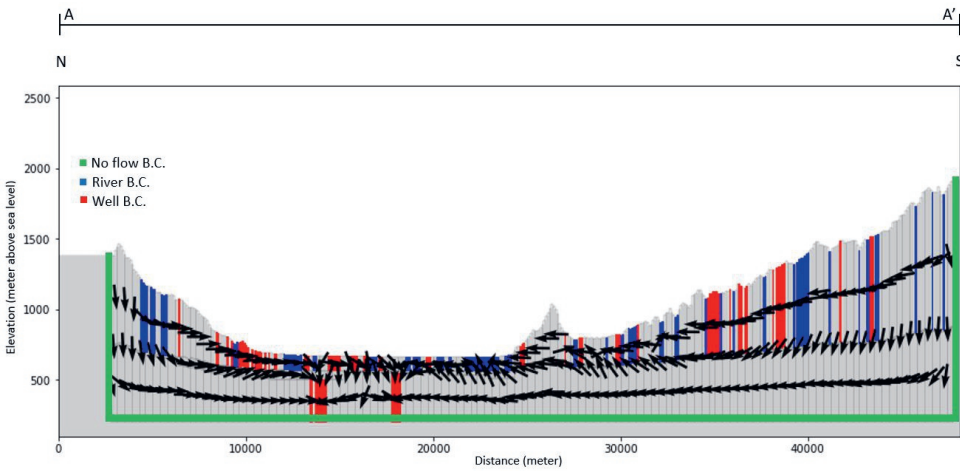


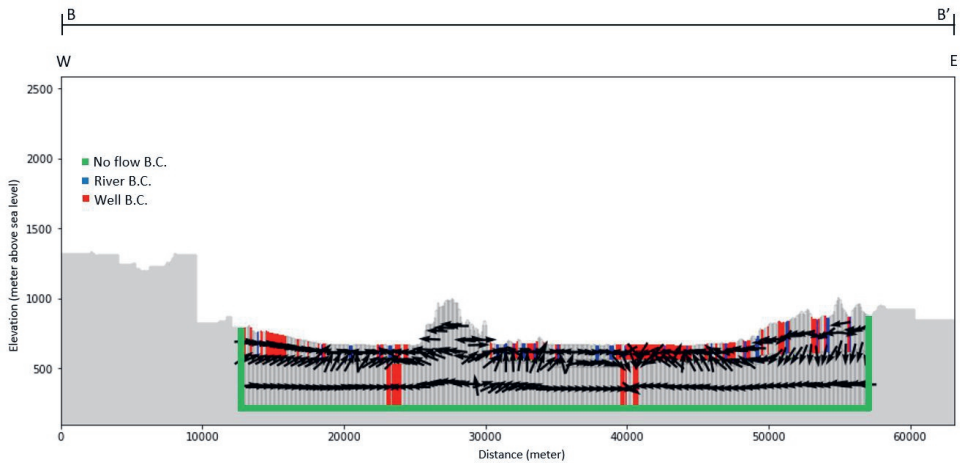
Figure 5.10: The spatial distribution of the intercell flow from the upper and to the lower aquifer. Negative flows mean the fluxes are heading outwards from the cells/layers, while positive flows represent inward fluxes.

Notable disparities in groundwater movement patterns are also evident between the relatively flat area in the middle of the basin and the higher elevated, steeper slope area at the basin’s periphery. Although the direct impact of groundwater abstraction in the lower elevated basin area on aquifer interaction is comprehensible, it’s intriguing to observe the substantial groundwater movement in the mountainous region, despite lower levels of groundwater abstraction in these areas. In the mountainous region, characterized by elevations higher than 1000 meters above sea level (ASL), the average vertical groundwater flow is approximately 0.63 mm/day, which is more than double the average rate observed across the entire basin. This trend persists throughout the basin: the higher the elevation, the more significant the contribution to the lower aquifer, even in areas with less groundwater abstraction. For elevations above 1200 and 1500 meters ASL, the average vertical groundwater flows increase to 0.77 and 0.88 mm/day, respectively. This observation suggests that the depletion of groundwater storage in the flat, central part of the basin, as indicated by declining groundwater tables, is primarily compensated by the inflow of groundwater from the basin’s higher-elevated periphery.

In addition to the analysis derived from the map view of the intercell flow, we also present analysis from north-south and west-east cross sections. Figure 5.11a and Figure 5.11b depict the normalized velocity vectors of groundwater flow in each layer. The blue and red bars in each figure indicate the grid cells where the river and well boundary conditions are applied, respectively. These bars do not represent the depth of the river or well but rather the grid cell in which the boundary conditions are applied. Another important note is that Figure 5.11 displays the velocity vectors representing the resultant vectors of the specific discharge in all directions and not intercell flow in a single direction.



(a) Velocity vector in the north-south cross-section.



(b) Velocity vector in the west-east cross-section.

Figure 5.11: The normalized velocity vectors in two cross-sections (a) north-south and (b) west-east directions. The blue and red bars in each figure indicate the whole cell where the river and well boundary conditions, respectively, are assigned. It is important to note that the bars do not represent the depth of the river or well, but the grid cell in which the boundary conditions are applied.

From the north-south cross-section (Figure 5.11a), we observe that in the upper layer’s cells located away from the groundwater abstraction boundary conditions, groundwater flows downward to the underlying aquifers. This trend is even more pronounced in the mountainous area on both sides of the figure, supporting our previous analysis of the higher elevated regions compensating for the groundwater abstraction in the lower part of

the basin. Near the groundwater abstraction boundary conditions applied in the upper layer, the velocity vectors generally point upward, aligning with the area in blue color shown in Figure 5.10a. Meanwhile, near similar boundary conditions but applied in the lower layer, the velocity vectors move downward. The groundwater flows through the aquitard, as they compensate for the abstracted deep groundwater. In the vicinity of the river boundary conditions, these fluxes create tension for the groundwater around the aquitard layer. They either flow upward to contribute to the river baseflow or downward to the confined layer, contributing to the aquifer interaction.

The west-east cross-section (Figure 5.11b) displays more compact velocity vectors. With small tributaries crossing through the west-east cross-section (compared to the north-south ones), there is less competition between the river and the aquifer interaction fluxes. Similar to the analysis derived from the north-south cross-section, most of the velocity vectors in the aquitard layer shown in Figure 5.11b are in line with our analysis derived from Figure 5.10a. In areas close to the river and groundwater abstraction boundary conditions are applied only to the upper unconfined layer, there are upward groundwater fluxes. However, in areas with intense groundwater abstraction from both layers and in the mountainous area, the velocity vectors are dominated by downward flow at an even steeper gradient. This indicates the cumulative impact of direct groundwater table drawdown due to domestic groundwater abstraction boundary conditions applied in the upper layer and indirect groundwater table drawdown due to aquifer interaction induced by the industrial groundwater abstraction boundary conditions applied in the lower layer.

5.3.8 Model simulation: Groundwater level changes

With an average of 187.70 Mm³ of groundwater annually flowing from the upper aquifer to the underlying aquifers, the groundwater level in the unconfined aquifer is inevitably affected. Although such aquifer interaction fluxes do not leave the groundwater storage as a whole, they do influence the groundwater table fluctuation; the groundwater level dwindles as a consequence of the net decline in the upper storage partition. Figure 5.12 below shows the spatial distribution and the magnitude of the groundwater level decrease in the BGB throughout the simulation period between 2005 and 2018.

Upon examination of the groundwater abstraction area and the spatial distribution of groundwater level decrease presented in Figure 5.12, a discernible correlation emerges between these two variables. It becomes evident that domestic groundwater abstraction from the upper aquifer primarily concentrates along the river and in the northwest and east regions of the basin. The expansion of industrial zones, driven by urban development, is particularly notable in proximity to densely populated areas, especially in the eastern section near the surface catchment outlet. In regions where groundwater abstraction occurs exclusively from the upper aquifer, and not from the lower aquifer, the average groundwater level drawdown equates to a net decline of approximately 2630.93 m³ per

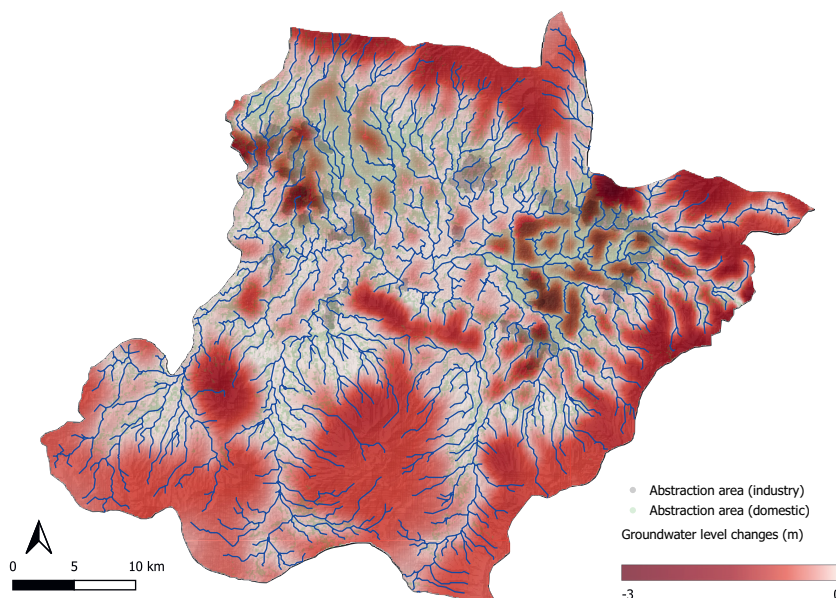


Figure 5.12: The spatial distribution of the groundwater level drawdown in the BGB throughout the simulation period between 2005 and 2018.

model grid cell in unconfined storage volume. This calculation is derived by comparing the groundwater level in the unconfined aquifer between the initial state in 2005 and the conclusion of the simulation in 2018. However, it's important to note that this figure is significantly influenced by the groundwater level changes in the eastern area of the basin. In this particular zone, where groundwater is drawn solely from the upper aquifer and the industrial groundwater abstraction exerts additional pressure, the decline in unconfined storage volume intensifies. When we calculate the net decline in unconfined storage volume specifically along the rivers, where surface water partially compensates for the groundwater abstracted from the unconfined storage, the value is notably lower at 851.91 m^3 per model grid cell. Conversely, in areas where groundwater is abstracted from both the upper and lower aquifers, the groundwater level drawdown is more pronounced. The average decline in unconfined storage volume in these areas amounts to 3126.57 m^3 per model grid cell, with the most substantial groundwater level drawdown reaching 3.32 meters. Interestingly, similar trends are observed in the undisturbed mountainous areas. Despite the absence of groundwater abstraction in these predominantly higher-elevated regions, the average groundwater level drawdown exceeds that of areas with groundwater abstraction. In these areas, the average net decline in unconfined storage volume is calculated to be as high as 6525.66 m^3 per model grid cell.

5.4 Discussion

5.4.1 Analysis limitation and the ideal data situation

Conducting hydrological and groundwater research in a data-scarce area inherently introduces a multitude of challenges and uncertainties. In this study, the fact that each of the data sources has its own limitations is the factor that keeps us away from a fuller analysis and a better-constrained model setup. It is imperative to recognize that the propagation of uncertainties within our simulation framework is a persistent challenge. This propagation initiates from the hydrological simulation, which estimates groundwater recharge, and extends through the groundwater flow simulation, which gauges groundwater response behavior to the inferred flow boundaries. This process encompasses a variety of elements, ranging from model input and parameterization to calibration data. Consequently, the need to effectively manage and address these uncertainties remains a pivotal task in our study. To tackle these complexities and enhance our understanding, we have implemented an EWT-based model evaluation approach. This approach serves as a valuable complement to the calibration of groundwater table and groundwater storage simulations, as previously documented in our earlier studies (Rusli et al., 2023a).

In our analysis of EWT data, it is important to note that these data are not available in the form of a time series and are instead based on measurements predating 2010. Consequently, any changes in the chemical composition of groundwater over the past decade are not represented within the dataset. Fortunately, the time scale of groundwater flow and its associated chemical reactions is notably slower than the movement of surface water (Winter et al., 1998; Schellenger and Hellweger, 2019). This characteristic supports our contention that the utilization of the once-at-a-time (OAT) measured EWT data remains pertinent for our subsequent analysis. However, it is essential to acknowledge that the available EWT data exhibit limitations in terms of their spatial distribution and data density. Similar to the data associated with the groundwater model, EWT data are predominantly concentrated in urban areas, which is logical considering that cities are focal points for human activities related to groundwater. Nevertheless, the scarcity of information pertaining to mountainous areas necessitates certain approaches, such as making assumptions and conducting spatial interpolations, to bridge these gaps. It is important to recognize that such techniques introduce uncertainties into our analysis.

Our study is not without the recognition of inherent risks associated with drawing conclusions from limited data quantities. For instance, while we estimate groundwater age using ^{14}C measurements, it is important to acknowledge that the intricacies of the process behind the estimated age remain undisclosed. It is plausible that this estimation can be influenced by the mixing of waters from two sources with extreme age differences, potentially distorting the average estimated age. Ideally, we would prefer data in the form of modern carbon percentages, however, we have utilized all the limited data available to

arrive at our results. In our MODPATH analysis, we should note that several assumptions are made in the simulations. Notably, we do not simulate the mixing and chemical reactions that may occur during groundwater transport. However, we contend that employing straightforward and justifiable approaches, supported by the available data, often yields higher reliability. This approach aligns with the findings of the previous study (Voss and Soliman, 2013). Beyond the availability of data to underpin our model, our approach is deeply intertwined with the objectives of our analysis. It is clear that reliance on a single approach, whether exclusively based on EWT data or solely on model-based evaluations, is inherently insufficient. To address this limitation, we adopt a comprehensive approach that draws from multiple sources of EWT data. Furthermore, our model evaluation also encompasses various perspectives from groundwater recharge, flow direction, age estimates, to aquifer interaction. The consistent alignment across these different facets offers compelling support for our proposal for incorporating EWT data, particularly in the context of data-scarce regions where the ideal data may be absent.

All the circumstances described above demonstrate the importance of an openly accessible integrated groundwater database system in the BGB, specifically, and in Indonesia and other data-scarce areas, in general. As we have shown in the EWT data, the borehole data, and even some fieldwork data, there have been numerous OAT measurements in the study area. Unfortunately, they are mostly done by independent projects, scattered among various parties: the government, the private sector, companies, consultants, and even individuals. The already-measured data, regrettably, are not adequately gathered, stored, and accessible to the public. Provided that the government could take advantage of this opportunity, i.e. by assisting in collating the available data and bridging the gap of information among the stakeholders, the challenge of data scarcity in conducting groundwater-related research in the BGB could be minimized.

5.4.2 EWT data-driven analysis and numerical model output comparison

From the description of the EWT data analysis and the output of the numerical groundwater flow model, we can see the agreement, in a qualitative sense, between the two approaches. Both methods are consistent in assessing the groundwater recharge spatial distribution, the regional groundwater flow direction, and in identifying the aquifer interaction through the vertical groundwater flows. The EWT data analysis strengthens the confidence in the numerical model accuracy, especially considering the limited calibration data available. Cooperatively, the numerical model provides invaluable quantitative information on the groundwater state. Compared to previous studies, most of our findings support and strengthen the groundwater modeling studies conducted in the study area. Having said that, we also observe a few deviations in our analysis, however, as opposed to some of the established notions of the groundwater flow system in the BGB.

In our study, the groundwater recharge spatial distribution is characterized by the collated EWT data and calculated using the previously set `wflow_sbm` model (Rusli et al., 2023a). Such setup has also been tested and proved to deliver good performances (Imhoff et al., 2020; Wannasin et al., 2021a). Combined with data from other studies (Taufiq et al., 2017), we found similarities in groundwater recharge potential in both higher and lower elevated areas in the BGB. The simulated groundwater recharge, naturally, shows some spatial variabilities, but it is calculated at a relatively narrow range between 0.7 and 0.9 mm/day across the basin. This is in contrast with some previous works analyzing the groundwater recharge in the BGB (Pujiindiyati and Satrio, 2013; Widodo, 2013), but at the same time, is supported, to a certain extent, by other works (Hutasoit, 2009; Delinom and Suriadarma, 2010). The discrepancies occur due to several factors, mostly as a consequence of the selected data and methods in estimating the groundwater recharge. While previous research relied on using limited input variables of only land use map, soil type, topography map, or EWT data, for example, we are the first study that combines all the factors into a comprehensive hydrological simulation.

The agreement between the EWT data analysis and the groundwater flow model simulation is also demonstrated by the derived regional groundwater flow. Both methods confirm the strong influence of the basin's topography on the directional pattern of the regional groundwater flow system. Following the elevation contour, the groundwater generally flows from the basin periphery inward to the basin's center. Several cones of depressions, as a consequence of highly concentrated groundwater abstraction, are detected by the groundwater age estimates data. However, the groundwater flow model is unable to replicate the local drawdowns due to its coarse horizontal spatial resolution. While the actual size of the abstraction wells is usually smaller than 1 meter in diameter, the grid size of our groundwater flow model is $100\text{m} \times 100\text{m}$, generating different cones of depression surface area as well as mismatched groundwater level drawdown. Utilizing MODFLOW's unstructured nested grid discretization in its model to represent the abstraction wells is computationally too demanding considering the high number of the estimated abstraction wells in the basin. Instead, results of regional-scale studies could assist in setting up a separate model that aims to imitate the groundwater behavior of local drawdown, as previous studies have implemented (Ebraheem et al., 2004; Sefelnasr et al., 2014).

From the groundwater age estimates, it is possible to not only qualitatively assess but also to quantitatively evaluate the model. This is achievable by using the Pearson correlation coefficient between the groundwater age estimates from water samples' radiocarbon content and ones from the model simulation. A correlation of 0.77 is attained, however, this is viable when a number of outliers are removed from the calculation. Visually, it is also apparent that there are locations where the estimates from both approaches result in significantly different values. This occurs due to several possible reasons. First, the MODPATH tracks the particle moving between the middle of the cell grid, which physically represents a $100\text{m} \times 100\text{m}$ area. In reality, moving within a cell itself might take a considerable

amount of time. There is also a large spatial coverage discrepancy between one point of the water sample with one grid cell, not even to mention the spatial variability within the grid, such as groundwater abstraction, soil layer thickness, etc. Second, while the groundwater travel time results in a magnitude of thousands of years, the boundary condition of the model still depends on the most recent climate forcing. While we could remove groundwater abstraction as the anthropogenic boundary from the model, simulating accurate groundwater recharge dating back hundreds of years ago is impossible, let alone thousands. Third, the flow path of groundwater is susceptible to change with groundwater abstraction in place, especially the deep one. In a cell where groundwater is abstracted, its flow path might be sourced from, for example, the northern part of the basin. However, when the groundwater abstraction boundary is removed, its flow path entry point moves to another location, even as far as the southern part of the basin. Under these two extremely different paths, the groundwater age estimates are expected to have large differences. All these factors are necessary to be taken into account when evaluating the agreement between the two approaches using the groundwater age estimates variable.

One of the most important agreements between both methods is their success in recognizing the aquifer interaction in the BGB. As has been specified above, the majority of basin-scale water balance analysis focus on the groundwater storage as one whole bucket instead of stratified partitions (Bhanja et al., 2018; Mehmood et al., 2022; Ramjeawon et al., 2022). In practice, the impact suffered by the groundwater level from the unconfined aquifer is more severe compared to the ones from the underlying aquifers and is disproportionate to the groundwater abstraction that occurs in different layers of aquifers. While our quantification of the aquifer interaction is discussed below, it is very important to first appreciate and be aware of the subsurface flow processes on groundwater moving from the upper aquifer to the underlying aquifers.

5.4.3 Layer-based groundwater budget zones

To implement our concept of analyzing groundwater storage as stratified partitions, we define the groundwater budget zonation based on its hydrogeological layer. By looking at the intercell flow from the upper aquifer (Figure 5.10a) and to the lower aquifer (Figure 5.10b), we actively attempt to estimate the aquifer interaction indicated by the EWT data. To the best of our knowledge, our study is the first to quantify and assess the exchange between the shallow and the deep groundwater in the BGB.

We can see that Figure 5.10a and Figure 5.10b almost exactly mirror each other. This describes the characteristics of the interspersing discontinuous aquitard layer in the BGB. While there is only limited data on the resistive aquitard layer, we know from the borehole data that in several locations, its thickness is relatively small compared to the extent of the aquifer, or even disconnected in a few places. The results suggest that the aquitard layer's capacity to prevent vertical groundwater movement is insufficient due to its properties

combination of spatially distributed thickness, specific storage, and hydraulic conductivity. However, we believe it still hinders the magnitude of the fluxes to a certain extent, as the confined storage is only partially refilled by the groundwater from the upper aquifer. Our ability to estimate the aquitard parameterization in our groundwater flow model is very limited, unfortunately, by the information and data availability in regard to this particular layer; borehole data spatial distribution and density, aquitard layer pumping tests and soil samplings, and aquitard piezometric head measurements are some examples of related data that could be improved. For an even more accurate aquifer interaction quantification in the future, the parameterization of the aquitard layer, grounded on reliable and comprehensive groundwater data, is very important. The importance of understanding the flow through the aquitard in this regard, previously so-called vertical groundwater movement, leakage, and/or aquitard drainage, has also been highlighted in previous research (Malama et al., 2007; Chen et al., 2018b; Luo et al., 2020).

Both the EWT data analysis and the groundwater flow model simulation also indicate that the unconfined groundwater storage is dwindling disproportionately compared to the groundwater abstraction, not only due to the domestic pumping but also to the aquifer interaction that is often not recognizable and quantifiable from a 'one groundwater storage bucket' concept. Using the model calculated groundwater level changes, we determine the unconfined aquifer storage decrease which results in an average rate of 51 Mm³/year. Such storage lost, notably from only the unconfined partition, contributes up to 60.3% of the total groundwater storage lost, estimated from our previous studies (Rusli et al., 2023a), despite the upper storage contributing to only 32.3% of the total groundwater abstraction. The different ratios in groundwater storage lost among the subsurface partitions and the groundwater storage as a whole as compared to the groundwater abstraction demonstrate the importance of understanding the subsurface processes when assessing the so-called 'groundwater storage change'. This is particularly important when the analysis method uses only a single approach, for example only remote sensing data of GRACE, only observation well data, or only numerical model simulation, as they might mislead the consequent analysis due to their different spatial representations in the vertical direction.

5.4.4 Spatial distribution of the groundwater level changes

As briefly mentioned in Section 5.3.8, we found a close correlation between the groundwater level changes and the estimated groundwater abstraction zones, which is straightforwardly intuitive. The interesting finding is that the so-called groundwater abstraction in the BGB occurs at various depths spatially, and the correspondence of the groundwater level changes is also found consistent with the vertical variation of the abstraction. The correlation of groundwater level changes to land use also extends to the river network estimates. Figure 5.12 clearly indicates the influence of surface water (river in particular) in compensating for the groundwater level drawdown, as the majority of areas around the river have significantly lower changes compared to the other areas. Such a relationship

between the abstraction area (and land use in this case), the river delineation, and the groundwater level changes emphasizes the importance of considering all involved aspects when formulating groundwater management policies and strategies, which has also been investigated, simulated, and discussed in previous studies (Levy and Xu, 2012; Petpongpan et al., 2021). There is also a correlation between the groundwater level changes and the topographical features of the basin. The fact that the higher elevated area suffers from the highest groundwater level drawdown despite having the smallest area of groundwater abstraction indicates the contribution from the mountain in sustaining the groundwater level in the urban area, which in the long run, theoretically, might cause groundwater basin closure (Molle et al., 2010; Zeinali et al., 2020; Pauloo et al., 2021).

Another interesting finding from the model simulation is the fact that the highest groundwater level change is calculated at only -3.32 meters. While this value might not seem significant, it represents the groundwater level change in the whole model grid cell with the size of $100\text{ m} \times 100\text{ m}$, not in one particular observation well. The local groundwater level change around the referred abstraction well, which typically has a diameter smaller than 1 meter, is theoretically much higher than the grid-representative groundwater head decrease. Such a circumstance where the simulated groundwater level change is found lower compared to the actual local drawdown due to its spatial resolution has also been noticed in other studies (Yidana et al., 2015; Pétré et al., 2019b). Therefore, understanding the circumstances of the observation wells data is very important in calibrating a numerical groundwater flow model representativeness.

5.5 Conclusions

In this study, we quantify the aquifer interaction, driven by multi-layer groundwater abstraction, in the BGB by utilizing the collated EWT data in conjunction with a numerical groundwater flow model during the period between 2005 and 2018. In addition, we also use the model simulation output to observe the impact of multi-layer groundwater abstraction on the spatial distribution of the groundwater level changes.

In the EWT data analysis, we focus on three data: (1) major ion elements, (2) groundwater age, and (3) stable isotope. We overlay our EWT data plot (Stiff diagrams, interpolated groundwater age profile, and $\delta^2\text{H}$ and $\delta^{18}\text{O}$ correlation) on the BGB map to qualitatively evaluate their spatial patterns, their values' changes, and their correlation with other available information, for example, land use and topographical distribution.

For the groundwater flow model setup, we use the previously developed groundwater flow model (Rusli et al., 2023a). The model parameterization is based on field and laboratory measurements, literature studies, population-based estimates, and hydrological simulation using the `wflow_sbm` model (Imhoff et al., 2020; Wannasin et al., 2021a). The simulation is run transiently between 2005 and 2018 in monthly time steps.

In evaluating the groundwater flow model, we assess the similarity between the EWT data analysis and the numerical model simulation results. Qualitatively, both methods are in agreement on interpreting the groundwater system in the BGB from the perspective of groundwater recharge spatial distribution, regional groundwater flow direction, groundwater age estimates, and aquifer interaction identification.

Based on the model simulation, we quantify the aquifer interaction at, on average, 0.110 m/year, which is relatively significant compared to the other groundwater fluxes. We also determine the unconfined aquifer storage volume decrease, calculated from the change in the groundwater table, resulting in an average declining rate of 51 Mm³/year. This number shows that the upper aquifer storage is dwindling at a rate that is disproportionate to its groundwater abstraction, hugely influenced by the aquifer interaction. The storage lost from only this partition contributes up to 60.3% of the total groundwater storage lost, despite contributing to only 32.3% of the groundwater abstraction. Additionally, we also investigate and examine the correlation between the groundwater level changes and the groundwater abstraction zones. Despite having the fewest groundwater abstraction zones, the mountainous area, unfortunately, suffers from the largest groundwater level drawdown, as well as the highest aquifer interaction, which in the long run could lead to potential basin closure (Molle et al., 2010; Pauloo et al., 2021).

Following our effort to collate the scattered groundwater-related data, we see the opportunity to initiate an open integrated groundwater database system in the BGB, specifically, and in Indonesia and other data-scarce areas, in general. The government as the authorized stakeholder has the most important role in bridging the groundwater-related data and information gap among researchers, practitioners, companies, and the public.

This study contributes to showing the importance of the quantification of aquifer interaction and groundwater level change dynamics driven by multi-layer groundwater abstraction in multi-layer hydrogeological settings. A better understanding of the groundwater flow mechanism will assist in deriving basin-scale groundwater policies and management strategies under the changing anthropogenic and climatic factors, thereby ensuring more sustainable groundwater management.



Chapter 6

Future groundwater availability projection



This chapter is mostly based on and adapted from:

S. Rusli, V. Bense, S. Mustafa, and A. Weerts (n.d.). “Assessing the significance of global climate model projections and groundwater abstraction scenarios on future basin-scale groundwater availability”.

in preparation

Abstract

Groundwater is under the pressure of changing climatic and increasing anthropogenic factors. In this study, we project the effect of these two factors on the projected future groundwater status. Climate projections of RCP4.5 and RCP8.5 from the Coupled Model Intercomparison Project Phase 6 (CMIP6) drive a one-way coupled Wflow_sbm and MODFLOW model. In addition, three plausible groundwater abstraction scenarios with diverging predictions from increasing, constant, to decreasing volumes and spatial distribution are used. Groundwater status projections are assessed for the short-term (2030), mid-term (2050), and long-term (2100) periods. We use the Bandung groundwater basin (BGB) as our study case, located 120 kilometers from the current capital city of Indonesia, Jakarta, which is currently under a relocation plan. Results show that changes in the projected climate input, including intensifying rainfall and rising temperature, do not propagate significant changes in groundwater recharge. Under the current unsustainable groundwater abstraction rate, the confined piezometric head is projected to drop up to 7.14 meters, 15.25 meters, and 29.51 meters in 2030, 2050, and 2100, respectively. When groundwater abstraction expands in proportion to the present population growth, the impact is worsened almost two-fold. In contrast, if the groundwater abstraction decreases because of the relocated capital city, the groundwater storage starts to show replenishment potential. As a whole, projected groundwater status changes are dominated by anthropogenic activity, and less so by changes in climatic forcing. The results of this study are expected to demonstrate and inform responsible parties in operational water management on the issue of the impact of projected climate forcing and anthropogenic activity on future groundwater status.

6.1 Introduction

Groundwater has been known to be over-exploited in many basins worldwide (Bierkens and Wada, 2019; Gleeson et al., 2020). In more than half of the sub-districts located in the northwestern part of Bangladesh, the estimated groundwater abstraction has a higher volume than the simulated groundwater recharge (Shahid et al., 2015). Even more drastically, twenty-one (out of twenty-three) provinces in China were diagnosed with groundwater over-exploitation-related problems (Lili et al., 2020). In the northeastern part of Brazil, the intensification of groundwater exploitation has caused piezometric surface drawdowns of up to 100 meters (Luna et al., 2017). In the archipelago part of Spain, Gran Canaria, the ensuing groundwater depletion would require a few decades to recover (Custodio et al., 2016). From all such cases, we can see the severe impact driven by anthropogenic activities through groundwater abstraction on the groundwater regime. Dwindling groundwater tables, depleting groundwater storage, and degrading groundwater quality, have led to various consequences such as land subsidence (Chen et al., 2022), wetland deterioration (Mancuso et al., 2020), groundwater pollution (Meng et al., 2022), and seawater intrusion (Momejian et al., 2019).

Besides anthropogenic activities, climatic change may also play an important role in a changing groundwater regime since groundwater recharge is the dominant driver of groundwater flow. Surface and soil properties aside, the generation process of groundwater recharge is modulated by precipitation, temperature, radiation, and other climate variables in the likely climate-dependent regions. The recent changes in these variables' patterns, frequencies, and extremes, have led to the alteration of the variable that directly regulates the groundwater table distribution. Several studies suggest that changes in climate contribute positively to the increase of groundwater recharge (Tillman et al., 2016; Patle et al., 2018; Gaye and Tindimugaya, 2019). This occurs as rainfall intensification has provided a higher volume of water, therefore providing an opportunity for more abundant groundwater resources. Some others advocate contrarily, where they estimate a decline in groundwater recharge as a consequence of climate change (Pardo-Igúzquiza et al., 2019; Anurag and Ng, 2022; Trásy-Havril et al., 2022). Mostly, the reduction is related to the higher potential evapotranspiration driven by the warming temperature. Some others found the trend to be less definitive, varying per case depending on various factors, and involving large uncertainties in its quantification (Meixner et al., 2016; Smerdon, 2017; Yawson et al., 2019; Wu et al., 2020; Wang et al., 2021a).

As much as both anthropogenic and climatic factors have influenced the groundwater regime in the past centuries even at the global scale (Döll et al., 2012), they also, to various extents, control the current and future status of the subsurface resource (Stevenazzi et al., 2017; Liu et al., 2022). Therefore, future groundwater resource prediction relies greatly on climate projections and anthropogenic scenarios. In regard to climate projection studies, the Coupled Model Intercomparison Project (CMIP) takes an important position in

coordinating the global climate models (GCMs) worldwide. In its current sixth development phase, CMIP6 (Eyring et al., 2016) distributes climate model outputs from numerous GCMs run by various model groups under different Representative Concentration Pathway (RCP) scenarios (IPCC, 2021), a set of pathways developed specifically on the span of projected radiative forcing values by the year 2100 (Vuuren et al., 2011). With numerous hydrological forcing projections available in multiple scenarios, it is possible to simulate future groundwater recharge using hydrological models, from catchment to global scales (Yuan et al., 2015; Zhao et al., 2021; Hua et al., 2022).

While climate variables have indirect repercussions on groundwater recharge as they are also controlled by other factors, in particular the basin surface and subsurface properties within a hydrological modeling framework, groundwater abstraction physically and directly removes the groundwater from subsurface storage. Regarding anthropogenic projection scenarios, many studies develop scenarios in which the groundwater abstraction rates increase (Chang et al., 2020; Ansari et al., 2021), in line with rising populations. Only a few studies projected the abstraction to decrease in the future, and in the case they do, it is estimated not as the likely scenario but as recommended policies with the aim to achieve sustainable abstraction rates. Nevertheless, in some specific basin-scale areas, decreasing future groundwater abstraction might be a real possibility, which is not less important to be studied in comparison to the increasing abstraction scenario. This becomes even more crucial as changes in anthropogenic factors are often quantified to be more influential to the groundwater level compared to changes driven by climatic factors (Varouchakis et al., 2015; Brewington et al., 2019; Mustafa et al., 2019).

In this study, we aim to envisage future groundwater availability under different climatic scenarios and multiple and diverging anthropogenic scenarios. The test basin is the Bandung groundwater basin (BGB), located in Java Island, Indonesia. While currently developed in a rising population trajectory, the Indonesia capital city relocation plan could steer the future groundwater abstraction down in the BGB. A detailed description of the affiliations between Jakarta, the current capital city, and the BGB is presented in a later section, along with the new capital city plan's short-term future schedule. Briefly summarized, the BGB and Jakarta are closely connected. The urban and industrial sector development in the study area is highly influenced by the demographic and socio-economic activity within and around the capital city. With the plan to relocate the capital, it is predicted that many aspects of the study area would be impacted, including the groundwater abstraction volume, rate, and spatial distribution. Later in this study, the projected groundwater abstraction scenario is the reflection of our interpretation regarding this potential impact. The comparable likelihood of future groundwater abstraction to either increase following the current trajectory or decrease as impacted by the capital city relocation plan makes this case study unique as compared to other study areas.

Under the future climatic forcing and groundwater abstraction uncertainties, in our analysis, we simulate the groundwater level and storage changes using a one-way coupled wflow_sbm and MODFLOW model (Rusli et al., 2023a; Rusli et al., 2023b). By applying multiple climatic forcing and abstraction scenarios, we aim to specifically (1) quantify the impact of future climate projection on groundwater recharge, and (2) assess the impact of the changing groundwater abstraction on groundwater status in the study area. It is expected that the outcome of this study would be useful to understanding the subsurface processes projection, generally, and is comparable with other basins with similar characteristics. We also believe that this study would provide valuable input for the BGB authorities to improve the current and future groundwater policy and management.

6.2 Material and methods

6.2.1 The influence of Jakarta and the new capital city plan on the BGB

Jakarta is a congested metropolitan city, with an area of 4,384 km², and a population density of 13,000 people per km². In 2019, there were up to 3.2 million commuters entering the Jakarta Metropolitan Area (JMA) daily (Martinez and Masron, 2020). Undoubtedly, Bandung City, the largest city within the BGB, is one of the cities with tangible mutual dependencies to Jakarta due to its neighboring distance (see Figure 6.1). The flows of demographic and socio-economic activities between these two cities make them often referred to as the Jakarta-Bandung mega-urban region (Pravitasari et al., 2018). The Cipularang Toll Road, one of the highway connections between Jakarta and Bandung, is even classified as the busiest corridor in Java Island (Andani et al., 2020).

The future of the groundwater regime in the BGB becomes uncertain with the latest geospatial planning of Indonesia. It is to move the capital city from Jakarta to Nusantara, located on a separate island in Borneo (Nugroho, 2020; Hackbarth and Vries, 2021; Mutaqin et al., 2021). With relocation starting in 2024 (Vries and Schrey, 2022), it would not only move the center of government but also mobilize part of the residents from Jakarta (Kodir et al., 2021). Therefore, the urban and industrial development in cities surrounding Jakarta, including those in the BGB, is predicted to be impacted. The Presidential Regulation of Indonesia number 63, 2022 (Indonesia, 2022) stated that the relocation is to be finalized in 2045. In the regulation's appendix, it is estimated that the population in Nusantara City would increase by eight folds, from around 150,000 people to more than 1.2 million people by the end of 2029 (Indonesia, 2022), with a considerable portion of the people actually relocated from JMA and its surrounding, including the BGB.

Considering the capital city relocation plan and the close affinity between our study area and Jakarta, it is reasonable to imagine that the former issue would influence the growth of the urban and industrial areas in the BGB. Indirectly, it would also be possible to forecast that the pressure of pumping groundwater to fulfill the water demand in

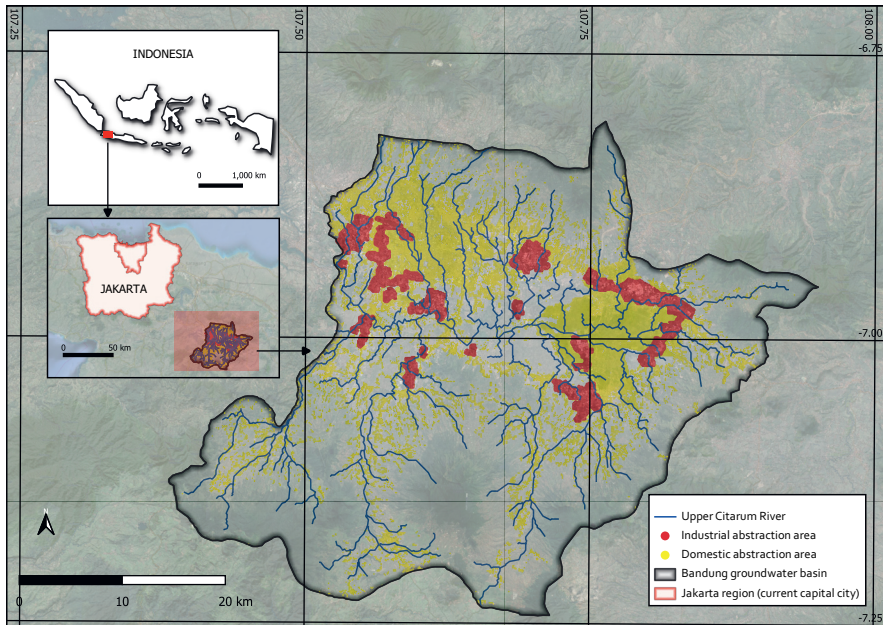


Figure 6.1: Overview of the BGB's relative position to Jakarta, the capital city of Indonesia. This image is adapted from Rusli et al. (2023b).

the future could be reduced. However, such a trend did not always happen in other former capital cities, such as Rio de Janeiro (Silva Jr and Pizani, 2003), Lagos (Healy et al., 2020), and Yangon (Hashimoto et al., 2022). In these three ex-capital cities, the economic growth carries on, despite being at different rates, and is translated to increasing groundwater abstraction. The uncertainties involving the future water resources, specifically groundwater abstraction, in the BGB are highly unsettling, thus multiple and diverging scenarios are necessary to be explored. Therefore, while the common conceptual understanding of groundwater abstraction projection is to increase in the future, in this study we define three scenarios with wide ranges, stretching from an increasing to decreasing future groundwater abstraction, described in Section 6.2.4.

6.2.2 Simulation workflow and temporal framework

There are two numerical simulations involved in the modeling framework within this study: (1) surface hydrological and (2) groundwater flow. The hydrological simulation is performed using the `Wflow_sbm` model, with two climate variables as its main forcing: the rainfall and the potential evapotranspiration. Hence, the climatic factors are included. This produces two outputs: the simulated river discharge and the groundwater recharge. While the simulated river discharge is used to evaluate the simulation performance, the

groundwater recharge is further used to force the succeeding model - the MODFLOW groundwater flow model. Aside from having the simulated groundwater recharge as its input, the groundwater flow model is also regulated by boundary conditions of groundwater abstraction, hence the anthropogenic factors. The outputs of the groundwater flow model include transient groundwater head (groundwater table for the unconfined layer and piezometric head for the confined layer) and groundwater storage changes.

We consider a two-phase simulation setup in this study based on the temporal categorization: the baseline and the future period. The baseline period is used as the 'control' of changes in the latter period; this is very important to note especially for variables whose projected changes are expressed in percentage relative to the benchmark. For the Wflow_sbm model hydrological simulation using Wflow_sbm and the MODFLOW model groundwater flow simulation, the benchmark period is set between 2005 and 2015. The baseline hydrological simulation was forced by the CHIRPS rainfall estimates (Funk et al., 2015), and the groundwater abstraction defined in the groundwater flow model was estimated upon population number and a number of literature reviews (Rusli et al., 2021). For the climate data temporal classification, the baseline period's temporal coverage starts from 1981 to 2015 following the categorization on the Copernicus Climate Data Store of MRI-ESM2-0 model group (Copernicus Climate Change Service, 2021). For the future period, we classify the temporal setting into three categories: the short-term future (up to 2030), the mid-term future (up to 2050), and the long-term future (up to 2100). These temporal classifications serve not only as the analysis checkpoints but also as the milestone for the projected groundwater abstraction spatial distribution. On the whole, Figure 6.2 outlines the role of the temporal setup in this study (in the horizontal direction), from the baseline (left box) to the future (right box) period, as well as the setup for subsequent hydrological and groundwater flow simulations (in the vertical direction) in each of the period.

6.2.3 Climate projection data and scenario

In this study, we develop two climatic scenarios that involve changes in projected rainfall and potential evapotranspiration, influenced by temperature and radiation. For the future period hydrological simulation, we use the CMIP6 (Coupled Model Intercomparison Project Phase 6) climate model runs (Eyring et al., 2016) under two greenhouse gas concentration trajectory scenarios: RCP (Representative Concentration Pathway) 4.5 and 8.5 (IPCC, 2021). The RCP4.5 is selected as the intermediate scenario, while the RCP8.5 is the extreme one. The considered variables are those required as the input to the Wflow_sbm model, specifically precipitation and near-surface air temperature as well as surface downwelling shortwave radiation and top-of-atmosphere (TOA) incident shortwave radiation. The latter three variables are used to estimate potential evapotranspiration using the method proposed by Bruin et al. (2016). All the mentioned climate model products are publicly available on the Copernicus Climate Data Store (Copernicus Climate Change Service, 2021).

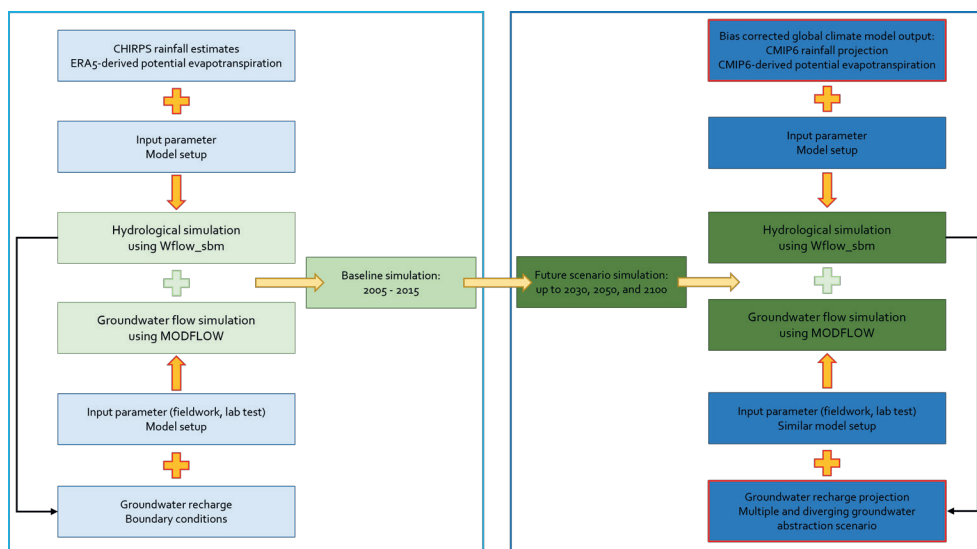


Figure 6.2: The overview of the modeling workflow. The left and right boxes show, respectively, the model setup during the baseline period and the future period. While both the hydrological and groundwater flow model's setup is similar during the two periods, the forcing data and boundary conditions are different and determined according to their respective configuration.

To select the model group, we apply criteria that the product should have (a) a spatial resolution of approximately $1^\circ \times 1^\circ$, (b) a daily temporal resolution for rainfall and temperature, and (c) a projection scenario of historical, RCP4.5, and RCP8.5; applicable to the four mentioned variables. Considering the criteria and other climate projection studies, we use the climate model outputs from the MRI-ESM2-0 model group (Yukimoto et al., 2019) for the precipitation and near-surface air temperature. We do not use an ensemble of multiple climate projection products for several reasons. First, as mentioned above, while the change in climate variables impacts the surface water cycle, it is mediated by the soil before subsequently affecting the subsurface water budgets. Therefore, climatic changes impact the groundwater recharge in a way lower magnitude compared to the surface variables, especially considering the governing control of soil within the groundwater recharge generation processes. This theory has been confirmed in many studies. In the Upper Colorado River basin, the groundwater recharge changes are projected to be under 10% relative to its baseline until 2100 despite the extreme climate change scenario (Tillman et al., 2016). In the Western United States, it was found that including the uncertainty bounds to the analysis projects no change to the groundwater recharge (Meixner et al., 2016). In the United Kingdom barley crop fields, the groundwater recharge is projected to change up to a minuscule 31 mm in 2050 under the largest reduction scenario (Yawson et al., 2019). Second, previous studies have found the anthropogenic

factor as the more dominant factor in groundwater level predictions compared to the climatic ones (Mustafa et al., 2019; Aslam et al., 2022). Combining 44 climatic scenarios from different RCPs and model groups to force their groundwater flow model, Mustafa et al. (2019) estimated that groundwater abstraction scenarios still hold up to 7.4 times higher influence on the projected groundwater level compared to the climatic scenarios. This is important, especially considering the computational cost that is generally way more demanding in simulating the climatic scenarios, which turns out to be less dominant in regulating the projected groundwater regime. Third, the MRI-ESM2-0 model group has also been suggested to perform well in CMIP6 outputs (Oruc, 2022), especially those related to cloud-related processes (Kawai et al., 2019). It has also proved to be one of the best-performing models in other studies, including in Southeast Asia region (Iqbal et al., 2021; Baghel et al., 2022), which is very close to our study area. It is not used for the global radiation data, however, as it does not cover the TOA incident shortwave radiation projection for the RCP 8.5. Therefore, for the global radiation data, we use the climate model output from the GFDL-ESM4 model group (Krasting et al., 2018), which qualifies for all the criteria mentioned above.

6.2.4 Groundwater abstraction scenarios

For the groundwater abstraction projection, we consider three diverging scenarios where the groundwater abstraction (a) increases, (b) stays constant, and (c) decreases in the future. Meanwhile, the groundwater abstraction during the baseline period is set according to estimates from our previous studies (Rusli et al., 2023a), increasing annually from 300 Mm^3 per year in 2005 to 495 Mm^3 per year in 2020. For all boundary conditions, the groundwater abstraction is distributed horizontally based on land use and vertically based on domestic/industrial water demand classification.

In this study, we propose a new approach to establishing the scenario where the future groundwater abstraction increases (scenario one). Commonly, the projected groundwater abstraction rate increases in proportion to the projected population growth. We indeed apply such a method to estimate the annual volume of the future groundwater abstraction in the study area, using an annual population growth rate of 1.36% referring to the United Nations' World Population Prospects, shown in Figure 6.3a. Under this scheme, the annual groundwater abstraction volume in 2030, 2050, and 2100 is projected to be 529, 839, and 1,346 Mm^3 per year, respectively. However, we have not yet found an approach that not only increases the abstraction rate but also expands its spatial distribution. Considering the currently high population density in the BGB, it is only logical that a surge in groundwater abstraction volume is accompanied by an enlargement of the abstraction area. In this paper, we expand the groundwater abstraction location by increasing the area of the initial abstraction location proportionally to the volume of abstraction.

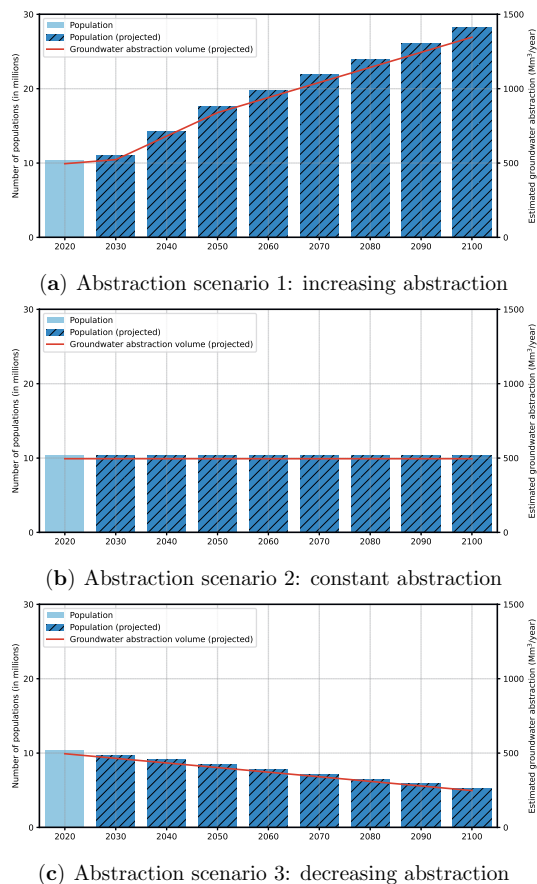


Figure 6.3: The three diverging scenarios of estimated groundwater abstraction volumes (right axis, Mm³/year) based on the projected number of population (left axis, millions).

The other two groundwater abstraction scenarios are based on Indonesia's capital city relocation plan. In the 'stay constant' scenario (scenario two), we assume that the urban and industrial area that is currently settling will continue to remain where they are now, with stagnant development (Figure 6.3b). Therefore, the groundwater abstraction rate is made constant from 2020 to 2100. In the decreasing groundwater abstraction scenario (scenario three), we assume that the capital city relocation would decrease the population of the BGB and water demand gradually in the future (Figure 6.3c). By 2100, it is assumed that the number population will be halved from 2020, therefore also decreasing the groundwater abstraction rate by 50% to 248 Mm³ per year, linearly interpolated. In scenarios two and three, the spatial distribution of the groundwater abstraction area remains constant with one in the baseline period.

Table 6.1: Climate dataset for bias adjustment and statistical downscaling

Variables	Climate model output	'Ground truth' data
Precipitation	MRI-ESM2-0	CHIRPS ¹
Near-surface air temperature	MRI-ESM2-0	ERA5-Land
Surface downwelling shortwave radiation	GFDL-ESM4	ERA5-Land
TOA incident shortwave radiation	GFDL-ESM4	ERA5-Land

¹ two CHIRPS products of different resolutions of $0.25^\circ \times 0.25^\circ$ and $0.05^\circ \times 0.05^\circ$ are used

6.2.5 Bias adjustment and statistical downscaling method of ISIMIP3b

In climate-related research, it is a common practice to employ bias correction when working with climate simulation data. This is done as they generally have different statistical attributes to climate observation data (Lange, 2019). The discrepancies occur due to various factors, such as differences in spatial resolution and systematic biases. Therefore, bias correction, involving two steps method of bias adjustment and statistical downscaling, is applied to bridge and minimize this gap. In this study, we apply the method tailored to the Inter-Sectoral Impact Model Intercomparison Project phase 3b (ISIMIP3b) for our bias correction (Lange, 2019; Lange, 2021).

Within the ISIMIP3b framework, two datasets are specified as benchmarks: (a) historical 'ground truth' data and (b) high-resolution data employed for the bias adjustment and statistical downscaling processes, respectively. In this study, we use CHIRPS estimates (Funk et al., 2015) with a spatial resolution of $0.25^\circ \times 0.25^\circ$ as the historical 'ground truth' rainfall estimates. Notably, the spatial resolution of the MRI-ESM2-0 model output is coarser than that of CHIRPS estimates. To align these datasets appropriately, the MRI-ESM2-0 model output is initially re-gridded and resampled to match the spatial resolution of CHIRPS before the bias adjustment was applied. As CHIRPS is available at an even higher resolution of $0.05^\circ \times 0.05^\circ$, we use it further as the benchmark for the statistical downscaling. The historical 'ground truth' estimates for the other variables (near-surface air temperature, surface downwelling shortwave radiation, and TOA incident shortwave radiation) are based on ERA5-Land hourly data (Copernicus Climate Change Service, 2019). All the datasets used for the application of ISIMIP3b in this paper are listed in Table 6.1.

6.2.6 Wflow_sbm model setup

The Wflow_sbm model is used to perform the hydrological simulation in this study. With model parameters that mostly represent physical characteristics, using Wflow_sbm makes it easier to intuitively interpret and correlate the parameter values with physical catchment properties. In the last decade, Wflow_sbm has been widely used in many hydrological modeling studies (López et al., 2016; Hassaballah et al., 2017; Gebremicael et al., 2019), including those in tropical regions in South East Asia (Rusli et al., 2021; Wannasin et al., 2021a), delivering good performance, shown by KGE, NSE, and RMSE metric.

We use a similar Wflow_sbm model setup for our previous study (Rusli et al., 2023a; Rusli et al., 2023b). Started with high-resolution model parameterization based upon point-scale (pedo)transfer functions (PTFs) (Imhoff et al., 2020), it is followed by downscaling designated to the model resolution of $0.08^\circ \times 0.08^\circ$. We use (a) SoilGrids database (Hengl et al., 2017) for soil-related parameters estimation, (b) Monthly Leaf Area Index climatology for daily interception calculation (Gash, 1979), (c) MERIT-DEM dataset (Yamazaki et al., 2017) for river network delineation (Eilander et al., 2020), and (d) vito land use map (Buchhorn et al., 2020) for deriving land-use related parameters. We simulate the recharge by previously calibrating the *MaxLeakage* parameter by optimizing the KGE value between the observed and the simulated discharge (Rusli et al., 2023a).

Precipitation and potential evapotranspiration data are the primary forcing data to run the Wflow_sbm model, besides the static maps input. In accordance with our temporal setting, we prepare and split the forcing data into the baseline and future projection periods. For the baseline period, CHIRPS rainfall estimates (Funk et al., 2015) and potential evapotranspiration derived from ERA5 temperature and global radiation data using the method from Bruin et al. (2016) are used. Using the Extended Triple Collocation method (McColl et al., 2014), CHIRPS products were found to perform well in estimating rainfall in the study area in our previous study (Rusli et al., 2021). In the future period, the forcing data are obtained from the bias-corrected climate projection: (1) the bias-corrected rainfall projections from the CMIP6 model output of the MRI-ESM2-0 model group and (2) the potential evapotranspiration derived from the bias-corrected near-surface air temperature projections from the CMIP6 model output of the MRI-ESM2-0 model group and the bias-corrected surface downwelling shortwave radiation and TOA incident shortwave radiation projections from the CMIP6 model output of the GFDL-ESM4 model group, based on two RCP scenarios (RCP4.5 and RCP8.5).

6.2.7 Groundwater flow MODFLOW model setup

The MODFLOW6 model, which solves the Darcy three-dimensional groundwater flow equation using the control-volume finite-difference (CVFD) method, is used to perform the groundwater flow simulation in this study. The model is built using the MODFLOW python package, flopy (Bakker et al., 2016).

The MODFLOW model parameterization in this study is based on the combination of literature reviews, fieldwork, and laboratory experiments. The model's subsurface vertical discretization is based upon collated borehole data (Rahiem, 2020), interpreted as a 3-layer model: the upper aquifer as the top layer, the thin interspersing aquitard as the middle layer, and the lower aquifer as the bottom layer. The hydraulic conductivities of the soil were measured by a combination of slug tests in the field, laboratory tests, and private company reports. They were then recalibrated by minimizing the difference between the simulated and the observed groundwater table (Rusli et al., 2023a). The K_h of the upper

and the lower aquifer are found in relatively similar ranges between 0.15 and 0.58 meters per day, as they are formed by a solitary geological formation. The K_v ranges between 3.0×10^{-4} and 6.0×10^{-4} meter per day. The aquitard is ten times less permeable than the aquifer, with K_h ranges between 1.5×10^{-2} and 5.8×10^{-2} meter per day and K_v ranges between 3.0×10^{-5} and 6.0×10^{-5} meter per day. The storage parameters are obtained from private company pumping test reports, and the river-related parameters were previously calibrated under steady-state conditions. The model parameters are spatially interpolated to produce gridded parameter values. The initial condition is defined by our previous simulation results at the designated time (Rusli et al., 2023a). The well package, related to groundwater abstraction, is set according to the scenario described in Section 6.2.4.

Similar to the hydrological simulation, we split the forcing data and the simulation period into two windows; the baseline period between 2005 and 2015, and the future projection period on short-term (up to 2030), mid-term (up to 2050), and long-term (up to 2100) future. Both periods are forced by the groundwater recharge simulated by the Wflow_sbm model, resulting in three different inputs as the drivers of the groundwater flow model: the baseline groundwater recharge, the future RCP4.5 groundwater recharge, and the future RCP8.5 groundwater recharge. With the combinations of different inputs and boundary conditions, six different outputs are produced from the groundwater flow simulation.

6.3 Results

6.3.1 Bias corrected rainfall projection

The statistical attributes of the rainfall estimates pre- and post- bias correction, as well as ones of the future scenarios, are summarized in Table 6.2. In the MRI-ESM2-0 model group 'historical' output pre-bias correction, the rainfall is, surprisingly, projected to decrease in general compared to the CHIRPS estimates (column 1) in both RCP4.5 (column 4) and RCP8.5 (column 6). These values are, however, prior to bias correction. The same trend of climate model underestimation in almost every statistical distribution is also found during the baseline period (column 1 and column 2), therefore bias correction is essential to be implemented. By applying the ISIMIP3b bias adjustment, we come up with baseline rainfall estimates that represent a better statistical fit to the CHIRPS estimates (column 3). Consequently, we apply the bias correction to the future scenario of RCP4.5 (columns 5) and RCP8.5 (columns 7).

To observe the seasonal impact on the projected climate scenario, we plot the monthly rainfall of the baseline period of CHIRPS and the future period of the bias-corrected RCP4.5 and RCP8.5 projections in Figure 6.4. During the rainy season between October and March, we can see that the projected rainfall has an increasing trend, with higher monthly rainfall especially from November to January. A contrasting trend is shown in the dry season between April and September, with lower monthly rainfall especially from July

Table 6.2: Application of ISIMIP3b bias correction to the rainfall estimates (in millimeters)

	Ground truth [†]	MRI-ESM2-0_historical data*		MRI-ESM2-0_RCP4.5		MRI-ESM2-0_RCP8.5	
	CHIRPS	Pre-**	Post-**	Pre-**	Post-**	Pre-**	Post-**
	(1)	(2)	(3)	(4)	(5)	(6)	(7)
Min	0.00	0.00	0.00	0.00	0.00	0.00	0.00
Q ₁	0.00	0.08	0.00	0.06	0.00	0.06	0.00
Median	4.67	0.97	4.17	2.81	5.45	2.39	5.18
Mean	7.61	5.74	7.62	6.87	8.70	6.64	8.52
Q ₃	12.50	9.19	12.53	11.41	14.60	10.92	14.26
Max	111.66	91.45	111.66	88.13	131.67	121.70	123.90

* historical data of the climate projection products have the temporal coverage of the baseline period (1981 - 2015)

** the pre- and post- columns represent the values pre- and post- bias-adjustment in the future periods (2015 - 2100)

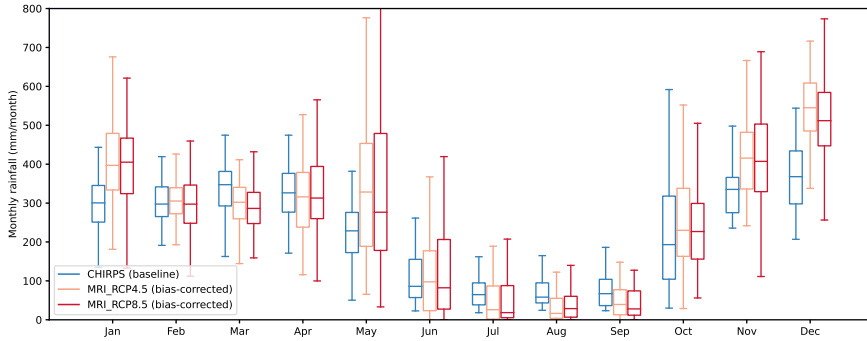
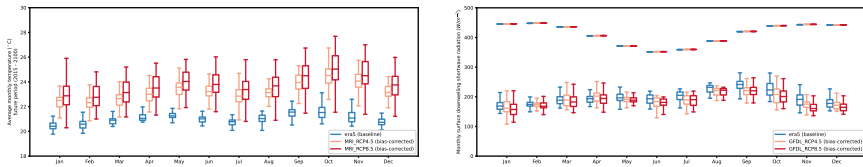


Figure 6.4: The comparison between the rainfall monthly statistics in the baseline period and in the two future climate scenarios (RCP4.5 and RCP8.5). The future rainfall estimates are bias-corrected using the ISIMIP3b bias correction method.

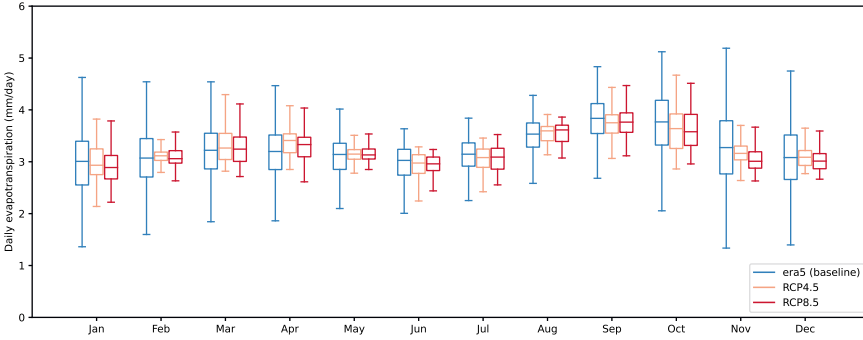
to September. In short, the wet period is projected to become wetter, and the dry period to be drier. We can also observe only small differences in the statistical quartiles between the two RCPs, with similar widths, mostly, between the orange and red boxes. The width of the minimum and maximum values, however, is more apparent. The magnitudes of the hydrological extremes are projected to be more pronounced in the future, therefore floods and droughts are predicted to be more severe than they currently are.

6.3.2 Bias-corrected potential evapotranspiration projection

We apply the bias-correction method of ISIMIP3b to the near-surface air temperature, surface downwelling shortwave radiation, and TOA incident shortwave radiation, in a similar fashion as one to the rainfall estimates. Figure 6.5a and 6.5b show the monthly near-surface air temperature and radiation projections, respectively. The monthly average temperature sharply increases from the baseline period of the aggregated ERA5-Land hourly estimates to the future period of the bias-corrected CMIP6 projections in all statistical attributes; quartiles, average, interquartile range, and extreme values. The



(a) Comparison between the temperature in the baseline period and in the two future climate scenarios (RCP4.5 and RCP8.5). (b) Comparison between the radiation in the baseline period and in the two future climate scenarios (RCP4.5 and RCP8.5).



(c) Comparison between the potential evapotranspiration in the baseline period and in the two future climate scenarios (RCP4.5 and RCP8.5).

Figure 6.5: The results on bias-corrected projections on three variables: (a) temperature, (b) radiation, and (c) potential evapotranspiration.

temperature, on the long-term average, is projected to be warmer by 2.21°C and 2.72°C in RCP4.5 and RCP8.5 scenarios, respectively. The projection on global radiation is based on the GFDL-ESM4 model group, with a tendency of slightly less surface downwelling shortwave radiation in the future. The TOA incident shortwave radiation remains almost constant throughout. On the radiation variable, the two different climatic scenarios of RCP4.5 and RCP8.5 do not seem to differ a lot in their statistical values.

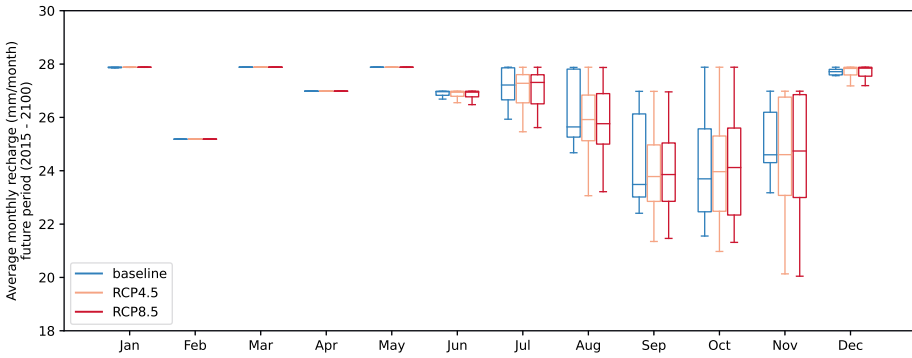
We use the three variables above to calculate potential evapotranspiration using the method of Bruin et al. (2016), with the result shown in Figure 6.5c. The range of the estimates is visually inconsistent between the baseline and the future period, as the future period is calculated in monthly time steps according to the temporal resolution of the radiation projections. Therefore, the variation between the statistical distribution is lower compared to ones of the baseline period, where it is available in the daily time step. The difference in the magnitude is considered low, as the highest difference in average daily potential evapotranspiration is less than 0.5 mm per day. Without looking at the seasonal variance, the annual daily potential evapotranspiration averages of the baseline period, the future RCP4.5 scenario, and the future RCP8.5 scenario are 3.24, 3.26, and 3.23 mm per day, respectively, which are relative to insignificant differences.

6.3.3 Groundwater recharge projection

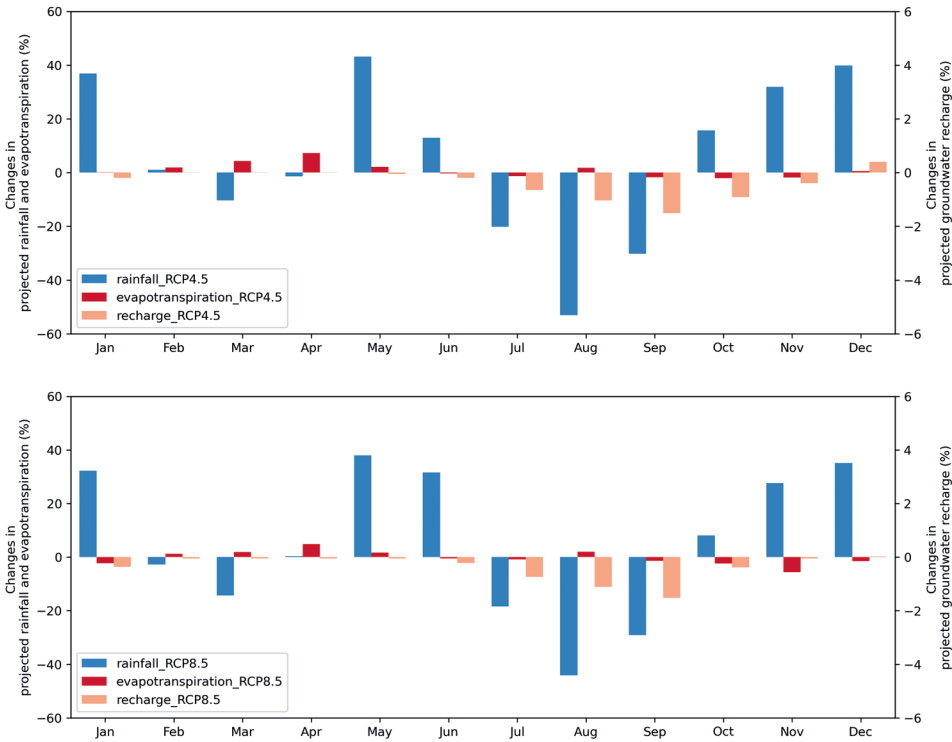
The projected rainfall and potential evapotranspiration drive the Wflow_sbm model to project groundwater recharge. A number of conceptual correlations are easily derivable in the projection of groundwater recharge: increased rainfall intensifies wet-season recharge, drier periods reduce dry-season recharge, rising temperatures limit soil infiltration, etc. As the difference in groundwater recharge in mm per day unit is relatively small, we accumulate the daily recharge to monthly recharge. The seasonal pattern of the monthly groundwater recharge is shown in Figure 6.6a. The values intrinsically represent the number of days in each month, therefore the groundwater recharge in the non-31-day months is lower than those in the 31-day months. The results are confirmed to be consistent in all the short-term, mid-term, and long-term future assessments of groundwater recharge.

Distinct groundwater recharge patterns emerge in relation to wet and dry seasons. Between the start of the wet season when the soil moisture starts to be saturated (December) and the beginning of the dry season when the soil's maximum capacity for storing water is still attained (May), the groundwater recharge could no longer increase despite the increasing rainfall. On the other hand, between the start of the dry season when the soil moisture starts to dry up (June) and the beginning of the wet season when the void spaces in the subsurface are still available for water to fill into (November), the magnitude of the groundwater recharge is relatively more subject to change. Having said that, during the latter period, differences in median and extreme recharge values are relatively small, although quartile values exhibit variations. Median values vary most significantly either in September (RCP4.5) or October (RCP8.5), with small increases of 1.27% and 1.79%, respectively. In all other months except June, groundwater recharge either slightly increases or remains relatively constant. Annually, the average groundwater recharge during the baseline period of 315.1 mm per year is projected to insignificantly increase to 316.1 mm per year for the RCP4.5 and 316.4 mm per year for the RCP8.5 scenario.

The results indicate the dominant role of the already-saturated soil in controlling the groundwater recharge processes in the BGB. When the soil's maximum capacity is reached, more rainfall leads to no change in the recharge processes. Instead, it leads to more water loss to evapotranspiration should the PET allows. It would also lead to an increase in surface runoff discharge. On average, the absolute relative change in the rainfall, temperature, and groundwater recharge estimates under the RCP4.5 scenario, respectively, are 31.03%, 10.71%, and 0.36%. The similar changes for the RCP8.5 scenario are 28.36%, 13.10%, and 0.44%. Figure 6.6b visually contrasts the magnitude of changes in rainfall and potential evapotranspiration on the left axis with groundwater recharge on the right axis, using a scale that is ten times larger, all represented as monthly averages. The average value is chosen over the median value, specifically for this figure, to take into account the projected extreme values. From the results, the change in the groundwater recharge is found to be far less responsive compared to its driver, especially the rainfall.



(a) Comparison between the simulated groundwater recharge in the baseline period and in the two future climate scenarios.



(b) Comparison between the projected average monthly rainfall, potential evapotranspiration, and groundwater recharge.

Figure 6.6: The results of (a) groundwater recharge projection and (b) its value relative to its driver of rainfall and potential evapotranspiration. The values are averaged over the future period, annually, up to 2100.

6.3.4 Groundwater level projection

The combination of two climatic and three groundwater abstraction scenarios results in six outcomes of projected groundwater level. For each outcome, there are three temporal checkpoints assigned as the milestone of the assessment: the short-term, the mid-term, and the long-term future in 2030, 2050, and 2100, respectively. There are also two layers of aquifers, the unconfined and the confined aquifers, to be assessed. As there are a lot of numbers to unpack, we discuss the results as per the abstraction scenario.

Generally, we focus on the maximum drawdown values of the groundwater table/piezometric head, as the change in the groundwater head is found to be highly localized, both from the simulation and observation perspective. Furthermore, the baseline groundwater abstraction area is estimated 'only' at 27.3% of the total basin area for the domestic groundwater abstraction, and even at 4.7% for the more intensive industrial abstraction. Taking the average or median value for the whole groundwater basin, therefore, would not be suitable to represent the severity of the groundwater abstraction impact, considering the high number of cells involved in the numerical simulation.

Under the increasing groundwater abstraction scenario, the groundwater level is projected to continue decreasing, as expected. The numbers are alarming, particularly for the confined aquifer, where the groundwater abstraction is spatially more concentrated with higher abstraction rates compared to one in the unconfined layer. Under the RCP4.5 scenario, the maximum piezometric head drawdown for the confined aquifer is projected to be at -10.04 meters in 2030, -19.98 meters in 2050, and -48.79 meters in 2100. Under the RCP8.5 scenario, these numbers are calculated at the same magnitude up to two decimals. The numbers are also concerning for the unconfined aquifers, as the groundwater table is projected to dwindle to up to -3.38 meters and -3.40 meters in the long run under the RCP4.5 and RCP8.5 scenarios, respectively. Based on the drawdown area, the trend shows that the impacted area is enlarged as the groundwater abstraction area expands. In the unconfined aquifer, respectively 74.6%, 80.5%, and 87.2% of the groundwater basin area is projected to experience groundwater table drawdown in 2030, 2050, and 2100 under the RCP4.5 scenario, obviously with varying magnitude. For the confined aquifers, the numbers representing the depression area are 70.5%, 72.9%, and 75.4%. Under the RCP8.5 scenario, these numbers are pretty much consistent, with a maximum of less than 1% difference from the RCP4.5 results.

The second abstraction scenario portrays the projection of the current situation in the study area. Should the anthropogenic pressure remains the same, the groundwater level, as expected, is projected to remain dwindling. The maximum confined piezometric head drawdown for 2030, 2050, and 2100 under the RCP4.5 scenario are -7.14, -15.25, and -29.51 meters. The numbers for the RCP8.5 scenario are very similar: -7.14, -15.28, and -29.51 meters. Similar to the increasing abstraction scenario, the unconfined aquifer groundwater table drawdown is noticeably lower compared to that of the confined aquifer,

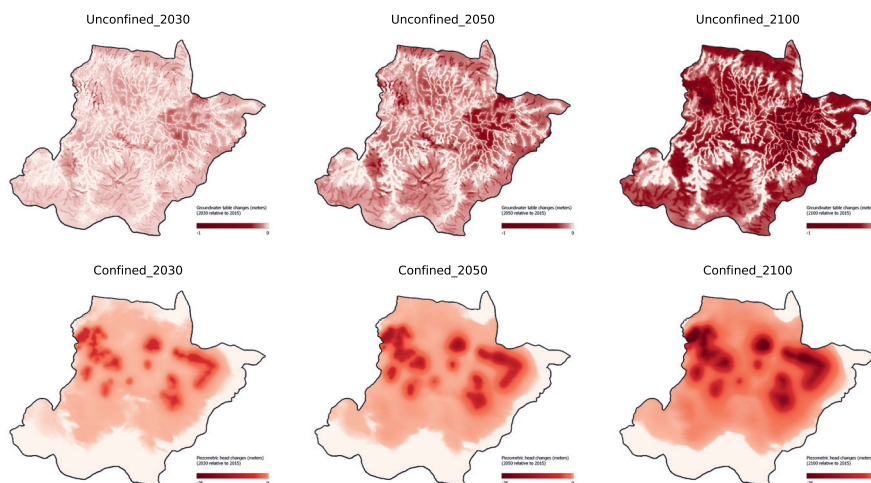


Figure 6.7: The spatial distribution of the projected groundwater head change under the RCP4.5 climatic scenario and the constant groundwater abstraction anthropogenic scenario. The three columns indicate the situation in the short-term (up to 2030), mid-term (up to 2050), and long-term (up to 2100) future, while the two rows represent the unconfined (top) and the confined (bottom) aquifers.

with a maximum drawdown of -2.58 and -2.60 meters in 2100 for RCP4.5 and RCP8.5, respectively. The drawdown area increases, with up to 84.7% and 75.0% of the groundwater basin area experiencing long-term dwindling groundwater heads in the unconfined and confined aquifer. Despite the lesser extent of the impacted area relative to the previous scenario, the vastly dominant area of decreasing groundwater head remains a concern. To visualize the time-series increasing impact of the groundwater head drawdown, Figure 6.7 shows the propagation of the groundwater head decline in the BGB under the RCP4.5 climatic scenario and the constant groundwater abstraction anthropogenic scenario.

The third abstraction scenario projects the groundwater abstraction to decrease, influenced by the relocation of Indonesia's capital city. Under this scenario, the groundwater is projected to be partially replenished between 2050 and 2100. This is indicated by the projected piezometric head drawdown that reaches -12.61 meters in 2050, but is calculated at -11.75 meters in 2100. Granted that -11.75 meters remain a net negative of groundwater head in the future, however, subsurface flows (and replenishment) are known to have a longer time scale as compared to surface flows to reach equilibrium. The fact that the piezometric head drawdown decreases signals an improving situation under scenario three. Having said that, the groundwater table in the unconfined aquifer is projected to decrease up to -2.58 and -2.93 meters under the RCP4.5 and RCP8.5 scenario, respectively. However, its drawdown area is projected to be smaller, going from 80.8% and 83.6% in

Table 6.3: Summary of projected maximum groundwater head drawdown under multiple climatic and anthropogenic scenarios

		Increasing abstraction		Constant abstraction		Decreasing abstraction	
		RCP4.5	RCP8.5	RCP4.5	RCP8.5	RCP4.5	RCP8.5
		(1)	(2)	(3)	(4)	(5)	(6)
2030	Unconfined	-0.98	-0.97	-0.89	-0.89	-0.89	-0.97
	Confined	-10.04	-10.04	-7.14	-7.14	-7.11	-7.11
2050	Unconfined	-1.69	-1.69	-1.49	-1.49	-1.49	-1.69
	Confined	-19.98	-19.98	-15.25	-15.28	-12.60	-12.61
2100	Unconfined	-3.38	-3.40	-2.58	-2.60	-2.58	-2.93
	Confined	-48.79	-48.79	-29.51	-29.51	-11.55	-11.75

2030 for RCP4.5 and RCP8.5 respectively to 75.5% and 76.7% in 2100. The response of groundwater replenishment is unique between the aquifer layers; the unconfined aquifer primarily reduces the drawdown area, while the confined aquifer relaxes the magnitude of the piezometric head drawdown. Nevertheless, it presents an opportunity for groundwater replenishment in the future given the right policy and management in the study area.

The two climatic scenarios, the three diverging abstraction scenarios, and the multiple assessment checkpoints as well as the two aquifer layers admittedly provide a lot of numbers to digest. Table 6.3 summarizes the maximum groundwater head drawdown in all involved scenarios, checkpoints, and layers in focus. The table makes it easy to see that the anthropogenic factor holds a more dominant influence on the status of the groundwater table in the future, with the climatic factor offering fewer changes in values due to the soil capacity control. This is shown by higher discrepancies when we are moving over the major columns, for example from column (1) to (3) to (5), compared to when we are moving over the minor columns, for example from column (1) to (2), (3) to (4), or (5) to (6). We can also see the propagation of the impact over time, from the major rows, and the more severe impact to the confined groundwater head compared to the unconfined groundwater table.

6.3.5 Groundwater storage projection

As stated above and shown in Figure 6.7, the drawdown impact of the groundwater abstraction is highly congregated. In the unconfined layer, the drawdown area is distributed under the abstraction area, while the area close to water bodies is less impacted. This occurs due to surface water and groundwater interaction, where the groundwater table is also regulated by the surface water elevation aside from the subsurface flow. In the confined aquifer, the highly elevated area on the surface is much less impacted compared to the one in the overlying aquifer, and the drawdown area is, in general, directly located under the abstraction area. Using only the groundwater head, although useful, could not capture the whole picture of the basin's groundwater regime projection. Therefore, we also assess the groundwater projections from the perspective of its integrated cumulative storage changes over time.

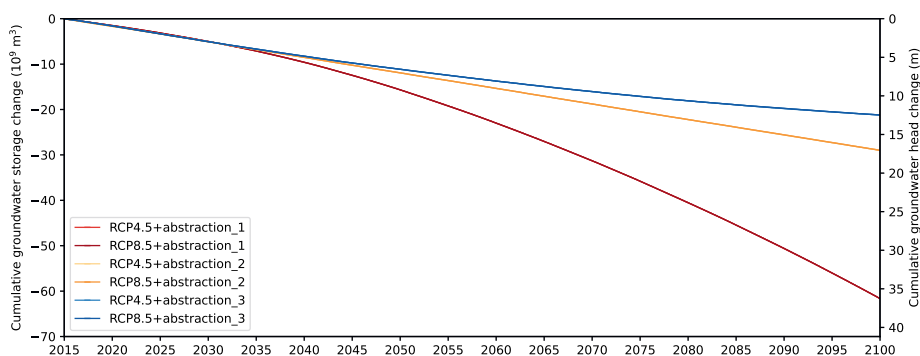


Figure 6.8: The cumulative projected groundwater storage changes from 2015 to 2100 for all climatic and anthropogenic scenarios.

Figure 6.8 shows the trajectory of each outcome in terms of its accumulated groundwater storage changes relative to the one in 2015 as the benchmark. Consistent with the earlier results, the difference between climatic scenarios is very thin, as lines with the same color are almost intersecting. However, the impact of the diverging abstraction scenario is visually apparent and even results in diverging groundwater storage change. Using the gradient of the storage depletion accumulation for scenario two as the benchmark, it gets up to 3.43 times steeper for scenario one and up to 0.40 times milder for scenario three during the most extreme year, both propagating in curve-shaped lines. The lines' shapes deliver important messages, as they indicate the uniquely diverging results of deteriorating, sustained, and improving groundwater storage depletion under the first scenario, second, and third scenarios, respectively. It is also notable that despite the indication of confined groundwater replenishment from the groundwater level perspective, assessment of the groundwater storage change suggests otherwise, further discussed in Section 6.4.2.

Under the constant abstraction scenario, the BGB storage is projected to lose almost 20 billion m^3 in the upcoming 85 years. While the number might seem exaggerated, it is actually equivalent to an average of 0.54 mm per day of storage depletion. The rate of storage depletion is relatively constant throughout the short-term, mid-term, and long-term future in this scenario, as per the abstraction rate. Under the increasing abstraction scenario, the long-term storage depletion is projected at -1.17 mm per day on average. This is a result of an escalating depletion, as the storage loss is averaged at -0.53 mm per day between 2015 and 2030, -0.86 mm per day between 2030 and 2050, and -1.48 mm per day between 2050 and 2100. Under the decreasing abstraction scenario, the long-term storage depletion is projected at -0.40 mm per day on average. This is the result of a withering depletion, despite the dwindling continuation, as the storage loss is averaged at -0.54 mm per day between 2015 and 2030, -0.49 mm per day between 2030 and 2050, and -0.33 mm per day between 2050 and 2100.

6.4 Discussion

6.4.1 Projections uncertainty

In climate projection studies, uncertainties are unavoidable as they are propagated from multiple sources: climate variability, climate model, and emission scenario (Latif, 2011). The natural climate variability is highly uncertain as Buser et al. (2010) suggested the extrapolative nature of climate variables which involved different biases in the scenario and the control period. Each model also has different responses to climatology and perturbation components uncertainties, for example, as stated by Adachi et al. (2019). To tackle the wide range of uncertainty bounds, many studies propose using an ensemble of climate projection products (Hawkins et al., 2016; Rajczak and Schär, 2017). Meanwhile, other studies promote the efficiency of bias correction to reduce the uncertainties of climate projection products as such a method takes into account the 'ground-truth' estimates of the corresponding climate variables (Lange, 2019; Wu et al., 2022).

In our study, climate projections uncertainty is also hardly avoidable. The range of projected climate in different model groups might vary to a certain extent. However, we believe that the uncertainties have been limited due to three reasons. First, the focus of the hydrological simulation is groundwater recharge, which is not solely controlled by climate variables. Indeed, climate plays an important role, as it provides the input to the basin that further generates recharge. However, the control of the groundwater recharge production is also regulated by the basin: its soil moisture capacity, its surface water cycle, its subsurface properties, etc. With the other simulation components' relatively known values, in this case, the Wflow_sbm model parameterization, the groundwater recharge estimates, therefore, are not singlehandedly impacted by the uncertainties of the climate projections. In fact, groundwater recharge is not projected to change by significant margins in some other studies, too (Meixner et al., 2016; Tillman et al., 2016; Yawson et al., 2019). Second, the primary goal of the study is to project groundwater availability, which is affected by both groundwater recharge and groundwater abstraction. Groundwater recharge projections exhibit a relatively narrow range of changes in the future, with anthropogenic factors exerting more significant influence (Mustafa et al., 2019; Aslam et al., 2022). In our scenario, the simulation results confirm that the three abstraction scenarios spanning from increasing to decreasing projection outweigh the uncertainty bounds propagated from the climatic scenario. Third, we also apply a bias correction method to the climate projection products, which has been proven in previous studies to effectively reduce climate projection uncertainties (Rahimi et al., 2021; Wu et al., 2022). Table 6.2 columns (1), (2), and (3) show a remarkable improvement in the bias-corrected climate model output. By bias-correcting the projected climate variables and taking into account the historical high-resolution 'ground truth' data as the benchmark, we believe the uncertainties of the climate projection have been significantly reduced.

6.4.2 Impact assessment on future groundwater level projections

As shown in the simulation workflow (Figure 6.2), future groundwater status is projected by altering climate forcing input and groundwater abstraction as the boundary condition. The former imparts its contribution to groundwater recharge estimates. However, as shown in Figure 6.6b, there are significant differences in the impact of climate variables' changes on the surface and the subsurface component of the water cycle. The rainfall median, not considering the seasonal fluctuation, is projected to change (either increase or decrease) up to 31.03% and 28.36% for RCP4.5 and RCP8.5 respectively. On the other hand, the projected change in the groundwater recharge is less than 1%, indicating a slower response of subsurface components to the climate change projection.

This result is limited, however, by the nature of the model one-way coupling. In our model setup, groundwater recharge is fully controlled by the surface processes and the mostly saturated soil. Physically, groundwater storage depletion due to groundwater abstraction would reduce soil water content. By that process, there would be more space for water to infiltrate, indicating two-way feedback between groundwater abstraction and groundwater recharge. A one-way coupled model, unfortunately, is not capable of incorporating such processes into its simulation. This further proves that basin properties possess equal, if not more, importance compared to the climate forcing in groundwater recharge projection. This looks site-specific, however, depending on the basin features, especially the land use/land cover type, the soil maximum capacity, and the subsurface properties. This also highlights the importance of basin-scale information in climate projection studies (Bhave et al., 2013; Jackson et al., 2015; Marcos-Garcia et al., 2023), which have been conducted largely in global scale studies.

The uncertainties of future anthropogenic factors, considering their large influence, should be the primary focus in future groundwater management. While the climatic factor is relatively intractable, groundwater abstraction activities, in terms of rates, volumes, and spatial distribution, are relatively manageable through groundwater policies and governance. Not to mention its more influential impact on the groundwater regime. Improving the understanding of subsurface response and bridging the key gap between science and policy should be the main focus while strengthening the law should be the responsibility of all involved stakeholders. The topic of climate change should not be blamed for degrading groundwater basin quality while the elephant in the room in the form of unsustainable groundwater abstraction is given less attention.

The simulation results also reveal the importance of multi-perspective assessment in groundwater regimes. On one side, Table 6.3 implies that the groundwater situation in the confined aquifer is improving under scenario three of groundwater abstraction, where the maximum piezometric head drawdown in 2100 is lower than one from 2050. On the other side, Figure 6.8 shows that the groundwater storage is still depleting, shown by the negative gradient of all the lines, including ones from the abstraction scenario three.

Such discrepancies occur as the two assessment variables, the groundwater head and the groundwater storage, represent two different dimensions. The groundwater head represents a point, or a single grid, value that constitutes local features, while the groundwater storage evaluates the basin-integrated response. Referring to only one assessment variable could lead to a misunderstanding of the process of the groundwater flow system. We discuss the interpretation of the two conflicting numbers in the following section.

6.4.3 Opportunities for groundwater replenishment

The different gradients shown in Figure 6.8 represent diverging directions of the groundwater storage over time. While all the results accumulate negative changes, the rate at which the groundwater storage is depleting differs among scenarios. With a decreasing groundwater abstraction scenario in the future, the depletion rate is also projected to decline. Admittedly, groundwater replenishment might take a comparably long time to reach a new equilibrium, considering the subsurface low flow velocity. The current declining, but slower, groundwater storage depletion, therefore, could be interpreted in two ways, either (1) the groundwater storage is still in a deterioration trend, or (2) the groundwater storage is actually being replenished, but has not yet reached the new equilibrium state. The latter hypothesis is supported by the values in Table 6.3, which at first glance might seem inconsistent with the results in Figure 6.8. By any means, the results in scenario three, which is highly possible due to the capital city relocation plan, suggest an opportunity for future groundwater replenishment, although it takes some time to yield a positive turning point. Consistent future groundwater head monitoring in the study area could provide crucial insight, which will assist in deriving adaptation policies in response to the capital city relocation.

We also notice different responses of unique groundwater 'replenishment' between the aquifer layers. In the unconfined aquifer, the primary response of the groundwater replenishment is to reduce the impacted drawdown area. While the groundwater table is dwindling in all future checkpoints, there are smaller (simulated) drawdown areas in 2100, even compared to ones in 2030. On the other hand, the confined aquifer responds by relaxing the magnitude of the piezometric head drawdown. This, presumably, is directly related to the spatial distribution of groundwater abstraction. The groundwater abstraction applied in the unconfined aquifer is more widespread with lower rates of abstraction. Therefore, the drawdown area is highly dependent on the spatial distribution. In the opposite to the unconfined aquifer, the groundwater abstraction applied in the confined aquifer is more concentrated with intense rates of abstraction. Decreasing the rate, consequently, delivers noticeable influences on the stressed piezometric head. This reveals an important opportunity for future groundwater policies: the governance of groundwater abstraction authorization should include not only the abstraction rate limitation but also the consideration of future and integrated geospatial planning of the study area.

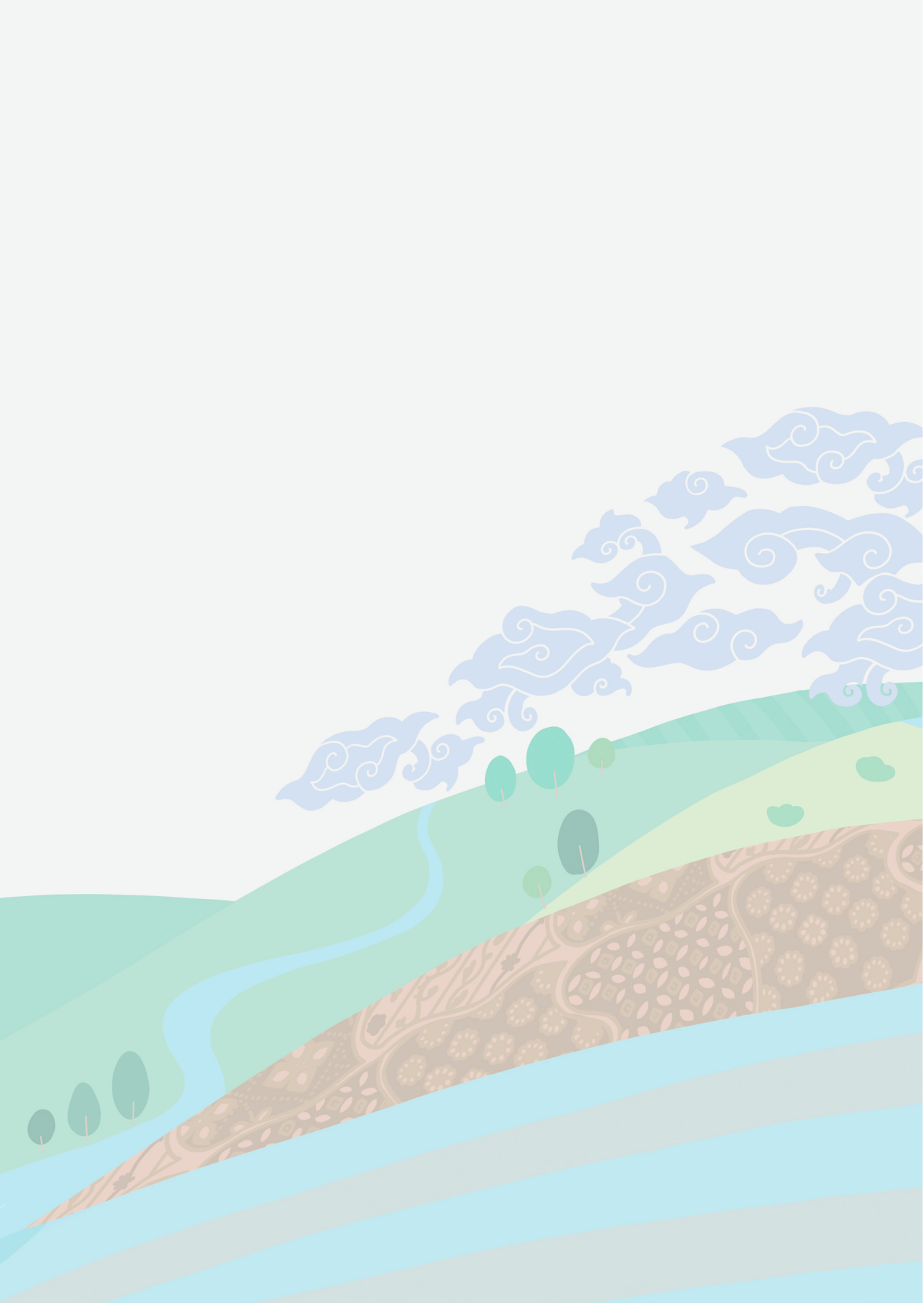
6.5 Conclusions

In this study, future groundwater availability under multiple climatic and diverging anthropogenic scenarios is projected. We simulate groundwater recharge projection using the hydrological model Wflow_sbm. The climate projection forcing is taken from the CMIP6 MRI-ESM2-0 model group, including the projected rainfall as well as the projected temperature and radiation data to estimate potential evapotranspiration. The Wflow_sbm model is forced with climate projections under RCP4.5 and RCP8.5 scenarios. Further, using the groundwater recharge projection as the groundwater flow driver, we simulate the subsurface flow under a groundwater abstraction scenario as the boundary condition. We develop three diverging scenarios; increasing groundwater abstraction as the most common approach, constant abstraction as the benchmark, and decreasing abstraction as a possibility. We take the BGB in Indonesia as our test case, located near Jakarta, the current capital city of Indonesia. The BGB has a wide range of uncertainties in terms of future groundwater abstraction, in response to the Indonesia capital city relocation plan, therefore nicely covering the three developed anthropogenic scenarios.

We apply the bias correction method of ISIMIP3b to the CMIP6 climate projection data before forcing it to the Wflow_sbm model. The bias correction reduces the uncertainty of the climate variables' projection, as the bias-corrected historical data show consistent statistical distributions to the 'ground-truth' data. Future rainfall and temperature median are projected to change by 31.03% and 10.71% under RCP4.5, and 28.36% and 13.10% under RCP8.5. Future groundwater recharge projection reveals the dominant control of the soil component in generating the groundwater recharge in the study area. The fact that there is less than a 1% change projected for the groundwater recharge variable under both climatic scenarios shows that most of the time, the recharge is already at its maximum capacity. During the rainy season, rainfall intensification could not generate more recharge. On the other hand, during the dry season, increasing rainfall drives higher recharge, however, during the dry period that is projected to be even drier, the deficit of groundwater recharge almost balances out those additional recharge.

As expected, under the increasing and constant groundwater abstraction scenario, the groundwater status is projected to drop. The maximum groundwater head drawdown rises over time, the drawdown area expands, and the groundwater storage depletes. However, a positive sign of groundwater replenishment potential is shown under the decreasing groundwater abstraction scenario, despite the conflicting numbers shown between the point-based groundwater level assessment and the basin-integrated groundwater storage assessment. Despite being slow and occurring between 2050 and 2100, there is a sign that the groundwater storage is going in the right direction to be refilled. It is also indicated that the groundwater table is highly regulated by not only the volume and rate of groundwater abstraction but also its spatial distribution. Comparing the results of climatic and anthropogenic impact, we conclude that groundwater abstraction propagates

a more significant impact on the simulated future groundwater availability. The findings of this study are expected to assist in deriving and improving the current and future groundwater policies and management strategies.



Chapter 7

Synthesis



This chapter synthesizes the results of the studies presented in this thesis. The chapter begins by addressing the research questions formulated in Chapter 1 based on specific objectives, followed by the answer to the primary objective. It is then followed up with the lesson learned on the challenges and strategies in dealing with and conducting groundwater studies in data-scarce areas. The last section is dedicated to discussing future opportunities in developing a research-based and practical approach to improving groundwater resource governance in developing countries. By using the Bandung groundwater basin as an example, this approach could be adopted to improve groundwater management in other developing regions.

7.1 Main findings

7.1.1 Water balance components estimates (Chapter 3)

The first research question in the first specific objective is *To what extent do different datasets and products differ in estimating water balance components in the Bandung groundwater basin?* To answer the question, multiple estimates on three water balance components: rainfall, actual evaporation, and river discharge are collated. For each variable, estimates determined by various methods are aggregated. Four rainfall products are assessed: ground observation, gauge-based interpolation, satellite product, and a combination of remote-sensing and station data. Additionally, hydrological model-based estimates and reanalysis products for actual evaporation and river discharge are incorporated, besides global estimates products and observation data. It is expected that discrepancies would occur among estimates, however, the extent was unknown. Besides using each estimate's statistical parameters, the Extended Triple Collocation (ETC) technique is also applied to quantify the discrepancies. While estimates on actual evaporation were found to be relatively consistent among products, the same trend cannot be concluded for rainfall and river discharge variables. Given **the extent of discrepancies** among the water balance components' estimates, it is highly recommended to consider **multiple estimates** in conducting hydrological water balance analysis in data-scarce areas.

The second research question on the first specific objective is *How well does a hydrological simulation using the Wflow_sbm model perform in comparison with other estimation methods?* In answering this question, the ETC technique is used to assess the simulated actual evaporation. It results in satisfactory estimates, with the r^2 of 0.70, better than that of 0.65 from ERA5 products. For river discharge estimates, discharge observation data is used as the benchmark value, with the assumption that it involves the least uncertainties. Using three metrics of Kling-Gupta Efficiency (KGE), Nash-Sutcliffe Efficiency (NSE), and Root Mean Square Error (RMSE), the river discharge estimates simulated using the Wflow_sbm model produce better results when compared to global reanalysis products of GloFAS-ERA5. Wflow_sbm model estimates are also visually in agreement with the

observed data. Considering local-scale data limitations to simulate the hydrological cycle in data-scarce areas, making use of a hydrological model with global parameterization, in particular the Wflow_sbm model, can be **beneficial** to estimate water balance components in a data-scarce area.

The last research question in the first specific objective, *Considering the uncertainty bounds in each of the surface water balance components, to what extent the definitive basin water storage change status can be determined?*, provides an insightful answer. In this study, it is revealed that the status of basin water storage change in the Bandung groundwater basin **cannot be definitively determined** considering the uncertainty bounds of the water balance components. Using different sets of water balance components estimates allows us to arrive at different conclusions: from decreasing to increasing water volume stored within the analyzed domain. The need to improve the accuracy and narrow the range of water storage change estimates is apparent from the results. Therefore, it is suggested to **incorporate a numerical groundwater flow model** so that the internal subsurface hydrological processes can be explored, simulated, and validated in further studies.

7.1.2 One-way coupled wflow_sbm and MODFLOW model (Chapter 4)

The first research question in the second specific objective is *How can the recharge estimates from the Wflow_sbm hydrological model be incorporated into groundwater flow simulation?* To integrate the Wflow_sbm model's groundwater recharge estimates into groundwater flow simulation, adjustments are necessary. While surface water estimates, like rainfall, are available at high temporal resolutions, groundwater flows at a slower rate. The Wflow_sbm groundwater recharge estimates in this study, for example, are produced in daily temporal resolution, while the groundwater flow model is run at monthly resolution. Thus, temporal aggregation of the Wflow_sbm model output is required to match the groundwater flow model temporal resolution. Additionally, spatial adjustments are also necessary to align the gridding system between the two models. In short, the incorporation of groundwater recharge simulated by the Wflow_sbm model largely involves **spatial and temporal adjustment to fit the designated groundwater flow model resolution**.

The answer to the second research question in the second specific objective, *To what extent can a parsimonious, yet reliable, groundwater flow model in the study area be constructed, considering the limited hydrogeological data availability?*, is model gradual development. Initially, the model is set up in a simple manner, featuring low spatial resolution, steady-state conditions, a single aquifer layer, and no flow boundary conditions. As new data slowly become available, they are **progressively incorporated** into the model as long as it is contextually justified. Borehole data are spatially interpolated to fill gaps in mountainous regions, and fieldwork test points are strategically distributed to address data sparsity in high elevated areas. River streams are delineated using the ArcGIS hydrology toolbox, while groundwater abstraction zones are derived from the national land

use database. On the whole, despite the limited hydrogeological data, alternative data sources are often available. However, **model representation should be prioritized over model complexification**, especially in data-scarce areas where excessive detail may not be justified but can lead to unnecessary complexity.

The last research question in the second specific objective is *What factors need to be considered in utilizing and, more importantly, contextualizing open-source remote-sensing-based global estimates of terrestrial water storage change (GRACE) in basin-scale model evaluation?* As groundwater head observations for calibration data are limited in the study area, the remote-sensing products of GRACE are used to compare the one-way coupled simulation results with and evaluate the one-way coupled model performance. However, several factors must be taken into account due to the difference in spatial resolution and coverage between the two estimates. While GRACE is measured on a $1^\circ \times 1^\circ$ domain, the basin-scale modeling is applied in a smaller area. **Discrepancies in characteristics** between the two domains are highly influential in interpreting the results of water storage change estimates. These differences involve variations in the **coverage area, topographical features (terrain slope)**, and subsequently **water storage change response time**. Incorporating these factors into the model evaluation improves the quality of the model performance assessment.

7.1.3 (Inter) Aquifer interaction quantification (Chapter 5)

The first question to address in the third specific objective is *To what extent can the result of a parsimonious groundwater flow model, built on limited hydrogeological data availability, be explored?* In Chapter 5, the simulation results are examined in greater depth compared to typical groundwater head output. The analysis focuses on the computed cell-to-cell flow, referred to as intercell flow, which represents the vertical **aquifer interactions across the aquitard**. Intercell flow quantifies the flow between connected cells in every direction: up, down, front, back, left, and right. The objective in addressing the research question is to not only assess the water budget of groundwater storage as a whole but also to analyze it for each layer of aquifers. Specifically, the investigation emphasizes intercell flow in the downward direction for the upper aquifer layer and in the upward direction for the bottom aquifer layer. By extracting this particular groundwater flow simulation results, it becomes possible to interpret the **groundwater flow mechanism and processes among different soil stratigraphy and aquifer systems**. These interpretations are elaborated on in the following two paragraphs.

With the absence of sufficient calibration data, the subsequent research question, *To what extent can EWT data analysis be incorporated in evaluating a groundwater flow model?*, becomes important. Given the impracticality of a quantitative approach in such circumstances, a qualitative model evaluation method is adopted. The focus is on bridging the evaluation gap by introducing EWT data into the equation. Chapter 5

is entirely dedicated to answering the question. In short, it involves the aggregation of qualitative analyses from EWT data. Investigations are carried out from the perspectives of **groundwater recharge spatial distribution, regional groundwater flow direction, groundwater age estimates**, and the **identification of aquifer interactions**. Although the resulting conclusions are limited in their quantitative aspects, the agreement observed between the numerical groundwater flow model and the EWT data analysis is encouraging. It serves to **enhance the model's credibility** and builds upon the approach taken in the second objective, where model evaluation is complemented with remote-sensing-based estimates of water storage changes.

The third research question in the third specific objective is *What is the impact of simultaneously abstracting groundwater from multiple depths and aquifers on groundwater head, storage, and aquifers' internal processes?* The simulation results confirm and expand on the established theory regarding the **direct and indirect impacts of groundwater abstraction** on the associated aquifer layers. It is evident that groundwater abstraction from a specific depth of an aquifer directly affects the hydraulic head of that same aquifer. In addition to that, it is also very likely that the hydraulic head of other aquifers - surrounding, overlaying, or underlying the point of abstraction - would be affected to some extent. With this knowledge, simultaneous groundwater abstraction from multiple aquifer layers clearly would induce multi-layer impact as well. This is confirmed by the results of the intercell flow and is even quantified. The analysis reveals that the **upper aquifer storage is decreasing at a rate that is disproportionate to its groundwater abstraction**. In the Bandung groundwater basin, specifically, the storage lost by outflow to the deeper aquifer contributes up to 60.3% of the total groundwater storage lost, despite contributing to only 32.3% of the groundwater abstraction.

7.1.4 Future groundwater availability (Chapter 6)

After model setup and evaluation, the one-way coupled model is applied to answer the research questions in the last specific objective. The first one is *How do the projected changes in climate variables in the Bandung groundwater basin influence groundwater recharge?* The projected trend of rainfall in the Bandung groundwater basin up to 2100 is calculated by applying bias correction to the CMIP6 climate model output. This correction is necessary to bridge the discrepancies of the statistical attributes among the climate variables estimates. In general, the rainy season is projected to be even wetter, while the dry season to be drier. Based on the projected temperature and global radiation, the potential evapotranspiration is projected to increase slightly. An important finding emerges from this analysis: the projected changes in the surface water component have **little influence on the projected groundwater recharge**. This is due to the soil moisture capacity being the controlling factor in the Bandung groundwater basin in generating recharge. Under the current climatic factor, more rainfall leads to negligible changes in

recharge generation once the soil's maximum capacity is reached. In the study area, the maximum monthly groundwater recharge change is quantified at 1.8%.

The second research question of the fourth specific objective is *What are the possibilities of groundwater abstraction changes in the Bandung groundwater basin, considering the capital city relocation plan of Indonesia?* The situation of the Bandung groundwater basin is quite unique. Capital city relocations are relatively rare events, let alone projecting future groundwater abstraction in a data-scarce and highly groundwater-dependent area that covers the capital's neighboring cities. Meanwhile, groundwater abstraction projection is often considered in many previous studies to be the most influential factor in future groundwater status projection, even when compared to climatic projection. Therefore, **multiple diverging scenarios** representing different trajectories for future groundwater abstraction are necessary to be developed. These scenarios encompass projections where groundwater abstraction is expected to **decrease**, be **constant**, and **increase** in the future. The abstraction wells' locations also have to be adjusted according to the changes in the abstraction rate. The aim is to capture a broad range of potential future groundwater availability scenarios, accounting for the various possibilities of groundwater abstraction. The variety of scenarios is also supposed to provide valuable insight that can assist in formulating adaptation policies in response to the capital city relocation plan.

The final research question is *To what extent do the changes in climatic forcing and anthropogenic activities, both each and combined, influence the future groundwater availability in the study area?* The two preceding paragraphs explained that climatic factor primarily affects the forcing component (groundwater recharge), while anthropogenic factors influence the boundary conditions (particularly groundwater abstraction) in the conceptualization of a groundwater flow model. For the **climatic factor**, despite the projected changes in climate variables, the basin parameters possess a substantially more influential control in generating groundwater recharge. The highest relative change of the monthly groundwater recharge median of 1.8% **does not propagate significant changes** to the simulated groundwater level and storage changes. The **anthropogenic factor**, however, **conveys a stronger effect** on the groundwater level and storage changes. These projections range from a depletion rate twice the current rate under increased abstraction to the potential for groundwater replenishment with decreasing abstraction. Combined, it is made clear that policies and regulations **focusing on groundwater abstraction management is the priority** to achieve future groundwater governance.

7.1.5 Answering the primary objective

With the specific objectives successfully achieved, this thesis delves deeper into the primary objective, which is to enhance the quantitative understanding of the groundwater system in a data-scarce area, primarily focusing on the Bandung groundwater basin. As groundwater flow is not detachable from the water cycle, this section also provides insights into the

hydrological cycle as a whole. The discussion below reports the state of the art of the surface water cycle in the study area before and after the completion of this thesis, followed by a similar analysis of the subsurface flow.

Indonesia, as a developing country, faces significant challenges in hydrological studies, particularly concerning data availability. In the Bandung groundwater basin, fortunately, several rainfall stations' measurements are (partially) accessible. Additionally, the growth of open-source remote sensing-based products has expanded opportunities for hydrological research in the region. However, studies that incorporate **multiple data sources**, employ **spatially distributed approaches**, and consider **uncertainty bounds** are still relatively scarce. To our knowledge, the majority of hydrological studies in and around the study area are conducted, still, on the basis of rainfall stations' dataset only. On the other hand, at the same time, many studies point out the low confidence in the reliability of using such an estimate. There are only an extremely limited number of studies in translating and interpreting the point data to spatially distributed hydrological variables' estimates, too. Conventional methods such as the Thiessen polygon to estimate areal rainfall or lumped modeling instead of a spatially distributed approach are still often used. On another note, in the few available publications, analysis of the water balance components' uncertainty bounds is often lacking. Even with only a limited source of rainfall estimates that is not openly accessible, large discrepancies are found among reports. This is compounded by further uncertainties in the hydrological model structure, calibration data, and so on, resulting in even larger discrepancies on other subsequent variables, for example, river discharge and basin water storage changes.

In this thesis, multiple estimates of water balance components are collated and compared to improve the understanding of the hydrological processes. The issue of spatially distributed modeling is tackled by performing hydrological simulation using a high-resolution **distributed Wflow_sbm model**, using global data to supply the model parameterization. With a wide variety of estimates from field measurements, interpolated point datasets, hydrological model simulation, remote sensing, and reanalysis products, the issues of uncertainty in estimating water balance components are addressed using the **uncertainties' quantification** of the Extended Triple Collocation (ETC) technique. The results indicate the importance of groundwater flow modeling in understanding the subsurface processes as well as the story of the water cycle as a whole. **Relying solely on the surface water components** to determine basin water storage changes leads to an **inconclusive deduction of the basin's overall status**, with results that are easily swayed and **highly sensitive to modelers' bias and decision-making processes**.

The central focus of this thesis, the groundwater system in the Bandung groundwater basin, has seen even **fewer research** efforts compared to surface water systems. Up until 2020, the Office of Mineral and Energy Resources (ESDM) of West Java Province was legally assigned the responsibility of managing groundwater in the study area. However,

the ESDM task extends far beyond a single topic of groundwater; it encompasses also the topic of energy generation from solar, water, biogas, and geothermal, as well as material, metal, and mineral mining, plus sub-urban area electrification. Given the extensive scope of their duties, conducting regional-scale groundwater research simultaneously was a challenge. Most of the groundwater research of old, to our knowledge, focuses on **problem identification and reports** (Wangsaatmaja et al., 2006; Gumilar et al., 2015; Tirtomihardjo, 2016). The cited papers outlined the general overview of the Bandung groundwater basin and provided some dwindling groundwater table measurements, along with figures on the increasing pressure for water supply. However, concrete and quantitative solutions were often elusive and obscured by uncertainties (Delinom, 2009; Delinom and Suriadarma, 2010; Abidin et al., 2012; Pujiindiyati and Satrio, 2013; Taufiq et al., 2017). The studies on groundwater modeling, in particular, were hampered by (1) the availability of a reliable distributed hydrological model that provides **dependable groundwater recharge estimates**, (2) limited computational power that restricts the **model's spatial resolution**, and (3) the nature of **open-source data** that were previously not so common within the scientific communities in the study area (especially before 2010), besides (4) the **insufficient and inadequate groundwater-related information**, such as borehole data, observation wells' data, and more, to build the well-grounded groundwater flow model. Nonetheless, some valuable and relevant findings from previous research remain applicable today and have been utilized in this thesis. For instance, the assignment of a no-flow boundary condition on the model's northern side boundary is based on earlier research that identified the influence of the Lembang geological fault on groundwater flow dynamics in the Bandung groundwater basin (Delinom and Suriadarma, 2010; Pujiindiyati and Satrio, 2013). Additionally, previous research efforts pointed to the existence of **aquifer interactions**, although quantifying these interactions was challenging given the limited information available at the time (Widodo, 2013; Taufiq et al., 2017). Overall, while earlier research in the Bandung groundwater basin faced various constraints, it laid the groundwork for subsequent studies and contributed valuable insights that continue to inform current research efforts.

This thesis addresses the four major challenges mentioned earlier to enhance the accuracy of groundwater flow quantification. Firstly, the groundwater recharge estimates were computed using the distributed Wflow_sbm model simulation calibrated by the river discharge measurement and, partially, the water storage change of GRACE. This approach is expected to **improve the precision and accuracy of groundwater recharge estimates**. Secondly, the groundwater flow model is set at a **higher spatial resolution**, with grid cells measuring up to 100 m × 100 m. To the best of our knowledge, this represents the most detailed model available for the study area. Thirdly, unlike the previous model, which was not freely accessible, the model developed in conjunction with this thesis has been **made available in an online** open-source repository. This ensures transparency and allows others to access and review the model configuration and

parameterization. Lastly, to address data scarcity, several initiatives were undertaken. **Collaboration with ESDM** was initiated to obtain as much relevant information as possible. A **field campaign** was conducted to gather additional data, and **existing data collation** efforts by previous researchers, such as Rahiem (2020) on borehole data and Irawan et al. (2016) on environmental water tracers data, were utilized. These efforts have collectively contributed to updated knowledge in the study area, covering (1) **improved groundwater recharge estimates**, (2) **reliable groundwater flow model**, (3) **groundwater flow mechanism understanding**, and even (4) **groundwater regime projection** under changing climatic forcing and anthropogenic activities.

7.2 Lessons learned on data-related strategy

After conducting the studies presented in this thesis, several lessons have been learned, particularly regarding data availability. These insights can serve as valuable guidance for improving the current data situation and laying a robust foundation for future data acquisition related to groundwater variables. Consequently, better data are expected to upgrade the quality of future groundwater modeling studies in the Bandung groundwater basin, specifically, and in other data-scarce areas, generally.

7.2.1 Challenges of data-scarcity

The primary challenge often encountered when initiating groundwater-related studies is the issue of **data quantity**. In this context, the term quantity could be associated with many things. Temporally, lack of data quantity may manifest as **data shortage**. Alternatively, it could also relate to **measurement frequency**. For example, having river discharge data spanning a long time frame but collected infrequently (e.g., annually) would provide limited insights into the behavior of the measured stream, particularly in the context of rapid and dynamic fluctuations, such as floods. Spatially, a lack of data quantity is linked with **point representation** over an area. Obviously, it is preferable to have more data points instead of a few or even a single point of measurement covering an area, although some factors need to be considered.

One crucial factor regarding the required number of data points is the **spatial variability** of the area in focus. In a heterogeneous area, a higher number of observation points is necessary to capture and understand the spatial variations adequately. On the contrary, in a homogeneous area where features exhibit little variation, fewer measurement points may suffice. In a data-scarce area with limited data points, using only available data immediately without context could lead to a misinterpretation of the actual integrated/aggregated system of the study area. Unfortunately, to understand the spatial variability itself, a lot of points of measurement are usually obligatory in advance. Therefore, to achieve well-distributed observation points considering a site's spatial variability, a **measurement network** also has to be established under a careful design.

Ensuring **data quality** is another critical aspect of data collection in groundwater flow modeling. Data quality pertains to the accuracy, precision, and repeatability of measurements. It is essential to have confidence in the data, especially when they are used for driving or calibrating models. Human-operated manual instruments are prone to human error, while automatic devices require periodic calibration and maintenance. Statistical analysis is typically used to evaluate data consistency, especially in detecting outliers, trends, and more. More importantly, in many instances, experienced researchers rely on their **intuition** and judgment to perform initial screenings of data quality, which can be crucial for identifying and addressing issues early in a research process.

Another important aspect in assessing data quality is the **representation of a measurement**. For example, groundwater table data from an observation well. Such data are typically used to evaluate a groundwater flow model simulation, where the groundwater head from both the observation and simulation are compared. However, it's important to recognize that the spatial scale of an observation well is typically much smaller than that of a grid cell in a groundwater flow model. As a result, the observed and simulated groundwater head values represent different **spatial coverages**, even though they measure the same variable. Consequently, the comparison reliability becomes a function of the actual basin system's homogeneity across the space covered by the grid cell size. In cases where the basin exhibits significant spatial variability, these comparisons may require careful interpretation. Additionally, the location of observation wells can introduce biases. Wells positioned near physical boundary conditions, such as surface water bodies or groundwater abstraction wells, may be influenced by their proximity to these features, leading to potential inaccuracies in the measurements. These factors should be considered when using observation well data in groundwater modeling and analysis.

Within the topic of data quality, good data also calls for **accurate and complete metadata**. It is important for hydrology and hydrogeology data, at minimum, to include information on measurement time, location, data type, size, and variables to measure. Providing measurement location and time, for example, is crucial for understanding spatial and temporal patterns and trends of the measured variables. Specifically, additional information should also be available depending on circumstances. For an observation well, details on well construction drawings and soil stratigraphy should be present. For a rainfall gauge, the elevation placements, device calibration history, and surrounding environments (canopy, building density, topography) should be attached to the data storage. This also applies to other observation data. With all the included information, metadata helps to contextualize data values, and might further assist in data screening.

Ultimately, a large quantity of high-quality data would only be useful should they be provided with **open accessibility**. There are, obviously, pros and cons in open-sourcing hydrology and hydrogeology data. Open-source data have the potential to reach higher numbers of users. As a result, it leads to more research that might be beneficial to the

study area and foster collaboration among the involved stakeholders. It also promotes transparency, which indirectly can enhance data quality. On the other hand, a solid and robust framework is necessary to initiate and maintain open-source data platforms. Quality control of data input is obligatory and becomes even stricter. However, as much effort is put in place to regulate data input, controlling public data usage and its output is far more complex nonetheless. Unverified research output based on open-source data might be overlooked, and worse, lead to misinterpretation in perceiving the actual situation. Therefore, in order to achieve good hydrology and hydrogeology data accessibility, a strong recommendation is made for the **involvement of government agencies**. Legal regulation in citing the use of open-source data could be mandated, and such an authority should only be bestowed to the official government bodies.

7.2.2 Strategies to overcome data-scarcity

As research in data-scarce areas is inevitable in the present time, in this section alternative approaches to gather insights and information in data-scarce areas are explored. Some require financial investment, but with careful planning, the gain would be valuable. Each point discussed below, though seemingly evident, warrants consideration due to its relevance in addressing data scarcity challenges. It is worth noting that the ultimate objective isn't simply to perpetually conduct research in data-scarce areas, but rather to empower these regions with the necessary resources to transform them into data-sufficient areas. This is further discussed in Section 7.3.

Under the situation where no open-source data are available, the significance of literature from **local sources** cannot be overstated, particularly those written in the local language of the study area. In various regions across the globe, many hydrology and hydrogeology data are meticulously collected but remain confined to local repositories, often due to resource limitations. Initiating collaboration with local legal parties responsible for groundwater data would unlock a number of opportunities. The same goes for engaging with local experts. As suggested in Chapter 4, the importance of local context is highly relevant for basin-scale studies. Therefore, local knowledge should be prioritized, both with and without the availability and accessibility of global-scale data.

Alternative data sources can also be found through direct interactions with government agencies and/or the private sector from other fields/disciplines. In the context of groundwater-related studies, access to geological documentation and other soil-related information specific to the study area is of paramount importance. Thankfully, these data are not the exclusive domain of hydrologists and hydrogeologists. Structural, geotechnical, and transportation engineers, and professionals from various other fields, are also in the same boat of gathering and assembling these details, each to their own needs in their projects. On that account, **multi-disciplinary collaboration** could commence not only in the data analysis phase but also during the data collation stage.

Doing **field campaign** is also a reliable alternative should such an option be available. Despite not being able to provide long-term measurement, in general, field campaigns could be designed as such to specifically suit the needs of the study. It is typically most useful to measure/estimate variables that are relatively persistent to change over time. At the very least, it provides the most recent status of the situation. With a well-planned follow-up, a field campaign also has the potential to add more information to a basin's overall knowledge should the measurement results be made open.

7.2.3 Knowledge prowess of multi-source data collation

The improvement of quantitative understanding of the groundwater system in the Bandung groundwater basin, which is the primary objective of this thesis, serves as a practical demonstration of the main topic discussed in this section. When examining each chapter and previous studies as distinct research sources, it becomes evident that the Bandung groundwater basin is indeed characterized by data scarcity. However, **collating data and estimates from multiple sources** proves to be a **powerful solution for overcoming data scarcity challenges**.

Estimating water storage changes typically relies on the mass balance approach, which involves approximating the water balance components. Prior to delving deeply into this subject in Chapter 3, numerous earlier studies on water balance budgets in the study area were limited by their reliance on single-source data, making them sensitive to selection bias. Chapter 3 demonstrates that by incorporating multiple estimates, it becomes possible to draw more robust conclusions, even in the face of significant uncertainties surrounding water storage change assessments.

The follow-up chapter in Chapter 4 also exemplifies that data collation does not only involve one variable in focus with a number of estimation methods but also multiple variables. Typically, groundwater flow model calibration relies solely on groundwater head measurements, but in this case, another variable comes into play: terrestrial water storage change estimates from GRACE. A reliable one-way coupled hydrological and groundwater flow model was even constructed by incorporating groundwater-related data from the private sector such as pumping test reports and borehole data, among others.

In Chapter 5, the model evaluation is further carried on by using the environmental water tracer data. When used solely for hydrogeochemistry studies, such data would have limited applications. Furthermore, these data were collected in various projects, and no continuous spatial monitoring network was established. Additionally, the measurements were taken at different times, which presents challenges in interpreting the situation. However, when combined with the groundwater flow model, these data offer a unique perspective on understanding the physical processes of subsurface flow. This comprehensive approach may not be achievable with the same level of confidence if the analysis were based solely on one data source.

7.3 Future opportunities

While the chapters of this thesis have primarily focused on the Bandung groundwater basin, it is important to consider future opportunities not only within this specific area but also in other data-scarce regions. Notably, extrapolating this analysis to other study areas requires careful contextualization and consideration of the local conditions and the surrounding environmental context. As a whole, the lessons learned and the strategies developed in this thesis are expected to serve as a valuable foundation for addressing data scarcity challenges in various regions.

From the analysis and modeling standpoint, there remain additional aspects to consider concerning the estimation of water balance components. While incorporating multiple approaches to quantify each component may offer even more benefits, investigating the **strategy for the optimal hydrological processes understanding** might be worth exploring. In addition to that, despite the parsimonious nature of the groundwater flow model in this study, it is imperative to include future data and information to enhance the **model's future representation** of the real-world system.

In terms of the coupling between the hydrological and groundwater flow models, this study adopts a one-way model coupling approach, primarily due to the differences in the timescales governing surface and subsurface processes. However, for prolonged simulations, transitioning to a **two-way model coupling** system is advisable. This method would enable the reciprocal feedback between groundwater abstraction that removes and groundwater recharge that brings in groundwater from and to the aquifer to be accurately simulated. Besides, this approach also allows for the determination of groundwater recharge rates from not only the surface processes but also the available storage within the groundwater system at a given simulation time.

Considering the current limitations in data quantity within the study area, it is advisable for future studies to prioritize **additional field campaigns**, particularly in areas where data remain limited. This recommendation arises from the uneven spatial distribution of data in the study area, with a concentration of data points in urban areas. Expanding measurement points in rural and mountainous regions would not only provide valuable information at specific locations but also enhance our understanding of the spatial variability within the Bandung groundwater basin. In a broader context, as previously discussed, increasing the number of data points can contribute to the development of more comprehensive datasets for future research and analysis.

From the time spent on the field, there are also noticeable major opportunities to assemble data that have been measured. A large number of projects have been taking place in the Bandung groundwater basin and many field measurements have been collected, from borehole data, pumping test data, and more. However, the results often belong and are confined to independent projects, particularly those initiated by the private sector.

Consequently, the utilization of these data is typically limited to the scope of their original purposes. To address this, a concerted effort in **data gathering** is necessary, ideally driven by collaboration between government agencies and private sector entities. This collaboration should encompass both historical and future data, mutually benefiting all stakeholders involved. Such an endeavor should be underpinned by the establishment of a robust groundwater database system to ensure the effective storage, retrieval, and management of this valuable information.

In the context of dependable measuring systems, it is imperative to conduct a comprehensive **assessment** of instrumentation. In data-scarce areas, the limited available data often exhibit questionable figures. Conversely, in data-sufficient areas, the majority of data tend to be relatively dependable. Although there is a lack of extensive studies on this subject, it is reasonable to hypothesize a **strong correlation between data quality and quantity**. While implementing groundwater data collection practices may be complex, maintaining and assessing ongoing measurement systems should be less intricate. This underscores the importance of investing in reliable instrumentation and regularly evaluating its performance to ensure the accuracy and credibility of the collected data.

To reiterate, the ultimate objective is not to perpetually operate in data-scarce areas but to empower these regions with the requisite resources to transform them into **data-sufficient areas**. In the specific context of the Bandung groundwater basin, this transformation would unlock numerous avenues for groundwater-related research, including studies on pollutant transport in groundwater, groundwater potential in mountainous regions, the impact of geological faults on groundwater flow, and various other topics. Achieving this transformation necessitates the establishment of a robust **groundwater data collection framework**, similar to initiatives undertaken in other data-scarce regions around the world. Such a framework would serve as the foundation for advancing our understanding of groundwater systems and addressing critical water resource challenges.

References

- Abe, Y., Y. Uchiyama, M. Saito, M. Ohira, and T. Yokoyama (2020). “Effects of bedrock groundwater dynamics on runoff generation: a case study on granodiorite headwater catchments, western Tanzawa Mountains, Japan”. *Hydrological Research Letters* 14.1, 62–67. DOI: 10.3178/hr1.14.62.
- Abidin, H. Z., I. Gumilar, H. Andreas, D. Murdohardono, and Y. Fukuda (2012). “On causes and impacts of land subsidence in Bandung Basin, Indonesia”. *Environmental Earth Sciences* 68.6, 1545–1553. DOI: 10.1007/s12665-012-1848-z.
- Abou Zaki, N., A. Torabi Haghighi, P. M. Rossi, M. J. Tourian, and B. Kløve (2019). “Monitoring Groundwater Storage Depletion Using Gravity Recovery and Climate Experiment (GRACE) Data in Bakhtegan Catchment, Iran”. *Water* 11.7. DOI: 10.3390/w11071456.
- Adachi, S. A., S. Nishizawa, K. Ando, T. Yamaura, R. Yoshida, H. Yashiro, Y. Kajikawa, and H. Tomita (2019). “An evaluation method for uncertainties in regional climate projections”. *Atmospheric Science Letters* 20.1, e877. DOI: <https://doi.org/10.1002/asl.877>. eprint: <https://rmets.onlinelibrary.wiley.com/doi/pdf/10.1002/asl.877>.
- Ahmadi, A. and M. Nasser (2020). “Do direct and inverse uncertainty assessment methods present the same results?” *Journal of Hydroinformatics* 22.4, 842–855. DOI: 10.2166/hydro.2020.190. eprint: <https://iwaponline.com/jh/article-pdf/22/4/842/844265/jh0220842.pdf>.
- Alfieri, L., V. Lorini, F. A. Hirpa, S. Harrigan, E. Zsoter, C. Prudhomme, and P. Salamon (2020). “A global streamflow reanalysis for 1980–2018”. *Journal of Hydrology X* 6, 100049. DOI: <https://doi.org/10.1016/j.hydroa.2019.100049>.
- Ali, R., D. McFarlane, S. Varma, W. Dawes, I. Emelyanova, G. Hodgson, and S. Charles (2012). “Potential climate change impacts on groundwater resources of south-western Australia”. *Journal of Hydrology* 475, 456–472. DOI: 10.1016/j.jhydrol.2012.04.043.
- Alley, W. M., T. E. Reilly, and O. L. Franke (1999). *Sustainability of ground-water resources*. ENGLISH. Tech. rep. Report. DOI: 10.3133/cir1186.

- Andani, I. G. A., L. La Paix Puello, and K. Geurs (2020). “Exploring the role of toll road construction on residential location choice in the Jakarta – Bandung region”. *Case Studies on Transport Policy* 8.2, 599–611. DOI: <https://doi.org/10.1016/j.cstp.2020.02.001>.
- Angelakis, A. N., K. S. Voudouris, and I. Mariolakos (2016). “Groundwater utilization through the centuries focusing on the Hellenic civilizations”. *Hydrogeology Journal* 24.5, 1311–1324. DOI: [10.1007/s10040-016-1392-0](https://doi.org/10.1007/s10040-016-1392-0).
- Ansari, A. H. M., R. Umar, N. us Saba, and S. Sarah (2021). “Assessment of Current and Future Groundwater Stress through Varied Scenario Projections in Urban and Rural Environment in Parts of Meerut District, Uttar Pradesh in Ganges Sub-basin”. *Journal of the Geological Society of India* 97.8, 927–934. DOI: [10.1007/s12594-021-1793-0](https://doi.org/10.1007/s12594-021-1793-0).
- Anurag, H. and G.-H. C. Ng (2022). “Assessing future climate change impacts on groundwater recharge in Minnesota”. *Journal of Hydrology* 612, 128112. DOI: <https://doi.org/10.1016/j.jhydrol.2022.128112>.
- Armanuos, A. M., A. Negm, C. Yoshimura, and O. C. S. Valeriano (2016). “Application of WetSpa model to estimate groundwater recharge variability in the Nile Delta aquifer”. *Arabian Journal of Geosciences* 9.10, 553. DOI: [10.1007/s12517-016-2580-x](https://doi.org/10.1007/s12517-016-2580-x).
- Aslam, R. A., S. Shrestha, M. N. Usman, S. N. Khan, S. Ali, M. S. Sharif, M. W. Sarwar, N. Saddique, A. Sarwar, M. U. Ali, and A. Arshad (2022). “Integrated SWAT-MODFLOW Modeling-Based Groundwater Adaptation Policy Guidelines for Lahore, Pakistan under Projected Climate Change, and Human Development Scenarios”. *Atmosphere* 13.12. DOI: [10.3390/atmos13122001](https://doi.org/10.3390/atmos13122001).
- Asoka, A., T. Gleeson, Y. Wada, and V. Mishra (2017). “Relative contribution of monsoon precipitation and pumping to changes in groundwater storage in India”. *Nature Geoscience* 10.2, 109–117. DOI: [10.1038/ngeo2869](https://doi.org/10.1038/ngeo2869).
- Asoka, A. and V. Mishra (2020). “Anthropogenic and Climate Contributions on the Changes in Terrestrial Water Storage in India”. *Journal of Geophysical Research: Atmospheres* 125.10, e2020JD032470. DOI: <https://doi.org/10.1029/2020JD032470>.
- Baghel, T., M. S. Babel, S. Shrestha, K. R. Salin, S. G. Viridis, and V. R. Shinde (2022). “A generalized methodology for ranking climate models based on climate indices for sector-specific studies: An application to the Mekong sub-basin”. *Science of The Total Environment* 829, 154551. DOI: <https://doi.org/10.1016/j.scitotenv.2022.154551>.
- Bakker, M., V. Post, C. D. Langevin, J. D. Hughes, J. T. White, J. J. Starn, and M. N. Fioren (2016). “Scripting MODFLOW Model Development Using Python and FloPy”. *Groundwater* 54.5, 733–739. DOI: <https://doi.org/10.1111/gwat.12413>.
- Bárdossy, A., C. Kilsby, S. Birkinshaw, N. Wang, and F. Anwar (2022). “Is Precipitation Responsible for the Most Hydrological Model Uncertainty?” *Frontiers in Water* 4. DOI: [10.3389/frwa.2022.836554](https://doi.org/10.3389/frwa.2022.836554).

- Besselaar, E. J. M. van den, G. van der Schrier, R. C. Cornes, A. S. Iqbal, and A. M. G. K. Tank (2017). “SA-OBS: A Daily Gridded Surface Temperature and Precipitation Dataset for Southeast Asia”. *Journal of Climate* 30.14, 5151–5165. DOI: 10.1175/jcli-d-16-0575.1.
- Bethke, C. M. and T. M. Johnson (2002). “Paradox of groundwater age”. *Geology* 30.2, 107–110. DOI: 10.1130/0091-7613(2002)030<0107:POGA>2.0.CO;2.
- Bhanja, S. N., X. Zhang, and J. Wang (2018). “Estimating long-term groundwater storage and its controlling factors in Alberta, Canada”. *Hydrology and Earth System Sciences* 22.12, 6241–6255. DOI: 10.5194/hess-22-6241-2018.
- Bhave, A. G., A. Mishra, and A. Groot (2013). “Sub-basin scale characterization of climate change vulnerability, impacts and adaptation in an Indian River basin”. *Regional Environmental Change* 13.5, 1087–1098. DOI: 10.1007/s10113-013-0416-8.
- Bierkens, M. F. P. and Y. Wada (2019). “Non-renewable groundwater use and groundwater depletion: a review”. *Environmental Research Letters* 14.6, 063002. DOI: 10.1088/1748-9326/ab1a5f.
- Bjerklie, D. M., D. Moller, L. C. Smith, and S. L. Dingman (2005). “Estimating discharge in rivers using remotely sensed hydraulic information”. *Journal of Hydrology* 309.1, 191–209. DOI: <https://doi.org/10.1016/j.jhydrol.2004.11.022>.
- Boluwade, A. (2020). “Spatial-Temporal Assessment of Satellite-Based Rainfall Estimates in Different Precipitation Regimes in Water-Scarce and Data-Sparse Regions”. *Atmosphere* 11.9, 901. DOI: 10.3390/atmos11090901.
- Bouaziz, L. J. E., F. Fenicia, G. Thirel, T. de Boer-Euser, J. Buitink, C. C. Brauer, J. De Niel, B. J. Dewals, G. Drogue, B. Grelier, L. A. Melsen, S. Moustakas, J. Nossent, F. Pereira, E. Sprokkereef, J. Stam, A. H. Weerts, P. Willems, H. H. G. Savenije, and M. Hrachowitz (2021). “Behind the scenes of streamflow model performance”. *Hydrology and Earth System Sciences* 25.2, 1069–1095. DOI: 10.5194/hess-25-1069-2021.
- Braadbaart, O. and F. Braadbaart (1997). “Policing the urban pumping race: Industrial groundwater overexploitation in Indonesia”. *World Development* 25.2, 199–210. DOI: 10.1016/s0305-750x(96)00102-7.
- Brewington, L., V. Keener, and A. Mair (2019). “Simulating Land Cover Change Impacts on Groundwater Recharge under Selected Climate Projections, Maui, Hawaii”. *Remote Sensing* 11.24. DOI: 10.3390/rs11243048.
- Bruin, H. A. R. de, I. F. Trigo, F. C. Bosveld, and J. F. Meirink (2016). “A Thermodynamically Based Model for Actual Evapotranspiration of an Extensive Grass Field Close to FAO Reference, Suitable for Remote Sensing Application”. *Journal of Hydrometeorology* 17.5, 1373–1382. DOI: 10.1175/jhm-d-15-0006.1.
- Buchhorn, M., B. Smets, L. Bertels, B. D. Roo, M. Lesiv, N.-E. Tsendbazar, L. Li, and A. Tarko (2020). *Copernicus Global Land Service: Land Cover 100m: version*

- 3 *Globe 2015-2019: Product User Manual*. Version Dataset v3.0, doc issue 3.3. DOI: 10.5281/zenodo.3938963.
- Buser, C. M., H. R. KÜNSCH, and A. WEBER (2010). “Biases and Uncertainty in Climate Projections”. *Scandinavian Journal of Statistics* 37.2, 179–199. DOI: <https://doi.org/10.1111/j.1467-9469.2009.00686.x>. eprint: <https://onlinelibrary.wiley.com/doi/pdf/10.1111/j.1467-9469.2009.00686.x>.
- Cao, Y., Z. Nan, and X. Hu (2012). “Estimating groundwater storage changes in the Heihe river basin using grace”. In: *2012 IEEE International Geoscience and Remote Sensing Symposium*. IEEE. DOI: 10.1109/igarss.2012.6351441.
- Chambel, A. (2015). “The role of groundwater in the management of water resources in the World”. *Proceedings of the International Association of Hydrological Sciences* 366, 107–108. DOI: 10.5194/piahs-366-107-2015.
- Chambers, L., D. Goody, and A. Binley (2019). “Use and application of CFC-11, CFC-12, CFC-113 and SF6 as environmental tracers of groundwater residence time: A review”. *Geoscience Frontiers* 10.5. Groundwater Arsenic Biogeochemistry, 1643–1652. DOI: <https://doi.org/10.1016/j.gsf.2018.02.017>.
- Chang, S. W., I.-M. Chung, M.-G. Kim, and B. A. Yifru (2020). “Vulnerability assessment considering impact of future groundwater exploitation on coastal groundwater resources in northeastern Jeju Island, South Korea”. *Environmental Earth Sciences* 79.22, 498. DOI: 10.1007/s12665-020-09254-2.
- Chatterjee, R., A. K. Jain, S. Chandra, V. Tomar, P. K. Parchure, and S. Ahmed (2018). “Mapping and management of aquifers suffering from over-exploitation of groundwater resources in Baswa-Bandikui watershed, Rajasthan, India”. *Environmental Earth Sciences* 77.5. DOI: 10.1007/s12665-018-7257-1.
- Chen, F., W. T. Crow, R. Bindlish, A. Colliander, M. S. Burgin, J. Asanuma, and K. Aida (2018a). “Global-scale evaluation of SMAP, SMOS and ASCAT soil moisture products using triple collocation”. *Remote Sensing of Environment* 214, 1–13. DOI: 10.1016/j.rse.2018.05.008.
- Chen, F., S. Wang, X. Wu, M. Zhang, A. A. Argiriou, X. Zhou, and J. Chen (2021). “Local Meteoric Water Lines in a Semi-Arid Setting of Northwest China Using Multiple Methods”. *Water* 13.17. DOI: 10.3390/w13172380.
- Chen, H., Y. Xue, and D. Qiu (2022). “Numerical simulation of the land subsidence induced by groundwater mining”. *Cluster Computing*. DOI: 10.1007/s10586-022-03771-4.
- Chen, J., C. Wilson, B. Tapley, B. Scanlon, and A. Güntner (2016). “Long-term groundwater storage change in Victoria, Australia from satellite gravity and in situ observations”. *Global and Planetary Change* 139, 56–65. DOI: <https://doi.org/10.1016/j.gloplacha.2016.01.002>.

- Chen, L., Q. He, K. Liu, J. Li, and C. Jing (2019). “Downscaling of GRACE-Derived Groundwater Storage Based on the Random Forest Model”. *Remote Sensing* 11.24. DOI: 10.3390/rs11242979.
- Chen, S., W. Ying, Z. Zhao-xian, C. Zhong-shuang, C. Jiang, and H. Qi-chen (2018b). “The drainage of the aquitard and its implication for groundwater exploitation in Hengshui City”. *JOURNAL OF GROUNDWATER SCIENCE AND ENGINEERING* 6.2, 84–91. DOI: 10.19637/j.cnki.2305-7068.2018.02.002.
- Chen, X., J. Goeke, J. F. Ayers, and S. Summerside (2003). “OBSERVATION WELL NETWORK DESIGN FOR PUMPING TESTS IN UNCONFINED AQUIFERS1”. *JAWRA Journal of the American Water Resources Association* 39.1, 17–32. DOI: <https://doi.org/10.1111/j.1752-1688.2003.tb01558.x>. eprint: <https://onlinelibrary.wiley.com/doi/pdf/10.1111/j.1752-1688.2003.tb01558.x>.
- Chinnasamy, P. and G. Agoramoorthy (2015). “Groundwater Storage and Depletion Trends in Tamil Nadu State, India”. *Water Resources Management: An International Journal, Published for the European Water Resources Association (EWRA)* 29.7, 2139–2152. DOI: 10.1007/s11269-015-0932-z.
- Closas, A., F. Molle, and N. Hernández-Mora (2017). *Sticks and carrots: managing groundwater overabstraction in La Mancha, Spain*. Tech. rep. DOI: 10.5337/2017.218.
- Condon, L. E., S. Kollet, M. F. P. Bierkens, G. E. Fogg, R. M. Maxwell, M. C. Hill, H.-J. H. Fransen, A. Verhoef, A. F. Van Loon, M. Sulis, and C. Abesser (2021). “Global Groundwater Modeling and Monitoring: Opportunities and Challenges”. *Water Resources Research* 57.12. e2020WR029500. DOI: <https://doi.org/10.1029/2020WR029500>. eprint: <https://agupubs.onlinelibrary.wiley.com/doi/pdf/10.1029/2020WR029500>.
- Copernicus Climate Change Service (2019). *ERA5-Land hourly data from 2001 to present*. DOI: 10.24381/CDS.E2161BAC.
- Copernicus Climate Change Service (2021). *CMIP6 climate projections*. DOI: 10.24381/CDS.C866074C.
- Coplen, T. B., A. L. Herczeg, and C. Barnes (2000). “Isotope Engineering—Using Stable Isotopes of the Water Molecule to Solve Practical Problems”. In: *Environmental Tracers in Subsurface Hydrology*. Boston, MA: Springer US, 79–110. DOI: 10.1007/978-1-4615-4557-6_3.
- Cowie, R., M. W. Williams, M. Wireman, and R. L. Runkel (2014). “Use of Natural and Applied Tracers to Guide Targeted Remediation Efforts in an Acid Mine Drainage System, Colorado Rockies, USA”. *Water* 6.4, 745–777. DOI: 10.3390/w6040745.
- Custodio, E., M. del Carmen Cabrera, R. Poncela, L.-O. Puga, E. Skupien, and A. del Villar (2016). “Groundwater intensive exploitation and mining in Gran Canaria and Tenerife, Canary Islands, Spain: Hydrogeological, environmental, economic and

- social aspects". *Science of The Total Environment* 557-558, 425–437. DOI: <https://doi.org/10.1016/j.scitotenv.2016.03.038>.
- Dams, J., E. Salvatore, T. Van Daele, V. Ntegeka, P. Willems, and O. Batelaan (2012). "Spatio-temporal impact of climate change on the groundwater system". *Hydrology and Earth System Sciences* 16.5, 1517–1531. DOI: 10.5194/hess-16-1517-2012.
- Dangar, S., A. Asoka, and V. Mishra (2021). "Causes and implications of groundwater depletion in India: A review". *Journal of Hydrology* 596, 126103. DOI: <https://doi.org/10.1016/j.jhydrol.2021.126103>.
- de Graaf, I., L. van Beek, Y. Wada, and M. Bierkens (2014). "Dynamic attribution of global water demand to surface water and groundwater resources: Effects of abstractions and return flows on river discharges". *Advances in Water Resources* 64, 21–33. DOI: <https://doi.org/10.1016/j.advwatres.2013.12.002>.
- de Graaf, I. E. M., R. L. P. H. van Beek, T. Gleeson, N. Moosdorf, O. Schmitz, E. H. Sultanudjaja, and M. F. P. Bierkens (2016). "A global-scale two-layer transient groundwater model: development and application to groundwater depletion". DOI: 10.5194/hess-2016-121.
- Delinom, R. M. (2009). "Structural geology controls on groundwater flow: Lembang Fault case study, West Java, Indonesia". *Hydrogeology Journal* 17.4, 1011–1023. DOI: 10.1007/s10040-009-0453-z.
- Delinom, R. M. and A. Suriadarma (2010). "GROUNDWATER FLOW SYSTEM OF BANDUNG BASIN BASED ON HYDRAULIC HEAD, SUBSURFACE TEMPERATURE, AND STABLE ISOTOPES". *Jurnal Riset Geologi dan Pertambangan* 19.2, 55. DOI: 10.14203/risetgeotam2010.v20.34.
- Döll, P., H. Hoffmann-Dobrev, F. Portmann, S. Siebert, A. Eicker, M. Rodell, G. Strassberg, and B. Scanlon (2012). "Impact of water withdrawals from groundwater and surface water on continental water storage variations". *Journal of Geodynamics* 59-60, 143–156. DOI: <https://doi.org/10.1016/j.jog.2011.05.001>.
- Dong, Y., Y. Xie, J. Zhang, A. J. Love, and X. Dai (2021). "Reliability of recharge rates estimated from groundwater age with a simplified analytical approach". *Hydrological Processes* 35.5, e14160. DOI: <https://doi.org/10.1002/hyp.14160>. eprint: <https://onlinelibrary.wiley.com/doi/pdf/10.1002/hyp.14160>.
- Doveri, M. and M. Mussi (2014). "Water Isotopes as Environmental Tracers for Conceptual Understanding of Groundwater Flow: An Application for Fractured Aquifer Systems in the "Scansano-Magliano in Toscana" Area (Southern Tuscany, Italy)". *Water* 6.8, 2255–2277. DOI: 10.3390/w6082255.
- Du, X., X. Lu, J. Hou, and X. Ye (2018). "Improving the Reliability of Numerical Groundwater Modeling in a Data-Sparse Region". *Water* 10.3. DOI: 10.3390/w10030289.

- Earman, S. and M. Dettinger (2011). “Potential impacts of climate change on groundwater resources – a global review”. *Journal of Water and Climate Change* 2.4, 213–229. DOI: 10.2166/wcc.2011.034.
- Ebraheem, A. M., S. Riad, P. Wycisk, and A. M. Sefelnasr (2004). “A local-scale groundwater flow model for groundwater resources management in Dakhla Oasis, SW Egypt”. *Hydrogeology Journal* 12.6, 714–722. DOI: 10.1007/s10040-004-0359-8.
- Eeman, S., P. G. B. De Louw, and S. E. A. T. M. Van der Zee (2017). “Cation exchange in a temporally fluctuating thin freshwater lens on top of saline groundwater”. *Hydrogeology Journal* 25.1, 223–241. DOI: 10.1007/s10040-016-1475-y.
- Eilander, D., W. van Verseveld, D. Yamazaki, A. Weerts, H. C. Winsemius, and P. J. Ward (2020). “A hydrography upscaling method for scale invariant parametrization of distributed hydrological models”. *Hydrology and Earth System Sciences Discussions* 2020, 1–34. DOI: 10.5194/hess-2020-582.
- Elliott, A. H., C. Rajanayaka, and J. Yang (2022). “Simplified Modelling of Coupled Surface-Groundwater Transport Using a Subcatchment Mass Balance Approach”. *Water* 14.3. DOI: 10.3390/w14030350.
- Eyring, V., S. Bony, G. A. Meehl, C. A. Senior, B. Stevens, R. J. Stouffer, and K. E. Taylor (2016). “Overview of the Coupled Model Intercomparison Project Phase 6 (CMIP6) experimental design and organization”. *Geoscientific Model Development* 9.5, 1937–1958. DOI: 10.5194/gmd-9-1937-2016.
- Fatolazadeh, F. and K. Goïta (2021). “Mapping terrestrial water storage changes in Canada using GRACE and GRACE-FO”. *Science of The Total Environment* 779, 146435. DOI: <https://doi.org/10.1016/j.scitotenv.2021.146435>.
- Felfelani, F., Y. Wada, L. Longuevergne, and Y. N. Pokhrel (2017). “Natural and human-induced terrestrial water storage change: A global analysis using hydrological models and GRACE”. *Journal of Hydrology* 553, 105–118. DOI: <https://doi.org/10.1016/j.jhydrol.2017.07.048>.
- Figuroa-Miranda, S., J. Tuxpan-Vargas, J. A. Ramos-Leal, V. M. Hernández-Madrigal, and C. I. Villaseñor-Reyes (2018). “Land subsidence by groundwater over-exploitation from aquifers in tectonic valleys of Central Mexico: A review”. *Engineering Geology* 246, 91–106. DOI: <https://doi.org/10.1016/j.enggeo.2018.09.023>.
- Frappart, F. and G. Ramillien (2018). “Monitoring Groundwater Storage Changes Using the Gravity Recovery and Climate Experiment (GRACE) Satellite Mission: A Review”. *Remote Sensing* 10.6. DOI: 10.3390/rs10060829.
- Funk, C., P. Peterson, M. Landsfeld, D. Pedreros, J. Verdin, S. Shukla, G. Husak, J. Rowland, L. Harrison, A. Hoell, and J. Michaelsen (2015). “The climate hazards infrared precipitation with stations—a new environmental record for monitoring extremes”. *Scientific Data* 2.1. DOI: 10.1038/sdata.2015.66.

- Gash, J. H. C. (1979). "An analytical model of rainfall interception by forests". *Quarterly Journal of the Royal Meteorological Society* 105.443, 43–55. DOI: <https://doi.org/10.1002/qj.49710544304>. eprint: <https://rmets.onlinelibrary.wiley.com/doi/pdf/10.1002/qj.49710544304>.
- Gaye, C. B. and C. Tindimugaya (2019). "Review: Challenges and opportunities for sustainable groundwater management in Africa". *Hydrogeology Journal* 27.3, 1099–1110. DOI: 10.1007/s10040-018-1892-1.
- Al-Gburi, H. F., B. S. Al-Tawash, O. S. Al-Tamimi, and C. Schüth (2022). "Stable isotope composition in precipitation and groundwater of Shwan Sub-Basin, Kirkuk governorate, northeast of Iraq". *Water Supply* 22.10, 7442–7459. DOI: 10.2166/ws.2022.327.
- Gebremicael, T., Y. Mohamed, and P. V. der Zaag (2019). "Attributing the hydrological impact of different land use types and their long-term dynamics through combining parsimonious hydrological modelling, alteration analysis and PLSR analysis". *Science of The Total Environment* 660, 1155–1167. DOI: 10.1016/j.scitotenv.2019.01.085.
- Getirana, A., M. Rodell, S. Kumar, H. K. Beaudoin, K. Arsenault, B. Zaitchik, H. Save, and S. Bettadpur (2020). "GRACE Improves Seasonal Groundwater Forecast Initialization over the United States". *Journal of Hydrometeorology* 21.1. DOI: 10.1175/JHM-D-19-0096.1.
- Ginkel, K. C. van (2016). "Water quality in the Upper Citarum River Basin: towards a better understanding of a heavily polluted catchment". *Student Undergraduate Research E-journal* 2.
- Gleeson, T., M. Cuthbert, G. Ferguson, and D. Perrone (2020). "Global Groundwater Sustainability, Resources, and Systems in the Anthropocene". *Annual Review of Earth and Planetary Sciences* 48.1, 431–463. DOI: 10.1146/annurev-earth-071719-055251. eprint: <https://doi.org/10.1146/annurev-earth-071719-055251>.
- Gleeson, T., N. Moosdorf, J. Hartmann, and L. P. H. van Beek (2014). "A glimpse beneath earth's surface: GLobal HYdrogeology MaPS (GLHYMPS) of permeability and porosity". *Geophysical Research Letters* 41.11, 3891–3898. DOI: <https://doi.org/10.1002/2014GL059856>.
- Gruber, A., C.-H. Su, W. T. Crow, S. Zwieback, W. A. Dorigo, and W. Wagner (2016). "Estimating error cross-correlations in soil moisture data sets using extended collocation analysis". *Journal of Geophysical Research: Atmospheres* 121.3, 1208–1219. DOI: 10.1002/2015jd024027.
- Gumilar, I., H. Z. Abidin, L. M. Hutasoit, D. M. Hakim, T. P. Sidiq, and H. Andreas (2015). "Land Subsidence in Bandung Basin and its Possible Caused Factors". *Procedia Earth and Planetary Science* 12. Proceeding of The 3rd International Symposium on Earthquake and Disaster Mitigation (The 3rd ISEDM), 47–62. DOI: <https://doi.org/10.1016/j.proeps.2015.03.026>.

- Gupta, H. V., H. Kling, K. K. Yilmaz, and G. F. Martinez (2009). “Decomposition of the mean squared error and NSE performance criteria: Implications for improving hydrological modelling”. *Journal of Hydrology* 377.1-2, 80–91. DOI: 10.1016/j.jhydrol.2009.08.003.
- Hachborn, E., A. Berg, J. Levison, and J. T. Ambadan (2017). “Sensitivity of GRACE-derived estimates of groundwater-level changes in southern Ontario, Canada”. *Hydrogeology Journal* 25.8, 2391–2402. DOI: 10.1007/s10040-017-1612-2.
- Hackbarth, T. X. and W. T. de Vries (2021). “An Evaluation of Massive Land Interventions for the Relocation of Capital Cities”. *Urban Science* 5.1. DOI: 10.3390/urbansci5010025.
- Hafizi, H. and A. A. Sorman (2022). “Assessment of 13 Gridded Precipitation Datasets for Hydrological Modeling in a Mountainous Basin”. *Atmosphere* 13.1. DOI: 10.3390/atmos13010143.
- Hallouin, T. (2019). *ThibHlln/hydroeval: General enhancements*. Version v0.0.3. DOI: 10.5281/zenodo.3402383.
- Han, J., N. Tangdamrongsub, C. Hwang, and H. Z. Abidin (2017). “Intensified water storage loss by biomass burning in Kalimantan: Detection by GRACE”. *Journal of Geophysical Research: Solid Earth*. DOI: 10.1002/2017jb014129.
- Haque, A., A. Salama, K. Lo, and P. Wu (2021). “Surface and Groundwater Interactions: A Review of Coupling Strategies in Detailed Domain Models”. *Hydrology* 8.1. DOI: 10.3390/hydrology8010035.
- Harrigan, S., E. Zsoter, L. Alfieri, C. Prudhomme, P. Salamon, F. Wetterhall, C. Barnard, H. Cloke, and F. Pappenberger (2020). “GloFAS-ERA5 operational global river discharge reanalysis 1979–present”. *Earth System Science Data* 12.3, 2043–2060. DOI: 10.5194/essd-12-2043-2020.
- Hashimoto, R., S. Kazama, T. Hashimoto, K. Oguma, and S. Takizawa (2022). “Planning methods for conjunctive use of urban water resources based on quantitative water demand estimation models and groundwater regulation index in Yangon City, Myanmar”. *Journal of Cleaner Production* 367, 133123. DOI: <https://doi.org/10.1016/j.jclepro.2022.133123>.
- Hassaballah, K., Y. Mohamed, S. Uhlenbrook, and K. Biro (2017). “Analysis of streamflow response to land use and land cover changes using satellite data and hydrological modelling: case study of Dinder and Rahad tributaries of the Blue Nile (Ethiopia–Sudan)”. *Hydrology and Earth System Sciences* 21.10, 5217–5242. DOI: 10.5194/hess-21-5217-2017.
- Hawkins, E., R. S. Smith, J. M. Gregory, and D. A. Stainforth (2016). “Irreducible uncertainty in near-term climate projections”. *Climate Dynamics* 46.11, 3807–3819. DOI: 10.1007/s00382-015-2806-8.

- Haylock, M. R., N. Hofstra, A. M. G. K. Tank, E. J. Klok, P. D. Jones, and M. New (2008). "A European daily high-resolution gridded data set of surface temperature and precipitation for 1950–2006". *Journal of Geophysical Research* 113.D20. DOI: 10.1029/2008jd010201.
- Healy, A., K. Upton, S. Capstick, G. Bristow, M. Tijani, A. MacDonald, I. Goni, Y. Bukar, L. Whitmarsh, S. Theis, K. Danert, and S. Allan (2020). "Domestic groundwater abstraction in Lagos, Nigeria: a disjuncture in the science-policy-practice interface?" *Environmental Research Letters* 15.4, 045006. DOI: 10.1088/1748-9326/ab7463.
- Hengl, T., J. M. de Jesus, G. B. M. Heuvelink, M. R. Gonzalez, M. Kilibarda, A. Blagotić, W. Shangguan, M. N. Wright, X. Geng, B. Bauer-Marschallinger, M. A. Guevara, R. Vargas, R. A. MacMillan, N. H. Batjes, J. G. B. Leenaars, E. Ribeiro, I. Wheeler, S. Mantel, and B. Kempen (2017). "SoilGrids250m: Global gridded soil information based on machine learning". *PLOS ONE* 12.2. Ed. by B. Bond-Lamberty, e0169748. DOI: 10.1371/journal.pone.0169748.
- Henriksen, H. J., L. Trolborg, A. L. Højberg, and J. C. Refsgaard (2008). "Assessment of exploitable groundwater resources of Denmark by use of ensemble resource indicators and a numerical groundwater–surface water model". *Journal of Hydrology* 348.1, 224–240. DOI: <https://doi.org/10.1016/j.jhydro1.2007.09.056>.
- Hersbach, H., B. Bell, P. Berrisford, S. Hirahara, A. Horányi, J. Muñoz-Sabater, J. Nicolas, C. Peubey, R. Radu, D. Schepers, A. Simmons, C. Soci, S. Abdalla, X. Abellan, G. Balsamo, P. Bechtold, G. Biavati, J. Bidlot, M. Bonavita, G. Chiara, P. Dahlgren, D. Dee, M. Diamantakis, R. Dragani, J. Flemming, R. Forbes, M. Fuentes, A. Geer, L. Haimberger, S. Healy, R. J. Hogan, E. Hólm, M. Janisková, S. Keeley, P. Laloyaux, P. Lopez, C. Lupu, G. Radnoti, P. Rosnay, I. Rozum, F. Vamborg, S. Villaume, and J.-N. Thépaut (2020). "The ERA5 global reanalysis". *Quarterly Journal of the Royal Meteorological Society* 146.730, 1999–2049. DOI: 10.1002/qj.3803.
- Hofstra, N., M. Haylock, M. New, P. Jones, and C. Frei (2008). "Comparison of six methods for the interpolation of daily, European climate data". *Journal of Geophysical Research* 113.D21. DOI: 10.1029/2008jd010100.
- Holland, M., C. Thomas, B. Livneh, S. Tatge, A. Johnson, and E. Thomas (2022). "Development and Validation of an In Situ Groundwater Abstraction Sensor Network, Hydrologic Statistical Model, and Blockchain Trading Platform: A Demonstration in Solano County, California". *ACS ES&T Water* 2.12, 2345–2358. DOI: 10.1021/acsestwater.2c00214.
- Holman, I. P., D. Tascone, and T. M. Hess (2009). "A comparison of stochastic and deterministic downscaling methods for modelling potential groundwater recharge under climate change in East Anglia, UK: implications for groundwater resource management". *Hydrogeology journal* v. 17.no. 7, pp. 1629-1641–2009 v.17 no.7. DOI: 10.1007/s10040-009-0457-8.

- Hu, Z., Q. Zhou, X. Chen, D. Chen, J. Li, M. Guo, G. Yin, and Z. Duan (2019). “Groundwater Depletion Estimated from GRACE: A Challenge of Sustainable Development in an Arid Region of Central Asia”. *Remote Sensing* 11.16, 1908. DOI: 10.3390/rs11161908.
- Hua, L., T. Zhao, and L. Zhong (2022). “Future changes in drought over Central Asia under CMIP6 forcing scenarios”. *Journal of Hydrology: Regional Studies* 43, 101191. DOI: <https://doi.org/10.1016/j.ejrh.2022.101191>.
- Hughes, J. D., C. D. Langevin, and E. R. Banta (2017). *Documentation for the MODFLOW 6 framework*. English. Tech. rep. Report. Reston, VA. DOI: 10.3133/tm6A57.
- Humphrey, V., L. Gudmundsson, and S. I. Seneviratne (2016). “Assessing Global Water Storage Variability from GRACE: Trends, Seasonal Cycle, Subseasonal Anomalies and Extremes”. *Surveys in Geophysics* 37.2, 357–395. DOI: 10.1007/s10712-016-9367-1.
- Huo, A., J. Peng, X. Chen, L. Deng, G. Wang, and Y. Cheng (2016). “Groundwater storage and depletion trends in the Loess areas of China”. *Environmental Earth Sciences* 75.16, 1167. DOI: 10.1007/s12665-016-5951-4.
- Huscroft, J., T. Gleeson, J. Hartmann, and J. Börker (2018). “Compiling and Mapping Global Permeability of the Unconsolidated and Consolidated Earth: GLobal HYdrogeology MaPS 2.0 (GLHYMPS 2.0)”. *Geophysical Research Letters* 45.4, 1897–1904. DOI: <https://doi.org/10.1002/2017GL075860>.
- Hutasoit, L. (2009). “Kondisi Permukaan Air Tanah dengan dan tanpa peresapan buatan di daerah Bandung: Hasil Simulasi Numerik”. *Indonesian Journal on Geoscience* 4.3. DOI: 10.17014/ijog.vol4no3.20093.
- Imhoff, R. O., W. J. van Verseveld, B. van Osnabrugge, and A. H. Weerts (2020). “Scaling Point-Scale (Pedo)transfer Functions to Seamless Large-Domain Parameter Estimates for High-Resolution Distributed Hydrologic Modeling: An Example for the Rhine River”. *Water Resources Research* 56.4. DOI: 10.1029/2019wr026807.
- Indonesia (2017). *Office of Energy and Mineral Resources Ministerial Regulation on Groundwater Basin*.
- Indonesia (2022). *Detail masterplan on Indonesia capital city*. Peraturan Presiden no 63 tahun 2022.
- IPCC (2021). *Climate Change 2021: The Physical Science Basis. Contribution of Working Group I to the Sixth Assessment Report of the Intergovernmental Panel on Climate Change*. Vol. In Press. Cambridge, United Kingdom and New York, NY, USA: Cambridge University Press. DOI: 10.1017/9781009157896.
- Iqbal, Z., S. Shahid, K. Ahmed, T. Ismail, G. F. Ziarh, E.-S. Chung, and X. Wang (2021). “Evaluation of CMIP6 GCM rainfall in mainland Southeast Asia”. *Atmospheric Research* 254, 105525. DOI: <https://doi.org/10.1016/j.atmosres.2021.105525>.
- Irawan, D. E., R. Suwarman, N. Ulfa, Irsyad, and Fadli (2016). *Final report: Groundwater open data map for Bandung area*.

- Izady, A., K. Davary, A. Alizadeh, A. N. Ziaei, A. Alipoor, A. Joodavi, and M. L. Brusseau (2014). "A framework toward developing a groundwater conceptual model". *Arabian Journal of Geosciences* 7.9, 3611–3631. DOI: 10.1007/s12517-013-0971-9.
- Jackson, C. R., J. P. Bloomfield, and J. D. Mackay (2015). "Evidence for changes in historic and future groundwater levels in the UK". *Progress in Physical Geography: Earth and Environment* 39.1, 49–67. DOI: 10.1177/0309133314550668. eprint: <https://doi.org/10.1177/0309133314550668>.
- Jaya, I. G. N. M., B. N. Ruchjana, A. S. Abdullah, and T. Toharudin (2020). "A relationship between temperature and precipitation over the contiguous Bandung city, Indonesia". *Communications in Mathematical Biology and Neuroscience*. DOI: 10.28919/cmbn/4868.
- Jian, J., D. Ryu, J. F. Costelloe, and C.-H. Su (2017). "Towards hydrological model calibration using river level measurements". *Journal of Hydrology: Regional Studies* 10, 95–109. DOI: <https://doi.org/10.1016/j.ejrh.2016.12.085>.
- Jing, M., F. Heße, R. Kumar, W. Wang, T. Fischer, M. Walther, M. Zink, A. Zech, L. Samaniego, O. Kolditz, and S. Attinger (2018). "Improved regional-scale groundwater representation by the coupling of the mesoscale Hydrologic Model (mHM v5.7) to the groundwater model OpenGeoSys (OGS)". *Geoscientific Model Development* 11.5, 1989–2007. DOI: 10.5194/gmd-11-1989-2018.
- Julian, M. M., M. Fink, S. Kralisch, and A. Brenning (2019). "Modelling of Hydrological Responses in the Upper Citarum Basin based on the Spatial Plan of West Java Province 2029 and Climate Change". *International Journal of Technology* 10.5, 866–875. DOI: <https://doi.org/10.14716/ijtech.v10i5.2376>.
- Jyolsna, P. J., B. V. N. P. Kambhammettu, and S. Gorugantula (2021). "Application of random forest and multi-linear regression methods in downscaling GRACE derived groundwater storage changes". *Hydrological Sciences Journal* 66.5, 874–887. DOI: 10.1080/02626667.2021.1896719.
- Karimi, L., M. Motagh, and I. Entezam (2019). "Modeling groundwater level fluctuations in Tehran aquifer: Results from a 3D unconfined aquifer model". *Groundwater for Sustainable Development* 8, 439–449. DOI: <https://doi.org/10.1016/j.gsd.2019.01.003>.
- Karszenberg, D., O. Schmitz, P. Salamon, K. de Jong, and M. F. Bierkens (2010). "A software framework for construction of process-based stochastic spatio-temporal models and data assimilation". *Environmental Modelling & Software* 25.4, 489–502. DOI: 10.1016/j.envsoft.2009.10.004.
- Katpatal, Y. B., C. Rishma, and C. K. Singh (2018). "Sensitivity of the Gravity Recovery and Climate Experiment (GRACE) to the complexity of aquifer systems for monitoring of groundwater". *Hydrogeology Journal* 26.3, 933–943. DOI: 10.1007/s10040-017-1686-x.
- Kawai, H., S. Yukimoto, T. Koshiro, N. Oshima, T. Tanaka, H. Yoshimura, and R. Nagasawa (2019). "Significant improvement of cloud representation in the global climate model

- MRI-ESM2". *Geoscientific Model Development* 12.7, 2875–2897. DOI: 10.5194/gmd-12-2875-2019.
- Kendall, C. and J. J. McDonnell (1998). *Isotope Tracers in Catchment Hydrology*. Elsevier. DOI: 10.1016/c2009-0-10239-8.
- Khezzani, B. and S. Bouchemal (2018). "Variations in groundwater levels and quality due to agricultural over-exploitation in an arid environment: the phreatic aquifer of the Souf oasis (Algerian Sahara)". *Environmental Earth Sciences* 77.4. DOI: 10.1007/s12665-018-7329-2.
- Kim, I. H. and J.-S. Yang (2018). "Prioritizing countermeasures for reducing seawater-intrusion area by considering regional characteristics using SEAWAT and a multicriteria decision-making method". *Hydrological Processes* 32.25, 3741–3757. DOI: 10.1002/hyp.13283.
- Kling, H., M. Fuchs, and M. Paulin (2012). "Runoff conditions in the upper Danube basin under an ensemble of climate change scenarios". *Journal of Hydrology* 424-425, 264–277. DOI: <https://doi.org/10.1016/j.jhydrol.2012.01.011>.
- Knoben, W. J. M., J. E. Freer, and R. A. Woods (2019). "Technical note: Inherent benchmark or not? Comparing Nash–Sutcliffe and Kling–Gupta efficiency scores". *Hydrology and Earth System Sciences* 23.10, 4323–4331. DOI: 10.5194/hess-23-4323-2019.
- Kodir, A., N. Hadi, I. Astina, D. Taryana, N. Ratnawati, and Idris (2021). "The dynamics of community response to the development of the New Capital (IKN) of Indonesia". In: *Development, Social Change and Environmental Sustainability*. Routledge, 57–61. DOI: 10.1201/9781003178163-13.
- Krasting, J. P., J. G. John, C. Blanton, C. McHugh, S. Nikonov, A. Radhakrishnan, K. Rand, N. T. Zadeh, V. Balaji, J. Durachta, C. Dupuis, R. Menzel, T. Robinson, S. Underwood, H. Vahlenkamp, K. A. Dunne, P. P. Gauthier, P. Ginoux, S. M. Griffies, R. Hallberg, M. Harrison, W. Hurlin, S. Malyshev, V. Naik, F. Paulot, D. J. Paynter, J. Ploshay, B. G. Reichl, D. M. Schwarzkopf, C. J. Seman, L. Silvers, B. Wyman, Y. Zeng, A. Adcroft, J. P. Dunne, R. Dussin, H. Guo, J. He, I. M. Held, L. W. Horowitz, P. Lin, P. Milly, E. Shevliakova, C. Stock, M. Winton, A. T. Wittenberg, Y. Xie, and M. Zhao (2018). *NOAA-GFDL GFDL-ESM4 model output prepared for CMIP6 CMIP*. DOI: 10.22033/ESGF/CMIP6.1407.
- Kumar, S., D. Machiwal, and B. S. Parmar (2019). "A parsimonious approach to delineating groundwater potential zones using geospatial modeling and multicriteria decision analysis techniques under limited data availability condition". *Engineering Reports* 1.5. DOI: 10.1002/eng2.12073.
- Kurukulasuriya, D., W. Howcroft, E. Moon, K. Meredith, and W. Timms (2022). "Selecting Environmental Water Tracers to Understand Groundwater around Mines: Opportunities

- and Limitations”. *Mine Water and the Environment* 41.2, 357–369. DOI: 10.1007/s10230-022-00845-y.
- Lamichhane, S. and N. M. Shakya (2019). “Alteration of groundwater recharge areas due to land use/cover change in Kathmandu Valley, Nepal”. *Journal of Hydrology: Regional Studies* 26, 100635. DOI: 10.1016/j.ejrh.2019.100635.
- Land Air, W. A. ((2020). *Factsheet: Groundwater basics*.
- Landerer, F. W. and S. C. Swenson (2012). “Accuracy of scaled GRACE terrestrial water storage estimates”. *Water Resources Research* 48.4. DOI: 10.1029/2011wr011453.
- Lange, S. (2019). “Trend-preserving bias adjustment and statistical downscaling with ISIMIP3BASD (v1.0)”. *Geoscientific Model Development* 12.7, 3055–3070. DOI: 10.5194/gmd-12-3055-2019.
- Lange, S. (2021). *ISIMIP3BASD*. Version 2.5.0. DOI: 10.5281/zenodo.4686991.
- Langevin, C. D., J. D. Hughes, E. R. Banta, R. G. Niswonger, S. Panday, and A. M. Provost (2017). *Documentation for the MODFLOW 6 Groundwater Flow Model*. Tech. rep. Report. Reston, VA. DOI: 10.3133/tm6A55.
- Larocque, M., P. G. Cook, K. Haaken, and C. T. Simmons (2009). “Estimating Flow Using Tracers and Hydraulics in Synthetic Heterogeneous Aquifers”. *Groundwater* 47.6, 786–796. DOI: <https://doi.org/10.1111/j.1745-6584.2009.00595.x>.
- Latif, M. (2011). “Uncertainty in climate change projections”. *Journal of Geochemical Exploration* 110.1. Sustainability of Geochemical Cycling, 1–7. DOI: <https://doi.org/10.1016/j.gexplo.2010.09.011>.
- Levy, J. and Y. Xu (2012). “Review: Groundwater management and groundwater/surface-water interaction in the context of South African water policy”. *Hydrogeology Journal* 20.2, 205–226. DOI: 10.1007/s10040-011-0776-4.
- Li, F., G. Pan, C. Tang, Q. Zhang, and J. Yu (2008). “Recharge source and hydrogeochemical evolution of shallow groundwater in a complex alluvial fan system, southwest of North China Plain”. *Environmental Geology* 55.5, 1109–1122. DOI: 10.1007/s00254-007-1059-1.
- Li, J., T. Li, S. Liu, and H. Shi (2018). “An Efficient Method for Mapping High-Resolution Global River Discharge Based on the Algorithms of Drainage Network Extraction”. *Water* 10.4.
- Li, Q., X. Liu, Y. Zhong, M. Wang, and S. Zhu (2021). “Estimation of Terrestrial Water Storage Changes at Small Basin Scales Based on Multi-Source Data”. *Remote Sensing* 13.16. DOI: 10.3390/rs13163304.
- Li, Y., H. Gong, L. Zhu, and X. Li (2017). “Measuring Spatiotemporal Features of Land Subsidence, Groundwater Drawdown, and Compressible Layer Thickness in Beijing Plain, China”. *Water* 9.1. DOI: 10.3390/w9010064.

- Li, Z., X. Li, Y. Wang, and S. M. Quiring (2019). “Impact of climate change on precipitation patterns in Houston, Texas, USA”. *Anthropocene* 25, 100193. DOI: <https://doi.org/10.1016/j.ancene.2019.100193>.
- Lili, Y., L. Minhua, C. Fei, D. Yueyuan, and L. Cuimei (2020). “Practices of groundwater over-exploitation control in Hebei Province”. *Water Policy* 22.4, 591–601. DOI: 10.2166/wp.2020.183. eprint: <https://iwaponline.com/wp/article-pdf/22/4/591/731181/022040591.pdf>.
- Lin, J., R. Ma, Y. Hu, Z. Sun, Y. Wang, and C. P. R. McCarter (2018). “Groundwater sustainability and groundwater/surface-water interaction in arid Dunhuang Basin, northwest China”. *Hydrogeology Journal* 26.5, 1559–1572. DOI: 10.1007/s10040-018-1743-0.
- Lin, M., A. Biswas, and E. M. Bennett (2020). “Socio-ecological determinants on spatio-temporal changes of groundwater in the Yellow River Basin, China”. *Science of The Total Environment* 731, 138725. DOI: 10.1016/j.scitotenv.2020.138725.
- Listiyani, N. and M. Y. Said (2018). “Political Law on the Environment: The Authority of the Government and Local Government to File Litigation in Law Number 32 Year 2009 on Environmental Protection and Management”. *Resources* 7.4, 77. DOI: 10.3390/resources7040077.
- Liu, H. and M. Rahman (2022). “Developing a parsimonious distributed land surface-subsurface hydrological model”. DOI: 10.5194/egusphere-egu22-5759.
- Liu, K., J. Zhang, and M. Wang (2022). “Drivers of Groundwater Change in China and Future Projections”. *Remote Sensing* 14.19. DOI: 10.3390/rs14194825.
- Liu, X., C. Liu, and W. Brutsaert (2020). “Mutual Consistency of Groundwater Storage Changes Derived From GRACE and From Baseflow Recessions in the Central Yangtze River Basin”. *Journal of Geophysical Research: Atmospheres* 125.24, e2019JD031467. DOI: <https://doi.org/10.1029/2019JD031467>.
- Liu, Y. and H. V. Gupta (2007). “Uncertainty in hydrologic modeling: Toward an integrated data assimilation framework”. *Water Resources Research* 43.7. DOI: <https://doi.org/10.1029/2006WR005756>.
- Longuevergne, L., C. R. Wilson, B. R. Scanlon, and J. F. Crétaux (2013). “GRACE water storage estimates for the Middle East and other regions with significant reservoir and lake storage”. *Hydrology and Earth System Sciences* 17.12, 4817–4830. DOI: 10.5194/hess-17-4817-2013.
- López, P. L., N. Wanders, J. Schellekens, L. J. Renzullo, E. H. Sutanudjaja, and M. F. P. Bierkens (2016). “Improved large-scale hydrological modelling through the assimilation of streamflow and downscaled satellite soil moisture observations”. *Hydrology and Earth System Sciences* 20.7, 3059–3076. DOI: 10.5194/hess-20-3059-2016.

- Luna, R. M. R. de, S. J. d. A. Garnés, J. J. d. S. P. Cabral, and S. M. dos Santos (2017). “Groundwater overexploitation and soil subsidence monitoring on Recife plain (Brazil)”. *Natural Hazards* 86.3, 1363–1376. DOI: 10.1007/s11069-017-2749-y.
- Luo, H., Z. Li, M. Luo, Q. Zhang, and W. A. Illman (2020). “An Analytical Method to Calculate Groundwater Released From an Aquitard Undergoing Nonlinear Consolidation”. *Water Resources Research* 56.9. e2020WR027320 2020WR027320, e2020WR027320. DOI: <https://doi.org/10.1029/2020WR027320>. eprint: <https://agupubs.onlinelibrary.wiley.com/doi/pdf/10.1029/2020WR027320>.
- Luo, X., W. Wu, D. He, Y. Li, and X. Ji (2019). “Hydrological Simulation Using TRMM and CHIRPS Precipitation Estimates in the Lower Lancang-Mekong River Basin”. *Chinese Geographical Science* 29.1, 13–25. DOI: 10.1007/s11769-019-1014-6.
- Lurtz, M. R., R. R. Morrison, T. K. Gates, G. B. Senay, A. S. Bhaskar, and D. G. Ketchum (2020). “Relationships between riparian evapotranspiration and groundwater depth along a semiarid irrigated river valley”. *Hydrological Processes* 34.8, 1714–1727. DOI: 10.1002/hyp.13712.
- Mabrouk, M., A. Jonoski, G. H. P. O. Essink, and S. Uhlenbrook (2018). “Impacts of Sea Level Rise and Groundwater Extraction Scenarios on Fresh Groundwater Resources in the Nile Delta Governorates, Egypt”. *Water* 10.11, 1690. DOI: 10.3390/w10111690.
- Malama, B., K. L. Kuhlman, and W. Barrash (2007). “Semi-analytical solution for flow in leaky unconfined aquifer–aquitard systems”. *Journal of Hydrology* 346.1, 59–68. DOI: <https://doi.org/10.1016/j.jhydrol.2007.08.018>.
- Mancuso, M., L. Santucci, and E. Carol (2020). “Effects of intensive aquifers exploitation on groundwater salinity in coastal wetlands”. *Hydrological Processes* 34.11, 2313–2323. DOI: <https://doi.org/10.1002/hyp.13727>. eprint: <https://onlinelibrary.wiley.com/doi/pdf/10.1002/hyp.13727>.
- Marcos-Garcia, P., M. Pulido-Velazquez, C. Sanchis-Ibor, M. García-Mollá, M. Ortega-Reig, A. Garcia-Prats, and C. Girard (2023). “From local knowledge to decision making in climate change adaptation at basin scale. Application to the Jucar River Basin, Spain”. *Climatic Change* 176.4, 38. DOI: 10.1007/s10584-023-03501-8.
- Martens, B., D. G. Miralles, H. Lievens, R. van der Schalie, R. A. M. de Jeu, D. Fernández-Prieto, H. E. Beck, W. A. Dorigo, and N. E. C. Verhoest (2017). “GLEAM v3: satellite-based land evaporation and root-zone soil moisture”. *Geoscientific Model Development* 10.5, 1903–1925. DOI: 10.5194/gmd-10-1903-2017.
- Martinez, R. and I. N. Masron (2020). “Jakarta: A city of cities”. *Cities* 106, 102868. DOI: <https://doi.org/10.1016/j.cities.2020.102868>.
- Mary P. Anderson, W. W. W. and R. J. Hunt (2015). *Applied Groundwater Modeling*. Elsevier. DOI: 10.1016/c2009-0-21563-7.

- Mazzoleni, M., L. Brandimarte, and A. Amaranto (2019). “Evaluating precipitation datasets for large-scale distributed hydrological modelling”. *Journal of Hydrology* 578, 124076. DOI: <https://doi.org/10.1016/j.jhydrol.2019.124076>.
- McCallum, J. L., P. G. Cook, and C. T. Simmons (2014). “Limitations of the Use of Environmental Tracers to Infer Groundwater Age”. *Groundwater* 53.S1, 56–70. DOI: 10.1111/gwat.12237.
- McColl, K. A., J. Vogelzang, A. G. Konings, D. Entekhabi, M. Piles, and A. Stoffelen (2014). “Extended triple collocation: Estimating errors and correlation coefficients with respect to an unknown target”. *Geophysical Research Letters* 41.17, 6229–6236. DOI: 10.1002/2014gl061322.
- McNamara, J. P., D. Tetzlaff, K. Bishop, C. Soulsby, M. Seyfried, N. E. Peters, B. T. Aulenbach, and R. Hooper (2011). “Storage as a Metric of Catchment Comparison”. *Hydrological Processes* 25.21, 3364–3371. DOI: <https://doi.org/10.1002/hyp.8113>. eprint: <https://onlinelibrary.wiley.com/doi/pdf/10.1002/hyp.8113>.
- Mehmood, K., B. Tischbein, M. Flörke, and M. Usman (2022). “Spatiotemporal Analysis of Groundwater Storage Changes, Controlling Factors, and Management Options over the Transboundary Indus Basin”. *Water* 14.20. DOI: 10.3390/w14203254.
- Meixner, T., A. H. Manning, D. A. Stonestrom, D. M. Allen, H. Ajami, K. W. Blasch, A. E. Brookfield, C. L. Castro, J. F. Clark, D. J. Gochis, A. L. Flint, K. L. Neff, R. Niraula, M. Rodell, B. R. Scanlon, K. Singha, and M. A. Walvoord (2016). “Implications of projected climate change for groundwater recharge in the western United States”. *Journal of Hydrology* 534, 124–138. DOI: <https://doi.org/10.1016/j.jhydrol.2015.12.027>.
- Melati, M. D., F. M. Fan, and G. B. Athayde (2019). “Groundwater recharge study based on hydrological data and hydrological modelling in a South American volcanic aquifer”. *Comptes Rendus Geoscience* 351.6, 441–450. DOI: <https://doi.org/10.1016/j.crte.2019.06.001>.
- Meng, L., J. Shi, Y. Zhai, R. Zuo, J. Wang, X. Guo, Y. Teng, J. Gao, L. Xu, and B. Guo (2022). “Ammonium Reactive Migration Process and Functional Bacteria Response along Lateral Runoff Path under Groundwater Exploitation”. *Sustainability* 14.14. DOI: 10.3390/su14148609.
- Meybeck, M. (2003). “5.08 - Global Occurrence of Major Elements in Rivers”. In: *Treatise on Geochemistry*. Ed. by H. D. Holland and K. K. Turekian. Oxford: Pergamon, 207–223. DOI: <https://doi.org/10.1016/B0-08-043751-6/05164-1>.
- Miralles, D. G., T. R. H. Holmes, R. A. M. De Jeu, J. H. Gash, A. G. C. A. Meesters, and A. J. Dolman (2011). “Global land-surface evaporation estimated from satellite-based observations”. *Hydrology and Earth System Sciences* 15.2, 453–469. DOI: 10.5194/hess-15-453-2011.

- Miro, M. E. and J. S. Famiglietti (2018). “Downscaling GRACE Remote Sensing Datasets to High-Resolution Groundwater Storage Change Maps of California’s Central Valley”. *Remote Sensing* 10.1. DOI: 10.3390/rs10010143.
- Misstear, B. D. R., L. Brown, and D. Daly (2009). “A methodology for making initial estimates of groundwater recharge from groundwater vulnerability mapping”. *Hydrogeology Journal* 17.2, 275–285. DOI: 10.1007/s10040-008-0342-x.
- Mitchell, M., A. Curtis, E. Sharp, and E. Mendham (2012). “Directions for social research to underpin improved groundwater management”. *Journal of Hydrology* 448-449, 223–231. DOI: <https://doi.org/10.1016/j.jhydrol.2012.04.056>.
- Moersidik, S. S., R. S. Arifin, E. T. B. Soesilo, D. M. Hartono, and Y. Latief (2015). “Project portfolio management to increase PDAM Tirtawening’s service coverage area”. In: *Water Resources Management VIII*. WIT Press. DOI: 10.2495/wrm150061.
- Moges, E., Y. Demissie, L. Larsen, and F. Yassin (2021). “Review: Sources of Hydrological Model Uncertainties and Advances in Their Analysis”. *Water* 13.1. DOI: 10.3390/w13010028.
- Mokadem, N., B. Redhaounia, H. Besser, Y. Ayadi, F. Khelifi, A. Hamad, Y. Hamed, and S. Bouri (2018). “Impact of climate change on groundwater and the extinction of ancient “Foggara” and springs systems in arid lands in North Africa: a case study in Gafsa basin (Central of Tunisia)”. *Euro-Mediterranean Journal for Environmental Integration* 3.1. DOI: 10.1007/s41207-018-0070-0.
- Molle, F., P. Wester, and P. Hirsch (2010). “River basin closure: Processes, implications and responses”. *Agricultural Water Management* 97.4. Comprehensive Assessment of Water Management in Agriculture, 569–577. DOI: <https://doi.org/10.1016/j.agwat.2009.01.004>.
- Momejian, N., M. Abou Najm, I. Alameddine, and M. El-Fadel (2019). “Groundwater Vulnerability Modeling to Assess Seawater Intrusion: a Methodological Comparison with Geospatial Interpolation”. *Water Resources Management* 33.3, 1039–1052. DOI: 10.1007/s11269-018-2165-4.
- Mora, A., J. Mählknecht, L. Rosales-Lagarde, and A. Hernández-Antonio (2017). “Assessment of major ions and trace elements in groundwater supplied to the Monterrey metropolitan area, Nuevo León, Mexico”. *Environmental Monitoring and Assessment* 189.8, 394. DOI: 10.1007/s10661-017-6096-y.
- Mustafa, S. M. T., M. M. Hasan, A. K. Saha, R. P. Rannu, E. Van Uytven, P. Willems, and M. Huysmans (2019). “Multi-model approach to quantify groundwater-level prediction uncertainty using an ensemble of global climate models and multiple abstraction scenarios”. *Hydrology and Earth System Sciences* 23.5, 2279–2303. DOI: 10.5194/hess-23-2279-2019.

- Mutaqin, D. J., M. B. Muslim, and N. H. Rahayu (2021). “Analisis Konsep Forest City dalam Rencana Pembangunan Ibu Kota Negara”. *Bappenas Working Papers* 4.1, 13–29. DOI: 10.47266/bwp.v4i1.87.
- Narulita, I. and W. Ningrum (2018). “Extreme flood event analysis in Indonesia based on rainfall intensity and recharge capacity”. *IOP Conference Series: Earth and Environmental Science* 118, 012045. DOI: 10.1088/1755-1315/118/1/012045.
- NASA/JPL (2019). *JPL GRACE and GRACE-FO Mascon Ocean, Ice, and Hydrology Equivalent Water Height Release 06 Version 02*. DOI: 10.5067/TEMSC-3MJ62.
- Nash, J. and J. Sutcliffe (1970). “River flow forecasting through conceptual models part I — A discussion of principles”. *Journal of Hydrology* 10.3, 282–290. DOI: 10.1016/0022-1694(70)90255-6.
- Neves, M. C., L. M. Nunes, and J. P. Monteiro (2020). “Evaluation of GRACE data for water resource management in Iberia: a case study of groundwater storage monitoring in the Algarve region”. *Journal of Hydrology: Regional Studies* 32, 100734. DOI: <https://doi.org/10.1016/j.ejrh.2020.100734>.
- Nolte, A., M. Eley, M. Schöniger, D. Gwapedza, J. Tanner, S. K. Mantel, and K. Scheihing (2021). “Hydrological modelling for assessing spatio-temporal groundwater recharge variations in the water-stressed Amathole Water Supply System, Eastern Cape, South Africa”. *Hydrological Processes* 35.6, e14264. DOI: <https://doi.org/10.1002/hyp.14264>. eprint: <https://onlinelibrary.wiley.com/doi/pdf/10.1002/hyp.14264>.
- Nugroho, H. (2020). “Pemindahan Ibu Kota Baru Negara Kesatuan Republik Indonesia ke Kalimantan Timur: Strategi Pemenuhan Kebutuhan dan Konsumsi Energi”. *Bappenas Working Papers* 3.1, 33–41. DOI: 10.47266/bwp.v3i1.53.
- Ochoa-González, G., D. Carreón-Freyre, A. Franceschini, M. Cerca, and P. Teatini (2018). “Overexploitation of groundwater resources in the faulted basin of Querétaro, Mexico: A 3D deformation and stress analysis”. *Engineering Geology* 245, 192–206. DOI: 10.1016/j.enggeo.2018.08.014.
- Oki, T. and S. Kanae (2006). “Global Hydrological Cycles and World Water Resources”. *Science* 313.5790, 1068–1072. DOI: 10.1126/science.1128845.
- Oruc, S. (2022). “Performance of bias corrected monthly CMIP6 climate projections with different reference period data in Turkey”. *Acta Geophysica* 70.2, 777–789. DOI: 10.1007/s11600-022-00731-9.
- Overeem, A., H. Leijnse, and R. Uijlenhoet (2011). “Measuring urban rainfall using microwave links from commercial cellular communication networks”. *Water Resources Research* 47.12. DOI: 10.1029/2010wr010350.
- Pandi, D., S. Kothandaraman, and M. Kuppusamy (2021). “Hydrological models: a review”. *International Journal of Hydrology Science and Technology* 12.3, 223–242. DOI:

- 10.1504/IJHST.2021.117540. eprint: <https://www.inderscienceonline.com/doi/pdf/10.1504/IJHST.2021.117540>.
- Pardo-Igúzquiza, E., A. J. Collados-Lara, and D. Pulido-Velazquez (2019). “Potential future impact of climate change on recharge in the Sierra de las Nieves (southern Spain) high-relief karst aquifer using regional climate models and statistical corrections”. *Environmental Earth Sciences* 78.20, 598. DOI: 10.1007/s12665-019-8594-4.
- Patle, G. T., D. K. Singh, and A. Sarangi (2018). “Modelling of climate-induced groundwater recharge for assessing carbon emission from groundwater irrigation”. *Current Science* 115.1, 64–73.
- Pauloo, R. A., G. E. Fogg, Z. Guo, and T. Harter (2021). “Anthropogenic basin closure and groundwater salinization (ABCSAL)”. *Journal of Hydrology* 593, 125787. DOI: <https://doi.org/10.1016/j.jhydrol.2020.125787>.
- Pesti, G., W. E. Kelly, and I. Bogardi (1994). “Observation network design for selecting locations for water supply wells”. *Environmetrics* 5.2, 91–110. DOI: <https://doi.org/10.1002/env.3170050202>. eprint: <https://onlinelibrary.wiley.com/doi/pdf/10.1002/env.3170050202>.
- Petpongpan, C., C. Ekkawatpanit, R. T. Bailey, and D. Kositgittiwong (2021). “Improving integrated surface water–groundwater modelling with groundwater extraction for water management”. *Hydrological Sciences Journal* 66.10, 1513–1530. DOI: 10.1080/02626667.2021.1948549.
- Pétré, M.-A., A. Rivera, and R. Lefebvre (2019a). “Numerical modeling of a regional groundwater flow system to assess groundwater storage loss, capture and sustainable exploitation of the transboundary Milk River Aquifer (Canada – USA)”. *Journal of Hydrology* 575, 656–670. DOI: 10.1016/j.jhydrol.2019.05.057.
- Pétré, M.-A., A. Rivera, and R. Lefebvre (2019b). “Numerical modeling of a regional groundwater flow system to assess groundwater storage loss, capture and sustainable exploitation of the transboundary Milk River Aquifer (Canada – USA)”. *Journal of Hydrology* 575, 656–670. DOI: <https://doi.org/10.1016/j.jhydrol.2019.05.057>.
- Pokhrel, Y. N., Y. Fan, G. Miguez-Macho, P. J.-F. Yeh, and S.-C. Han (2013). “The role of groundwater in the Amazon water cycle: 3. Influence on terrestrial water storage computations and comparison with GRACE”. *Journal of Geophysical Research: Atmospheres* 118.8, 3233–3244. DOI: 10.1002/jgrd.50335.
- Pollock, D. W. (2016). *User guide for MODPATH Version 7—A particle-tracking model for MODFLOW*. English. Tech. rep. Report. Reston, VA, 41. DOI: 10.3133/ofr20161086.
- Post, V. E., A. Vandenbohede, A. D. Werner, Maimun, and M. D. Teubner (2013). “Groundwater ages in coastal aquifers”. *Advances in Water Resources* 57, 1–11. DOI: <https://doi.org/10.1016/j.advwatres.2013.03.011>.

- Prasetya, R., A. R. As-syakur, and T. Osawa (2012). "Validation of TRMM Precipitation Radar satellite data over Indonesian region". *Theoretical and Applied Climatology* 112.3-4, 575–587. DOI: 10.1007/s00704-012-0756-1.
- Pravitasari, A. E., E. Rustiadi, S. P. Mulya, Y. Setiawan, L. N. Fuadina, and A. Murtadho (2018). "Identifying the driving forces of urban expansion and its environmental impact in Jakarta-Bandung mega urban region". *IOP Conference Series: Earth and Environmental Science* 149.1, 012044. DOI: 10.1088/1755-1315/149/1/012044.
- Pujiindiyati, E. and S. Satrio (2013). "Aplikasi Isotop Alam (18O, 2H dan 14C) untuk Studi Dinamika Air Tanah dan Hubungannya dengan Air Sungai di Daerah Bandung". *EKSPLORIUM* 34.2, 99–110. DOI: 10.17146/eksplorium.2013.34.2.2803.
- Putman, A. L., R. P. Fiorella, G. J. Bowen, and Z. Cai (2019). "A Global Perspective on Local Meteoric Water Lines: Meta-analytic Insight Into Fundamental Controls and Practical Constraints". *Water Resources Research* 55.8, 6896–6910. DOI: <https://doi.org/10.1029/2019WR025181>. eprint: <https://agupubs.onlinelibrary.wiley.com/doi/pdf/10.1029/2019WR025181>.
- Rahaman, M., B. Thakur, A. Kalra, and S. Ahmad (2019). "Modeling of GRACE-Derived Groundwater Information in the Colorado River Basin". *Hydrology* 6.1, 19. DOI: 10.3390/hydrology6010019.
- Rahiem, M. A. (2020). *Hydrogeological Information of Bandung Basin, Indonesia*.
- Rahimi, R., H. Tavakol-Davani, and M. Nasseri (2021). "An Uncertainty-Based Regional Comparative Analysis on the Performance of Different Bias Correction Methods in Statistical Downscaling of Precipitation". *Water Resources Management* 35.8, 2503–2518. DOI: 10.1007/s11269-021-02844-0.
- Rahimzadegan, M. and S. A. Entezari (2019). "Performance of the Gravity Recovery and Climate Experiment (GRACE) method in monitoring groundwater-level changes in local-scale study regions within Iran". *Hydrogeology Journal* 27.7, 2497–2509. DOI: 10.1007/s10040-019-02007-x.
- Rajabi, M. M., B. Ataie-Ashtiani, and C. T. Simmons (2018). "Model-data interaction in groundwater studies: Review of methods, applications and future directions". *Journal of Hydrology* 567, 457–477. DOI: <https://doi.org/10.1016/j.jhydrol.2018.09.053>.
- Rajczak, J. and C. Schär (2017). "Projections of Future Precipitation Extremes Over Europe: A Multimodel Assessment of Climate Simulations". *Journal of Geophysical Research: Atmospheres* 122.20, 10, 773–10, 800. DOI: <https://doi.org/10.1002/2017JD027176>. eprint: <https://agupubs.onlinelibrary.wiley.com/doi/pdf/10.1002/2017JD027176>.
- Ramjeawon, M., M. Demlie, and M. Toucher (2022). "Analyses of groundwater storage change using GRACE satellite data in the Usutu-Mhlathuze drainage region, north-eastern South Africa". *Journal of Hydrology: Regional Studies* 42, 101118. DOI: <https://doi.org/10.1016/j.ejrh.2022.101118>.

- Rashidi, H., N. M. N. Sulaiman, N. A. Hashim, L. Bradford, H. Asgharnejad, and M. M. Larijani (2021). “Wax removal from textile wastewater using an innovative hybrid baffle tank”. *The Journal of The Textile Institute* 112.2, 223–232. DOI: [10.1080/00405000.2020.1736484](https://doi.org/10.1080/00405000.2020.1736484).
- Rateb, A., B. R. Scanlon, D. R. Pool, A. Sun, Z. Zhang, J. Chen, B. Clark, C. C. Faunt, C. J. Haugh, M. Hill, C. Hobza, V. L. McGuire, M. Reitz, H. Müller Schmied, E. H. Sutanudjaja, S. Swenson, D. Wiese, Y. Xia, and W. Zell (2020). “Comparison of Groundwater Storage Changes From GRACE Satellites With Monitoring and Modeling of Major U.S. Aquifers”. *Water Resources Research* 56.12, e2020WR027556. DOI: <https://doi.org/10.1029/2020WR027556>.
- Rodell, M., J. Chen, H. Kato, J. S. Famiglietti, J. Nigro, and C. R. Wilson (2007). “Estimating groundwater storage changes in the Mississippi River basin (USA) using GRACE”. *Hydrogeology Journal* 15.1, 159–166. DOI: [10.1007/s10040-006-0103-7](https://doi.org/10.1007/s10040-006-0103-7).
- Rodell, M., I. Velicogna, and J. S. Famiglietti (2009). “Satellite-based estimates of groundwater depletion in India”. *Nature* 460.7258, 999–1002. DOI: [10.1038/nature08238](https://doi.org/10.1038/nature08238).
- Rusli, S., V. Bense, S. Mustafa, and A. Weerts (n.d.). “Assessing the significance of global climate model projections and groundwater abstraction scenarios on future basin-scale groundwater availability” (). in preparation.
- Rusli, S., V. Bense, A. Taufiq, and A. Weerts (2023a). “Quantifying basin-scale changes in groundwater storage using GRACE and one-way coupled hydrological and groundwater flow model in the data-scarce Bandung groundwater Basin, Indonesia”. *Groundwater for Sustainable Development* 22, 100953. DOI: <https://doi.org/10.1016/j.gsd.2023.100953>.
- Rusli, S., A. Weerts, S. Mustafa, D. Irawan, A. Taufiq, and V. Bense (2023b). “Quantifying aquifer interaction using numerical groundwater flow model evaluated by environmental water tracer data: Application to the data-scarce area of the Bandung groundwater basin, West Java, Indonesia”. *Journal of Hydrology: Regional Studies* 50, 101585. DOI: <https://doi.org/10.1016/j.ejrh.2023.101585>.
- Rusli, S., A. Weerts, A. Taufiq, and V. Bense (2021). “Estimating water balance components and their uncertainty bounds in highly groundwater-dependent and data-scarce area: An example for the Upper Citarum basin”. *Journal of Hydrology: Regional Studies* 37, 100911. DOI: <https://doi.org/10.1016/j.ejrh.2021.100911>.
- Rusli, S. R., D. Yudianto, and J.-t. Liu (2015). “Effects of temporal variability on HBV model calibration”. *Water Science and Engineering* 8.4, 291–300. DOI: <https://doi.org/10.1016/j.wse.2015.12.002>.
- Russo, T. A. and U. Lall (2017). “Depletion and response of deep groundwater to climate-induced pumping variability”. *Nature Geoscience* 10.2, 105–108. DOI: [10.1038/ngeo2883](https://doi.org/10.1038/ngeo2883).

- Ryguis, M., A. Novellino, E. Hussain, F. Syafiudin, H. Andreas, and C. Meisina (2023). “A Clustering Approach for the Analysis of InSAR Time Series: Application to the Bandung Basin (Indonesia)”. *Remote Sensing* 15.15. DOI: 10.3390/rs15153776.
- Rzepecka, Z. and M. Birylo (2020). “Groundwater Storage Changes Derived from GRACE and GLDAS on Smaller River Basins—A Case Study in Poland”. *Geosciences* 10.4. DOI: 10.3390/geosciences10040124.
- Saha, K., P. Dash, X. Zhao, and H.-m. Zhang (2020). “Error Estimation of Pathfinder Version 5.3 Level-3C SST Using Extended Triple Collocation Analysis”. *Remote Sensing* 12.4, 590. DOI: 10.3390/rs12040590.
- Salam, M., M. J. M. Cheema, W. Zhang, S. Hussain, A. Khan, M. Bilal, A. Arshad, S. Ali, and M. A. Zaman (2020). “Groundwater Storage Change Estimation Using Grace Satellite Data In Indus Basin”. *Big Data In Water Resources Engineering (BDWRE)* 1.1, 10–15. DOI: <https://doi.org/10.26480/bdwre.01.2020.10.15>.
- Salim, A. G., I. W. S. Dharmawan, and B. H. Narendra (2019). “Pengaruh Perubahan Luas Tutupan Lahan Hutan Terhadap Karakteristik Hidrologi DAS Citarum Hulu”. *Jurnal Ilmu Lingkungan* 17.2, 333. DOI: 10.14710/jil.17.2.333-340.
- Sanford, W. (2002). “Recharge and groundwater models: an overview”. *Hydrogeology Journal* 10.1, 110–120. DOI: 10.1007/s10040-001-0173-5.
- Sauvageot, H. (1994). “Rainfall measurement by radar: a review”. *Atmospheric Research* 35.1, 27–54. DOI: 10.1016/0169-8095(94)90071-x.
- Schellekens, J., verseve, M. Visser, hewinsemius, tanjaeuser, laurenebouaziz, sandercdvries, cthiange, hboisgon, DirkEilander, F. Baart, aweerts, DanielTollenaar, Pieter9011, ctenvelden, arthur-lutz, M. Jansen, and Imme1992 (2020). *openstreams/wflow: Bug fix release for 2020.1*. Version 2020.1.1. DOI: 10.5281/zenodo.3859967.
- Schellenger, F. L. and F. L. Hellweger (2019). “Phosphorus loading from onsite wastewater systems to a lake (at long time scales)”. *Lake and Reservoir Management* 35.1, 90–101. DOI: 10.1080/10402381.2018.1541031.
- Schneider, S. H., T. L. Root, and M. D. Mastrandrea, eds. (2011). *Encyclopedia of Climate and Weather*. Oxford University Press. DOI: 10.1093/acref/9780199765324.001.0001.
- Scholz, R. W., H. A. Mieg, and J. E. Oswald (2000). “Transdisciplinarity in Groundwater Management — Towards Mutual Learning of Science and Society”. *Water, Air, and Soil Pollution* 123.1, 477–487. DOI: 10.1023/A:1005292328778.
- Scott, K. A. (2020). “Extended Categorical Triple Collocation for Evaluating Sea Ice/Open Water Data Sets”. *IEEE Geoscience and Remote Sensing Letters*, 1–5. DOI: 10.1109/lgrs.2020.2990332.
- Sefelnasr, A., W. Gossel, and P. Wycisk (2014). “Three-dimensional groundwater flow modeling approach for the groundwater management options for the Dakhla oasis,

- Western Desert, Egypt". *Environmental Earth Sciences* 72.4, 1227–1241. DOI: 10.1007/s12665-013-3041-4.
- Seo, S., R. D. Bhowmik, A. Sankarasubramanian, G. Mahinthakumar, and M. Kumar (2019). "The role of cross-correlation between precipitation and temperature in basin-scale simulations of hydrologic variables". *Journal of Hydrology* 570, 304–314. DOI: 10.1016/j.jhydrol.2018.12.076.
- Serrat-Capdevila, A., J. B. Valdés, J. G. Pérez, K. Baird, L. J. Mata, and T. Maddock (2007). "Modeling climate change impacts – and uncertainty – on the hydrology of a riparian system: The San Pedro Basin (Arizona/Sonora)". *Journal of Hydrology* 347.1, 48–66. DOI: <https://doi.org/10.1016/j.jhydrol.2007.08.028>.
- Setiawan, A. M., Y. Koesmaryono, A. Faqih, and D. Gunawan (2017). "Observed and blended gauge-satellite precipitation estimates perspective on meteorological drought intensity over South Sulawesi, Indonesia". *IOP Conference Series: Earth and Environmental Science* 54, 012040. DOI: 10.1088/1755-1315/54/1/012040.
- Shahid, S., X.-J. Wang, M. Moshir Rahman, R. Hasan, S. B. Harun, and S. Shamsudin (2015). "Spatial assessment of groundwater over-exploitation in northwestern districts of Bangladesh". *Journal of the Geological Society of India* 85.4, 463–470. DOI: 10.1007/s12594-015-0238-z.
- Shamsudduha, M., R. G. Taylor, D. Jones, L. Longuevergne, M. Owor, and C. Tindimugaya (2017). "Recent changes in terrestrial water storage in the Upper Nile Basin: an evaluation of commonly used gridded GRACE products". DOI: 10.5194/hess-2017-146.
- Shawul, A. A., S. Chakma, and A. M. Melesse (2019). "The response of water balance components to land cover change based on hydrologic modeling and partial least squares regression (PLSR) analysis in the Upper Awash Basin". *Journal of Hydrology: Regional Studies* 26, 100640. DOI: 10.1016/j.ejrh.2019.100640.
- Shen, H., M. Leblanc, S. Tweed, and W. Liu (2015). "Groundwater depletion in the Hai River Basin, China, from in situ and GRACE observations". *Hydrological Sciences Journal* 60.4, 671–687. DOI: 10.1080/02626667.2014.916406.
- Shen, S.-L. and Y.-S. Xu (2011). "Numerical evaluation of land subsidence induced by groundwater pumping in Shanghai". *Canadian Geotechnical Journal* 48.9, 1378–1392. DOI: 10.1139/t11-049. eprint: <https://doi.org/10.1139/t11-049>.
- Silva Jr, G. and T. Pizani (2003). "Vulnerability assessment in coastal aquifers between Niterói and Rio das Ostras, Rio de Janeiro State, Brazil". *Rev Lat Am Hidrogeol* 3.1, 93–99.
- Singh, A. (2014). "Groundwater resources management through the applications of simulation modeling: A review". *Science of The Total Environment* 499, 414–423. DOI: <https://doi.org/10.1016/j.scitotenv.2014.05.048>.

- Siswanto, S. Y. and F. Francés (2019). “How land use/land cover changes can affect water, flooding and sedimentation in a tropical watershed: a case study using distributed modeling in the Upper Citarum watershed, Indonesia”. *Environmental Earth Sciences* 78.17, 550. DOI: [10.1007/s12665-019-8561-0](https://doi.org/10.1007/s12665-019-8561-0).
- Skaskevych, A., J. Lee, H. C. Jung, J. Bolten, J. L. David, F. S. Policelli, I. B. Goni, G. Favreau, S. San, and C. M. Ichoku (2020). “Application of GRACE to the estimation of groundwater storage change in a data-poor region: A case study of Ngadda catchment in the Lake Chad Basin”. *Hydrological Processes* 34.4, 941–955. DOI: <https://doi.org/10.1002/hyp.13613>.
- Smerdon, B. D. (2017). “A synopsis of climate change effects on groundwater recharge”. *Journal of Hydrology* 555, 125–128. DOI: <https://doi.org/10.1016/j.jhydrol.2017.09.047>.
- Smith, R. G. and S. Majumdar (2020). “Groundwater Storage Loss Associated With Land Subsidence in Western United States Mapped Using Machine Learning”. *Water Resources Research* 56.7, e2019WR026621. DOI: <https://doi.org/10.1029/2019WR026621>.
- Sorensen, J. P. R., J. Davies, G. Y. Ebrahim, J. Lindle, B. P. Marchant, M. J. Ascott, J. P. Bloomfield, M. O. Cuthbert, M. Holland, K. H. Jensen, M. Shamsudduha, K. G. Villholth, A. M. MacDonald, and R. G. Taylor (2021). “The influence of groundwater abstraction on interpreting climate controls and extreme recharge events from well hydrographs in semi-arid South Africa”. *Hydrogeology Journal* 29.8, 2773–2787. DOI: [10.1007/s10040-021-02391-3](https://doi.org/10.1007/s10040-021-02391-3).
- Sreedevi, P. D., P. D. Srekanth, and D. V. Reddy (2021). “Deuterium Excess of Groundwater as a Proxy for Recharge in an Evaporative Environment of a Granitic Aquifer, South India”. *Journal of the Geological Society of India* 97.6, 649–655. DOI: [10.1007/s12594-021-1740-0](https://doi.org/10.1007/s12594-021-1740-0).
- Staudinger, M., J. Seibert, and H. J. van Meerveld (2021). “Representation of Bi-Directional Fluxes Between Groundwater and Surface Water in a Bucket-Type Hydrological Model”. *Water Resources Research* 57.9, e2020WR028835. DOI: <https://doi.org/10.1029/2020WR028835>. eprint: <https://agupubs.onlinelibrary.wiley.com/doi/pdf/10.1029/2020WR028835>.
- Stevenazzi, S., M. Bonfanti, M. Masetti, S. V. Nghiem, and A. Soricetta (2017). “A versatile method for groundwater vulnerability projections in future scenarios”. *Journal of Environmental Management* 187, 365–374. DOI: <https://doi.org/10.1016/j.jenvman.2016.10.057>.
- Stiff Henry A., J. (1951). “The Interpretation of Chemical Water Analysis by Means of Patterns”. *Journal of Petroleum Technology* 3.10, 15–3. DOI: [10.2118/951376-G](https://doi.org/10.2118/951376-G).
- Stoffelen, A. (1998). “Toward the true near-surface wind speed: Error modeling and calibration using triple collocation”. *Journal of Geophysical Research: Oceans* 103.C4, 7755–7766. DOI: [10.1029/97jc03180](https://doi.org/10.1029/97jc03180).

- Su, K., W. Zheng, W. Yin, L. Hu, and Y. Shen (2022). “Improving the Accuracy of Groundwater Storage Estimates Based on Groundwater Weighted Fusion Model”. *Remote Sensing* 14.1. DOI: 10.3390/rs14010202.
- Sun, A. Y. (2013). “Predicting groundwater level changes using GRACE data”. *Water Resources Research* 49.9, 5900–5912. DOI: 10.1002/wrcr.20421.
- Sun, F., H. Shao, T. Kalbacher, W. Wang, Z. Yang, Z. Huang, and O. Kolditz (2011). “Groundwater drawdown at Nankou site of Beijing Plain: model development and calibration”. *Environmental Earth Sciences* 64.5, 1323–1333. DOI: 10.1007/s12665-011-0957-4.
- Sun, Q., C. Miao, Q. Duan, H. Ashouri, S. Sorooshian, and K.-L. Hsu (2018). “A Review of Global Precipitation Data Sets: Data Sources, Estimation, and Intercomparisons”. *Reviews of Geophysics* 56.1, 79–107. DOI: <https://doi.org/10.1002/2017RG000574>. eprint: <https://agupubs.onlinelibrary.wiley.com/doi/pdf/10.1002/2017RG000574>.
- As-syakur, A. R., T. Tanaka, T. Osawa, and M. S. Mahendra (2013). “Indonesian rainfall variability observation using TRMM multi-satellite data”. *International Journal of Remote Sensing* 34.21, 7723–7738. DOI: 10.1080/01431161.2013.826837.
- Tanachaichoksirikun, P. and U. Seeboonruang (2020). “Distributions of Groundwater Age under Climate Change of Thailand’s Lower Chao Phraya Basin”. *Water* 12.12. DOI: 10.3390/w12123474.
- Tang, Y., M. Hooshyar, T. Zhu, C. Ringler, A. Y. Sun, D. Long, and D. Wang (2017). “Reconstructing annual groundwater storage changes in a large-scale irrigation region using GRACE data and Budyko model”. *Journal of Hydrology* 551. Investigation of Coastal Aquifers, 397–406. DOI: <https://doi.org/10.1016/j.jhydro.2017.06.021>.
- Tangdamrongsub, N. and M. Šprlák (2021). “The Assessment of Hydrologic- and Flood-Induced Land Deformation in Data-Sparse Regions Using GRACE/GRACE-FO Data Assimilation”. *Remote Sensing* 13.2. DOI: 10.3390/rs13020235.
- Tapiador, F. J., F. Turk, W. Petersen, A. Y. Hou, E. García-Ortega, L. A. Machado, C. F. Angelis, P. Salio, C. Kidd, G. J. Huffman, and M. de Castro (2012). “Global precipitation measurement: Methods, datasets and applications”. *Atmospheric Research* 104-105, 70–97. DOI: <https://doi.org/10.1016/j.atmosres.2011.10.021>.
- Tarigan, A. K., S. Sagala, D. A. A. Samsura, D. F. Fiisabilillah, H. A. Simarmata, and M. Nababan (2016). “Bandung City, Indonesia”. *Cities* 50, 100–110. DOI: 10.1016/j.cities.2015.09.005.
- Taufiq, A., T. Hosono, K. Ide, M. Kagabu, I. Iskandar, A. J. Effendi, L. M. Hutasoit, and J. Shimada (2017). “Impact of excessive groundwater pumping on rejuvenation processes in the Bandung basin (Indonesia) as determined by hydrogeochemistry and modeling”. *Hydrogeology Journal* 26.4, 1263–1279. DOI: 10.1007/s10040-017-1696-8.

- Thomas, C. (1994). "Water in crisis: a guide to the world's fresh water resources". *International Affairs* 70.3, 557–557. DOI: [10.2307/2623756](https://doi.org/10.2307/2623756).
- Tillman, F. D., S. Gangopadhyay, and T. Pruitt (2016). "Changes in groundwater recharge under projected climate in the upper Colorado River basin". *Geophysical Research Letters* 43.13, 6968–6974. DOI: <https://doi.org/10.1002/2016GL069714>.
- Tirtomihardjo, H. (2016). "Chapter 10 - Groundwater Environment in Bandung, Indonesia". In: *Groundwater Environment in Asian Cities*. Ed. by S. Shrestha, V. P. Pandey, B. R. Shivakoti, and S. Thatikonda. Butterworth-Heinemann, 193–228. DOI: <https://doi.org/10.1016/B978-0-12-803166-7.00010-6>.
- Trásy-Havril, T., S. Szkolnikovics-Simon, and J. Mádl-Szőnyi (2022). "How Complex Groundwater Flow Systems Respond to Climate Change Induced Recharge Reduction?" *Water* 14.19. DOI: [10.3390/w14193026](https://doi.org/10.3390/w14193026).
- Trenberth, K. E. (2011). "Changes in precipitation with climate change". *Climate Research* 47.1-2, 123–138. DOI: [10.3354/cr00953](https://doi.org/10.3354/cr00953).
- Turek, M. E., Q. De Jong van Lier, and R. A. Armindo (2022). "Parameterizing field capacity as the upper limit of available water in bucket-type hydrological models". *Computers and Electronics in Agriculture* 194, 106801. DOI: <https://doi.org/10.1016/j.compag.2022.106801>.
- Turnadge, C. and B. D. Smerdon (2014). "A review of methods for modelling environmental tracers in groundwater: Advantages of tracer concentration simulation". *Journal of Hydrology* 519, 3674–3689. DOI: <https://doi.org/10.1016/j.jhydrol.2014.10.056>.
- Varouchakis, E. A., G. P. Karatzas, and G. P. Giannopoulos (2015). "Impact of irrigation scenarios and precipitation projections on the groundwater resources of Viannos Basin at the island of Crete, Greece". *Environmental Earth Sciences* 73.11, 7359–7374. DOI: [10.1007/s12665-014-3913-2](https://doi.org/10.1007/s12665-014-3913-2).
- Verma, K. and Y. B. Katpatal (2020). "Groundwater Monitoring Using GRACE and GLDAS Data after Downscaling Within Basaltic Aquifer System". *Groundwater* 58.1, 143–151. DOI: <https://doi.org/10.1111/gwat.12929>. eprint: <https://ngwa.onlinelibrary.wiley.com/doi/pdf/10.1111/gwat.12929>.
- Vertessy, R. A. and H. Elsenbeer (1999). "Distributed modeling of storm flow generation in an Amazonian rain forest catchment: Effects of model parameterization". *Water Resources Research* 35.7, 2173–2187. DOI: [10.1029/1999wr900051](https://doi.org/10.1029/1999wr900051).
- Vorobevskii, I., R. Kronenberg, and C. Bernhofer (2020). "Global BROOK90 R Package: An Automatic Framework to Simulate the Water Balance at Any Location". *Water* 12.7, 2037. DOI: [10.3390/w12072037](https://doi.org/10.3390/w12072037).
- Vos, L. de, H. Leijnse, A. Overeem, and R. Uijlenhoet (2017). "The potential of urban rainfall monitoring with crowdsourced automatic weather stations in Amsterdam". *Hydrology and Earth System Sciences* 21.2, 765–777. DOI: [10.5194/hess-21-765-2017](https://doi.org/10.5194/hess-21-765-2017).

- Voss, C. I. and S. M. Soliman (2013). “The transboundary non-renewable Nubian Aquifer System of Chad, Egypt, Libya and Sudan: classical groundwater questions and parsimonious hydrogeologic analysis and modeling”. *Hydrogeology Journal* 22.2, 441–468. DOI: 10.1007/s10040-013-1039-3.
- Voudouris, K., M. Valipour, A. Kaiafa, X. Y. Zheng, R. Kumar, K. Zanier, E. Kolokytha, and A. Angelakis (2018). “Evolution of water wells focusing on Balkan and Asian civilizations”. *Water Supply* 19.2, 347–364. DOI: 10.2166/ws.2018.114.
- Vries, W. T. de and M. Schrey (2022). “Geospatial Approaches to Model Renewable Energy Requirements of the New Capital City of Indonesia”. *Frontiers in Sustainable Cities* 4. DOI: 10.3389/frsc.2022.848309.
- Vuuren, D. P. van, J. Edmonds, M. Kainuma, K. Riahi, A. Thomson, K. Hibbard, G. C. Hurtt, T. Kram, V. Krey, J.-F. Lamarque, T. Masui, M. Meinshausen, N. Nakicenovic, S. J. Smith, and S. K. Rose (2011). “The representative concentration pathways: an overview”. *Climatic Change* 109.1, 5. DOI: 10.1007/s10584-011-0148-z.
- Wang, S., M. Zhang, C. E. Hughes, J. Crawford, G. Wang, F. Chen, M. Du, X. Qiu, and S. Zhou (2018). “Meteoric water lines in arid Central Asia using event-based and monthly data”. *Journal of Hydrology* 562, 435–445. DOI: 10.1016/j.jhydro1.2018.05.034.
- Wang, S.-J., C.-H. Lee, C.-F. Yeh, Y. F. Choo, and H.-W. Tseng (2021a). “Evaluation of Climate Change Impact on Groundwater Recharge in Groundwater Regions in Taiwan”. *Water* 13.9. DOI: 10.3390/w13091153.
- Wang, T.-Y., P. Wang, Y.-C. Zhang, J.-J. Yu, C.-Y. Du, and Y.-H. Fang (2019). “Contrasting groundwater depletion patterns induced by anthropogenic and climate-driven factors on Alxa Plateau, northwestern China”. *Journal of Hydrology* 576, 262–272. DOI: <https://doi.org/10.1016/j.jhydro1.2019.06.057>.
- Wang, X., Y. Geng, W. Zhou, Y. Li, and H. Luo (2021b). “Quantification and Regionalization of the Interaction between the Doumen Reservoir and Regional Groundwater in the Urban Plains of Northwest China”. *Water* 13.4, 540. DOI: 10.3390/w13040540.
- Wang, Z., M. Xue, K. Huang, and Z. Liu (2011). “Textile Dyeing Wastewater Treatment”. In: *Advances in Treating Textile Effluent*. Ed. by P. J. Hauser. Rijeka: IntechOpen. Chap. 5. DOI: 10.5772/22670.
- Wangsaatmaja, S., A. D. Sutadian, and M. A. N. Prasetiati (2006). “A Review of Groundwater Issues in the Bandung Basin, Indonesia: Management and Recommendations”. *International Review for Environmental Strategies* 2, 425–442.
- Wannasin, C., C. Brauer, R. Uijlenhoet, W. van Verseveld, and A. Weerts (2021a). “Daily flow simulation in Thailand Part I: Testing a distributed hydrological model with seamless parameter maps based on global data”. *Journal of Hydrology: Regional Studies* 34, 100794. DOI: 10.1016/j.ejrh.2021.100794.

- Wannasin, C., C. Brauer, R. Uijlenhoet, W. van Verseveld, and A. Weerts (2021b). “Daily flow simulation in Thailand Part II: Unraveling effects of reservoir operation”. *Journal of Hydrology: Regional Studies* 34, 100792. DOI: 10.1016/j.ejrh.2021.100792.
- Wati, T., A. Sopaheluwakan, and F. Fatkhuroyan (2018). “Comparison Pan Evaporation Data with Global Land-surface Evaporation GLEAM in Java and Bali Island Indonesia”. *Indonesian Journal of Geography* 50.1, 87. DOI: 10.22146/ijg.30926.
- Westerberg, I. K., A. E. Sikorska-Senoner, D. Viviroli, M. Vis, and J. Seibert (2022). “Hydrological model calibration with uncertain discharge data”. *Hydrological Sciences Journal* 67.16, 2441–2456. DOI: 10.1080/02626667.2020.1735638. eprint: <https://doi.org/10.1080/02626667.2020.1735638>.
- Widodo, L. E. (2013). “Estimation of Natural Recharge and Groundwater Build up in the Bandung Groundwater Basin Contributed from Rain Water Infiltration and Inter-aquifer Transfer”. *Procedia Earth and Planetary Science* 6, 187–194. DOI: 10.1016/j.proeps.2013.01.025.
- Winter, T. C., J. W. Harvey, O. L. Franke, and W. M. Alley (1998). *Ground water and surface water: A single resource*. DOI: 10.3133/cir1139.
- Wu, M., J. Wu, J. Lin, X. Zhu, J. Wu, and B. X. Hu (2018). “Evaluating the interactions between surface water and groundwater in the arid mid-eastern Yanqi Basin, northwestern China”. *Hydrological Sciences Journal* 63.9, 1313–1331. DOI: 10.1080/02626667.2018.1500744.
- Wu, W.-Y., M.-H. Lo, Y. Wada, J. S. Famiglietti, J. T. Reager, P. J.-F. Yeh, A. Ducharne, and Z.-L. Yang (2020). “Divergent effects of climate change on future groundwater availability in key mid-latitude aquifers”. *Nature Communications* 11.1, 3710. DOI: 10.1038/s41467-020-17581-y.
- Wu, X., Q. Xiao, J. Wen, and D. You (2019). “Direct Comparison and Triple Collocation: Which Is More Reliable in the Validation of Coarse-Scale Satellite Surface Albedo Products”. *Journal of Geophysical Research: Atmospheres* 124.10, 5198–5213. DOI: 10.1029/2018jd029937.
- Wu, Y., C. Miao, X. Fan, J. Gou, Q. Zhang, and H. Zheng (2022). “Quantifying the Uncertainty Sources of Future Climate Projections and Narrowing Uncertainties With Bias Correction Techniques”. *Earth's Future* 10.11. e2022EF002963. DOI: <https://doi.org/10.1029/2022EF002963>. eprint: <https://agupubs.onlinelibrary.wiley.com/doi/pdf/10.1029/2022EF002963>.
- Yamazaki, D., D. Ikeshima, R. Tawatari, T. Yamaguchi, F. O’Loughlin, J. C. Neal, C. C. Sampson, S. Kanae, and P. D. Bates (2017). “A high-accuracy map of global terrain elevations”. *Geophysical Research Letters* 44.11, 5844–5853. DOI: 10.1002/2017gl072874.

- Yang, X., N. Wang, Q. Liang, A. Chen, and Y. Wu (2021). “Impacts of Human Activities on the Variations in Terrestrial Water Storage of the Aral Sea Basin”. *Remote Sensing* 13.15. DOI: 10.3390/rs13152923.
- Yawson, D., M. Adu, B. Mulholland, T. Ball, K. Frimpong, S. Mohan, and P. White (2019). “Regional variations in potential groundwater recharge from spring barley crop fields in the UK under projected climate change”. *Groundwater for Sustainable Development* 8, 332–345. DOI: <https://doi.org/10.1016/j.gsd.2018.12.005>.
- Yeh, W. W.-G. (2015). “Review: Optimization methods for groundwater modeling and management”. *Hydrogeology Journal* 23.6, 1051–1065. DOI: 10.1007/s10040-015-1260-3.
- Yidana, S. M., C. Alo, M. O. Addai, O. F. Fynn, and S. K. Essel (2015). “Numerical analysis of groundwater flow and potential in parts of a crystalline aquifer system in Northern Ghana”. *International Journal of Environmental Science and Technology* 12.12, 3805–3818. DOI: 10.1007/s13762-015-0805-2.
- Yidana, S. M., E. K. Vakpo, P. A. Sakyi, L. P. Chegbeleh, and T. M. Akabzaa (2019). “Groundwater–lakewater interactions: an evaluation of the impacts of climate change and increased abstractions on groundwater contribution to the Volta Lake, Ghana”. *Environmental Earth Sciences* 78.3, 74. DOI: 10.1007/s12665-019-8076-8.
- Yin, J., S. Guo, L. Gu, Z. Zeng, D. Liu, J. Chen, Y. Shen, and C.-Y. Xu (2021). “Blending multi-satellite, atmospheric reanalysis and gauge precipitation products to facilitate hydrological modelling”. *Journal of Hydrology* 593, 125878. DOI: <https://doi.org/10.1016/j.jhydrol.2020.125878>.
- Yin, W., L. Hu, M. Zhang, J. Wang, and S.-C. Han (2018). “Statistical Downscaling of GRACE-Derived Groundwater Storage Using ET Data in the North China Plain”. *Journal of Geophysical Research: Atmospheres* 123.11, 5973–5987. DOI: <https://doi.org/10.1029/2017JD027468>.
- Yirdaw, S. Z. and K. R. Snelgrove (2011). “Regional Groundwater Storage from GRACE over the Assiniboine Delta Aquifer (ADA) of Manitoba”. *Atmosphere-Ocean* 49.4, 396–407. DOI: 10.1080/07055900.2011.623915.
- Yu, D., J. Yang, L. Shi, Q. Zhang, K. Huang, Y. Fang, and Y. Zha (2019). “On the uncertainty of initial condition and initialization approaches in variably saturated flow modeling”. *Hydrology and Earth System Sciences* 23.7, 2897–2914. DOI: 10.5194/hess-23-2897-2019.
- Yuan, F., Y.-K. Tung, and L. Ren (2015). “Projection of future streamflow changes of the Pearl River basin in China using two delta-change methods”. *Hydrology Research* 47.1, 217–238. DOI: 10.2166/nh.2015.159. eprint: <https://iwaponline.com/hr/article-pdf/47/1/217/369161/nh0470217.pdf>.

- Yuanyuan, M., Z. Xuegang, and L. Zhijia (2013). “Coupled Simulation of Xinanjiang Model with MODFLOW”. *Journal of Hydrologic Engineering* 18.11, 1443–1449. DOI: 10.1061/(ASCE)HE.1943-5584.0000706.
- Yukimoto, S., T. Koshiro, H. Kawai, N. Oshima, K. Yoshida, S. Urakawa, H. Tsujino, M. Deushi, T. Tanaka, M. Hosaka, H. Yoshimura, E. Shindo, R. Mizuta, M. Ishii, A. Obata, and Y. Adachi (2019). *MRI MRI-ESM2.0 model output prepared for CMIP6 CMIP*. DOI: 10.22033/ESGF/CMIP6.621.
- Zeinali, M., A. Azari, and M. M. Heidari (2020). “Multiobjective Optimization for Water Resource Management in Low-Flow Areas Based on a Coupled Surface Water–Groundwater Model”. *Journal of Water Resources Planning and Management* 146.5, 04020020. DOI: 10.1061/(ASCE)WR.1943-5452.0001189.
- Zhang, L., S. Yi, Q. Wang, L. Chang, H. Tang, and W. Sun (2019). “Evaluation of GRACE mascon solutions for small spatial scales and localized mass sources”. *Geophysical Journal International* 218.2, 1307–1321. DOI: 10.1093/gji/ggz198.
- Zhao, Y., N. Dong, Z. Li, W. Zhang, M. Yang, and H. Wang (2021). “Future precipitation, hydrology and hydropower generation in the Yalong River Basin: Projections and analysis”. *Journal of Hydrology* 602, 126738. DOI: <https://doi.org/10.1016/j.jhydrol.2021.126738>.
- Zhong, Y., W. Feng, V. Humphrey, and M. Zhong (2019). “Human-Induced and Climate-Driven Contributions to Water Storage Variations in the Haihe River Basin, China”. *Remote Sensing* 11.24. DOI: 10.3390/rs11243050.
- Zhong, Y., M. Zhong, W. Feng, Z. Zhang, Y. Shen, and D. Wu (2018). “Groundwater Depletion in the West Liaohe River Basin, China and Its Implications Revealed by GRACE and In Situ Measurements”. *Remote Sensing* 10.4. DOI: 10.3390/rs10040493.
- Zhu, M., S. Wang, X. Kong, W. Zheng, W. Feng, X. Zhang, R. Yuan, X. Song, and M. Sprenger (2019a). “Interaction of Surface Water and Groundwater Influenced by Groundwater Over-Extraction, Waste Water Discharge and Water Transfer in Xiong’an New Area, China”. *Water* 11.3, 539. DOI: 10.3390/w11030539.
- Zhu, R., B. F. Croke, and A. J. Jakeman (2020a). “Diffuse groundwater recharge estimation confronting hydrological modelling uncertainty”. *Journal of Hydrology* 584, 124642. DOI: <https://doi.org/10.1016/j.jhydrol.2020.124642>.
- Zhu, R., H. Zheng, B. F. Croke, and A. J. Jakeman (2020b). “Quantifying climate contributions to changes in groundwater discharge for headwater catchments in a major Australian basin”. *Science of The Total Environment* 729, 138910. DOI: 10.1016/j.scitotenv.2020.138910.
- Zhu, S., F. Zhang, Z. Zhang, H.-t. Kung, and A. Yushanjiang (2019b). “Hydrogen and Oxygen Isotope Composition and Water Quality Evaluation for Different Water Bodies in the Ebinur Lake Watershed, Northwestern China”. *Water* 11.10. DOI: 10.3390/w11102067.

-
- Zimmermann, I., H. Fleige, and R. Horn (2017). “Longtime effects of deep groundwater extraction management on water table levels in surface aquifers”. *Journal of Soils and Sediments* 17.1, 133–143. DOI: 10.1007/s11368-016-1489-z.
- Al-Zyoud, S., W. Rühaak, E. Forootan, and I. Sass (2015). “Over Exploitation of Groundwater in the Centre of Amman Zarqa Basin—Jordan: Evaluation of Well Data and GRACE Satellite Observations”. *Resources* 4.4, 819–830. DOI: 10.3390/resources4040819.

Statement of authorship contribution

Steven Rusli proposed the origin of the broader idea in this thesis. Later, Albrecht Weerts and Victor Bense assisted in reshaping, refining, and sharpening the concept into concrete research objectives. For the content of this thesis, chapter by chapter, the contributions from all the involved individuals are listed below.

The following initials are abbreviated from the names as follow:

SR = Steven R. Rusli (WUR)

AW = Albrecht H. Weerts (Deltares/WUR)

VB = Victor F. Bense (WUR)

SM = Syed M.T. Mustafa (WUR)

AT = Ahmad Taufiq (Ministry of Public Work and Housing, Indonesia)

DEI = Dasapta Erwin Irawan (Institut Teknologi Bandung, Indonesia)

Chapter 1 (introduction):

Writing	: SR
Supervision	: AH, VB

Chapter 2 (study area):

Conceptualization	: SR
Resources & data collection	: SR, AH, AT, DEI
Writing	: SR
Supervision	: AH, VB

Chapter 3:

Conceptualization	: SR, AH, VB
Methodology	: SR, AH, VB
Data collection	: SR, AH, VB, AT
Modeling	: SR with contribution from AH
Data analysis	: SR, AH, VB
Writing	: SR
Supervision	: AH, VB, AT

Chapter 4:

Conceptualization	: SR, AH, VB
Methodology	: SR, AH, VB
Data collection	: SR, AT
Modeling	: SR in consultation with AH, VB
Data analysis	: SR, AH, VB
Writing	: SR
Supervision	: AH, VB

Chapter 5:

Conceptualization	: SR, AH, VB, DEI
Methodology	: SR, AH, VB
Data collection	: SR, AT, DEI
Modeling	: SR in consultation with AH, VB
Data analysis	: SR, AH, VB, DEI
Writing	: SR
Supervision	: AH, VB, SM, DEI

Chapter 6:

Conceptualization	: SR, AH, VB, SM
Methodology	: SR, AH, VB, SM
Data collection	: SR
Modeling	: SR in consultation with AH, VB, SM
Data analysis	: SR, AH, VB, SM
Writing	: SR
Supervision	: AH, VB, SM

Chapter 7 (synthesis):

Writing	: SR
Supervision	: AH, VB

Acknowledgements

A-1. I give thanks to You, who strengthens me, with a grateful heart.

The highest gratitude and appreciation are most fittingly addressed to my invaluable family; my wife Marlitha Egi, my son Gavriel Brandon Rusli, and my future child(ren). Your everlasting, never-ending, and wholehearted support radiates love, joy, peace, and hope. Profoundly, you complete me in the most fundamental way; you trust me with the right to bear the responsibility, as a man, of a husband and a father. You give me purposes of provision and protection. Marlitha, I hope you will be everlastingly happy choosing me as your man. Of all the titles I have been privileged to have, 'your husband' was, is, and will always be the one I'm happiest with. Gavriel, be a righteous man. Be a courageous man. Be the best version of yourself, someone that you will be proud of. Never in doubt, your parents will make sure that you do. Together, let's continue building our heaven on earth, forever and always!

On behalf of our little family, the recognition is also extended to our parents, siblings, and relatives. You teach us endurance, resilience, and tenacity, not only by words but also by example. Thanks for all the care, time, and sweat you sacrificed to shape us the way we are today; and for the compassion, kindness, and smiles to brighten up our days. I will never forget the lesson you taught us: to be honest and to be brave when you are right, even though the world is against you. I promise that these legacies will be passed on to generations, and will only thrive.

In the focus of this thesis, I thank the (extended) supervising team. Albrecht and Victor, thank you for your consistent support throughout the journey, especially for your patience with my limited scientific quality, and for your trust in my capacity to eventually overcome those challenges gradually. Humbly, I recognized the sluggishness of my early performance. Extra work to catch up with the quality requirement was necessary, particularly in coding, systematic thinking, and formulating ideas, but none of you gave up on me. Albrecht, thank you for the assistance in initiating the Wflow_sbm model. Your direct problem-solving approach boosted my confidence in working on the first paper. Victor, I vividly remember the first time I was unsure of how to start building the groundwater flow model. Your response to my unreasonable concern was direct, straightforward, and detached from any unnecessary virtue-signaling emotions. 'At some point, you have to start, so why

don't do it now' and 'Just start' were some of the short advice you gave. You might not remember it, but looking back to that time now, that was unquestionably the best answer I could hope for. I deeply appreciate both of your approaches to handling my frequent unnecessary insecurity and I apologize for any shortcomings. To the other contributors, thank you for the direction in writing this thesis. Syed, thank you for your hands-on and detailed approach to every single discussion. Looking forward to other even more fruitful collaboration papers in the future. Pak Ahmad Taufiq and Pak Dasapta Erwin Irawan, I appreciate the assistance in the data collection phase of this thesis, as well as the discussion we had throughout the journey.

For my work colleagues and friends, it has been a pleasure sharing these last 4.5 years with you. Pak Suryadi, Mo, Ko Sony, Pak Doddi, and Bu Ida, thanks for helping to make this even possible, to begin with. None of this story would have happened without each of your help. Germano, Sjoukje, Linda, and Iris, it is a privilege to go through the PhD experience in the same stages with you. Good luck finishing your PhDs! I wish you all the best future, full of blessings. Luca, Rose, Khoa, Bob, Harro, Joao, Henk, Derk, Titus, Jingwei, and everyone whose names I can't mention one by one, cheers for all the memories we created. Thank you, Luca, for welcoming my family to my dream city, Rome. My son still keeps the Roman wolf doll that you gave him until now. Rose, I can't say thank you enough to you. You managed to put a lock on my mouth so many times, preventing me from causing so many potential problems with my opinion. Khoa, thank you for always being the most relatable person in the group. Good luck to the future of your family. Bob, what a pleasure to treat each other with Dutch and Indonesian lunch! Thank you, Harro, for the considerate conversations we had. You have been the bridge between me and the Dutch. Thank you, Joao, Henk, and Derk, for your willingness to listen to my perspective. The way I look at the world is by far the minority in the current Western culture. The three of you have provided the ears that bear my complaints. Titus, thank you for your willingness for the last-minute help to even work during your weekend time. Jingwei, thank you for the help in organizing the space for a lot of celebrations. Thank you, Nick, for the last-minute grammar check on the thesis title and propositions. Bart and Kryss, thanks for the modesty in sharing the working space. Claudia, thanks for always being the kindest person around. Tamara, thanks for all the earnest assistance. Farid and Vina, Dyon (and wife), Metta (and husband), and Adham, cheers for the joint struggle until the finish line. Hugo, Tya, Silvia, and members of Wageningen Ekklesia Christian Fellowship, your presence has been more than a blessing to us. Ko Khris, Ci Filla, Pak Didik, Ci Lingling, and all associates in Indonesia, thanks for the moral support and all the other positive things you provided. For all of us, success!

A-(-1). Beloved, I pray that all may go well with you and that you may be in good health, as it goes well with your soul.

About the author

Steven Reinaldo Rusli was born in Bandung, Indonesia on July 2nd, 1991. He finished his bachelor's degree in the Civil Engineering Department of Universitas Katolik Parahyangan, Indonesia, in 2012, with the undergraduate thesis topic of flood control study of a tidal-influenced river in Borneo Island, Indonesia. After his graduation, he continued working on various engineering consultation projects and teaching part-time as a laboratory assistant. He joined the double degree program in Water Resources Engineering from Universitas Katolik Parahyangan, Indonesia, and Hohai University, China, and graduated in 2015. His master's thesis topic focused on the assessment of parameter uncertainties of two hydrological models under various temporal variabilities. Since then, he reversed his position: working in academia as a full-time lecturer at Universitas Katolik Parahyangan and in water resources projects as a part-time consultant. He started his PhD at Wageningen University and Research in 2019, with a research focus on groundwater flow modeling in a data-scarce and highly-groundwater-dependent area of the Bandung groundwater basin. After his graduation, he plans to continue working in academia and is aiming to be a full professor one day, hopefully in Indonesia.

Outside of his professional position, Steven has several outside hobbies - mainly music and football - which he hopes his child(ren) will like, too. He enjoys spending time the most with his family though. Without the family, there will not be the same Steven today. Marlitha, his wife, is fulfilling her purpose flawlessly: she loves her husband and their children, she is discreet, chaste, keepsers at home, good, and obedient to her husband. Thank you, Marlitha, you are worth loving. You are worth melting for. Gavriel has been the finest first-born son we could have ever asked for. Grow, son, and be a man who is the best version of you, for surely there is a future, and your hope will not be cut off. I have no greater joy than to hear that you are living according to the truth. Don't let anyone look down on you because you are young, but set an example for the believers in speech, conduct, love, faith, and purity. Thank you, Gavriel, you are worth fighting for. You are worth protecting. For my future child(ren), if we are trusted and blessed, you are worth dreaming of. You are worth hoping for. See you later, fingers crossed! How good and pleasant it is when we live together in unity!

Peer-reviewed Journal Publications | In this thesis

- Rusli, S.**, A. Weerts, A. Taufiq, and V. Bense (2021). “Estimating water balance components and their uncertainty bounds in highly groundwater-dependent and data-scarce area: An example for the Upper Citarum basin”. *Journal of Hydrology: Regional Studies* 37, 100911. DOI: <https://doi.org/10.1016/j.ejrh.2021.100911>.
- Rusli, S.**, V. Bense, A. Taufiq, and A. Weerts (2023a). “Quantifying basin-scale changes in groundwater storage using GRACE and one-way coupled hydrological and groundwater flow model in the data-scarce Bandung groundwater Basin, Indonesia”. *Groundwater for Sustainable Development* 22, 100953. DOI: <https://doi.org/10.1016/j.gsd.2023.100953>.
- Rusli, S.**, A. Weerts, S. Mustafa, D. Irawan, A. Taufiq, and V. Bense (2023b). “Quantifying aquifer interaction using numerical groundwater flow model evaluated by environmental water tracer data: Application to the data-scarce area of the Bandung groundwater basin, West Java, Indonesia”. *Journal of Hydrology: Regional Studies* 50, 101585. DOI: <https://doi.org/10.1016/j.ejrh.2023.101585>.
- Rusli, S.**, V. Bense, S. Mustafa, and A. Weerts (n.d.). “Assessing the significance of global climate model projections and groundwater abstraction scenarios on future basin-scale groundwater availability” (). in preparation.

Peer-reviewed Journal Publications | Other

- Yudianto, D., B. M. Ginting, S. Sanjaya, **S. Rusli**, and A. Wicaksono (2021). “A Framework of Dam-Break Hazard Risk Mapping for a Data-Sparse Region in Indonesia”. *ISPRS International Journal of Geo-Information* 10.3. DOI: [10.3390/ijgi10030110](https://doi.org/10.3390/ijgi10030110).
- Hateren, T. C. van, H. J. Jongen, H. Al-Zawaidah, J. G. Beemster, J. Boekee, L. Bogerd, S. Gao, C. Kannen, I. van Meerveld, S. I. de Lange, F. Linke, R. B. Pinto, J. O. Remmers, J. Ruijsch, **S. R. Rusli**, R. C. van de Vijzel, J. P. Aerts, S. M. Agoungbome, M. Anys, S. B. Ramírez, T. van Emmerik, L. Gallitelli, G. C. Gesualdo, W. G. Otero, S. Hanus, Z. He, S. Hoffmeister, R. O. Imhoff, T. Kerlin, S. M. Meshram, J. Meyer, A. M. Oliveira, A. C. Müller, R. Nijzink, M. Scheller, L. Schreyers, D. Sehgal, P. F. Tasserion, A. J. Teuling, M. Trevisson, K. Waldschläger, B. Walraven, C. Wannasin, J. Wienhöfer, M. J. Zander, S. Zhang, J. Zhou, J. Y. Zomer, and B. W. Zwartendijk (2023). “Where should hydrology go? An early-career perspective on the next IAHS Scientific Decade: 2023–2032”. *Hydrological Sciences Journal* 68.4, 529–541. DOI: [10.1080/02626667.2023.2170754](https://doi.org/10.1080/02626667.2023.2170754). eprint: <https://doi.org/10.1080/02626667.2023.2170754>.



*Netherlands Research School for the
Socio-Economic and Natural Sciences of the Environment*

D I P L O M A

for specialised PhD training

The Netherlands research school for the
Socio-Economic and Natural Sciences of the Environment
(SENSE) declares that

Steven Reinaldo Rusli

born on the 2nd of July 1991 in Bandung, Indonesia

has successfully fulfilled all requirements of the
educational PhD programme of SENSE.

Wageningen, 6th of February 2024

Chair of the SENSE board

Prof. dr. Martin Wassen

The SENSE Director

Prof. Philipp Pattberg

The SENSE Research School has been accredited by the Royal Netherlands Academy of Arts and Sciences (KNAW)



K O N I N K L I J K E N E D E R L A N D S E
A K A D E M I E V A N W E T E N S C H A P P E N



The SENSE Research School declares that **Steven Reinaldo Rusli** has successfully fulfilled all requirements of the educational PhD programme of SENSE with a work load of 46.1 EC, including the following activities:

SENSE PhD Courses

- o Environmental research in context (2019)
- o Research in context activity: 'Coordinating two simultaneous webinars, as the organizers and the speakers, on the topic of 'Hydrology in Indonesia'(2020)

Other PhD and Advanced MSc Courses

- o Groundwater flow modeling with Modflow, Python, and Flopy , Hatarilabs (2020)
- o Applied groundwater modeling, IHE Delft (2021)
- o QGIS for groundwater modelling application, Australian Water School (2021)
- o Groundwater modelling with Python, Australian Water School (2022)
- o Applied groundwater modeling with MODFLOW and ModelMuse, Hatarilabs (2023)

External training at a foreign research institute

- o Engineering profession program, Indonesian Engineer Association, Indonesia (2021)

Management and Didactic Skills Training

- o Organizing the 'Tour the PhD' trip to other institutes abroad (2022)
- o Guest lecturer at the InHolland Hogeschool Honours Programme in Haarlem (2023)

Oral Presentations

- o *Estimating the water balance and uncertainty bounds in a highly groundwater-dependent and data-scarce area: An example for the upper Citarum basin.* European Geosciences Union 2022, 26 - 30 April 2021 Vienna, Austria (online)
- o *Estimating basin-scale groundwater storage change component in data-scarce area of Bandung Basin, West Java, Indonesia, using groundwater modeling and GRACE data.* European Geosciences Union 2022, 23 - 27 May 2022, Vienna, Austria
- o *Groundwater flow system behavior in Bandung groundwater basin.* Wageningen-Indonesia Scientific Exposure (WISE) 2023, 8 March 2022 Wageningen, the Netherlands
- o *Quantifying aquifer interaction using numerical groundwater flow model evaluated by environmental water tracers data: Application in Bandung groundwater basin, Indonesia.* European Geosciences Union 2023, 24 - 28 April 2023 Vienna, Austria

SENSE coordinator PhD education

Dr. ir. Peter Vermeulen

The research presented in this thesis was financially supported by the Indonesian Endowment Fund for Education (*Lembaga Pengelola Dana Pendidikan/LPDP*), the Ministry of Finance of the Republic of Indonesia through the program of *Beasiswa Unggulan Dosen Indonesia/BUDI*, Grant number: LOG2429202221533732. Financial support from Wageningen University and Research and LPDP for printing this thesis is gratefully acknowledged.

© 2024 Steven Reinaldo Rusli

Cover design by Fatimah Zahra (Instagram @fazamatahari) and Steven R. Rusli

Additional lay-out and printing by ProefschriftMaken — proefschriftmaken.nl

Printed on FSC Certified paper

